Base Compaction Specification Feasibility Analysis

Hani H. Titi, Ph.D., P.E., M.ASCE
Habib Tabatabai, Ph.D., P.E., S.E.
Emil Bautista, M.Sc.
Andrew Druckrey, M.Sc.

Department of Civil Engineering and Mechanics
University of Wisconsin-Milwaukee

Ahmed Faheem, Ph.D.

Bloom Companies, LLC
Milwaukee, WI

Erol Tutumluer, Ph.D.

Civil and Environmental Engineering
University of Illinois at Urbana-Champaign

WisDOT ID no. 0092-11-02

December 2012

Research & Library Unit

Wisconsin Highway Research Program

WISCONSIN DOT

PUTTING RESEARCH TO WORK

Base Compaction Specification Feasibility Analysis

Hani H. Titi, Ph.D., P.E., M.ASCE
Habib Tabatabai, Ph.D., P.E., S.E.
Emil Bautista, M.Sc.
Andrew Druckrey[1], M.Sc.
Department of Civil Engineering and Mechanics
University of Wisconsin-Milwaukee
3200 N. Cramer St.
Milwaukee, WI 53211

Ahmed Faheem, Ph.D.
Bloom Companies, LLC
10501 W. Research Drive, Suite 100
Milwaukee, WI 53226

And

Erol Tutumluer, Ph.D.
Civil and Environmental Engineering
University of Illinois at Urbana-Champaign
205 N. Mathews Ave., Urbana, IL 61801

Final Report

Submitted to

Wisconsin Highway Research Program
Wisconsin Department of Transportation
WisDOT Research & Library Unit
4805 Sheboygan Avenue, Room 104
P.O. Box 7915
Madison, WI 53707

December 2012

[1] Former graduate student at UW-Milwaukee; current Ph.D. student, University of Tennessee, Knoxville

Executive Summary

The objective of this research is to establish the technical engineering and cost analysis concepts that will enable WisDOT management to objectively evaluate the feasibility of switching construction specification philosophies for aggregate base. In order to accomplish this goal, field and laboratory testing program as well as comprehensive survey of highway agencies practices on base layer construction in the U.S. and Canada were conducted. This research proposed construction specifications for aggregate base course layers.

This research investigated the performance of aggregate base layers for existing Hot Mix Asphalt (HMA) pavements and for HMA pavement under construction through field and laboratory tests on pavement layers and pavement materials. Eleven existing HMA pavement projects with aggregate base course layers constructed in the last few years were selected for non-destructive testing and evaluation using the Falling Weight Deflectometer (FWD) and visual distress surveys. In six of these projects, issues related to the aggregate base stability and uniformity were observed and reported during HMA layer paving. Later, these pavements exhibited various levels of distresses that included cracking (longitudinal, transverse, and alligator), aggregate base failure, and pavement surface roughness/irregularities (in terms of ride quality). The remaining five pavement projects, in which no issues related to aggregate base layer behavior during construction were reported, performed well after construction. These projects were subjected to FWD testing along approximately one-mile test section per project. The existing HMA pavements that showed early distresses exhibited high levels of spatial variability and non-uniformity in aggregate base course layers, as demonstrated by FWD testing and backcalculated base layer modulus. The existing HMA pavements that performed well exhibited low levels of spatial variability and uniformity in aggregate base course layers, as shown by the FWD test results and the backcalculated base layer modulus.

In addition, field and laboratory tests were conducted on 10 projects during base course layer construction to evaluate the quality of the constructed base layers. Base aggregates were also collected from these sites for laboratory testing. The field testing program consisted of the in place density by the sand cone method, the dynamic cone penetration (DCP) test, the light weight deflectometer (LWD) test, and the GeoGauge test. Laboratory tests conducted are the particle size analysis, the standard compaction test (AASHTO T 99), and the repeated load triaxial test (AASHTO T 307) for determining the resilient modulus.

Analyses were conducted on field and laboratory test results. High spatial variability in field density and moisture content exists in base course layers under construction, as demonstrated by the relative compaction test results. High variability exists along the depth of base course layers, as demonstrated by the dynamic cone penetrometer test results and the estimated profile of California Bearing Ratio (CBR) along the depth of the investigated base layers. Spatial variability and non-uniformity

were also demonstrated by the results of the light weight deflectometer and GeoGauge, in which the layer modulus varies within a large range of values.

The mechanistic-empirical pavement design method (Mechanistic-Empirical Design of New and Rehabilitated Pavement Structures) was used to perform sensitivity analysis for the effect of the base course layer modulus on pavement performance. Results of the analysis demonstrated that Wisconsin pavements with a lower base layer modulus exhibited earlier fatigue bottom-up cracking and developed more rutting. The sensitivity analysis was conducted utilizing DARWin-ME software. Wisconsin data and pavement design input parameters for STH 33, Port Washington were used in the analysis.

A comprehensive survey was designed and conducted by communication with state highway agencies in the U.S. and Canada to obtain the current state of practice on the Quality Control/Quality Assurance (QC/QA) of constructed aggregate base layer. The results of the survey showed that four highway agencies out of 62 in the U.S. and Canada use subjective observation for accepting constructed aggregate base layers. The survey also indicated that 42% of the highway agencies are thinking of new methodologies such as modulus-based specification to replace/complement their current density-based specifications. Current state of practice and research in the U.S. is focused on the modulus-based specifications and developing such specifications for QC/QA. This is demonstrated by the Indiana DOT's move to use/implement the LWD tests for base layer characterization, and by a major National Cooperative Highway Research Program (NCHRP) project 10-84 (Modulus-Based Construction Specification for Compaction of Earthwork and Unbound Aggregate) and NCHRP Synthesis 20-05/Topic 43-03 (Practices for Unbound Aggregate Pavement Layers) on modulus-based characterization of aggregate base layers.

DISCLAIMER

This research was funded through the Wisconsin Highway Research Program by the Wisconsin Department of Transportation and the Federal Highway Administration under Project 0092-11-02. The contents of this report reflect the views of the authors, who are responsible for the facts and accuracy of the data presented herein. The contents do not necessarily reflect the official views of the Wisconsin Department of Transportation or the Federal Highway Administration at the time of publication.

This document is disseminated under the sponsorship of the Department of Transportation in the interest of information exchange. The United States Government assumes no liability for its contents or use thereof. This report does not constitute a standard, specification or regulation.

The United States Government does not endorse products or manufacturers. Trade and manufacturers' names appear in this report only because they are considered essential to the object of the document.

Technical Report Documentation Page

1. **Report No.** WHRP	2. **Government Accession** No	3. **Recipient's Catalog No**
4. **Title and Subtitle** Base Compaction Specification Feasibility Analysis		5. **Report Date** December 2012 6. **Performing Organization Code** Wisconsin Highway Research Program
7. **Authors** Hani H. Titi, Habib Tabatabai, Ahmed Faheem, Emil Bautista, Erol Tutumluer, and Andrew Druckrey		8. **Performing Organization Report:** No.
9. **Performing Organization Name and Address** Department of Civil Engineering and Mechanics University of Wisconsin-Milwaukee 3200 N. Cramer St. Milwaukee, WI 53211		10. **Work Unit No. (TRAIS)** 11. **Contract or Grant No.** WHRP 0092-11-02
12. **Sponsoring Agency Name and Address** Wisconsin Highway Research Program Wisconsin Department of Transportation WisDOT Research & Library Unit 4805 Sheboygan Avenue, Room 104 P.O. Box 7915 Madison, WI 53707		13. **Type of Report and Period Covered** Final Report, 10/2010 – 12/2012 14. **Sponsoring Agency Code**
15. **Supplementary Notes**		

16. **Abstract**

The objective of this research is to establish the technical engineering and cost analysis concepts that will enable WisDOT management to objectively evaluate the feasibility of switching construction specification philosophies for aggregate base. In order to accomplish this goal, field and laboratory testing programs were conducted on existing HMA pavements and on base layers under construction as well as comprehensive survey was conducted on highway agencies practices pertaining to base layer construction in the U.S. and Canada. This research proposed construction specifications for aggregate base course layers.

The existing HMA pavements that showed early distresses exhibited high levels of spatial variability and non-uniformity in aggregate base course layers, as demonstrated by FWD testing and backcalculated base layer modulus. The existing HMA pavements that performed well exhibited low levels of spatial variability and high uniformity in aggregate base course layers, as shown by the FWD test results and the backcalculated base layer modulus.

High spatial variability in field density and moisture content exists in base course layers under construction, as demonstrated by the relative compaction test results. In addition, spatial variability and non-uniformity were also demonstrated by the results of the Light Weight Deflectometer (LWD) and GeoGauge, in which the layer modulus varies within a large range of values.

17. **Key Words** Aggregate base layer, base construction specifications, FWD, HMA pavement, QC/QA, LWD, density-based specifications, modulus-based specifications, DARWin-ME		18. **Distribution Statement** No restriction. This document is available to the public through the National Technical Information Service 5285 Port Royal Road Springfield VA 22161	
19. **Security Classif.(of this report)** Unclassified	19. **Security Classif. (of this page)** Unclassified	20. **No. of Pages** 127	21. **Price**

Form DOT F 1700.7 (8-72) Reproduction of completed page authorized

Acknowledgements

This research project is financially supported by Wisconsin Highway Research Program (WHRP)–Wisconsin Department of Transportation (WisDOT).

The authors acknowledge the help, support, and guidance provided by the POC members: Scot Schwandt, Judith Ryan, and Tom Brokaw.

The authors acknowledge the help of the Barry Paye in identifying number of the base layer construction projects. The help and support of the project engineers at various locations is greatly acknowledged, namely, Paul D. Piccione, Bloom Companies (STH 33); Bill Niemi, Bloom Companies (I-90/94/39), Jason Schrandt, Strand Associates, Inc. (USH 12); Ryan Erkkila, Coleman Engineering (USH 141); Bryan Lampshire, Graef (CTH JJ), Robert Anderson, Gremmer Associates (USH 45–CTH I), Lucas Budden, WisDOT-NW Region (CTH B).

The authors also acknowledge the work conducted in the field and lab by UW-Milwaukee graduate and undergraduate students: Issam Qamhia, Vahid Alizadeh, Vince Difrances, Mohammed Aljuboori, and Benjamin Roberts.

The help and contribution of Jay Schabelski, Romus Inc., is gratefully acknowledged.

The authors thank Ed Hall, Humboldt Inc., for donating the GeoGauge during field testing. The LWD was leased from Dynatest International; the help provided by Gary Mitchell to facilitate the lease of the LWD is appreciated. FWD testing was conducted by ERI International of Savoy, IL. The help of Abas Butt is appreciated.

The help of Dr. Aaron Coenen during FWD field testing is appreciated.

The authors thank John Siekmeier, Mn/DOT for his help with regard to Mn/DOT practices and research experience on base course layers construction.

The authors thank Nayyar Siddiki, Indiana DOT, for his help with regard to Indiana DOT practices and research experience on base course layers construction.

The authors also thank Michelle Schoenecker, Senior Technical Grant Writer at UW-Milwaukee, for reviewing and editing the manuscript.

Table of Contents

List of Figures

List of Tables

Chapter 1
Introduction

1.1 Problem Statement

For approximately the last fifteen years, Wisconsin Department of Transportation (WisDOT) construction specifications have been transitioning from “method” specifications to “performance” specifications; however, WisDOT’s base aggregates specifications have not yet made that transition. These specifications rely on construction method terms such as “Standard Compaction” to provide contractors and department construction managers and inspectors with the necessary guidance and acceptance measures to construct good-performing, quality aggregate bases. However, review of the “Standard Compaction” description reveals the use of ambiguous and rather subjective terminology such as “appreciable displacement.” WisDOT SS 301 also uses terms such as “soft” and “spongy” to identify adequate foundation preparation prior to base aggregate placement. As a result, such ambiguous terminology leads to accepted base layers that exhibit variable stiffness values that contribute to hot mix asphalt (HMA) pavement performance issues.

Flexible pavement design includes unbound granular layers (as defined by WisDOT SS 305) as part of the overall pavement structure. Pavement designers could increase the cost-effectiveness of a pavement if the engineering properties of a given pavement material are more consistent and correlated with *specification performance criteria*. A base aggregate specification that is based on the performance criteria for compaction will improve pavement structural designs and reduce the construction costs and delays arising from base failures during construction.

Many other state highway agencies are using performance-based specifications for base aggregates—what is the feasibility for WisDOT to transition to this type of specification in order to realize greater cost savings related to HMA expenditures and resultant pavement performance?

1.2 Research Objectives

The proposed research will establish the technical engineering and cost analysis that will enable WisDOT management to objectively evaluate the feasibility of switching specification philosophies for base aggregate materials. This research will also provide technical recommendations for a proposed performance-based base aggregate specification. This performance-based specification should use performance criteria in terms of a minimum and uniform stiffness measurement parameter consistent with modern technology and mechanistic-empirical pavement design guide (MEPDG) pavement design input parameters. Furthermore, these criteria should be consistent with other pavement layer performance-based specifications.

1.3 Background

To achieve long-lasting constructed pavements with minimized distress levels and good ride quality, controlling the construction quality of the unbound granular base layers is critical. Different methods are available for quality control and quality assurance (QC/QA) of constructed aggregate base course layers. These methods are based on different concepts/theories and include density-based and modulus-based methods. Some of these methods achieve QC/QA by performing spot-test evaluations or by continuous characterization of the base course layer. Spot-test evaluations are usually conducted based on in-place density measurements, which is not a load-bearing indicator. The majority of state highway agency specifications require the laboratory compaction test (e.g., AASHTO T 99 or T 180) to determine a target density (the maximum dry unit weight) as a basis for the QC/QA of compacted aggregate base layers. Moreover, spot-test methods include the modulus-based methods using portable devices such as the light weight deflectometer (LWD), dynamic cone penetrometer (DCP) and GeoGauge. Continuous monitoring of the constructed aggregate base layers quality can also be achieved using the intelligent compaction technique.

While spot-test and continuous measurements are being used in various capacities, observation and personal judgment is still used by four highway agencies in the U.S., including Wisconsin. This practice employs subjective terminology such as “appreciable displacement” to judge the quality of constructed base layers—thus, the determination of a well-compacted base is left to the judgment of field engineers. Such methods may not lead to uniformly constructed base course layers, potentially leading to distressed pavements and early deterioration. Therefore, the objective of the QC/QA is to ensure the construction of high-quality, good-performing, and long-lasting pavements. This is achieved through quality acceptance (QA) by QC/QA procedures and specifications through laboratory and field tests and measurements on unbound base materials and constructed base layers.

1.4 Organization of the Report

This report is organized in seven chapters. Chapter One introduces the problem statement and objective of the research. The literature review and synthesis is presented in Chapter Two, and the research methodology is discussed in Chapter Three. Chapters Four and Five present a detailed analysis for field and laboratory testing programs with critical analysis of the outcome. A framework for base layer construction specifications is presented in Chapter Six. The conclusions and recommendations are provided in Chapter Seven.

Chapter 2
Background

This chapter presents a synthesis of the literature review conducted on the characterization of unbound granular materials (aggregates) in base course layers and their influence on flexible pavement performance. Laboratory and field methods of testing unbound materials and constructed unbound base layers are discussed, and methods of quality acceptance (QA) of constructed unbound base course layers are emphasized. In addition, the current state of practice with regard to the QA of constructed unbound base layers is presented through a detailed survey of state highway agencies in the U.S. and Canada.

2.1 Significance of Unbound Base Layers for Pavement Performance

The use of unbound aggregates as base course layers in the construction of flexible pavements is common practice in the U.S. and around the world. Unbound base layers function by supporting traffic load from the asphalt concrete surface layer and dissipating and transferring such load to the underlying pavement layer or subgrade. Therefore, the unbound aggregate layers comprise a significant intermediate component in pavement stability and performance.

Performance of unbound aggregate materials in base course layers depends on the characteristics/properties of the individual aggregate particles and the interaction behavior of group of particles associated/aggregated in matrix (e.g., in base course layer). The importance of the individual particle properties comes from its influence on the group behavior within the matrix. Particle properties include (1) particle size, (2) particle shape, (3) particle texture, (4) particle angularity, (5) particle durability, (6) specific gravity, (7) absorption, (8) particle toughness, and (9) particle mineralogical composition. Properties of aggregate within matrix (such as base layer) include: (1) shear strength, (2) stiffness, (3) density, (4) resistance to permanent deformation, (5) permeability, and (6) frost susceptibility (Saeed et al. 2001).

The individual characteristics of aggregate particles (e.g., shape, angularity, texture) define their ability for interlocking behavior in a packed matrix, such as in base course layers, to provide the desirable structural stability to support traffic loads. Proper construction of aggregate base layers will produce densely packed materials with good interlocking among the particles, leading to increased shear strength and stability and decreased permanent deformation as the void space between particles is minimized. A lack of stability in the base course layers results in the lateral movement of aggregates, thereby causing pavement distress (Barksdale, 2001).

As previously described, the particle and matrix properties of aggregate particles and unbound base layers influence the performance of flexible pavements. Within the context of appropriate construction of these layers, the pavements are expected to perform very well;

however, poor and inadequate construction of base course layers can lead to poor pavement performance and early distress and deterioration. Flexible pavement distresses such as fatigue cracking, rutting/corrugations, depressions, and frost heave can be attributed to the poor performance of unbound aggregate base course layers (Saeed et al., 2001). Table 2.1 summarizes distresses of flexible pavements attributed to the poor performance of unbound base layers, and the base layers' contributing factors to such distresses.

Saeed et al. (2001) discussed the distresses (presented in Table 2.1) that are attributed to the poor performance of unbound base course layers. Below is a description of these distresses: Fatigue cracking occurs in areas subjected to repeated traffic loading. Cracking starts as fine, longitudinal hairline cracks running parallel to one another in the wheel path. High flexibility in the aggregate base allows excessive bending strains in the asphalt concrete surface. The same result can also be caused by inadequate thickness of the aggregate base. Changes in the base properties with time can render the base inadequate to support loads. The contributing factors to fatigue cracking related to the base layer are: (a) low elastic modulus of the base layer, (b) improper gradation, (c) high fines content, (d) high moisture levels, (e) lack of adequate particle angularity and surface texture (poor interlocking), and (f) degradation under repeated loads and freeze-thaw cycling.

Rutting results from permanent deformation in one or more layers or at the subgrade, usually caused by consolidation and/or lateral movement of the material due to load. Rutting appears as a longitudinal surface depression in the wheel path and may not be noticeable, except during and following rainfall. Inadequate shear strength in the base allows lateral displacement of particles with applications of wheel loads, causing a decrease in the base layer thickness in the wheel path. Inadequate density causes settlement of the base. The contributing factors to rutting are: (a) low shear strength of aggregate base, (b) inadequate compaction, as illustrated by low density, (c) improper gradation, (d) high fines content, (e) high moisture levels, (f) lack of adequate particle angularity and surface texture, and (g) degradation under repeated loads and freeze-thaw cycling.

Depressions are caused by inadequate initial compaction or non-uniform material conditions, which further reduce the volume with load applications. Depressions differ from rutting because they are localized deformations that are bound to specific area. Because they occur at a location where the pavement foundation is "soft" (i.e., under-compacted or cannot be compacted to target density). The contributing factors to this distress are: (a) low density of base material, and (b) weak foundation.

Frost heave appears as an upward bulge in the pavement surface and may be accompanied by surface cracking, including alligator cracking with resulting potholes. Ice lenses are created within the base/subbase during freezing temperatures as moisture is pulled from below by capillary action. During spring thaw, large quantities of water are released from the

Table 2.1: Flexible pavement distresses and contributing factors (Saeed et al. 2001).

Distress	**Description of Distress**	**Base Failure Manifestation**	**Contributing Factors**
Fatigue Cracking	Fatigue cracking first appears as fine, longitudinal hairline cracks running parallel to one another in the wheel path and in the direction of traffic; as the progresses the cracks will interconnect, forming many-sided, sharp angled pieces (resulting in the commonly termed "alligator cracking"); eventually cracks become wider, and in later stages some spalling occurs with loose pieces prevalent. Fatigue cracking occurs only in areas subjected to repeated traffic loading.	Lack of base stiffness causes high deflection/strain in the asphalt concrete surface under repeated wheel distress loads, resulting in fatigue cracking of the asphalt concrete surface. Alligator cracking only occurs in areas where repeated wheel loads are applied. High flexibility in the base allows excessive bending strains in the asphalt concrete surface. The same result can also be caused by inadequate thickness of the base. Changes in the base properties with time can render the base to support loads.	Low modulus base Improper gradation High fines content High moisture level Lack of adequate particle angularity and surface texture Degradation under repeated loads and freeze-thaw cycling
Rutting	Rutting appears as a longitudinal surface depression in the wheel path and may not be noticeable, except during and following rains. Pavement uplift may occur along the sides of the rut. Rutting results from a permanent deformation in one or more pavement layers or subgrade, usually caused by consolidation and/or lateral movement of the materials due to load.	Inadequate shear strength in the base allows lateral displacement of particles with applications of wheel loads and results in a decrease in the base layer thickness in the wheel path. Rutting may also result from consolidation of the base due to inadequate initial density. Changes in base properties with time due to poor durability or frost effects can result in rutting.	Low shear strength Low density of base material Improper gradation High fines content High moisture level Lack of adequate particle angularity and surface texture Degradation under repeated loads and freeze-thaw cycling
Depressions	Depressions are localized low areas in the pavement surface caused by settlement of the foundation soil or consolidation in the subgrade or base/subbase layers due to improper compaction. Depressions can contribute to roughness and can cause hydroplaning when filled with water.	Inadequate initial compaction or nonuniform material conditions result in additional reduction in volume with load applications. Changes in material conditions due to poor durability or frost effects may also result in localized densification with eventual fatigue failure.	Low density of base material
Frost Heave	Frost heave appears as an upward bulge in the pavement surface and may be accompanied by surface cracking, including alligator cracking with resulting potholes. Freezing of underlying layers resulting in an increased volume of material cause the upheaval. An advanced stage of the distortion mode of distress resulting from differential heave is surface cracking with random orientation and spacing.	Ice lenses are created within the base/subbase during freezing temperatures, particularly when freezing occurs slowly, as moisture is pulled from below by capillary action. During spring thaw, large quantities of water are released from the frozen zone, which can include all unbound materials.	Freezing temperatures Source of water Permeability of material high enough to allow free moisture movement to the freezing zone

frozen zone, which can include all unbound materials. The contributing factors to this distress are: (a) freezing temperatures, (b) source of water, (c) and permeability of material high enough to allow free moisture movement to the freezing zone.

2.1.1 Characterization of Aggregate Particle Properties

The aggregates particle properties/characteristics that are important for the performance of aggregate layers and how they are determined by laboratory tests are discussed here in detail. The aggregate handbook (Barksdale, 2001) provides a detailed description of aggregate properties, as well as quantification tests. NCHRP Project 4-23, "Performance-Related Tests of Aggregates for Use in Unbound Pavement Layers (NCHRP Report 453)," summarized the most important tests that relate to the performance of aggregates in unbound pavement layers.

Gradation (Particle Size Distribution) is the distribution of different aggregate particles by size. Well-graded aggregates indicate good strength of the mixture despite the application. The particle size distribution that allows for the maximum amount of aggregate to be included in a unit volume of mixture can be considered the optimum gradation for most construction applications.

Particle Shape is the shape of the individual aggregate particles. Desired aggregates for an unbound aggregate base are angular, cubical particles for developing aggregate interlock, which increases the shear strength of the base layer.

Particle Texture is the degree of roughness or irregularity of the surface of an aggregate particle. The use of rough aggregates will increase the strength of an unbound aggregate base.

Toughness is the resistance to fracture from impact, and it is closely related to the absence of brittleness.

Particle Strength is the magnitude of the tensile and/or compressive stress that an individual aggregate particle can withstand before failure occurs. Determining the strength of individual aggregate particles is difficult because the particles have varying sizes and shapes.

Particle Stiffness is the resistance of an aggregate particle to deformation, as usually indicated by the modulus of elasticity of the particle. A high degree of stiffness is preferred for most construction applications.

Permeability is defined as the capacity of an aggregate particle, or group of particles, to transmit a fluid. The grading and density of the mixture of aggregate particles determines the overall permeability of a group of particles. The coefficient of permeability of unbound aggregate materials ranges from 0.001 to 100,000 ft/day (Saeed et al., 2001).

Frost Susceptibility is associated with aggregate resistance to freeze-thaw, and this is defined as the ability of an aggregate to resist deterioration due to cyclic freezing and thawing. When some types of aggregates are wet and subjected to freeze-thaw cycles, general flaking and cracking can occur. The resistance to freeze-thaw is influenced by the volume and size of accessible pores in the aggregate.

Various test methods are available to evaluate the properties of unbound granular materials and how these properties influence pavement performance in terms of distresses, structural stability, and ride quality. Table 2.2 describes the relationship between aggregate properties/test and pavement-performance parameters.

Table 2.2: Relationship between aggregate properties and pavement-performance parameters (after Saeed et al. 2001).

Pavement Type	Performance Parameter	Related Aggregate Property	Test Parameters that May Relate to Performance
Flexible	Fatigue Cracking	Stiffness	Resilient modulus, Poisson's ratio, gradation, fines content, particle angularity and surface texture, frost susceptibility, degradation of particles, density
	Rutting Corrugations	Shear Strength	Failure stress, angle of internal friction, cohesion, gradation, fines content, particle geometrics (texture, shape, angularity), density, moisture effects
	Fatigue Cracking, Rutting, Corrugations	Toughness	Particle strength, particle degradation, particle size, gradation, high fines
		Durability	Particle deterioration, strength loss
		Frost Susceptibility	Permeability, gradation, percent minus 0.02 mm size, density, fines type
		Permeability	Gradation, fines content, density

The following tests are conducted on aggregates to assess their performance in base course layers (Table 2.3):

Screening Tests:

i. ***Sieve Analysis:*** Gradation is used to indicate permeability, frost susceptibility, and shear strength. Test methods: AASHTO T 2: Standard Method of Test for Sampling of Aggregates, AASHTO T 11: Standard Method of Test for Materials Finer than 75-µm (No. 200) Sieve in Mineral Aggregates by Washing, and AASHTO T 27: Standard Method of Test for Sieve Analysis of Fine and Coarse Aggregates.

ii. ***Atterberg Limits:*** Ensures that fine materials will have the correct amount of shear strength and not too much change in volume as it expands and shrinks with different moisture contents. Liquid Limit (LL) of aggregate fraction passing sieve # 40 (0.425-mm) is determined using standard test procedure AASHTO T 89; plastic limit (PL) is determined using AASHTO T 90 test procedure. Test methods: AASHTO T 89: Standard

Method of Test for Determining the Liquid Limit of Soils, and AASHTO T 90: Standard Method of Test for Determining the Plastic Limit and Plasticity Index of Soils.

iii. ***Moisture-Density Relationship:*** Compaction of aggregate materials generally increases density, shear strength, and stiffness, and decreasing permeability with increasing moisture content prior to a point of maximum density beyond which the trends reverse. Test methods: AASHTO T 99: Standard Method of Test for Moisture-Density Relations of Soils Using a 2.5-kg (5.5-lb) Rammer and a 305-mm (12-in.) Drop and AASHTO T 180 Standard Method of Test for Moisture-Density Relations of Soils Using a 4.54-kg (10-lb) Rammer and a 457-mm (18-in.) Drop.

iv. ***Specific Gravity:*** Known as the ratio of the mass of a given volume of aggregate solids to the mass of an equal volume of water. A high specific gravity provides stability to the system without requiring increased layer thickness or increased track cross-section. Test methods: AASHTO T 84: Specific Gravity and Absorption of Fine Aggregate and AASHTO T 85: Specific Gravity and Absorption of Coarse Aggregate.

v. ***Absorption:*** Indicates the ability of aggregates to retain moisture due to porosity. Particles with high absorption are less durable and may experience freeze-thaw and soundness problems. Test methods: AASHTO T 84: Specific Gravity and Absorption of Fine Aggregate and AASHTO T 85: Specific Gravity and Absorption of Coarse Aggregate.

vi. ***Flat and Elongated Particles:*** Can break under compaction and change gradation. An excess of these particles may interfere with compaction and consolidation. Standard test: ASTM D4791: Standard Test Method for Flat Particles, Elongated Particles, or Flat and Elongated Particles in Coarse Aggregate.

vii. ***Uncompacted Voids:*** Provides a good overall indicator of the potential for resisting permanent deformation and it is a function of particle shape, angularity, and surface texture. Test methods: AASHTO TP 33: Standard Test Method for Uncompacted Void Content of Fine Aggregate (as Influenced by Particle Shape, Surface Texture and Grading) and ASTM C1252: Standard Test Methods for Uncompacted Void Content of Fine Aggregate (as Influenced by Particle Shape, Surface Texture, and Grading).

Durability

i. ***Magnesium or Sodium Sulfate Soundness***: Estimates aggregates' resistance to weathering. Test method: AASHTO T 104: Soundness of Aggregate by Use of Sodium or Magnesium Sulfate.

ii. ***Unconfined Freeze-Thaw Test:*** Test method: AASHTO T 103 Standard Method of Test for Soundness of Aggregates by Freezing and Thawing.

Shear Strength Tests

i. ***Shear Strength:*** Considered as the most important aggregate property that affects the performance of unbound base layers. The static triaxial test is the most common test to measure shear strength. Test methods: AASHTO T 296: Standard Method of Test for Unconsolidated, Undrained Compressive Strength of Cohesive Soils in Triaxial Compression.

ii. ***California Bearing Ratio (CBR)***: is a comparative measure of the shearing resistance of aggregate and it is a widely used method, as a strength parameter, of pavement structures. Test method: AASHTO T 193: Standard Method of Test for The California Bearing Ratio.

Stiffness

i. ***Resilient Modulus:*** The elastic modulus based on the recoverable strain under repeated loads. Test method: AASHTO T 307: Standard Method of Test for Determining the Resilient Modulus of Soils and Aggregate Materials.

Toughness and Abrasion Resistance

i. ***Micro-Deval Test:*** Indicates the potential of an aggregate to degrade. Test method: AASHTO T 327: Standard Method of Test for Resistance of Coarse Aggregate to Degradation by Abrasion in the Micro-Deval Apparatus.

ii. ***Los Angeles Abrasion.*** Test method: AASHTO T 96: Standard Method of Test for Resistance to Degradation of Small-Size Coarse Aggregate by Abrasion and Impact in the Los Angeles Machine.

Frost Susceptibility

i. ***Tube Suction Test:*** Measures the amount of free water that exists within an aggregate sample.

2.2 Factors Affecting Construction/Compaction of Aggregate in Base Layer

Construction of aggregate base course layers consists of placing/spreading the aggregate materials in lifts of determined thickness and the subsequent compaction, under specified moisture content, using rollers. Compaction is defined as the process of densification of aggregate materials by reducing void space between aggregate particles through the application of mechanical energy. Water acts as lubricant in the compaction, because it facilitates the relative movement/reorientation of aggregate particles and sliding to achieve a more packed state of aggregation. Compaction leads to a dense state of compactness (dense aggregate matrix) with strong particle-to-particle interlocking/interaction, which affects the performance of the aggregate base layers in terms of: (1) reducing deformation/settlements, (2) increasing the shear strength and thus providing structural stability, (3) improving the bearing capacity of granular base layers, and (4) controlling undesirable volume change caused by frost action, swelling, and shrinkage (Holtz, 1990).

Table 2.3: Selected aggregate characterization tests (After Saeed et al., 2001)

Aggregate Property	Test Method	Test Reference	Test Parameter
Screening Tests	Sieve Analysis	T 27, T 11[a]	Particle Size Distribution
	Atterberg Limits	T 89, T 90[a]	PL, LL, PI
	Specific Gravity and Absorption	T 84, T 85[a]	Specific Gravity
	Moisture/Density Relationship	T 99, T 180[a]	Maximum Dry Density
	Flat and Elongated Particles	D 4971[b]	F or E, F, and E
	Uncompacted Void Content	TP 33[a]	Percent Uncompacted void
	Shape and Texture	D 3398[b]	Particle shape and texture index
Shear Strength	Static Triaxial Shear	T 296[a]	C, ϕ, shear strength
	Repeated Load Triaxial		Deviator stress
	California Bearing Ratio	T 193[a]	CBR
Stiffness	Repeated Load Triaxial	**	Resilient modulus
Frost Susceptibility	Tube Suction Test	*	Dielectric constant
	Index Method	*	F categories
Toughness and Abrasion	Los Angeles Abrasion	C 131[b]	%loss, passing #12 sieve
	Aggregate Impact Value	BS 812[c]	% loss, passing BS 2.40 mm sieve
	Aggregate Crushing Value	BS 812[c]	% loss, passing BS 2.40 mm sieve
	Micro-Deval Test	TP 58-99[a]	% loss, passing #16 sieve
	Gyratory Degradation		Before and after gradation
Durability	Sulfate Soundness	T 104[a]	Weighted average loss
	Aggregate Durability Index	T 210, T 176[a]	Durability index

a: AASHTO reference test method

b: ASTM reference test method

c: British reference test method

*: No test method is currently available

**: Test method is developed in this research

According to the Manual for Highway Construction (AASHTO, 1990), the factors that affect compaction include moisture content, gradation, and compaction effort. Molenaar and Niekerk (2002) studied the influence of gradation, composition, and degree of compaction on the mechanical characteristics of unbound base course materials made from recycled concrete and masonry. The researchers investigated the influence of these factors at a range of degrees of compaction, as estimated by the single point Proctor density (SPPD). They concluded that the degree of compaction has the largest influence on the resilient characteristics (stiffness), the resistance to permanent deformation, and on the cohesion of the material. The gradation with a large number of fines appeared to have the highest cohesion.

Laboratory aggregate compaction tests, used to establish target density for field evaluation of compaction, are based on impact/dropped load (AASHTO T 99, AASHTO T 180, ASTM D698 and ASTM D1557). Adu-Osei et al. (2000) indicated that vibratory and gyratory laboratory compaction procedures are considered more realistic for providing both adequate modulus and strength in laboratory compacted samples, and for simulating properly field loading and applied stress conditions under vibratory rollers. The use of vibratory compaction for establishing the compaction characteristics of granular soils is covered under ASTM D7382, no such specification is provided by AASHTO (Tutumluer, 2012).

Kaya et al. (2012) compared the effects of impact compaction and vibratory compaction on the mechanical behavior of unbound aggregate base materials. Comparing the gradation of aggregate specimens before and after compaction, they observed that impact compaction caused a change in aggregate gradation through crushing and particle breakage. This ultimately increased the optimum moisture content value. No such particle crushing and resulting change in gradation were observed for specimens prepared using the vibratory compaction method. Although the vibratory compaction method resulted in higher CBR values, the resilient modulus values for specimens prepared using impact compaction were consistently higher, except for one aggregate type (Tutumluer, 2012).

Holubec (1969) found that increased density improves the properties of unbound aggregates with angular particles more than for aggregates with rounded particles, provided there is no increase in the pore pressure during repetitive loading. Generally, increasing the density of a granular material makes the aggregate layer stiffer and reduces the magnitude of the resilient and permanent deformation response to both static and dynamic loads (Seyhan and Tutumluer, 2002).

Particle size distribution and the amount of fines are important factors in achieving a dense state of compactness in aggregate base layers. Arnold et al. (2007) conducted a study on one aggregate source at different gradations to optimize gradation for maximum rut resistance using the repeated load triaxial test. The results showed that the grading envelope found from this study is very tight, indicating that optimum gradation can be achieved with minimal tolerance. In addition, the study found that fine gradation has a lower strength when wet compared with coarse gradation, while the opposite is the case when dry. Furthermore, finer gradations were found to be constructed with less segregation and lower total voids to minimize any further densification after opening a pavement to traffic. Arnold et al. (2007) offered acceptable range of variation of each particle size for the gradations studies to optimize rutting resistance as measured by the repeated axial load test. The particle sizes in Table 2.4 are represented in SI units.

Table 2.4: Recommended gradation envelope variations around a measured particle size distribution for the repeated triaxial loading sample (Arnold et al., 2007).

Sieve size (mm)	**Acceptable variation around measured particle size distribution (PSD).**
	%
37.50	-
19.00	±5
9.50	±5
4.75	±4
2.36	±3
1.18	the > of ±14% of the measured PSD or ±2
0.600	the > of ±14% of the measured PSD or ±1
0.300	the > of ±14% of the measured PSD or ±1
0.150	the > of ±14% of the measured PSD or ±1
0.075	the > of ±14% of the measured PSD or ±1

Arnold et al. (2007) also investigated multiple specifications in the world. A total of 12 countries' specifications were listed with respect to their gradation envelop. Figures 2.1 and 2.2 show the upper and lower gradation limits as presented by Arnold et al. (2007).

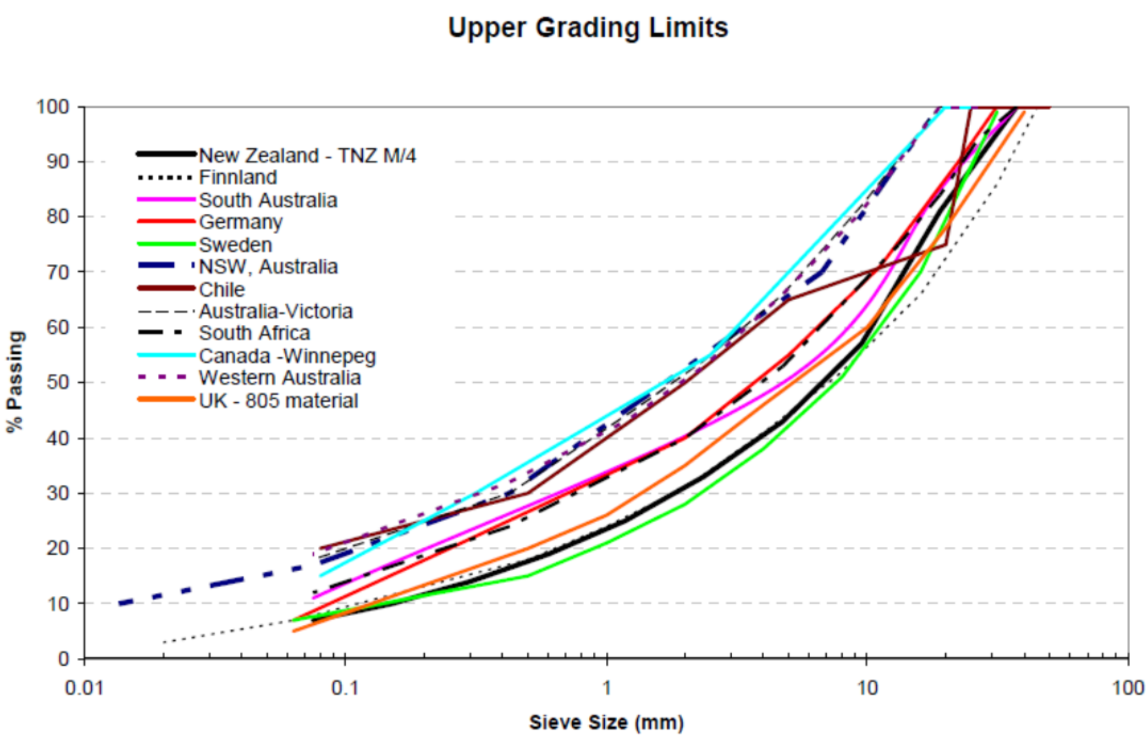

Figure 2.1: Upper gradation limits for base aggregate specifications in 12 countries (Arnold et al., 2007).

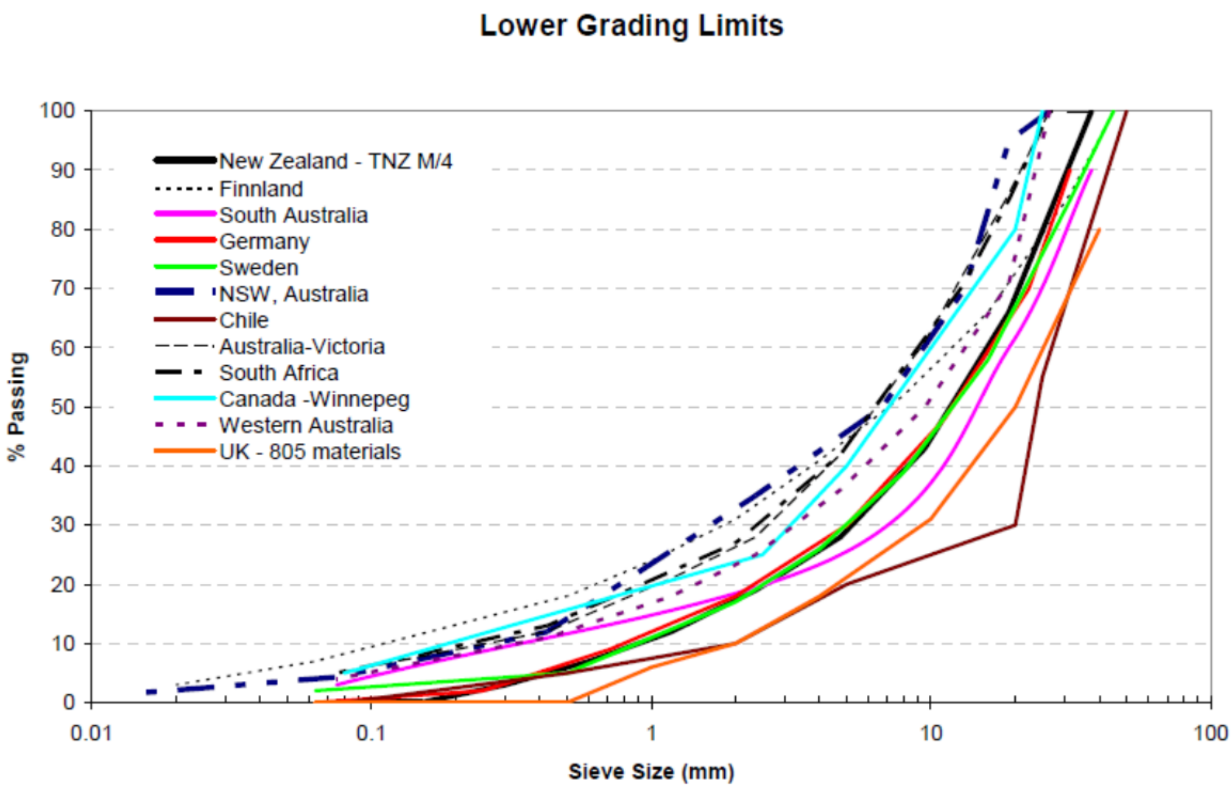

Figure 2.2: Lower gradation limits for base aggregate specifications in 12 countries (Arnold et al., 2007).

According to the following equation, the gradation power (*n*) is used to control the gradation type and packing:

$$p = 100\left(\frac{d}{D}\right)^{n} \tag{2.1}$$

Where:

p = percent passing sieve size d
D = maximum particle size and
n = number commonly has a range between 0.3 (fine grading) and 0.6 (coarse grading).

Lay (1984) proposed a value of *n* ranging from 0.45 and 0.50 as indicator for best packing. Belt et al. (1997) found that maximum resistance to permanent deformation can be achieved at *n*-value of 0.4. Bennert and Maher (2003) conducted a study on multiple aggregate sources and concluded that different materials perform differently with respect to gradation. In general the literature showed that well-graded base with fines exhibited higher mechanical stability with variations, depending on material type and physical parameters. This explains the high variability of gradation envelop ranges specified by the different countries shown in Figures 2.1 and 2.2, and in Table 2.5.

Moisture has adverse effects on the performance of unbound aggregate layers in pavement structures, and it can affect aggregates in three different ways: (1) make them stronger with capillary suction, (2) make them weaker by causing lubrication between the particles, and (3) reduce the effective stress between particle contact points due to increasing pore water pressure, thereby decreasing the strength (Tutumluer 2012).

Table 2.5: Ranges for *n*-values in the world (after Arnold et al., 2007).

	Lower limits (coarse side)	Upper limits (fine side)
New Zealand	0.61	0.4
Finland	0.38	0.38
Germany	0.58	0.33
South Australia	0.61	0.37
Sweden	0.55	0.47
United Kingdom	0.68	0.35
Chile	0.95	0.3
Canada	0.58	0.3
Australia-Victoria	0.5	0.3
Australia-Western Australia	0.57	0.3
South Africa	0.5	0.31

Tutumluer et al. (2009) compared relative impacts of molding (as-compacted) moisture content and plasticity of fines on the permanent deformation behavior of both crushed (dolomite) and uncrushed (gravel) aggregate materials with percent passing sieve #200 (P_{200}) = 12%. As shown in Figure 2.3, a drastic reduction in aggregate performance occurs when plastic fines are combined with increased molding moisture, i.e., compared permanent deformation of gravel at 110% of the optimum moisture content with plastic and non-plastic fines, as shown in Figure 2.3b.

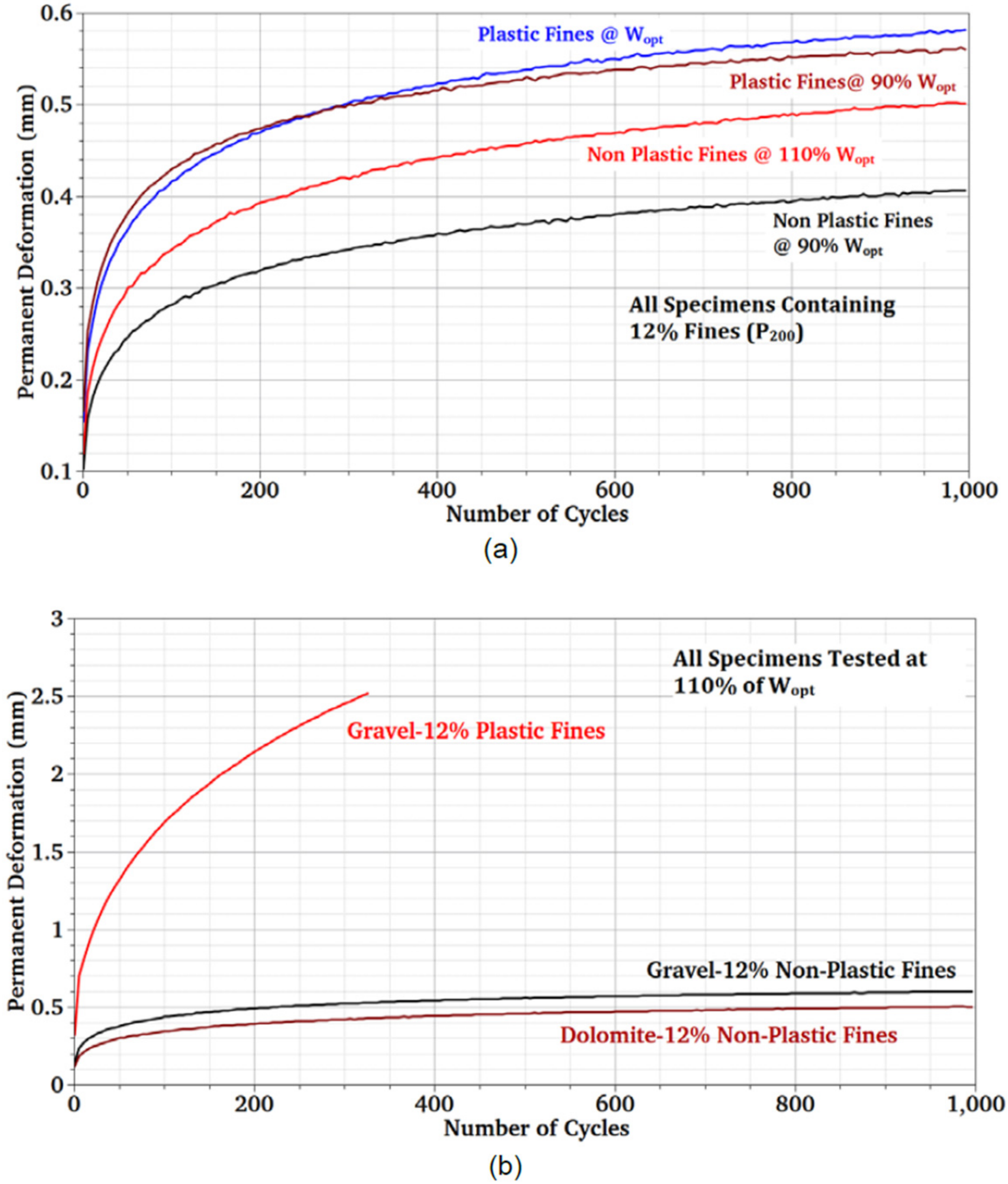

Figure 2.3: Relative effects of varying moisture content and the plasticity of fines on the permanent deformation behavior of crushed and uncrushed aggregates (Tutumluer et al., 2009).

2.3 Characterization of Unbound Granular Base Layers

To achieve long-lasting constructed pavements with minimized distress levels and good ride quality, it is highly important to control the construction quality of the unbound granular base layers. Different methods are available for the quality control and quality assurance (QC/QA) of constructed aggregate base course layers, which are based on different concepts/theories, including density-based and modulus-based methods. In addition, some of these methods achieve QC/QA by performing spot-test evaluations and others by continuous characterizing the base course layer. Spot-test evaluations are usually conducted based on in-place density measurements, which is not a load-bearing indicator. The majority of state highway agencies specifications require the laboratory compaction test (e.g., AASHTO T 99 and T 180) to determine a target density (the maximum dry unit weight) as basis for QC/QA of compacted aggregate base layers. Moreover, spot-test methods include the modulus-based methods using portable devices such as the light weight deflectometer (LWD), Dynamic Cone Penetrometer (DCP) and GeoGauge.

Continuous monitoring of the constructed aggregate base layers quality can also be achieved using the intelligent compaction technique. While spot-test and continuous measurements are being used in various capacities, observation and personal judgment is still used by four highway agencies in the U.S., including Wisconsin. This practice employs subjective terminology such as “appreciable displacement” to judge the quality of constructed base layers, which means that the determination of a well-compacted base is left to the judgment of field engineers. Such method may not lead to a uniformly constructed base course layers and therefore could lead to distressed pavements and early deterioration.

Therefore, the objective of QC/QA is to ensure that high-quality, good-performing and long-lasting pavements are constructed. This is conducted through quality acceptance (QA) by QC/QA procedures and specifications through laboratory and field tests and measurements on unbound base materials and constructed base layers, as described below.

2.3.1 Laboratory Methods

Currently, there are three well-known methods for pavement design: the Asphalt Institute (AI) method, the 1993 AASHTO method, and the AASHTO Mechanistic-Empirical Pavement Design Guide (MEPDG). The AASHTO 1993 design guide and the MEPDG use two important design input parameters for the material properties, Poisson’s ratio (ν) and the resilient modulus (M_R). Poisson’s ratio is defined as the ratio of the lateral strain to the axial strain of a given material. It has a relatively small effect on pavement responses; therefore, it is customary to assume a reasonable value for use in design. For untreated granular material, this value ranges between 0.30 and 0.40; a value of 0.35 is typically used (Huan, 1993).

Repeated Load Triaxial Test

This test is used to determine the resilient modulus under conditions simulating the physical conditions and stress states of pavement materials. The test is performed by applying a sequence of repeated or cyclic loads on compacted soils/aggregate specimens, simulating repeated traffic wheel loading. The AASHTO T 307 standard test method covers the procedures for preparing and testing untreated subgrade soils and untreated base/subbase materials for determining the resilient modulus. The unbound aggregate specimen is compacted using impact compaction or other methods in layers inside a 6-inch diameter mold. The density of the compacted specimen reflects the in-place wet density obtained in the field using AASHTO T 239 or T 191, with the moisture content of the laboratory-compacted specimen similar to the in-situ moisture content obtained in the field using AASHTO T 238.

If the in-situ moisture content or the in-place density values are not available, then the percentage of maximum dry density and the corresponding optimum moisture content by AASHTO T 99 or T 180 should be used. After proper compaction of the specimen is performed, it is mounted inside a triaxial chamber and confining pressure is applied. The testing is initiated with the application of conditioning load cycles, and then various levels of deviatoric stresses. The resilient modulus is determined by averaging the recoverable deformation of the last five deviatoric loading cycles at each confining pressure and deviatoric stress. The resilient modulus value at a confining pressure and deviatoric stress levels, corresponding with the unbound base layer location within the pavement system, is selected as the design value (AASHTO T 307).

The resilient modulus is the basic material property, which is defined as the elastic modulus based on the recoverable strain under repeated loads (Figure 2.4).

$$M_R = \frac{\sigma_d}{\varepsilon_r} \quad \textbf{(2.2)}$$

Where: σ_d = deviator stress, which is the axial stress in excess of the confining pressure in a triaxial compression test, and ε_r = elastic strain (recoverable).

This design input parameter is related to the stiffness and provides a way to characterize the pavement materials response under a variety of conditions and stress states, which simulate the conditions in a pavement subjected to moving/repeated wheels loads. This basic material characteristic property can be determined using established laboratory test protocols and evaluated in-situ either from nondestructive or intrusive tests.

Titi et al. (2012) conducted repeated load triaxial tests on crushed limestone aggregates from Wisconsin. The aggregate particles characteristics indicated good quality in terms of particle shape, angularity, and texture, as shown in Figure 4.5. In addition, the aggregates conform to particles size distribution specification limits (upper and lower limits of sizes and fine content) of Wisconsin DOT, as depicted in Figure 4.6.

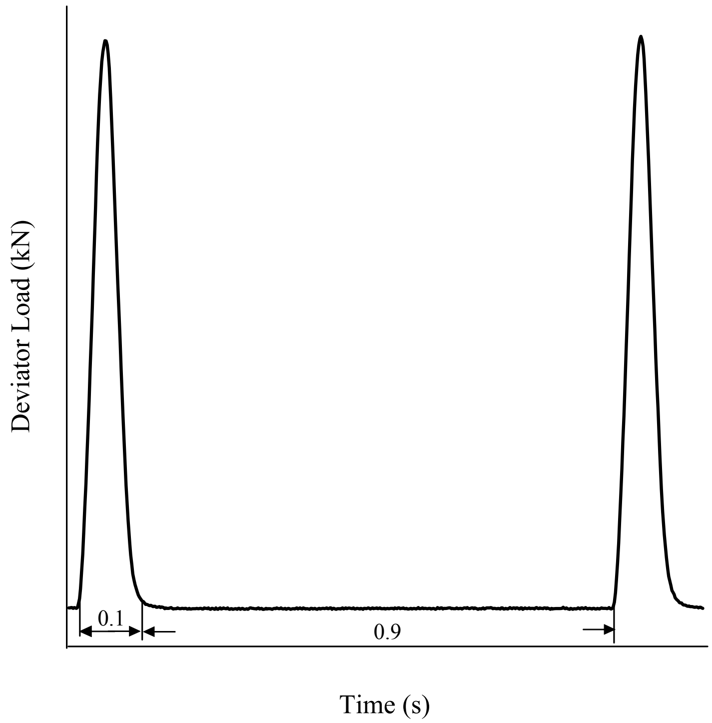

(a) Shape and duration of repeated load

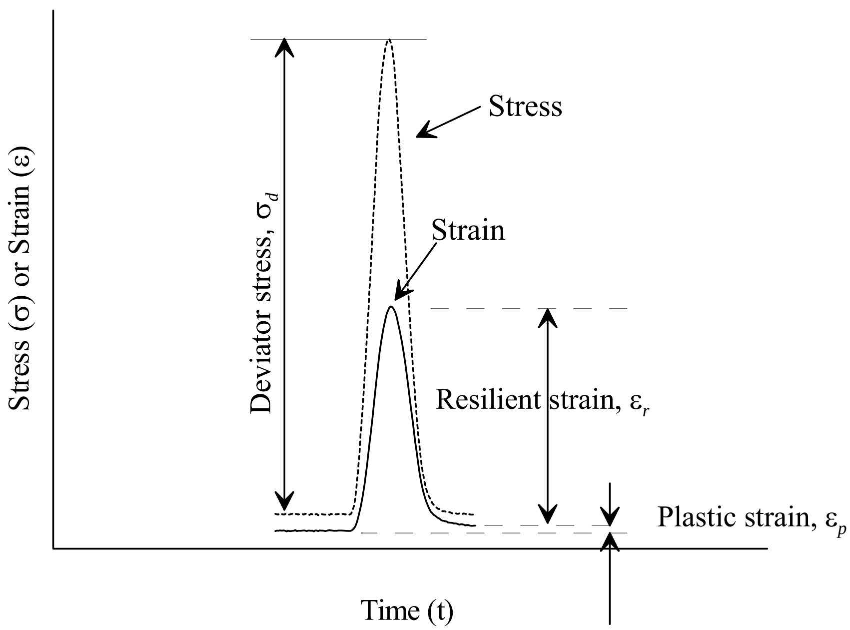

(b) Stresses and strains of one load cycle

Figure 2.4: Definition of the resilient modulus in a repeated load triaxial test (after Titi et al., 2004),

Figure 2.5: Typical crushed limestone aggregate from Wisconsin (Titi et al. 2012).

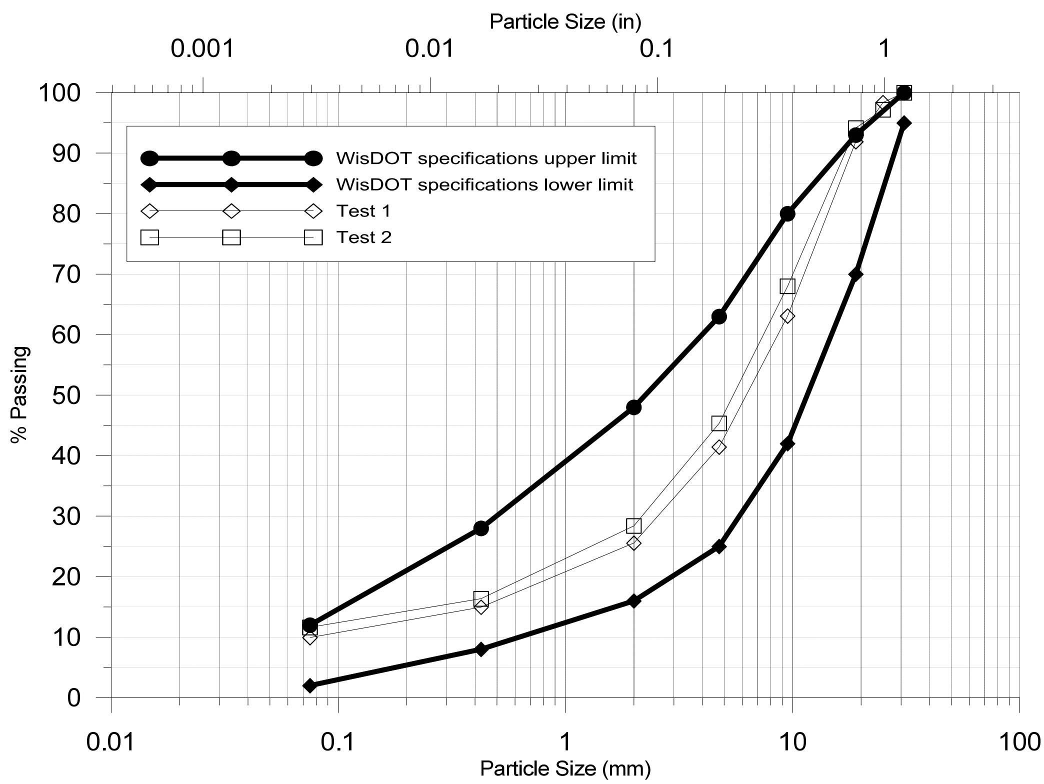

Figure 2.6: Particle size distribution for a typical limestone aggregate from Wisconsin (Titi et al., 2012).

The results of repeated load triaxial test on crushed aggregate are shown in Figure 2.7. The resilient modulus values of crushed aggregate increase with the increase of bulk stress, as well as with the increase of confining pressures indicated good interlocking of aggregates matrix. AASHTO T 307 produces a wide range of resilient modulus variation based on stress state. Von

Quintus et al. (2009) calculated a target resilient modulus of base aggregate at low confining pressure of 6 psi and deviator stress of 6 psi to reflect base layer modulus for comparison with field measurements. Applying this concept to the data presented in Figure 2.7, the typical resilient modulus value will be about (bulk stress = 24 psi) 18.5 ksi. Such value could be used to reflect the modulus of unbound aggregate layer compacted at maximum density and optimum moisture content.

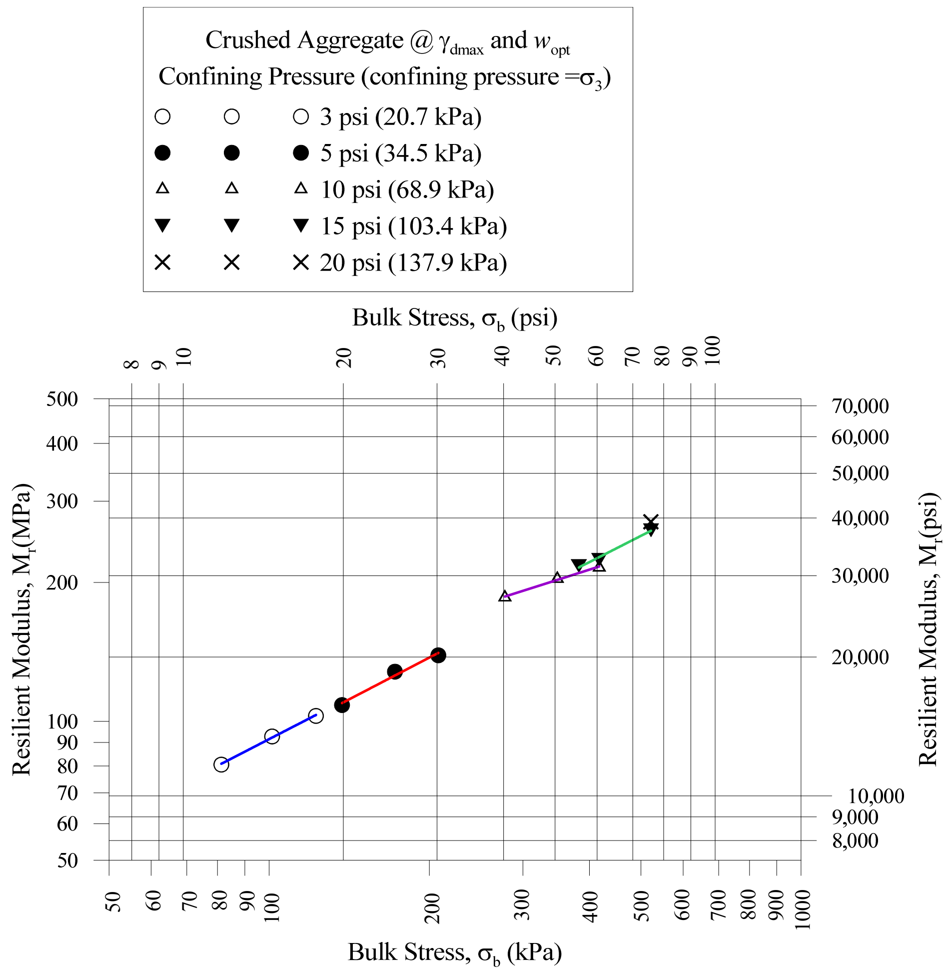

Figure 2.7: Resilient modulus test results for typical limestone aggregate at γ_{dmax} and w_{opt} (Titi et al., 2012).

Eggen and Brittnacher (2004) investigated the influences on the support strength of crushed aggregate base course due to gradational, regional, and source variations. They conducted testing to evaluate the resilient modulus of 37 aggregate sources in Wisconsin. The objective was to evaluate how variables, such as physical characteristics, material type, source lithology and regional factors influence the resilient modulus. The variation of resilient modulus with the bulk stress is presented in Figure 2.8. For a typical base course layer bulk stress level of 24 psi, the resilient modulus values vary between 11 and 22 ksi with an average values of 16.5 ksi. Eggen and Brittnacher (2004) concluded that that resilient modulus did not differ between and/gravel pit and quarry groups, and that carbonate quarries generally gave significantly higher resilient modulus values than Precambrian, felsic-plutonic quarries. They also stated that changing gradation of the base course from a given source affected resilient modulus test results, but not consistently or predictably. They also indicated that certain physical parameters were found to influence resilient modulus in some of the geologic subsets; however, none of the correlations were strong enough to predict resilient modulus with sufficient confidence.

California Bearing Ratio Test

The California Bearing Ratio (CBR) test is conducted according to AASHTO T 193 "Standard Method of Test for the California Bearing Ratio." The test is conducted by compacting aggregate in a 6 in. diameter mold to form a specimen 4.6 in. high, with maximum allowed particle size of 0.75 in. The test can be conducted on soaked or dry specimens. Soaked specimens are conditioned for 96 hours in water to simulate wet pavement conditions. The specimen is subjected to penetration of 3 in^2 area plunger at 0.05 in/minute. The CBR value is determined from the penetration pressure at 0.1 or 0.2 in. The standard crushed aggregate materials has a CBR of 100%, however, a high-quality, dense-graded crushed stone commonly has CBR values in excess of 80% (Tutumluer 2012).

2.3.2 Field Test Methods

Field test methods for characterizing aggregate base layers can be divided into nondestructive test (NDT) methods, and minimally intrusive and intrusive methods. There has been significant improvement in the NDT technologies for characterizing base course materials, including ground-penetrating radar (GPR), falling weight deflectometer (FWD), light weight deflectometer (LWD), GeoGauge, and penetration technology such as dynamic cone penetrometer (DCP). NCHRP synthesis 382 (Puppala 2008) and NCHRP report 626 (Von Quintus et al., 2009) provided detailed information and data on various technologies applicable for characterizing unbound aggregate base layers.

The importance of evaluating these technologies and their ability to characterize unbound aggregate base layers come from the new mechanistic-empirical pavement design (MEPDG), in which pavement layer modulus is a key material property required for designing new and rehabilitated flexible pavements. Implementation of mechanistic-empirical pavement design and availability of these NDT technologies for predicting pavement performance will help increase the use of such technologies (Von Quintus et al., 2009).

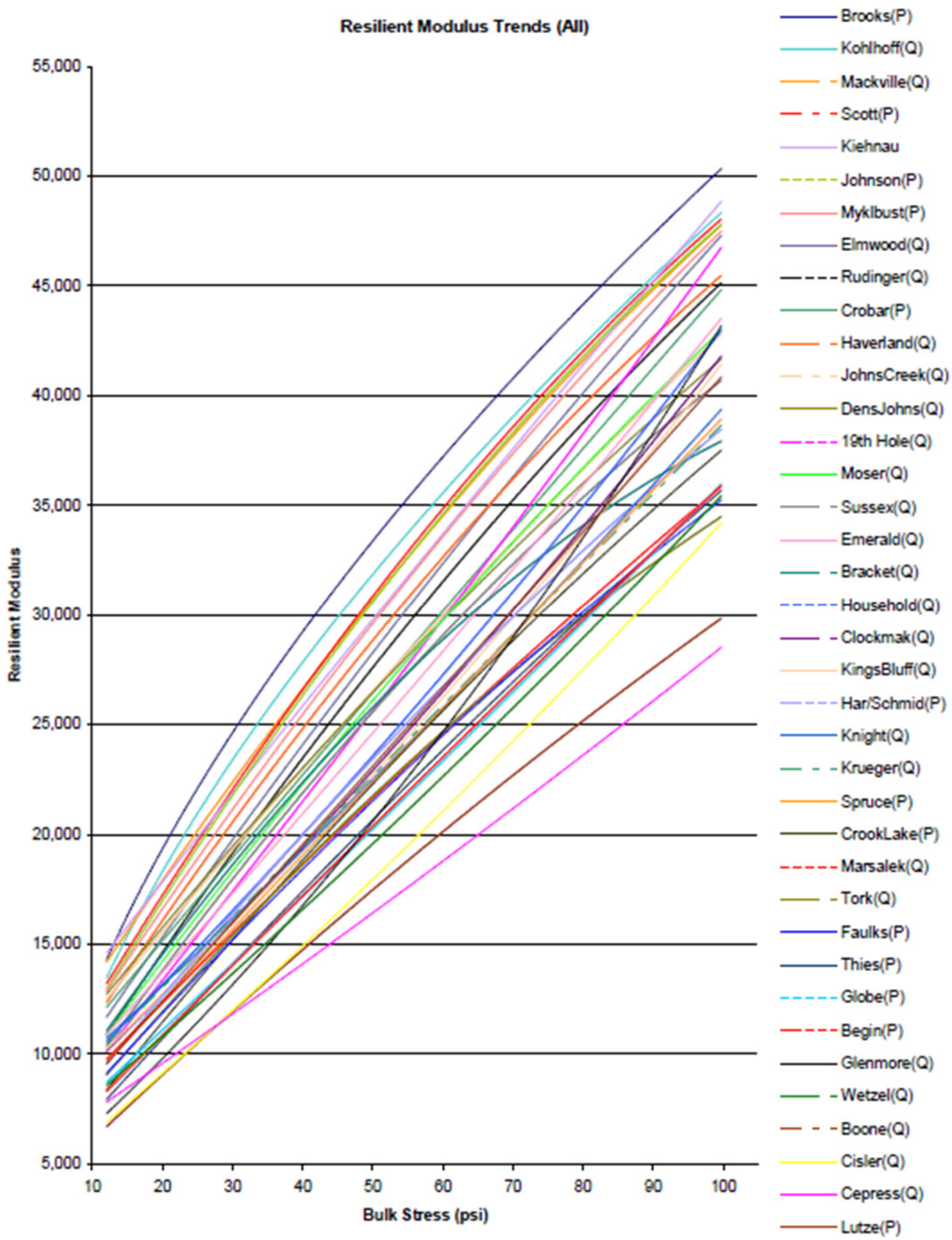

Figure 2.8: Resilient modulus values in psi (lb/in^2) for 37 Wisconsin aggregate samples (Eggen and Brittnacher, 2004).

Von Quintus et al. (2009) identified NDT technologies that are available for immediate implementation and routine use in QC/QA of constructed unbound aggregate layers. These technologies were identified based on their ability to recognize construction anomalies and to predict material properties indicative of pavement performance. Based on this, Von Quintus et al. (2009) recommended the GeoGauge for estimating the modulus of unbound layers for its readiness and ease of used for routine practice.

The layer thickness and modulus are needed structural properties for predicting pavement performance and are termed as quality characteristics as defined in the TRB circular E-C307 (Von Quintus et al., 2009). Methods and technologies used for characterizing the unbound aggregate base layers and materials for both structural design and mixture design (gradation) are summarized in Tables 2.6 and 2.7.

Table 2.6: Summary of material and layer properties used for design and acceptance of flexible pavements and HMA overlays (after Von Quintus et al., 2009).

Pavement Layer	Material-Layer Property		Property Needed For:		
			Structural Design	Mixture Design	Acceptance
HMA Layers; Dense-Graded Mixtures	Density – Air Voids at Construction		Yes	Yes	√
	Voids in Mineral Aggregate		Yes	Yes	√
	Effective Asphalt Binder Content		Yes	Yes	√
	Voids Filled with Asphalt			Yes	
	Gradation		Yes	Yes	√
	Asphalt Binder Properties		Yes	Yes	
	IDT Strength and Creep Compliance		Yes	Yes	
	Dynamic Modulus		Yes	Yes	
	Flow Time or Flow Number			Yes	
	Smoothness, Initial		Yes		√
Unbound Layers: Dense Graded Granular Base, Embankment Soils	Density		Yes	Yes	√
	Water Content		Yes	Yes	
	Gradation		Yes	Yes	√
	Minus 200 Material		Yes	Yes	√
	Plasticity Index (Atterberg Limits)		Yes	Yes	
	Resilient Modulus		Yes	Yes	
	Strength	CBR or R-Value	Yes	Yes	
		DCP; Penetration Rate	Yes		
IDT – Indirect Tensile Test CBR – California Bearing Ratio DCP – Dynamic Cone Penetrometer					

Table 2.7: NDT methods used to measure properties and features of flexible pavements in-place (after Von Quintus et al., 2009).

Type of Property or Feature		NDT Technologies and Methods: HMA Layers	NDT Technologies and Methods: Unbound Aggregate Base and Soil Layers
Volumetric	Density	• GPR • Non-Nuclear Gauges: PQI, PaveTracker	• GPR • Non-Nuclear Gauges: EDG, Purdue TDR
	Air Voids or Percent Compaction	• GPR • Infrared Tomography • Acoustic Emissions • Roller-Mounted Density Devices	• GPR • Rolled-Mounted Density Devices
	Fluids Content	• GPR	• GPR • Non-Nuclear Gauges; EDG, Purdue TDR
	Gradation; Segregation	• GPR • Infrared Tomography • ROSAN	• NA.
	Voids in Mineral Aggregate	• GPR (Proprietary Method)	• NA.
Structural	Thickness	• GPR • Ultrasonic; Impact Echo, SPA, SASW • Magnetic Tomography	• GPR • Ultrasonic; SPA, SASW •
	Modulus; Dynamic or Resilient	• Ultrasonic; SPA, SASW • Deflection-Based; FWD, LWD • Roller-Mounted Response System, Asphalt Manager	• Impact/Penetration; DCP, Clegg Hammer • GPR • Ultrasonic; DSPA, SPA, SASW • Deflection-Based; FWD, LWD • Steady-State Vibratory: GeoGauge • Roller-Mounted Response Systems
	Bond/Adhesion Between Lifts	• GPR • Ultrasonic; SASW, Impulse Response • Infrared Tomography	NA.
Functional	Profile ; IRI	• Profilograph , Profilometer, Inertial Profilers	NA.
	Noise	• Noise Trailers	NA.
	Friction	• CT Meter, ROSAN	NA.

SPA- Seismic Pavement Analyzer
PSPA- Portable Seismic Pavement Analyzer
SASW- Spectral Analysis of Surface Waves
LWD- Light Weight Deflectometer
ROSAN- Road Surface Analyzer
EDG- Electrical Density Gauge
TDR- Time Domain Reflectometry

- DSPA- Dirt Seismic Pavement Analyzer
- PQI- Pavement Quality Indicator
- DCP- Dynamic Cone Penetrometer
- CT- Circular Texture
- FWD- Falling Weight Deflectometer

As summarized in Tables 2.6 and 2.7, GPR is used for volumetric-base property characterization of unbound aggregate base layers, and deflection and ultrasonic-based technologies are used for estimating structural properties of aggregate base layers.

1. *Falling Weight Deflectometer (FWD)*

This testing device is used to measure pavements pavement surface deflection due to impact load. In the test, an impulse load is applied to the pavement surface by a weight mass dropped from a specified height, and then measures deflections using sensors (e.g., geophones) placed over the pavement surface. The deflections are used to calculate the modulus of pavement layers. Different moduli for each layer are assumed through back calculation routines. An algorithm is used to predict the deflections of the pavement surface. If the pattern and magnitude of the predicted deflections match with the measured deflections, then the assumed moduli are reported as the moduli of the pavement layers (NCHRP 382). Figure 2.9a shows the FWD during pavement testing.

2. *Light Weight Deflectometer (LWD)*

This testing device is the portable version of the FWD. The LWD device consists of the weight (hammer) on a pole and the sensors (geophones) in a plate on the ground, all encompassed in one, connected, and portable structure. The sensors are connected to a hand-held computer by wireless remote technology such as wireless PDA, Bluetooth, and GPS (Grontmij - Carl Bro 2010). Using equations that assume underlying layers as homogenous elastic half-space, dynamic forces and velocities measurements are converted to elastic stiffness of the base or subgrade, which is correlated to the Young's modulus of the granular base and subgrade layers. Figure 2.9b depicts the LWD.

3. *GeoGauge*

This test device is a portable instrument that can measure the stiffness properties of subgrade and unbound aggregate base layers. Small displacements are induced in the soil using a harmonic oscillator operating over a frequency of 100 to 196 Hz to estimate stiffness. The average stiffness values at 25 frequencies are used to determine the stiffness properties of the measured layer.

4. *Dynaflect*

Dynaflect is a lightweight, two-wheel trailer equipped with an automated data acquisition and control system. This test is performed by placing sensors on the pavement and striking a predetermined load on the pavement structure. The load is generated by two counter-rotating eccentric steel weights, which rotate at a constant frequency of 8 Hz. This movement generates dynamic loads of approximately 500 labs in magnitude (Choubane et al., 2000).

The sensors then measure the deflection when the load has been applied. Theoretical or empirical formulations are then used to analyzed the deflections and determine the modulus of the subgrade and base.

5. *Seismic Pavement Analyzer (SPA)*

The seismic pavement analyzer is used to monitor construction and deterioration in the pavement layers by determining the Young's modulus of elasticity and shear modulus of the different layers in the pavement system. This test takes one minute, which makes it relatively quick, and measures deformations induced by a large hammer that generates low-frequency vibrations, and by small hammer that generates high-frequency vibrations (Nazarian et al., 1995, 2003, 2005).

(a) FWD performing pavement surface testing.

(b) LWD testing on aggregate base course layers

Figure 2.9: Deflection based NDT on pavement layers.

6. *Dynamic Cone Penetrometer (DCP)*

The DCP is a testing device that measures penetration rate induced by a sliding hammer weight that drives a slender shaft into the compacted base and subgrade. It is widely used to estimate density, strength, or stiffness of in-situ soils by determining parameters such as dynamic cone resistance (q_d) or DCP index (DCPI) in millimeters per blow or inches per blow or blows per 300 mm penetration. One major limitation is the lack of standardization of the testing device. Different size cones, hammer weights, and drop heights have been used, resulting in different energies applied by each device (NCHRP 382). Compaction quality control and assurance is one of the applications of this device. The DCP measurements are reported in the literature to correlate with multiple mechanical properties (Baus, 2006).

Siekmeier et al. (2009) conducted a comprehensive study on LWD and DCP use for characterizing unbound aggregate layers in Minnesota for Mn/DOT. They concluded that the LWD and DCP should be implemented more widely in the state of Minnesota. The authors proposed limits for the DCP and LWD as function of base gradation (Table 2.8).

Table 2.8: DCP and LWD target values for granular materials (after Siekmeier et al., 2009).

Grading Number	Moisture Content	Target DPI	Target DPI Modulus CSIR	Target LWD Modulus Dynatest	Target LWD Modulus Zorn	Target LWD Deflection Zorn
GN	**%**	**mm/drop**	**MPa**	**MPa**	**MPa**	**mm**
3.1-3.5	5-7	10	97	120	80	0.38
	7-9	12	80	100	67	0.45
	9-11	16	59	75	50	0.60
3.6-4.0	5-7	10	97	120	80	0.38
	7-9	15	63	80	53	0.56
	9-11	19	49	63	42	0.71
4.1-4.5	5-7	13	73	92	62	0.49
	7-9	17	55	71	47	0.64
	9-11	21	44	57	38	0.79
4.6-5.0	5-7	15	63	80	53	0.56
	7-9	19	49	63	42	0.71
	9-11	23	40	52	35	0.86
5.1-5.5	5-7	17	55	71	47	0.64
	7-9	21	44	57	38	0.79
	9-11	25	37	48	32	0.94
5.6-6.0	5-7	19	49	63	42	0.71
	7-9	24	38	50	33	0.90
	9-11	28	32	43	29	1.05

On the other hand, Baus and Li (2006) conducted a study on granular base materials to investigate the factors affecting the mechanical stability of compacted base layers. In investigating the effect of the base layer thickness, the measured modulus using the FWD showed that the influence of the base thickness varies for every material type. Figure 2.10 shows the variation in modulus where the base thickness varies from 6 to 12 in. The figure shows that the maximum modulus value varies depending on the granular material used. In addition, the crushed limestone (CL) is the only granular material that exhibited the most change in modulus with changing the thickness; however, it is also the material that yielded the highest modulus values for all thicknesses.

One of the commonly used LWD devices is the Dynatest model number 3031. This device comes with a standard drop weight of 22 lbs. (10 kg.) and also two additional drop weights of 11 lbs (5 kg.) each. When used with the standard drop weight, the LWD weighs 48 lbs. (22 kg.) and produces approximately 1,300-lbf peak loads with the 7.8 in (200 mm) diameter loading plate. A precision load cell measures the magnitude of the impact force and the time history and peak value of the impact force from the standard 22 lbs. (10 kg.) or the optional 33 lbs. (15 kg.) or 44 lbs. (15 kg.) drop weight setups. A hole located through the loading plate and instrumented with a seismic transducer (geophone) measures the center deflection time history and peak value. This measured deflection is used to estimate the elastic modulus from the LWD (E_{LWD}).

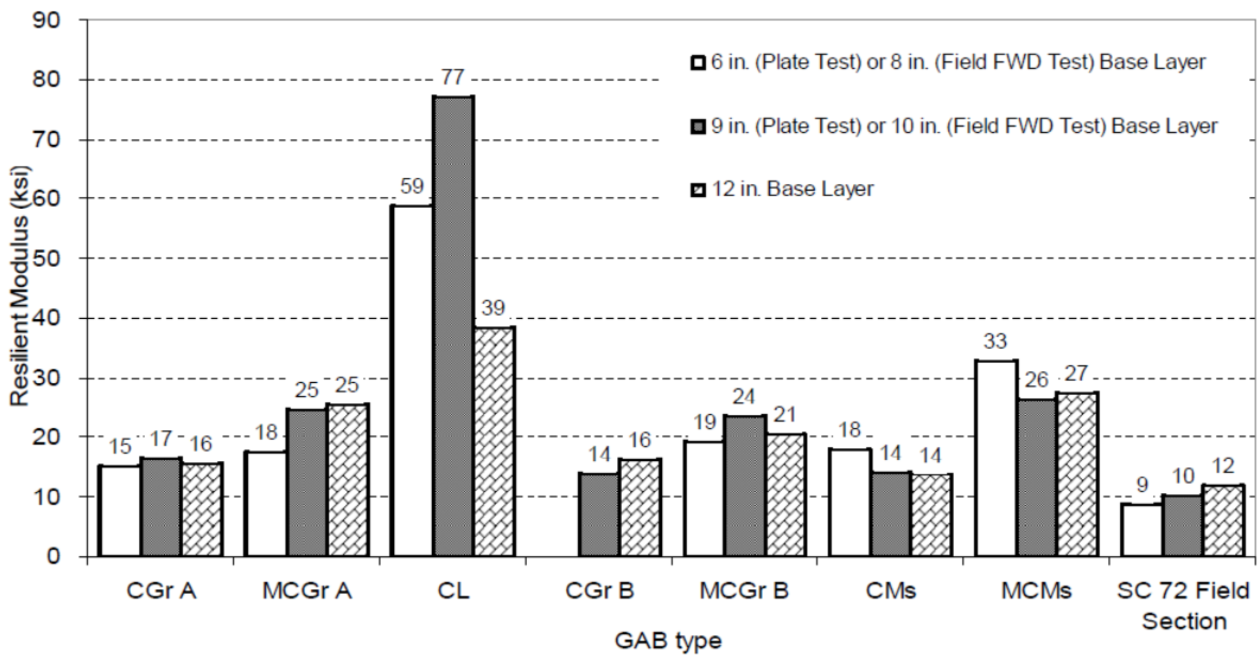

Figure 2.10: Variation of modulus as measured by the static plate load and field FWD on different type of aggregate base (after Baus and Li, 2006).

Equation 2.3 is used to calculate E_{LWD} from the measured deflections from the LWD apparatus as follows:

$$E_{LWD} = \frac{2(1-\nu^2)\,\sigma \times R}{\delta_c} \qquad \textbf{(2.3)}$$

Where:

σ = applied stress
R = plate radius

δ_c = center deflection
ν = Poisson's ratio

The stiffness/modulus gauge is a hand-portable device that provides a simple, rapid, and precise method to measure in-place stiffness and material modulus of compacted subgrade, subbase, and base course layers. This device, also known as the Humboldt Stiffness Gauge or GeoGauge, was originally developed to detect land mines by the defense industry. Its introduction was a collaborated effort between Humboldt, Bolts, Beranek, and Newman from Cambridge, Massachusetts and CAN Consulting Engineers from Minneapolis, Minnesota (Fiedler et al., 1998).

According to Humboldt, the GeoGauge can be used to simply and rapidly build the quantitative basis for implementing mechanistic-empirical pavement design by cataloging as-built resilient modulus in a fraction of the time required for laboratory measurements. The GeoGauge measures the force imparted to the soil and the resulting surface deflection as a function of frequency. This device imparts deflections to the ground as small as 0.00005″ (1.27×10^{-6} m) at 25 discreet frequencies that range from 100 to 196 Hz. The GeoGauge stiffness, H_{SG}, is based on the average of 25 stiffness values obtained at 25 different frequencies. CNA Consulting Engineers proposed the following equation to convert the GeoGauge stiffness, H_{SG}, to soil elastic modulus, E_{SG}.

$$\boldsymbol{E_G = H_{SG} \frac{(1-\nu^2)}{1.77R}} \tag{2.4}$$

Where:
E_G = elastic modulus (MPa)
H_{SG} = GeoGauge stiffness reading in MN/m
ν = Poisson's ratio and,
R = Radius of GeoGauge foot (2.25″ or 57.15 mm)

This apparatus rest on the aggregate base layer surface through a ring-shaped foot and weighs about 22 lbs. (10 kg), it has a diameter of approximately 11″ (28 cm) and a height of approximately 10″ (25.4 cm).

The Dynamic Cone Penetrometer was developed in 1956 in Australia by a company called Scala for quick characterization of subgrade soils. Currently, the DCP is widely used to characterize soils and unbound pavement layers in addition to estimating lift thicknesses and locations of underlying soil layers. According to the ASTM D6951, the standard DCP apparatus consists of a 5/8 inch diameter steel rod, divided in two parts known as the upper and lower shafts, a replaceable or disposable 60° cone tip, a 17.6-lb hammer, a vertical scale, a coupler assembly or anvil, and a handle.

Performing the DCP operation is simple and straight forward. After assembling the equipment, the 17.6- lb hammer is raised to a height of 22.6 inches and dropped under its own weight. This energy is used to drive the conical tip into the material being tested. The number of hammers drops (blows) is recorded, as well as the corresponding penetration depth of the lower shaft of the DCP. The penetration depth per blow is termed the DCP penetration index (DPI) or as the penetration rate (PR). The DPI or PR is recorded in unit length (inches or millimeters) per blow and it is used to estimate the strength of a layer of the pavement and/or the overall strength of the unbound materials. It can also be used to identify the boundaries between the different layers of the pavement system.

In the U.S., several highway agencies are using the DCP to assess the in-situ strength of pavement layers. State highway agencies in Minnesota and Louisiana have developed specifications on the use of DCP as a pavement foundation characterization tool. Mn/DOT has been using the DCP as an acceptance tool for compacting pavement edge drain trenches since 1993, and more recently for the acceptance of compacting base material. Some of the reasons that make this device attractive to use are its low cost and simple way of transportation.

The PR is calculated by subtracting the previous vertical scale penetration rate reading from the present reading and dividing this difference by the difference of blow counts. Many studies have been developed to correlate DCP penetration rate to pavement strength and stiffness.

It is well documented that Mn/DOT is one of the state departments of transportation that has used the DCP extensively. In 1991 Mn/DOT was first introduced to the DCP and since then has used the DCP for different applications, including determining pavement rehabilitation strategies and locating layers in pavement structures, supplementing foundation testing for design, identifying weak spots in constructed embankments, using the DCP as an acceptance testing tool, locating boundaries of required subcuts, and determining thaw/freeze depth during spring. Mn/DOT developed specification limits of PR based on soil type under the assumption of adequate confinement near the surface to be tested. To identify these limiting values, Mn/DOT conducted and analyzed more than 700 DCP tests and recommended PR limiting values of one inch/blow (25 mm/blow) for clay and silt, seven mm/blow (0.28 inch/blow) for select granular materials and five mm/blow (0.20 inch/blow) for Class 3 special materials.

Over the years many researchers have worked with the DCP to characterize the layers of a pavement system and used the penetration rate to correlate with other pavement design parameters such as CBR. Some of these correlations are described below.

Penetration Ratio and California Bearing Ratio Correlation

According to Gabr (2000), most of the correlations developed between DCP PR and CBR measurements were directed to subgrade soils with a few on aggregate base courses and seem to have coincided to the form:

$$\boldsymbol{log}\ (\boldsymbol{CBR}) = \boldsymbol{a} + \boldsymbol{b}\,\mathbf{log}(\boldsymbol{PR}) \qquad \textbf{(2.5)}$$

Where:

CBR = California Bearing Ratio,

PR = DCP penetration rate (mm/blow),

a = constant that ranges from 2.44 to 2.56, and

b = constant that ranges from -1.07 to -1.16.

Kleyn (1975) worked on developing a laboratory-based correlation between DCP and CBR on 2,000 specimens. He noticed that when the moisture content changed while maintaining the compaction level at standard Proctor effort, the DCP data varied similar to that of the CBR. Based on these findings, he concluded that the DCP-CBR relationship is independent of moisture content. The correlation developed under his study was:

$$\boldsymbol{log}\ (\boldsymbol{CBR}) = \mathbf{2.62} - \mathbf{1.27}\ \mathbf{log}(\boldsymbol{PR}) \qquad \textbf{(2.6)}$$

Harison (1987) found that a good correlation exists between CBR and DCP for clay-like soils, well-graded sand, and gravel. In his study, Harison developed correlations for each individual type of material tested, as well as general correlation for all the materials tested. The developed correlations by Harison (1987) are based on DCP tests conducted in the laboratory on samples compacted in standard CBR molds. Equations 2.7 and 2.8 show the relationship of the CBR the PR for gravel materials and the general correlation.

$$\boldsymbol{log}\ (\boldsymbol{CBR}) = \mathbf{2.55} - \mathbf{0.96}\ \mathbf{log}(\boldsymbol{PR}) \qquad \textbf{(2.7)}$$

$$\boldsymbol{log}\ (\boldsymbol{CBR}) = \mathbf{2.81} - \mathbf{1.32}\ \mathbf{log}(\boldsymbol{PR}) \qquad \textbf{(2.8)}$$

Harison (1987) stated that it is preferable to establish a single equation, which has general applicability than a set of equations, each for a particular material. With this correlation, all materials tested can be represented to an accuracy of ± 10%. He also found that moisture content, dry density, and soaking processes do not affect the relationship between CBR and DCP.

Livneh and Ishai (1987) conducted DCP and in-situ CBR testing on a wide range of undisturbed and compacted fine-grained soil samples, with and without saturation. Flexible molds with variable controlled lateral pressures were used to test compacted granular soils. Based on their results, Livneh and Ishai (1987) proposed the following correlation:

$$\boldsymbol{log\ (CBR) = 2.2 - 0.71\ \log(PR)^{1.5}} \quad \textbf{(2.9)}$$

Webster et al. (1992), working with the U.S. Army Corps of Engineers, developed a relationship for a wide range of granular and cohesive materials. This correlation was developed between the DCP penetration rate and CBR strength values required for operation of aircraft and military vehicles on unsurfaced soils. Webster et al. (1992) collected a database of field CBR versus DCP values from many sites and different soil types. The database was used to compare results published by Van Vuuren (1969), Kleyn (1975), Harison (1987), and Livneh and Ishai (1987). He found general agreement between the various sources of information and proposed the following equation:

$$\boldsymbol{log\ (CBR) = 2.465 - 1.12\ \log(PR)} \quad \textbf{(2.10)}$$

or

$$\boldsymbol{CBR = \frac{292}{DCP^{1.12}}} \quad \textbf{(2.11)}$$

Ese (1995) used the DCP for road-strengthening design purposes in Norway in 23 road sections with base courses of well-graded gravel, each 20 m long and with a homogenous distress pattern. He determined that a value of 2.6 mm/blow is a limit value for good road performance indication; higher values indicated poor road performance. Ese (1995) conducted laboratory and field testing to five existing pavement structures of various ages and a wide range of fines contents in the natural gravel base course. The results showed correlation existed between the penetration rate and the stability of an aggregate base course (ABC), and that this correlation was independent of the moisture content and dry densities. The developed correlation was compared with correlations developed by Kleyn (1975), Smith and Pratt (1983) and Livneh (1987). He found that the correlation he developed yielded higher values of CBR, especially at low DCP values; therefore, he decided to calibrate the correlation by comparing field CBR values and laboratory CBR values. Ese (1995) found that the average ratio between field CBR and laboratory CBR was 1.7. He used this average ratio as a calibration factor and applied it to the laboratory-generated correlation:

$$\boldsymbol{log\ (CBR) = 2.438 - 1.065\ \log(PR)} \quad \textbf{(2.12)}$$

Gabr (2000) investigated the potential of using the DCP as an instrument to evaluate pavement performance. His approach was to develop a model to predict the distress levels of pavements layers on subgrade and aggregate base course. The researcher's goal was to discern the integrity of the subgrade and aggregate base course by using the developed model. Gabr

(2000) conducted a testing program that included laboratory and field testing. The laboratory testing included compacting base aggregates specimens under various conditions representative of compactive efforts according to AASHTO T 99 and T 180 in CBR molds, performing CBR tests, and then penetrating the specimen with the DCP device. These specimens were assembled in the lab to meet a specified gradation and 86 blows/layer were used to compact five layers of material in a 7-inch mold. Gabr (2000) found that for both compactive efforts, as the moisture content was increased, the CBR increased slightly and the PR decreased up to a moisture content of 5.4%. As the moisture content was increased from 5.4% to 6%, the PR increased and the CBR decreased.

Field testing included CBR tests on the aggregate base and DCP tests on the aggregate base and subgrade layers for four sites constructed with aggregate base course material. Information regarding the pavement and base thickness, nuclear moisture density, pavement age, and traffic load also was collected. DCP testing was done under confined and unconfined conditions. The confined condition is when the DCP test is conducted on top of the asphalt surface layer; the unconfined condition is when the DCP test is conducted after removing the asphalt surface layer.

Gabr (2000) found that the unconfined PR measurements for the base layer ranged from 3.1 to 3.9 mm/blow, and for the confined condition values ranged from 2.2 to 5.6 mm/blow. Nuclear density gauge measurements were also taken at the sites and indicated that the field moisture content ranges from 4.4 to 5.2% with dry densities range from 2.21 to 2.28 Mg/m^3. In this study a correlation was developed between CBR and DCP on the base material tested as:

$$\boldsymbol{log\ (CBR) = 1.4 - 0.55\ \log(PR)} \qquad \textbf{(2.13)}$$

This correlation is specific to the type of material tested under this study. The aggregate base course material tested was Granitic in origin with a specific gravity of 2.78 and high abrasion resistance.

A model also was developed to predict the distress conditions ratings of the pavement. This proposed model followed the AASHTO design guidelines for flexible pavement and was develop using the PR measurements to construct a terminal serviceability $p_t = 2.5$. These lines define the boundary between good and bad road conditions.

Penetration Rate and Moduli Correlation

The resilient modulus is one of the most important material properties used today in the design of pavements, and it is considered a required input for determining the stress-strain characteristics of pavement structures subjected to traffic load. Over the years, correlations have been developed to determine modulus from CBR or DCP results. Heukelom and Klomp (1962) tested fine-grained soils with a soaked CBR of 10 or less, and proposed an equation that correlates modulus to CBR. Equation 2.14 was adopted by the 1993 AASHTO Guide for Design of Pavement Structures for estimating resilient modulus.

$$\boldsymbol{M_R\ (psi) = 1500 * CBR} \quad \text{or} \quad \boldsymbol{M_R\ (MPa) = 10.34 * CBR} \tag{2.14}$$

The proposed correlation was developed from a modulus range from 750 to 3,000 times the CBR. Powell et al. (1984) proposed a relationship between CBR and modulus. Equation 2.15 has been widely accepted.

$$\boldsymbol{E\ (psi) = 2550 * CBR^{0.64} \quad or \quad E_{MPa} = 10.34 * CBR^{0.64}} \tag{2.15}$$

Chen et al. (2001) conducted more than 60 DCP tests on two pavements used for accelerated pavement testing to assess the validities of empirical equations proposed in previous literature to compute layer moduli from data with the DCP. One of his objectives was to recommend a method for estimating the modulus through DCP testing. Chen et al. (2001) used the U.S. Army Corps of Engineers equation to correlate DCP to CBR, and then used the Powell et al. (1984) equation to estimate modulus from CBR values.

Chen et al. (2001) also conducted FWD multidepth deflectometer and laboratory tests to compare with the estimated modulus values from DCP. He found that the comparison between DCP and FWD multidepth deflectometer yielded compatible results, and laboratory-determined subgrade modulus values were slightly higher than the ones obtained from the DCP and FWD multidepth deflectometer.

Pen (1990) reviewed the available methods of analysis for FWD deflection data and verified the estimated elastic moduli of the pavement layers. He worked with five different analysis methods that incorporated three different models. He correlated the results obtained from the different analysis methods with DCP data and found good correlations for subgrade and subbase modulus.

The correlations for subgrade modulus (E_{sg}) are shown in equations 2.16 and 2.17 and were derived under the following data limits: 30 MN/m^2 < E_{sg} < 250 MN/m^2 and 12 mm/blow < DCP < 70 mm/blow

$$\boldsymbol{E_{sg} = 1780 * DCP^{-0.89}} \tag{2.16}$$

$$\boldsymbol{E_{sg} = 4594 * DCP^{-1.17}} \tag{2.17}$$

The correlation for subbase modulus (E_3) is shown in equations 2.18 and was derived under the following data limits: 60 MN/m^2 < E_3 < 300 MN/m^2 and 1.5 mm/blow < DCP < 10 mm/blow

$$\boldsymbol{E_3 = 419 * DCP^{-0.85}} \tag{2.18}$$

It was not possible to find a relationship between DCP and unbound base modulus (E_2) computed with any of the methods used. Pen (1990) suggested that this could be due to the fact that DCP is not a satisfactory method of differentiating the strengths of strong granular base.

Penetration Rate and Shear Strength

Ayers (1989) worked on a study to evaluate the efficacy of the DCP for estimating the shear strength of granular materials. He postulated that the use of the DCP has been limited in part, because of a lack of correlations relating DCP penetration values with fundamental material properties such as cohesion (c), and friction angle (ϕ), properties that are important to many mechanistic-empirical analysis and design procedures.

Ayers (1989) conducted DCP and rapid loading triaxial shear tests on six granular materials compacted at three density levels. The granular materials used were sand, dense-graded sandy gravel, crushed dolomitic ballast, and ballast with 7.5, 15 and 22.5 of a non-plastic crushed-dolomitic fines material called FA-20 material and composed of 96% passing the No. 4 sieve and 2% passing the No. 200 sieve.

2.4 Base Compaction Survey

This section presents the results of a survey conducted to obtain the current state of the practice by highway agencies in the U.S. and Canada on aggregate base construction and quality control/quality assurance. Survey results are analyzed and evaluated.

2.4.1 Conducting the Survey

The research team designed a survey with various questions to obtain the current state of practice of highway agencies in the U.S. and Canada on aggregate base construction and QC/QA. The survey questionnaire is presented in Appendix A.

The research team conducted the survey by e-mail and phone calls after contacting each highway agency to identify engineers who can answer the survey questionnaire. Conducting the survey was challenging and time-consuming; in some cases, it was not possible for one engineer to answer the survey questions, and thus we were directed to contact other engineers within the same highway agency.

The 50 Departments of Transportation (DOTs) in the U.S. and 13 Ministries of Transportation (MOTs) in Canada were contacted to answer the survey questionnaire. Out of the 50 state DOTs, Alaska DOT did not respond to the repeated requests of the research team. All Canadian MOTs submitted answers to the survey questionnaire.

2.4.2 Analysis of the Survey

Forty-nine state DOTs answered the survey questionnaire. The answers and collected information were compiled into spreadsheet files to facilitate data analysis and presentation in graphical format. The answers were analyzed using Map Viewer software in order to highlight the individual highway agency response to the different survey questions.

Highway agency engineers who answered the survey questionnaire are involved with aggregate materials as follows: 42% in aggregate materials testing, 32% in specifications, 18% in construction, and 8% in production, as shown in Figure 2.11. These results are normalized for 100% with engineers are involved in more than one part.

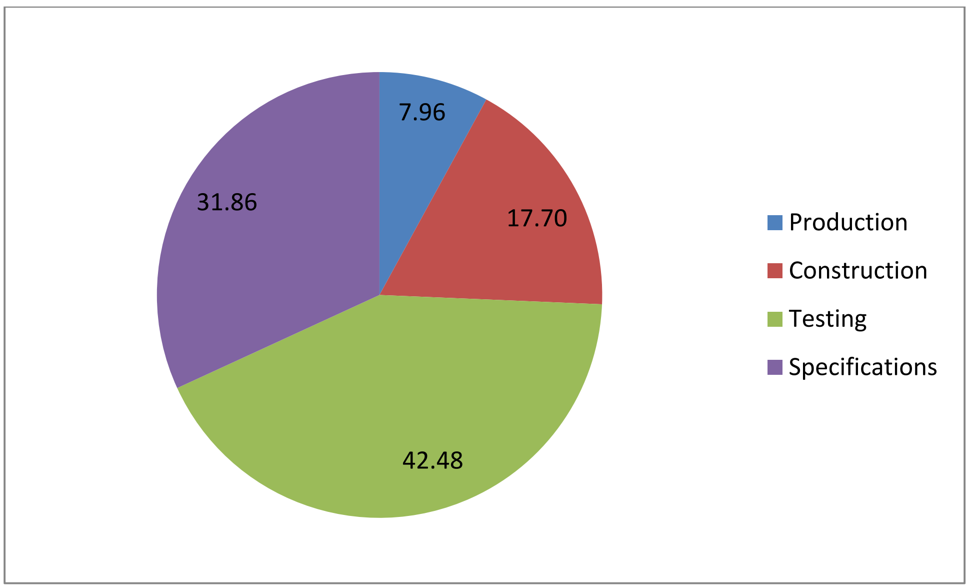

Figure 2.11: Involvement capacities of highway agencies engineers in aggregate materials.

Quality control and quality assurance (QC/QA) of constructed aggregate base layers is implemented mainly using density-based specifications with a percentage of 90.3. Only 6.5% of highway agencies use observation-based specifications and 3.2% implement performance-based specification. Figure 2.12 depicts a pie chart of those percentages and a map identifying the individual state DOT response.

When asked about methods to establish target density for evaluating in-place compaction, 71% of highway agencies use ASTM or AASHTO standard procedures, and 17% use their own procedures modified from ASTM or AASHTO, as depicted in Figure 2.13.

Figure 2.14 presents the response of highway agencies with respect to methods used to measure in-place density. The majority of state highway agencies use the nuclear density gauge to measure in-place density and field moisture content with 62.9% using AASHTO or ASTM standard, and 21% using their own modified standard procedure. The share of usage for the sand cone method is 14.5%.

State highway agency responses on the acceptance limits for the relative compaction are shown in Figure 2.15. The majority of highway agencies require that achieved relative compaction of more than or equal to 95% with 93.1% of the responses require this level.

Modulus-based QC/QA devices are also used by highway agencies to evaluate aggregate base layer construction. Figure 2.16 shows that 15.2% of highway agencies use the FWD, 9.1% use the DCP, and 1.52% use the LWD. However, 70% do not implement or use any stiffness/ modulus-based method.

Construction of the aggregate base layer is carried out in lifts with various thicknesses. As presented in Figure 2.17, 43.5% of highway agencies specify the lift thickness of 6 in. versus 29% who require 8 in. Only 16.1% of highway agencies allow 12-in lift thickness in aggregate base layers construction. It should also be noted that all surveyed highway agencies implement gradation specifications for aggregates used in base layer construction

There is no significant impact of implementing QC/QA specifications for base layer construction on schedules and activities in a project. About 62.9% of the surveyed highway agencies report no impact on project timelines versus 12.9% who stated that QC/QA will cause delays in project timelines. Figure 2.18 displays a pie chart of the answers of the surveyed highway agencies. In terms of impact on project budgets and cost, 53.2% of the surveyed highway agencies said that implementing QC/QA for base layer construction has no impact on the project budget (no increase in cost), while 21% said the project budget will increase to account for such implementation, as depicted in Figure 2.19.

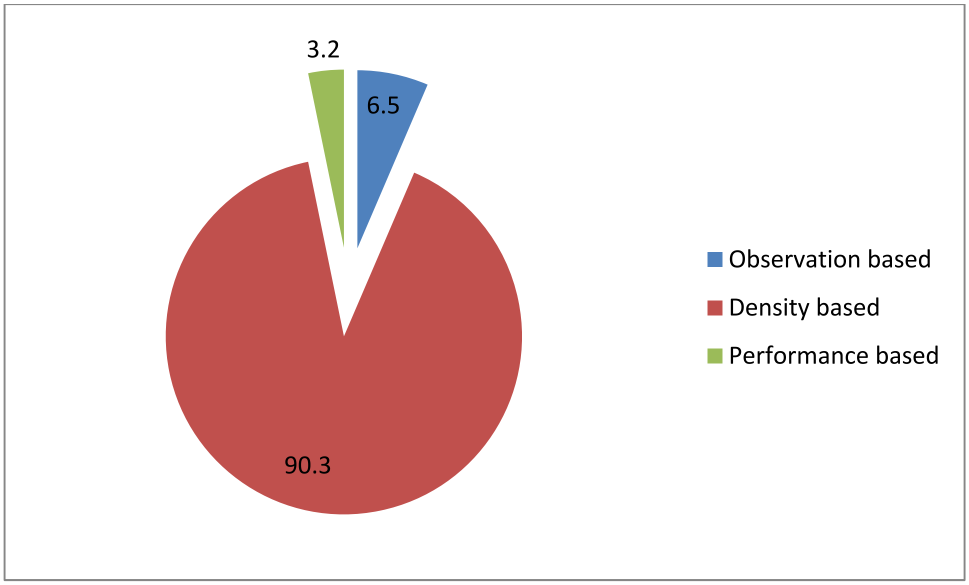

(a) Categories of QC/QA

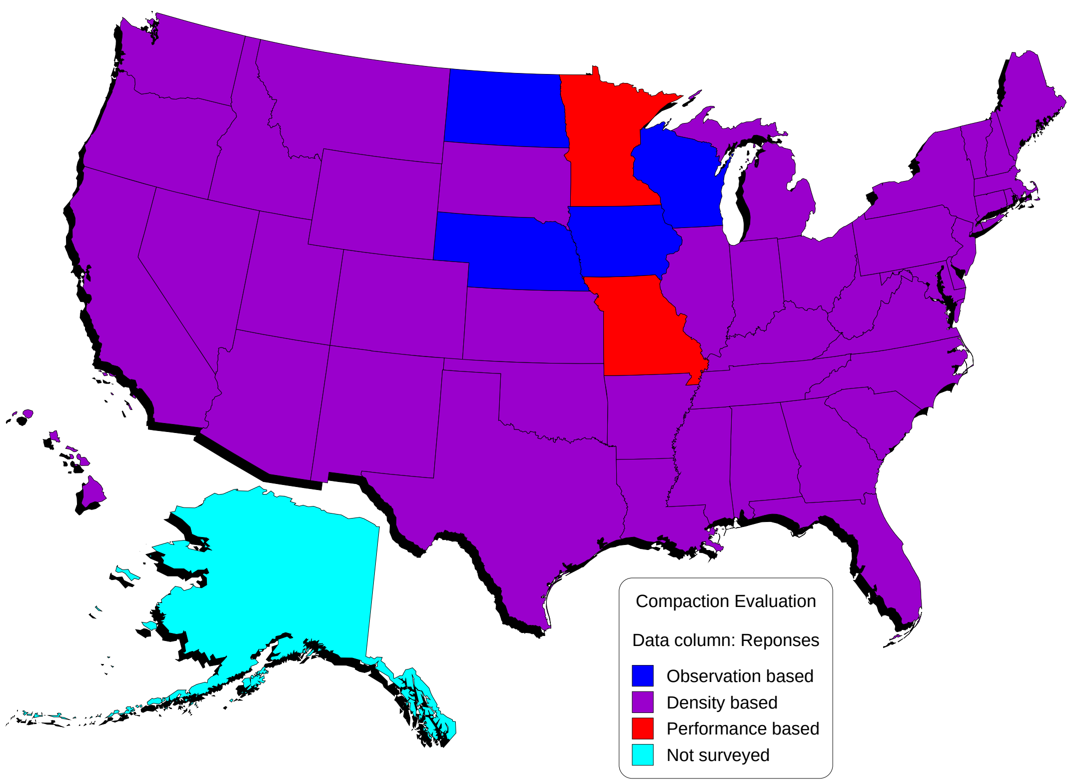

(b) U.S. State DOTs – map representation

Figure 2.12: Response of highway agencies on QC/QA of constructed aggregate base layers.

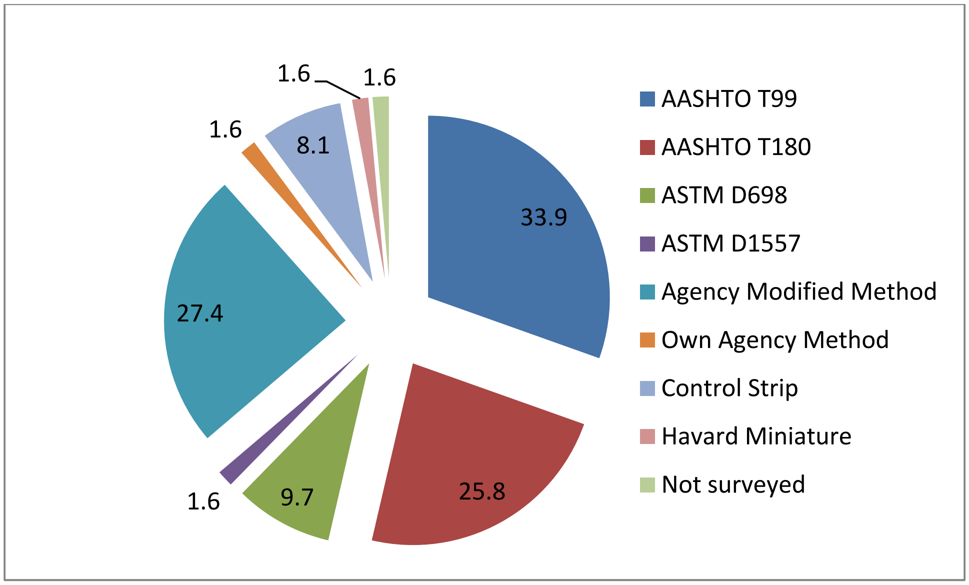

AASHTO T99 and ASTM D698: Standard Proctor compaction test
AASHTO T180 and ASTM 1557 ➔ Modified Proctor compaction test

Figure 2.13: Methods used by highway agencies to establish target density for aggregate base layer compaction control.

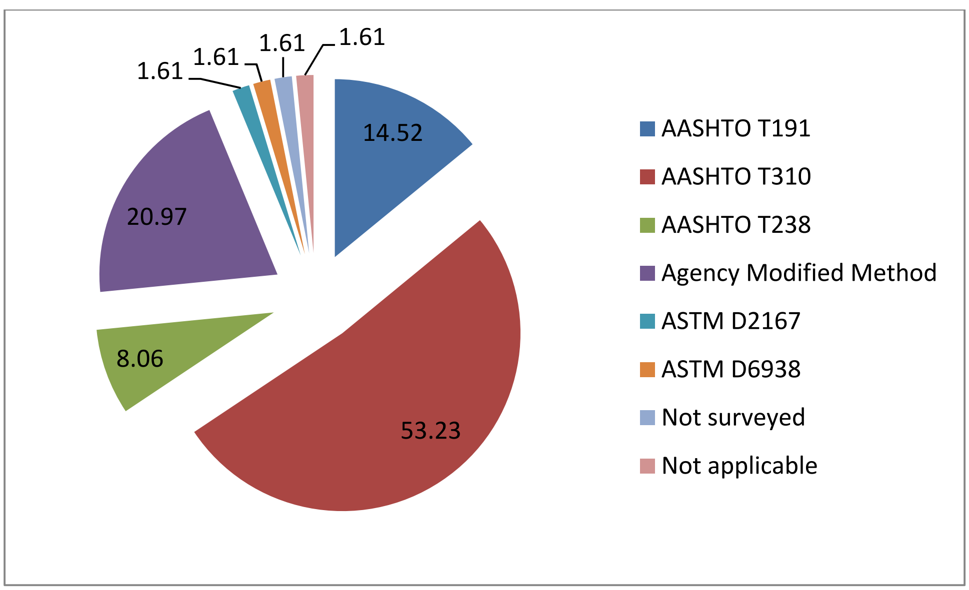

AASHTO T 191: In place density by sand cone method
AASHTO T 310 and ASTM D6938: In place density and moisture content by unclear gauge
AASHTO T 238: In place density by unclear gauge
ASTM D2167: In place density by rubber balloon

Figure 2.14: Methods used by highway agencies to measure in-place density of compacted aggregate base layers.

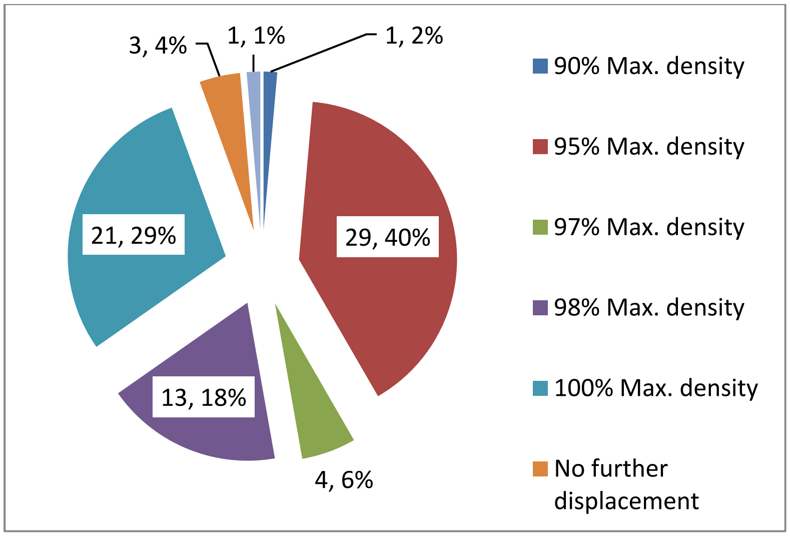

(a) Results by percentage of target density

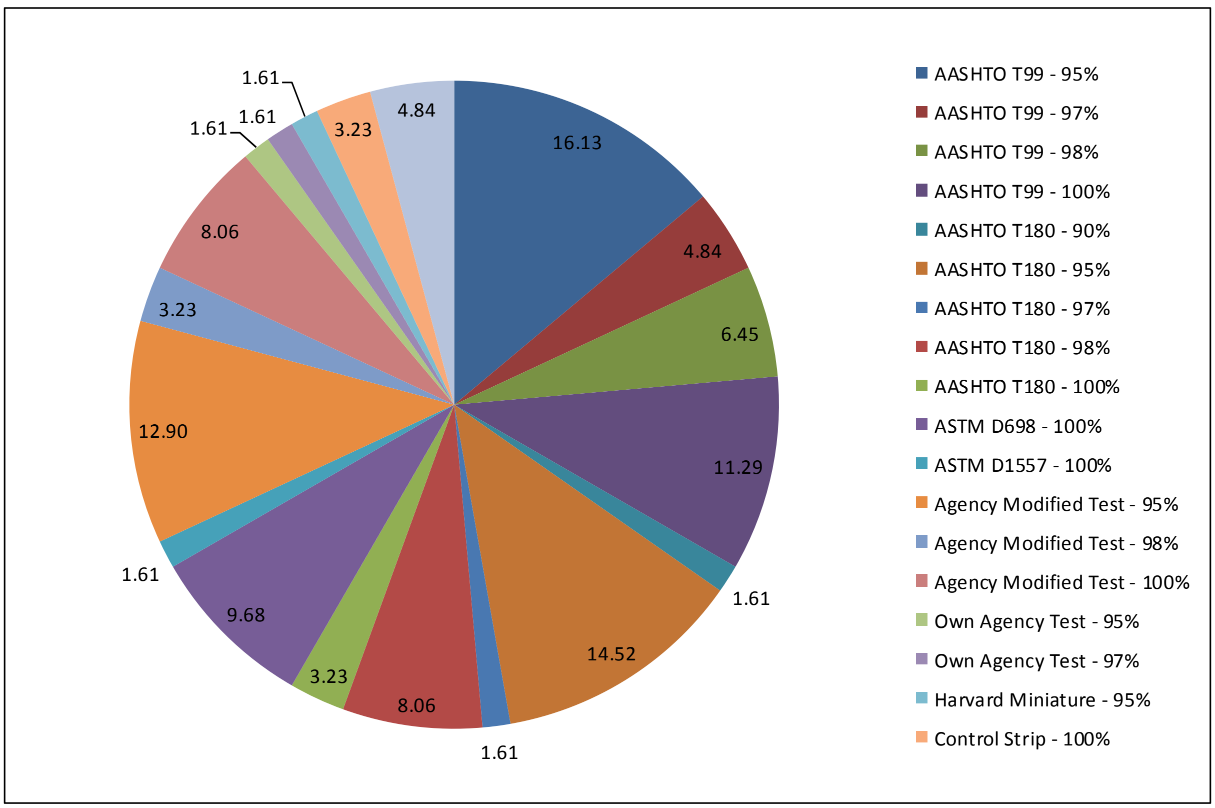

(b) Results by percentage of target density determined by specific method

AASHTO T 99 and ASTM D698: Standard Proctor compaction test
AASHTO T 180 and ASTM 1557 → Modified Proctor compaction test

Figure 2.15: Relative compaction limits implemented by state highway agencies for acceptance of constructed aggregate base layers.

Finally, 42% of the surveyed highway agencies believe there is a need to implement new methodologies for QC/QA of aggregate base layer construction, versus 58% who believe the current methods are satisfactory, as shown in Figure 2.20. Table 2.9 presents the ASTM and AASHTO standard procedures mentioned in the survey.

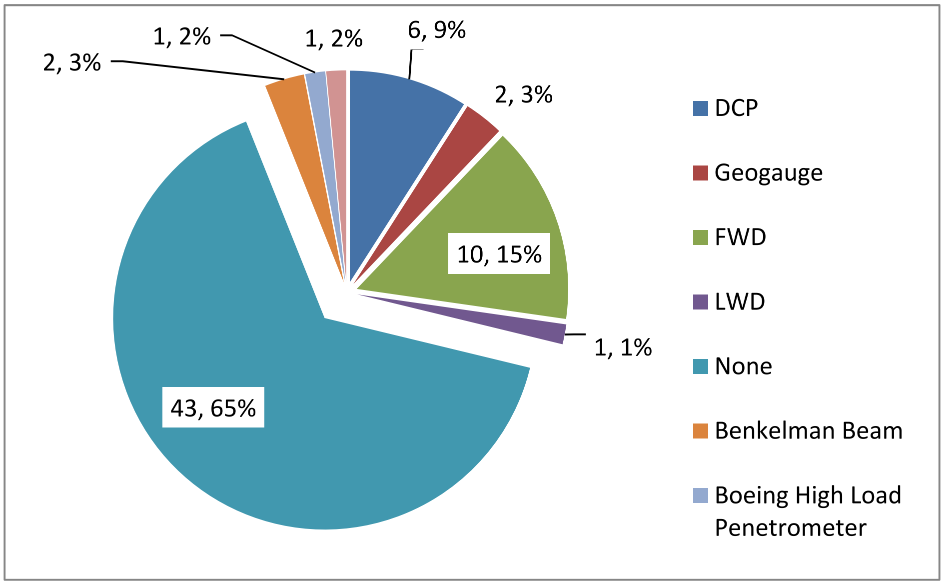

Figure 2.16: Methods used by highway agencies for field measurement of stiffness/modulus of aggregate base course layers.

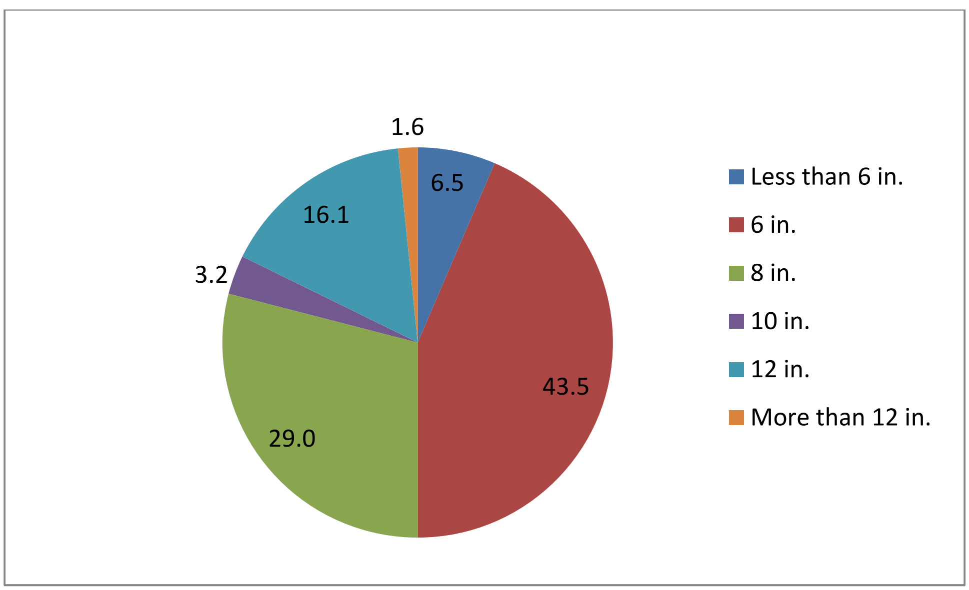

Figure 2.17: Aggregate base layer lift thickness required for construction.

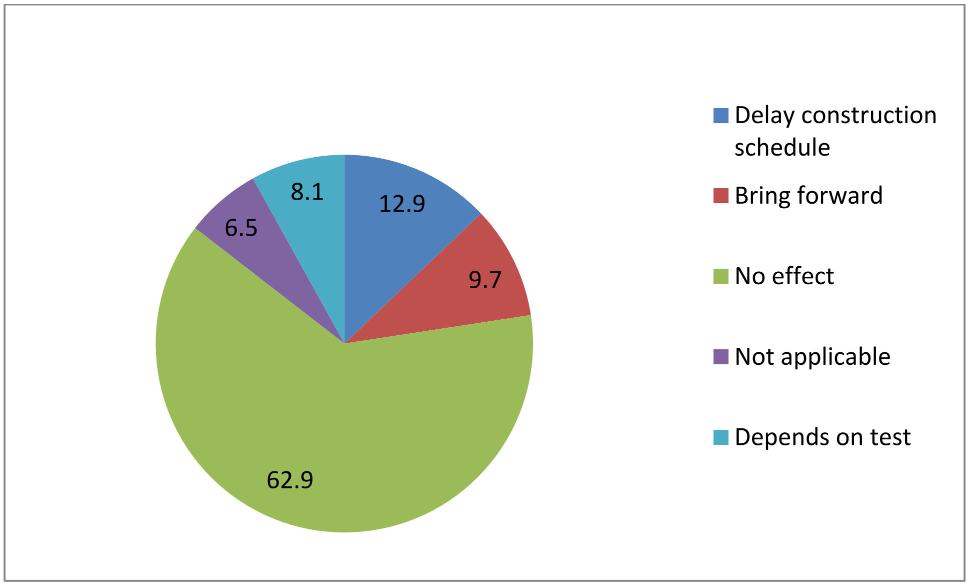

Figure 2.18: Impact of implementing QC/QA specifications on timelines and project schedules.

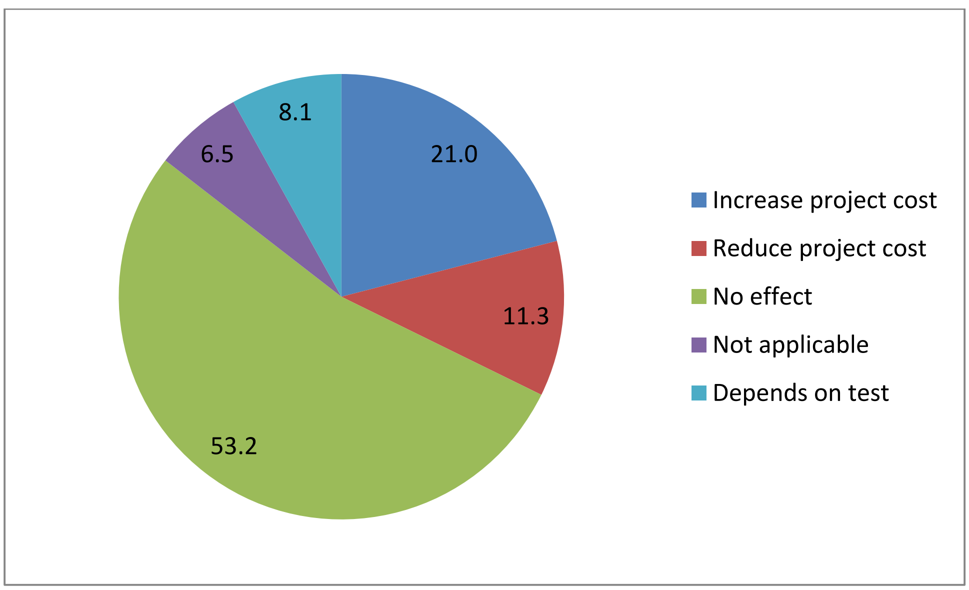

Figure 2.19: Impact of implementing QC/QA specifications on project budget and cost.

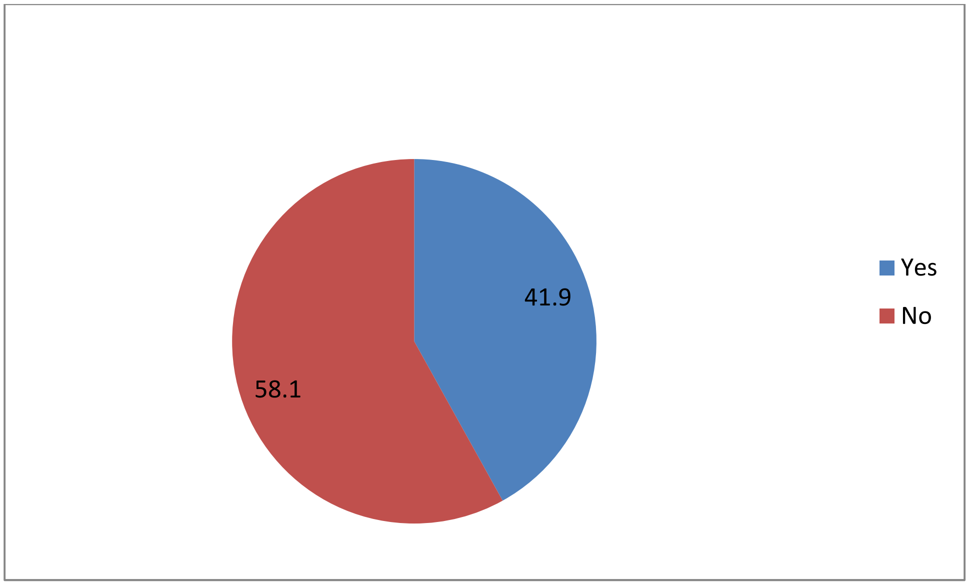

Figure 2.20: The need to implement new methodologies for QC/QA of constructed aggregate base layers.

Table 2.9: ASTM and AASHTO standard procedures mentioned in the survey.

Test		AASHTO Specification	ASTM Specification
Laboratory Max. Density and Optimum Moisture Content	Standard Proctor	AASHTO T 99	ASTM D698
	Modified Proctor	AASHTO T 180	ASTM D1557
Relative Compaction (In-Place Density)	Sand Cone	AASHTO T 191	ASTM D1556
	Nuclear Gauge	AASHTO T 238	ASTM D6938
		AASHTO T 310	
	Rubber Balloon	--	ASTM D2167
In-Place Stiffness/Modulus	DCP	--	ASTM D6951
	GeoGauge	--	ASTM D6758
	FWD	--	ASTM D4694
	LWD	--	ASTM E2583

AASHTO T 99 Standard Method of Test for Moisture-Density Relations of Soils Using a 2.5-kg (5.5-lb) Rammer and a 305-mm (12-in.) Drop

AASHTO T 180 Standard Method of Test for Moisture-Density Relations of Soils Using a 4.54-kg (10-lb) Rammer and a 457-mm (18-in.) Drop

AASHTO T 191 Standard Method of Test for Density of Soil In-Place by the Sand-Cone Method

AASHTO T 238 Standard Method of Test for Density of Soil In-Place by Nuclear Methods (Shallow Depth)

AASHTO T 310 Standard Method of Test for Density of Soil In-Place by Nuclear Methods (Shallow Depth)

ASTM D698 Standard Test Methods for Laboratory Compaction Characteristics of Soil Using Standard Effort (12 400 ft-lbf/ft^3 (600 kN-m/m^3))

ASTM D1557 Standard Test Methods for Laboratory Compaction Characteristics of Soil Using Modified Effort (56,000 ft-lbf/ft^3 (2,700 kN-m/m^3))

ASTM D1556 Standard Test Method for Density and Unit Weight of Soil in Place by the Sand-Cone Method

ASTM D2167 Standard Test Method for Density and Unit Weight of Soil in Place by the Rubber Balloon Method

ASTM D4694 Standard Test Method for Deflections with a Falling-Weight Type Impulse Load Service

ASTM D6758 Standard Test Method for Measuring Stiffness and Apparent of Soil and Soil Aggregate In Place by Electro Mechanical Method

ASTM D6938 Standard Test Method for In Place Density and Water Content of Soil and Soil Aggregate by Nuclear Methods (Shallow Depth)

ASTM D6951 Standard Test Method for Use of The Dynamic Cone Penetrometer in Shallow Pavement Applications

ASTM E2583 Standard Test Method for Measuring Deflections with a Light Weight Deflectometer (LWD)

Chapter 3
Research Methodology

This chapter describes the methods and tests used to investigate field projects and collected base aggregates both in the field in the laboratory. Eleven existing hot mix asphalt (HMA) pavement projects were subjected to nondestructive testing using the Falling Weight Deflectometer (FWD). Visual pavement distress surveys were also carried out for these projects. Moreover, 10 aggregate base course projects under construction were subjected to field testing and evaluation using the Light Weight Deflectometer (LWD), Dynamic Cone Penetrometer (DCP), sand cone test for in-place unit weight (density), and GeoGauge. Laboratory tests of compaction, particle size analysis, and resilient modulus were conducted on materials obtained from aggregate base course projects at the pavement research laboratory at UW-Milwaukee.

3.1 Non-Destructive Testing and Evaluation of Existing Pavements

The Project Oversight Committee (POC) with coordination with the research team identified and selected 11 existing HMA pavement projects for field testing. The selected projects are HMA pavements with aggregate base courses that were constructed in the last few years. Five of the selected projects showed good performance during service life and the rest of the projects exhibited different types and levels of distresses, which were attributed to variability in aggregate base course layer performance. Figure 3.1 depicts the locations of the investigated projects in Wisconsin and Table 3.1 presents summary information about these projects.

3.1.1 Falling Weight Deflectometer Tests

The research team contracted with Engineering & Research International (ERI), Inc. from Savoy, IL to perform the FWD testing. The research team traveled with ERI team to select and test sections and execute the traffic control plan. Once arrived at the project site, the research team conducted windshield visual distress survey/evaluation of the whole length of the project to select representative test section(s). In some projects, two test sections were identified when different distress levels were observed.

The FWD test was conducted according to the standard test procedure of ASTM D4694: Standard Test Method for Deflections with a Falling-Weight-Type Impulse Load Device. ERI KUAB FWD was used with three different load drops of 5,000, 9,000, and 12,000 lb. Nine geophones were used to record pavement surface deflection located at the center of the loading plate and at 8, 12, 18, 24, 36, 48, 60, and 72 in. behind the loading plate. Pavement surface temperature and air temperature were recorded at each test point. In addition, GPS coordinates were acquired for each test point at all projects. Figure 3.2 show the FWD during testing at STH 77 in Washburn County.

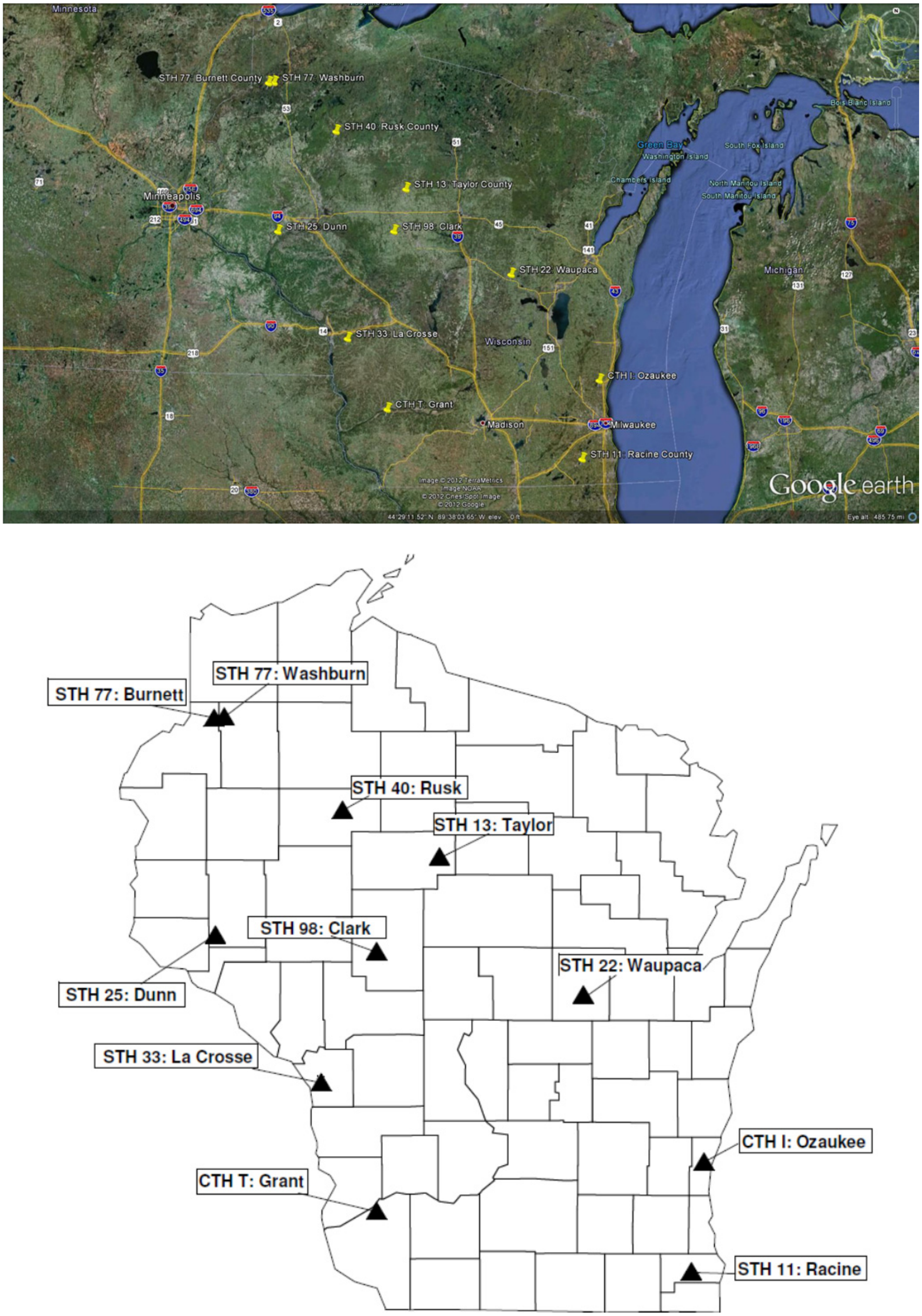

Figure 3.1: Locations of the investigated existing HMA pavement projects in Wisconsin.

Table 3.1: Summary of HMA pavements subjected to FWD testing.

Group	Project	Section	Length (ft.)	FWD Test Interval (ft.)	Existing Typical Sections	
					HMA (in.)	Base (in.)
I (Low performance variability of aggregate base)	STH 33 – LaCrosse	1	3,000	100	6.00	21.00
		2	2,000	100	6.00	21.00
	STH 11 – Racine	-	4,800	100	6.25	9.50
	STH 22-54 – Waupaca	-	5,500	100	6.00	14.00
	CTH T – Grant	1	3,000	100	4.00	14.00
		2	2,000	100	4.00	14.00
	STH 77 – Burnett	-	5,000	100	5.00	10.00
II (High performance variability of aggregate base)	STH 13 – Taylor	1	550	25	6.00	18.00
		2	3,000	100	6.00	18.00
	STH 40 - Rusk	1	4,000	100	4.00	9.00
		2	4,000	100	4.00	9.00
		1	100	10	4.00	9.00
		2	100	10	4.00	9.00
	STH 77 – Washburn	-	5,000	100	5.00	10.00
	STH 98 – Clark	-	5,000	100	4.50	12.00
	STH 25 – Dunn	-	5,000	100	4.50	16.00
	CTH I – Ozaukee	-	5,000	100	5.25	11.00

Figure 3.2: The KUAB FWD used in nondestructive testing of the existing HMA pavement projects.

The total length of FWD testing for each project was about 5,000 ft. at 100 ft. spacing. STH 40 in Rusk County was subjected to FWD testing along both lanes and at two different spacing of 10 and 100 ft. to obtain results at more close intervals.

3.1.2 Visual Distress Survey

Visual distress surveys for all investigated projects were conducted to obtain data needed to estimate pavement condition. The distress survey was conducted for one 250-ft section at each project location. The section was selected to be representative of the pavement condition. At project sites were two test sections were selected for FWD test, two survey sections were taken. Pavement distresses were identified, measured and recorded for each of the investigated test sections. Pavement distresses were identified and quantified according to the FHWA distress identification manual. Figure 3.3 shows pavement surface condition during the visual distress survey.

(a) STH 33 (b) STH 25

Figure 3.3: Pavement surface conditions at selected investigated HMA pavements.

3.2 Field Testing of Aggregate Base under Construction

The research team and POC identified 10 aggregate base construction projects for field testing and evaluation. Base aggregates were also collected from these sites for laboratory testing. Figure 3.4 depicts map of Wisconsin showing the county locations of the selected projects. Table 3.2 presents summary of information on these projects. The field testing program consisted of conducting the in place density by the sand cone method, the Dynamic Cone Penetration Test, the Light Weight Deflectometer test, and GeoGauge test. Table 3.3 presents summary of field and laboratory tests conducted.

Table 3.2: Base course layer thickness for the investigated projects.

Projects	**Base Course Layer Thickness (in)**
STH 13 – Marshfield	6
CTH JJ – Outagamie	10
USH 45 – Larsen	6
STH 33 – Port Washington	13.5
STH 33 – Saukville	16.5
US 12 – Dane	15
CTH B – Woodville	10
I 90-94-39 – Dane	5.5-7.5
STH 33 – Saukville Ramp	16.5
US 141 – Beecher	17

Table 3.3: Summary of tests conducted on aggregate base materials and layers.

Projects	Field Testing				Laboratory Testing		
	Sand Cone	DCP	LWD	GeoGauge™	Grain Size Distribution	Standard Proctor	Resilient Modulus
STH 13 – Marshfield	✓	✓	✗	✗	✓	✓	✓
CTH JJ – Outagamie	✓	✓	✗	✗	✓	✓	✓
USH 45 – Larsen	✓	✓	✗	✗	✓	✓	✓
STH 33 – Port Washington	✓	✓	✗	✗	✓	✓	✓
STH 33 – Saukville	✓	✓	✗	✗	✓	✓	✓
US 12 – Dane	✓	✓	✓	✗	✓	✓	✓
CTH B – Woodville	✓	✓	✓	✓	✓	✓	✓
I 90-94-39 – Dane	✓	✓	✓	✓	✓	✓	✓
STH 33 – Saukville Ramp	✓	✓	✓	✗	✓	✓	✓
US 141 – Beecher	✓	✓	✓	✗	✓	✓	✓

3.2.1 In-Place Density by the Sand Cone Method

The standard test procedure AASHTO T 191: "*Standard Method of Test for Density of Soil In-Place by the Sand-Cone Method*," was used to determine the in-place unit weight of the compacted base aggregate materials. A test section of 1,200 ft. was selected for most projects where the in-place density test was performed every 200 ft. spacing. In projects where space was limited by construction activities, the in-place density was conducted every 100 ft. spacing. In most cases, six in-place density tests were conducted. Figure 3.5 show the in-place density test by the sand cone method conducted on USH 12 in Madison and on USH 141 near Beecher.

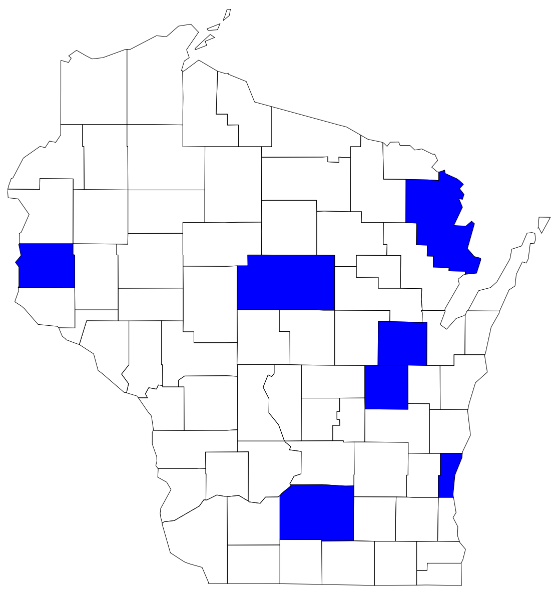

Figure 3.4: Counties where the investigated base construction projects are located.

a) USH 12

b) USH 141

Figure 3.5: In-place density test by the sand cone method.

3.2.2 Dynamic Cone Penetration Test

A dynamic cone penetrometer with a single-mass hammer was used to perform tests on the project sites. The DCP was driven into the aggregate base layer by the impact of a single-mass 17.6 lb. hammer dropped from a height of 22.6 in. The test was conducted according to the standard test procedure described by ASTM D6951: "*Standard Test Method for Use of the Dynamic Cone Penetrometer in Shallow Pavement Applications*." For most field projects, 12 tests were conducted at 100 ft. spacing in which the cone was driven through the whole aggregate base course layer. Figure 3.6 depicts the DCP test on two project sites.

3.2.3 Light Weight Deflectometer Test

The research team acquired a light weight deflectometer from Dynatest for use in this research. The LWD was used according to the standard procedure: ASTM E2583 - 07(2011) Standard Test Method for Measuring Deflections with a Light Weight Deflectometer (LWD). Different test plans were used for different projects in some of which a test grid was created to establish contour maps of calculated layer modulus. Figure 3.7 depicts the LWD during testing for this research.

a) CTH I (USH 45), Larsen   b) STH 33, Port Washington

Figure 3.6: Dynamic cone penetration test on aggregate base course layers.

Figure 3.7: LWD testing on USH 141 (left) and on CTH B (right).

3.2.4 GeoGauge Test

The GeoGauge was obtained from Humboldt and used on two test sites. This was due to time constraints and equipment availability. The GeoGauge was used at the same test point locations before LWD test was conducted. Also, GeoGauge testing was performed on grid configuration to create a contour map of layer moduli.

3.3 Laboratory Testing of Base Aggregate

Representative aggregate samples were collected from the investigated sites during unbound base layer construction and transported to the pavement research laboratory at UW-Milwaukee. Figure 3.8 depicts aggregate sample collected from base course layer constructed at USH 45 – CTH I in Larsen.

Figure 3.8: Aggregate sample collected for laboratory tests at USH 45, Larsen.

The following laboratory tests were conducted on base aggregate collected from project sites:

1. Particle size analysis: AASHTO T 26: Sieve Analysis of Fine and Coarse Aggregates (AASHTO T 11)
2. Compaction test: AASHTO T 99: Moisture-Density Relations of Soils Using a 2.5kg (5.5lb) Rammer and a 305-mm (12-in.) Drop
3. Repeated load triaxial test: AASHTO T 307: Determining the Resilient Modulus of Soils and Aggregate Materials

Repeated load triaxial test was conducted on aggregates compacted at maximum dry unit weight and optimum moisture content for most samples. A special six inch diameter mold was used to produce specimens for the repeated load triaxial test. Pictures of the mold and the compaction process are show in Figure 3.9. Preparing and compacting aggregate specimens were conducted according to AASHTO T 307 standard procedure. After preparation, specimens housed in the triaxial cell are mounted on the dynamic test system for repeated load triaxial test as depicted in Figure 3.10. After the test was concluded the specimen was inspected.

Figure 3.9: Preparation of aggregate specimens for repeated load triaxial test.

Figure 3.10: Mounting the six-inch diameter specimen on the dynamic test system.

Chapter 4
Analyses of Non-Destructive Evaluation of Existing HMA Pavements

This chapter presents the results of the non-destructive evaluation (NDE) conducted on 11 existing HMA pavements using FWD testing. The results of the FWD tests are presented, analyzed and evaluated. In addition, the results of the visual distress survey and subsequent analysis are discussed.

4.1 FWD Results and Analysis

Falling Weight Deflectometer tests were conducted on 11 existing HMA pavements located at various areas across Wisconsin, as depicted in Figure 3.1. As previously stated, these projects were selected by the POC to comprise a population that is representative of typical HMA pavement construction. On six of these projects, issues related to the aggregate base stability and uniformity were observed and reported during HMA layer paving. Later, these projects exhibited various levels of distresses that included cracking (longitudinal, transverse, and alligator), aggregate base failure, and pavement surface roughness/irregularities (in terms of ride quality). The other five projects, in which no issues related to aggregate base layer behavior during construction were reported, performed well after construction.

The investigated projects were categorized in two groups: Group I that includes HMA pavements that did not exhibit high variability in aggregate base performance during HMA paving, and Group II of HMA pavements with reported high variability in aggregate base layer behavior during HMA paving. Table 3.1 presented the listing of HMA pavements in both groups and details of the typical pavement sections.

Collected FWD test data were analyzed using the pavement layer moduli back-calculation software from ERI, Inc. The back calculation program is widely used to estimate pavement layer moduli from FWD test results. The analysis was conducted at UWM with consultation from ERI, Inc. to obtain the field/analysis experience of ERI engineers with FWD testing and analysis. Pavement typical sections of the investigated projects were obtained from WisDOT files and existing pavement layer thicknesses were used in the analysis (Table 3.1). All analysis steps necessary to predict layer moduli values were executed. For example, pavement deflections were normalized to the 9,000 lb. load and then adjusted for temperature variations.

The variation with distance of the deflection under the loading plate (D_0) for all investigated HMA pavements is shown in Figure 4.1. In general, D_0 variation range is between 5 and 15 mils. Figures 4.1b and 4.1c depict the variation of D_0 with distance for Group I and Group II projects, respectively. Inspection of these figures indicates, generally, that the distribution of D_0 with distance for Group I projects is more consistent/uniform with less variability compared with the distribution of D_0 for Group II projects. For example, for STH 11 in Racine County (Group I), D_0 varies between 4.87 and 7.86 mils with an average of 6.03 and coefficient of variation of 12.7%. On the other hand, D_0 for STH 25 in Dunn County ranges from 6.75 to 14.57 mils with an average of 10.38 and coefficient of variation of 20.4%. Table 4.1 presents a summary of average D_0 and COV values for all investigated projects. Figures 4.2 and 4.3 present the average D_0 and COV for D_0 along with the error bar for all investigated projects, respectively.

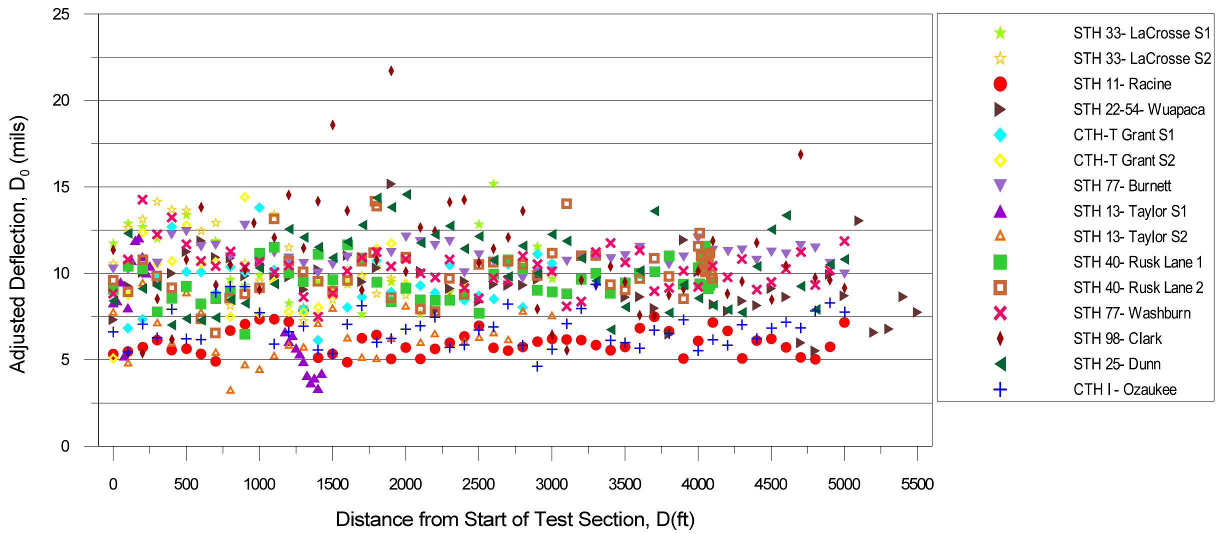

(a) All investigated HMA pavements

Figure 4.1: Variation of D_0 along test sections for the investigated HMA pavements.

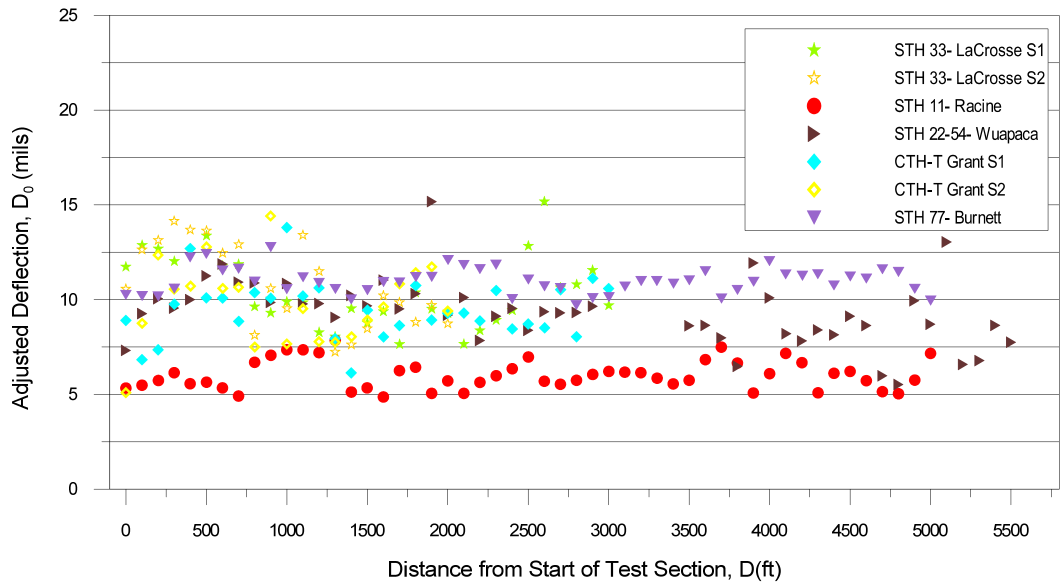

(b) Group I HMA pavements

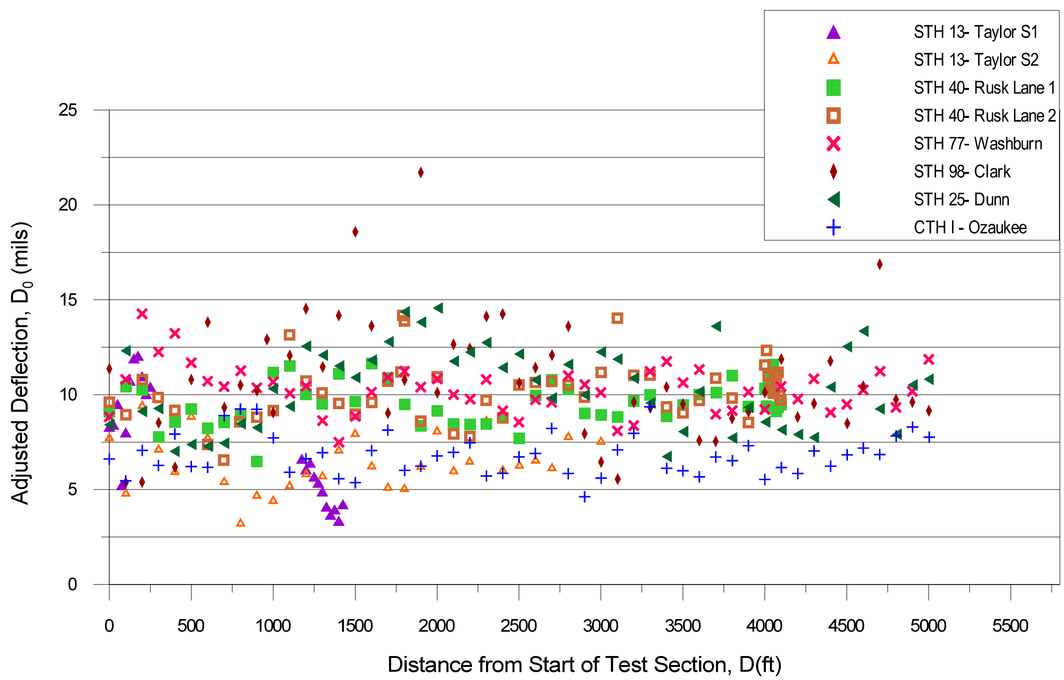

(c) Group II HMA pavements

Figure 4.1 (cont.): Variation of D_0 along test sections for the investigated HMA pavements.

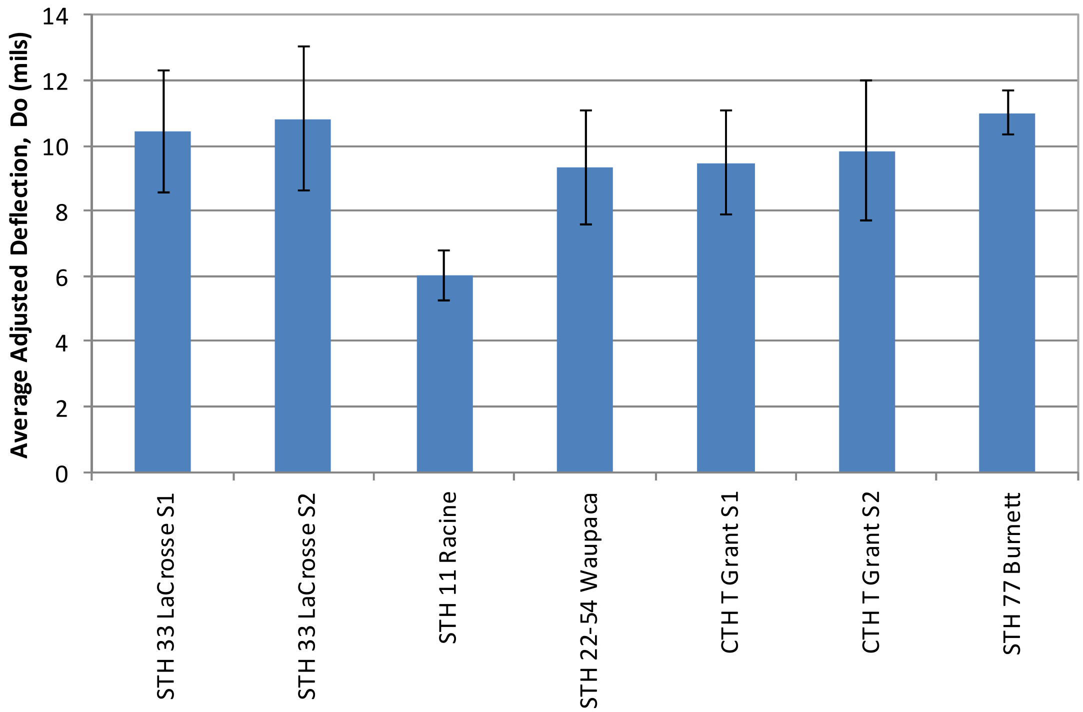

(a) Group I HMA pavements

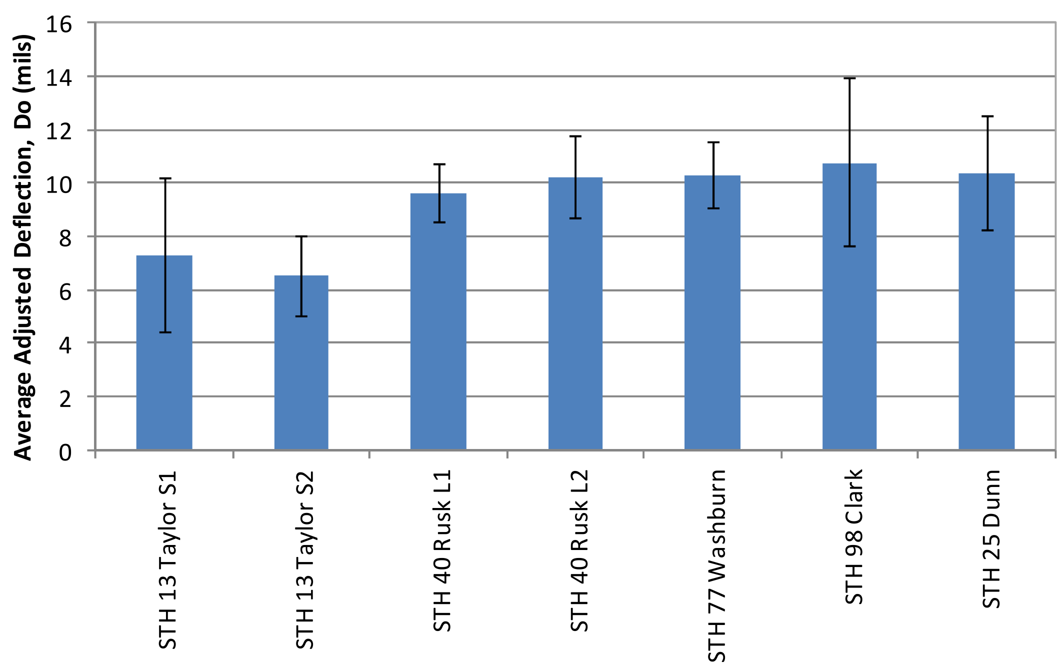

(b) Group II HMA pavements

Figure 4.2: Average D_0 deflection, with error bar, for all investigated HMA pavements.

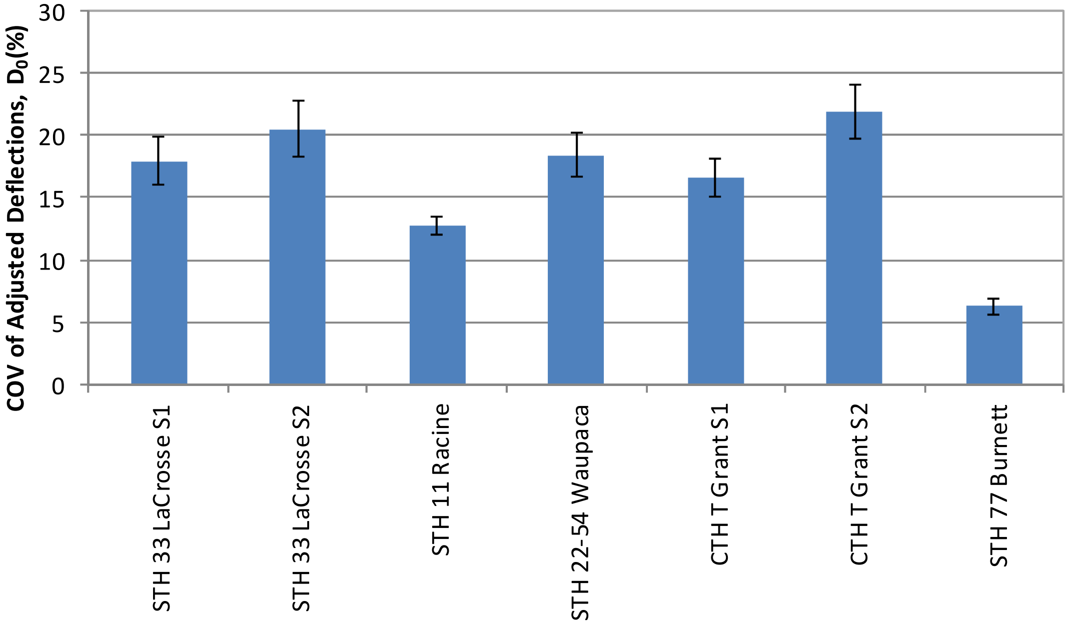

(a) Group I HMA pavements.

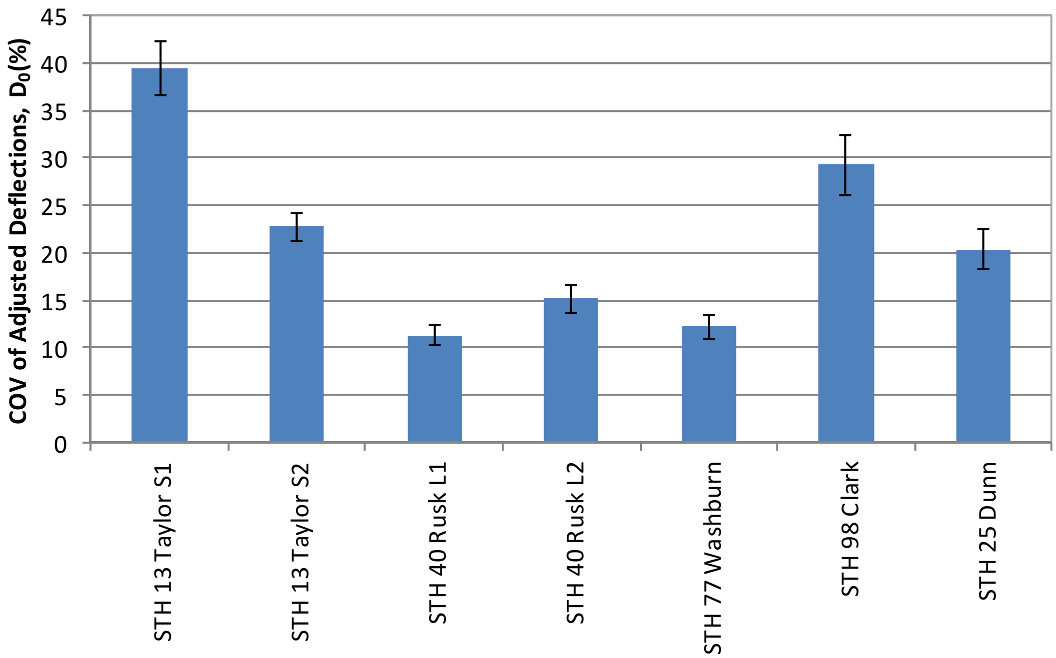

(b) Group II HMA pavements

Figure 4.3: COV of D_0 deflection, with error bars, for all investigated HMA pavements.

Table 4.1: Summary of HMA pavements subjected to NDE.

Group	Project	Section	Average D_0 (mils)	COV for D_0 (%)
I (Low performance variability of aggregate base)	STH 33 – LaCrosse	1	10.44	18
		2	10.81	21
	STH 11 – Racine	-	6.03	13
	STH 22-54 – Waupaca	-	9.33	18
	CTH T – Grant	1	9.47	17
		2	9.82	22
	STH 77 – Burnett	-	11.00	6
II (High performance variability of aggregate base)	STH 13 – Taylor	1	7.28	39
		2	6.51	23
	STH 40 – Rusk	1	9.60	11
		2	10.20	15
	STH 77 – Washburn	-	10.29	12
	STH 98 – Clark	-	10.76	29
	STH 25 – Dunn	-	10.38	20
	CTH I – Ozaukee	-	6.82	16

The backcalculated layer moduli for the HMA surface layers, aggregate base course layers, and subgrade soil for all investigated projects are depicted in Figures 4.4, 4.7 and 4.9, respectively.

The backcalculated modulus for the HMA layer (E_{HMA}) for all investigated pavements varies significantly among the projects and within the individual project. As an example, for STH 11, E_{HMA} ranges from 490 to 1,894 ksi with an average of 1,177 ksi and COV equals 28%. The maximum and minimum E_{HMA} as well as average and COV values are summarized in Table 4.2. The distribution with distance of E_{HMA} for Group I and II pavements is depicted in Figure 4.4 (b and c). Examination of the plots shows the variability of E_{HMA} in projects within both groups with E_{HMA} values tend to be lower for projects in Group II. The average E_{HMA} for Group I projects varies between 201 and 1,177 ksi with COV ranges from 16 to 57%. For Group II projects, the average E_{HMA} ranges from 155 to 704 ksi with COV varies between 17 and 123%. It should be noted that the low backcalculated layer modulus for the HMA layer in number of Group II projects is due to deteriorated and distressed pavement surface. Figure 4.5 depicts pictures of distressed pavement surface at STH 98 and STH 13 part of Group II projects. It should be noted that distressed HMA surface layers will exhibit low backcalculated elastic modulus. On the other hand, pavement surface layers for projects within Group I did not exhibit surface distresses, as shown in Figure 4.6.

The variability in E_{HMA} is not necessarily and exclusively dependent on the base course layer variability; there are other factors that may influence the mechanical stability of HMA such as mix design, compaction temperature, compaction effort, density, and variability in layer thickness.

Table 4.2: Statistical summary of backcalculated layer moduli for investigated HMA pavements

Group	Project	Section	Average			COV			Maximum			Minimum		
			E_{HMA} (ksi)	E_{Base} (ksi)	$E_{Subgrade}$ (ksi)	E_{HMA} (%)	E_{Base} (%)	$E_{Subgrade}$ (%)	E_{HMA} (ksi)	E_{Base} (ksi)	$E_{Subgrade}$ (ksi)	E_{HMA} (ksi)	E_{Base} (ksi)	$E_{Subgrade}$ (ksi)
I	STH 33 – LaCrosse	1	349	34	15	25	24	23	522	51	22	146	18	10
		2	322	34	16	23	24	22	459	46	24	209	16	11
	STH 11 – Racine	-	1,177	36	28	28	19	16	1,894	61	42	490	24	22
	STH 22-54 - Waupaca	-	944	27	20	57	43	23	2,908	76	38	242	7	12
	CTH T – Grant	1	201	50	30	19	11	28	325	58	53	144	35	20
		2	213	49	28	16	18	36	281	76	62	155	34	15
	STH 77 – Burnett	-	700	27	20	18	26	12	1,034	39	24	466	16	15
II	STH 13 – Taylor	1	345	72	33	123	65	35	1,615	164	54	81	9	17
		2	234	61	34	52	51	18	598	160	51	92	17	22
	STH 40 – Rusk	1	210	48	25	48	16	17	755	58	39	132	19	19
		2	211	50	24	61	16	16	884	59	37	109	21	17
	STH 77 - Washburn	-	302	50	23	50	47	14	768	95	33	148	19	16
	STH 98 – Clark	-	155	59	20	17	20	31	202	121	40	54	38	8
	STH 25 – Dunn	-	704	55	17	54	37	34	2,227	92	33	167	22	10
	CTH I – Ozaukee	-	246	45	38	59	44	24	671	84	63	102	16	21

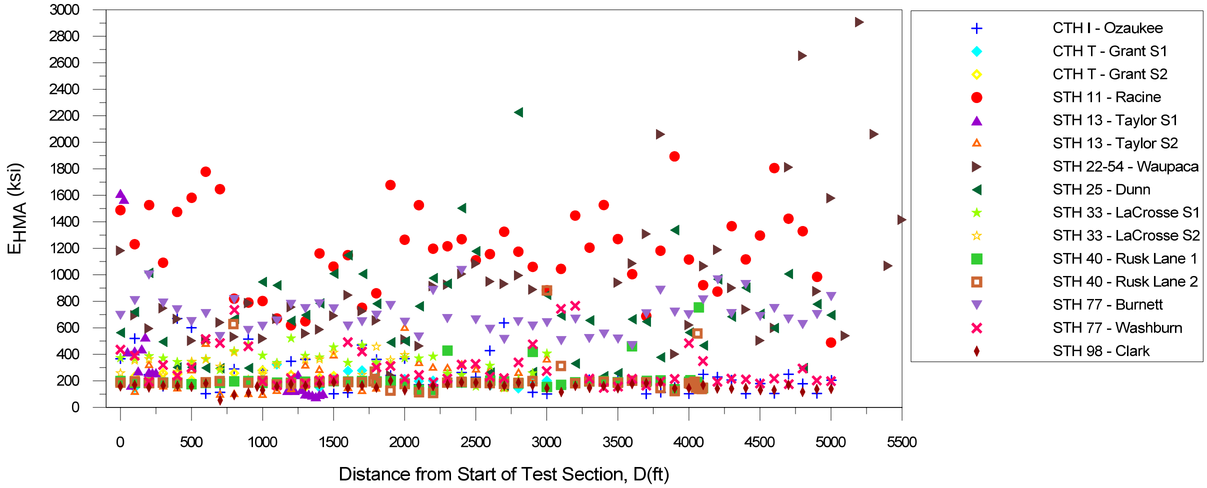

(a) All investigated HMA pavements.

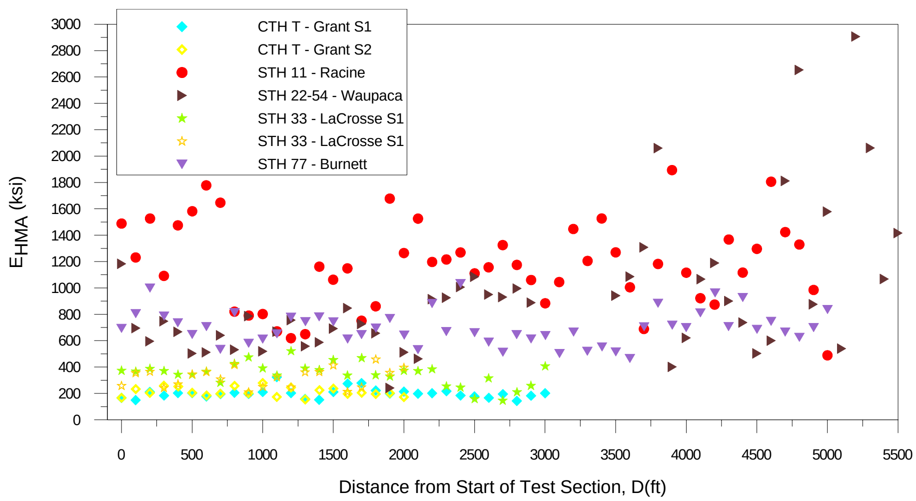

(b) Group I HMA pavements

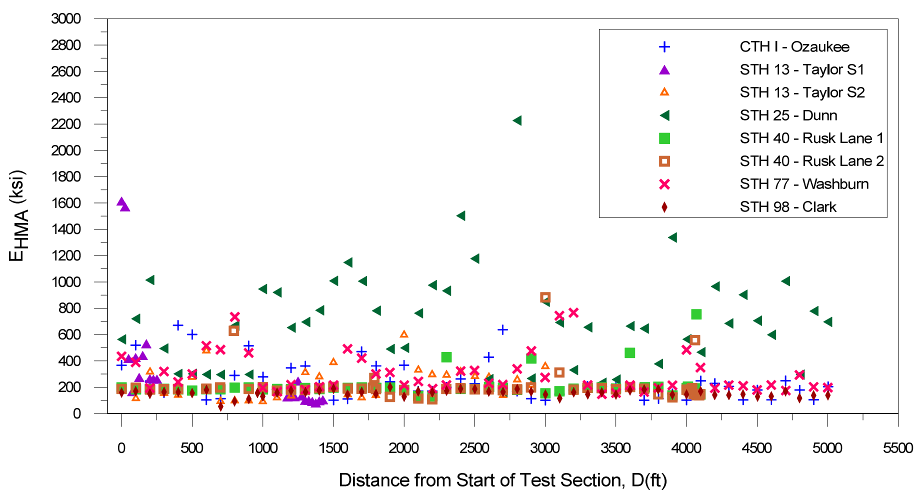

(b) Group II HMA pavements

Figure 4.4: Backcalculated elastic modulus (E_{HMA}) for HMA pavement layer.

(a) STH 98

(b) STH 13

Figure 4.5: Distresses pavement surfaces at selected Group II HMA projects.

(a) CTH T

(b) STH 33

(c) STH 77

Figure 4.6: Pavement surfaces at selected Group I HMA projects.

The distribution with distance of the backcalculated elastic modulus for the aggregate base layers (E_{Base}) for all investigated projects is presented in Figure 4.7. Inspection of Figure 4.7a indicates significant variability of E_{Base} within the individual project and among projects with a range between 7 and 164 ksi. The backcalculated modulus for the aggregate base layer for STH 11 ranges from 24 to 61 ksi with an average of 36 ksi and COV equals 19%. In addition, E_{Base} for STH 25 ranges from 22 to 92 ksi with an average E_{Base} equal to 55 ksi and COV of 37%. The maximum and minimum backcalculated E_{Base} as well as the average and COV for each project were presented earlier in Table 4.2. Figures 4.7b and 4.7c show the distribution with distance of E_{Base} for Group I and II projects, respectively. For Group I projects, E_{Base} variability is relatively lower with a minimum E_{Base} of 7 and a maximum of 76 ksi. The average E_{Base} values for projects in Group I range between 27 and 50 ksi with COV range from 11 to 43%. It is important to note that in Group I, there is only one project with high COV (43%) while COV values for the rest of the projects are less than or equal to 26%. Figure 4.7b clearly indicates the relative uniformity, consistency, and less variability of the backcalculated E_{Base} distribution along test sections of projects within Group I. On the other hand, the variability of E_{Base} is higher, in general, for Group II projects with minimum E_{Base} of 9 and maximum of 164 ksi. The average E_{Base} values for projects in Group II vary between 45 and 72 ksi with COV range from 16 to 65%. Figure 4.8c depicts the lack of uniformity, inconsistency, and high variability of the backcalculated E_{Base} distribution along test sections for majority of projects within Group II.

The variability of aggregate base layers of the investigated projects is evident from the statistical analysis of the backcalculated modulus, E_{Base}. In order to examine the variability of aggregate base layers on small scale, FWD testing was conducted on one 100 ft. section on STH 40 in Rusk County with 10 ft. spacing along both East Bound (EB) and West Bound (WB) lanes. The results of the backcalculated E_{Base} along the grid configuration were used to create a contour map as shown in Figure 4.8. The backcalculated E_{Base} varies from minimum E_{Base} of 19 ksi to maximum E_{Base} of 59 ksi. Inspection of the Figure 4.8 indicates that the “area with low E_{Base}” of the aggregate base layer is located across the pavement between distance marker of 60 to 80 ft. on the EB lane and 50 to 70 ft. on the WB lane.

The distribution with distance of backcalculated subgrade modulus ($E_{Subgrade}$) for all investigated pavements is presented in Figure 4.9. The variability with distance of subgrade modulus is evident in all investigated projects. For STH 11, $E_{Subgrade}$ ranges from 22 to 42 ksi with an average of 28 ksi and COV equals 16%, while $E_{Subgrade}$ for STH 25 varies between 10 and 33 ksi with an average E_{Base} equal to 17 ksi and COV of 34%. The distribution with distance of $E_{Subgrade}$ for Group I and II pavements is depicted in Figure 4.10 (b and c). The average $E_{Subgrade}$ for Group I projects varies between 15 and 30 ksi with COV ranges from 12 to 36%. For Group II projects, the average $E_{Subgrade}$ ranges from 17 to 38 ksi with COV varies between 14 and 35%. In general and based on the average $E_{Subgrade}$ values, the variability of subgrade for projects of both groups is approximately within a similar range. The maximum and minimum predicted $E_{Subgrade}$ as well as average and COV values are summarized in Table 4.2.

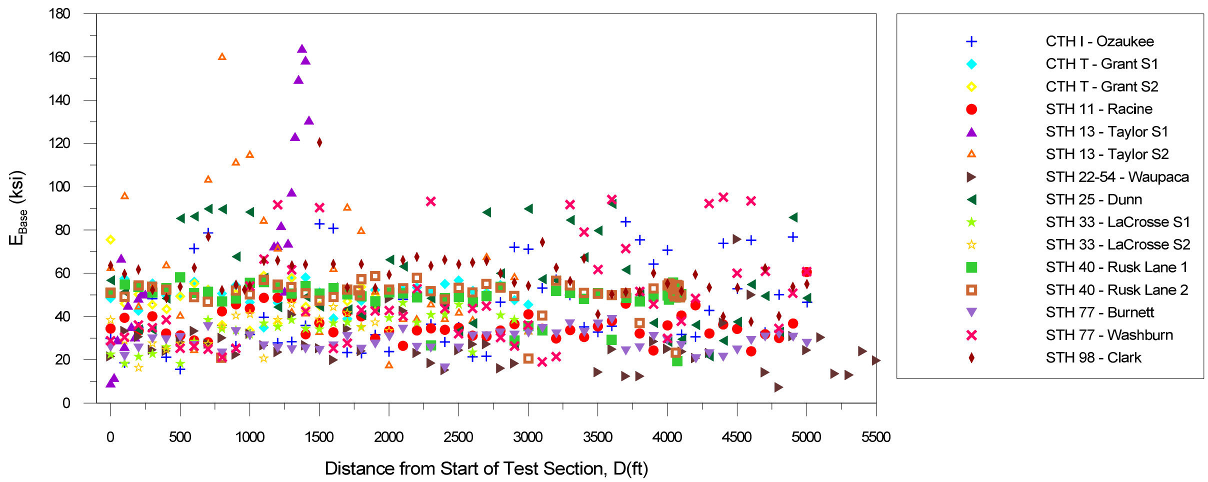

(a) All investigated HMA pavements

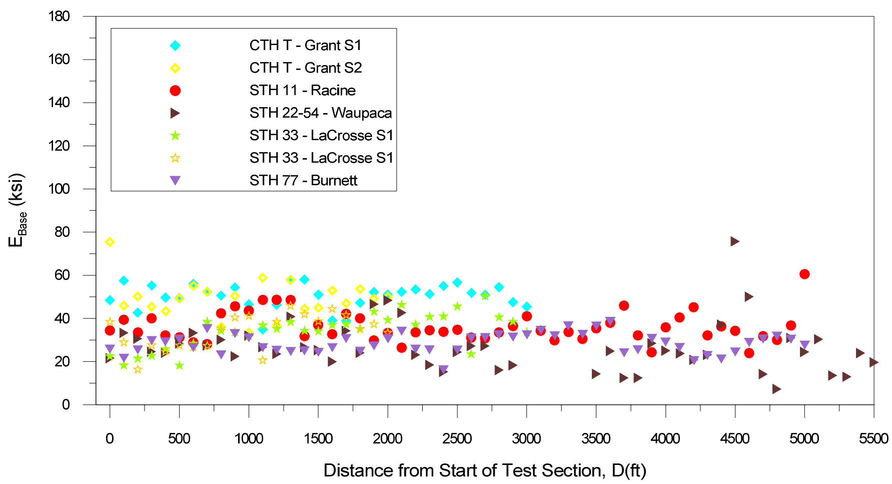

(b) Group I HMA pavements

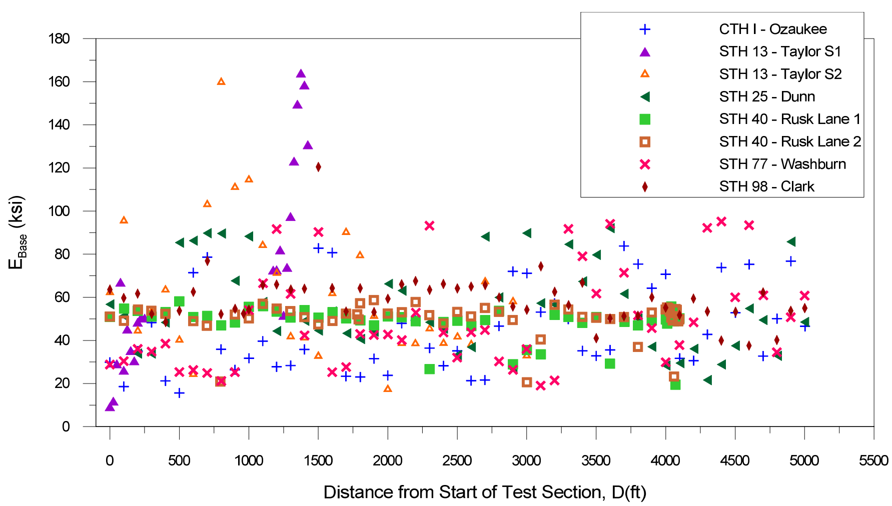

(c) Group II HMA pavements

Figure 4.7: Predicted elastic modulus (E_{Base}) for the aggregate base layer.

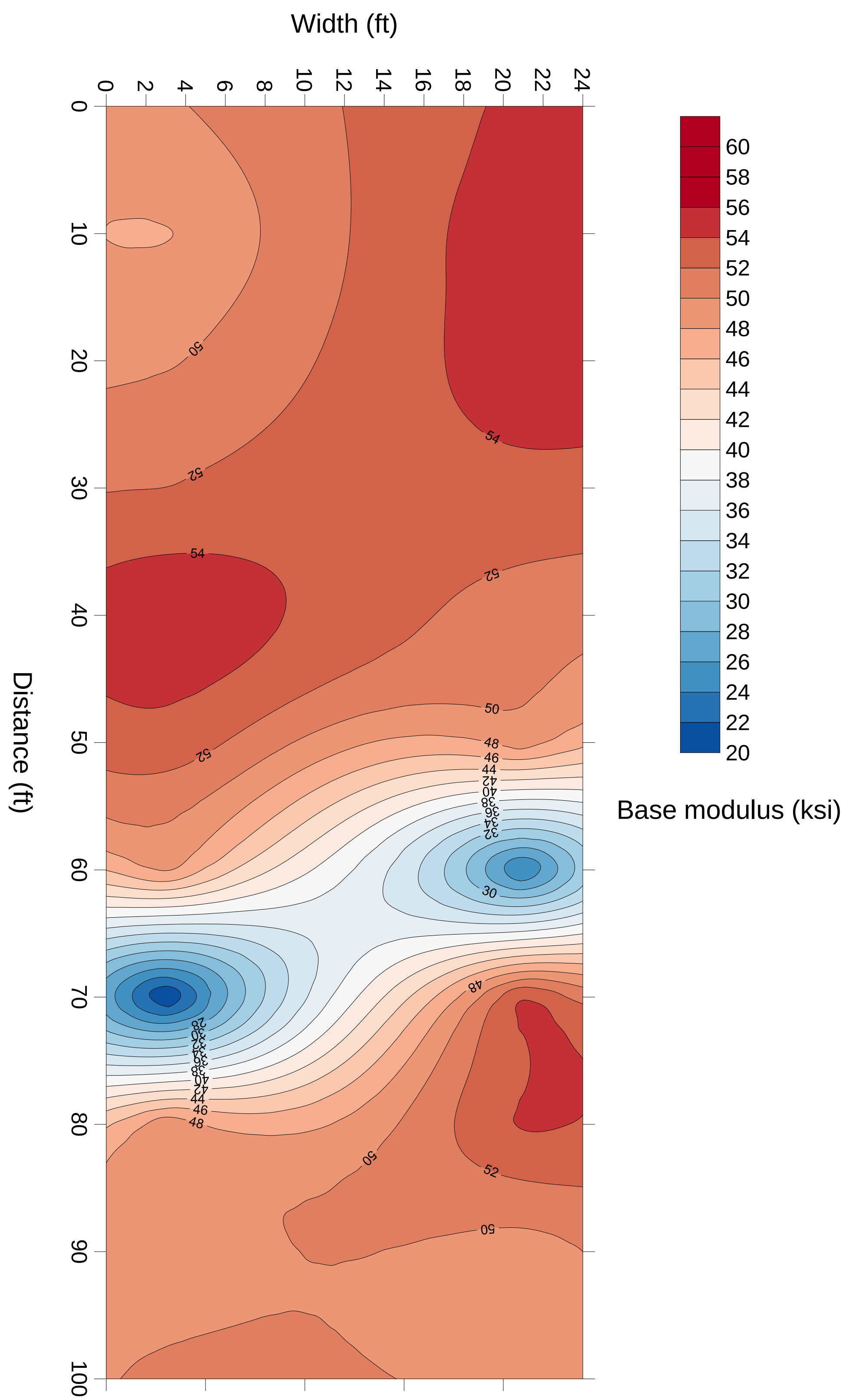

Figure 4.8: Contour of backcalculated elastic modulus (E_{Base}) for the aggregate base layer for STH 40, Rusk County.

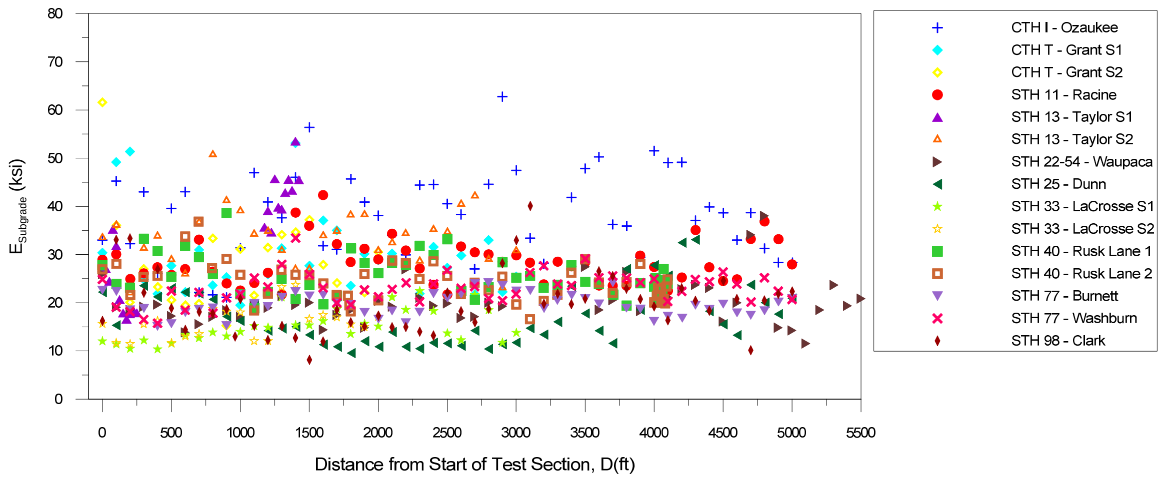

(a) All investigated HMA pavements.

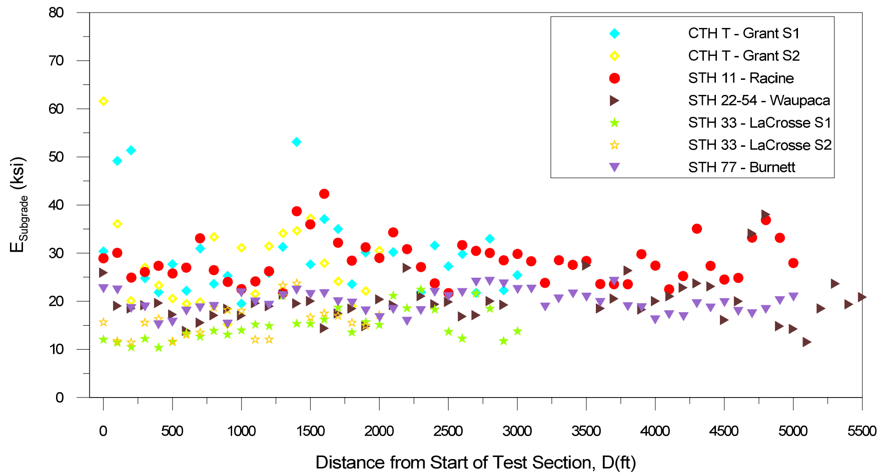

(b) Group I HMA pavements

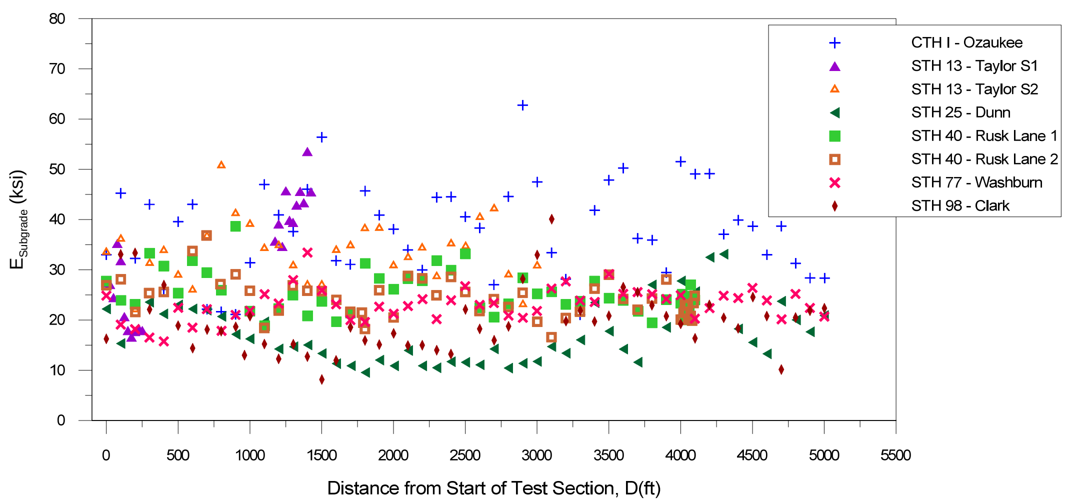

(c) Group II HMA pavements

Figure 4.9: Backcalculated subgrade modulus ($E_{Subgrade}$).

4.2 Summary Observation on FWD Results

The variability of backcalculated layer moduli within each investigated project and among projects was presented in the previous section. Table 4.2 summarized the results statistical information including maximum, minimum, average, and COV of layer moduli using all collected data points.

Figures 4.10 and 4.11 present the backcalculated layer moduli values for each project in a Whisker-box plot format with Group I projects located on the left side of the plot. The plots show the range, median, outliers, and extremes when considering 90 percentile of the backcalculated layer moduli. Figures 4.10 and 4.11 show the relative variation of backcalculated layer moduli for base and subgrade.

Figures 4.12 to 4.15 present the results of the statistical on base and subgrade backcalculated layer moduli. Inspection of the data indicates the following:

1. The average E_{Base} for Group I projects ranges from 27 to 50 ksi with COV varies between 11 and 43%. The average E_{Base} of all Group I projects is 36.7 ksi with average COV of 23.6%.
2. The average E_{Base} for Group II projects ranges from 45 to 72 ksi with COV varies between 16 and 65%. The average E_{Base} of all Group II projects is 55 ksi with average COV of 37%.
3. The average $E_{Subgrade}$ for Group I projects ranges from 15 to 30 ksi with COV varies between 12 and 36%. The average $E_{Subgrade}$ of all Group I projects is 22.5 ksi with average COV of 22.9%.
4. The average $E_{Subgrade}$ for Group II projects ranges from 17 to 38 ksi with COV varies between 14 and 35%. The average $E_{Subgrade}$ of all Group II projects is 26.8 ksi with average COV of 23.6%.

This analysis indicates that subgrade modulus variability within the projects of both groups is relatively low and within close range. The average subgrade modulus for projects of Group II is slightly higher. This provides uniform and consistent subgrade reference to evaluate aggregate base modulus on uniform subgrade conditions that are approximately similar for all investigated projects. This observation is important, because it normalizes the potential effect of the subgrade on the performance of the different pavements studied. Therefore, the next steps in analysis focuses on the base layer consistency/uniformity and the influence on the surface layer performance.

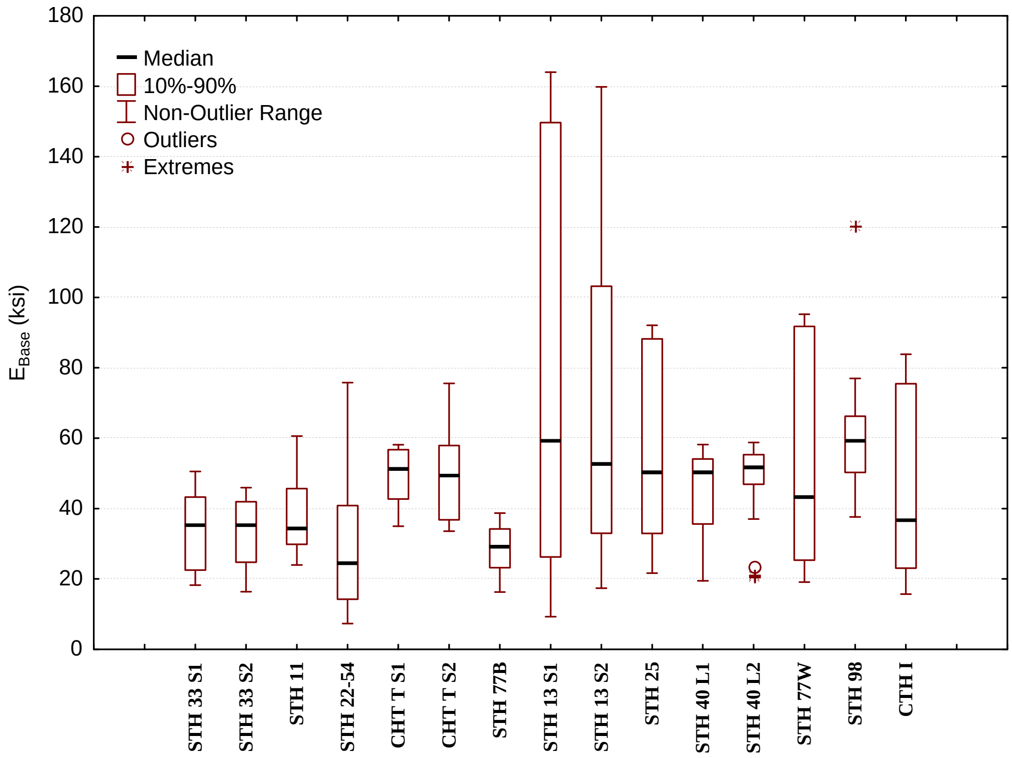

Figure 4.10: Whisker-box plot for 90 percentile of E_{Base} of the investigated projects.

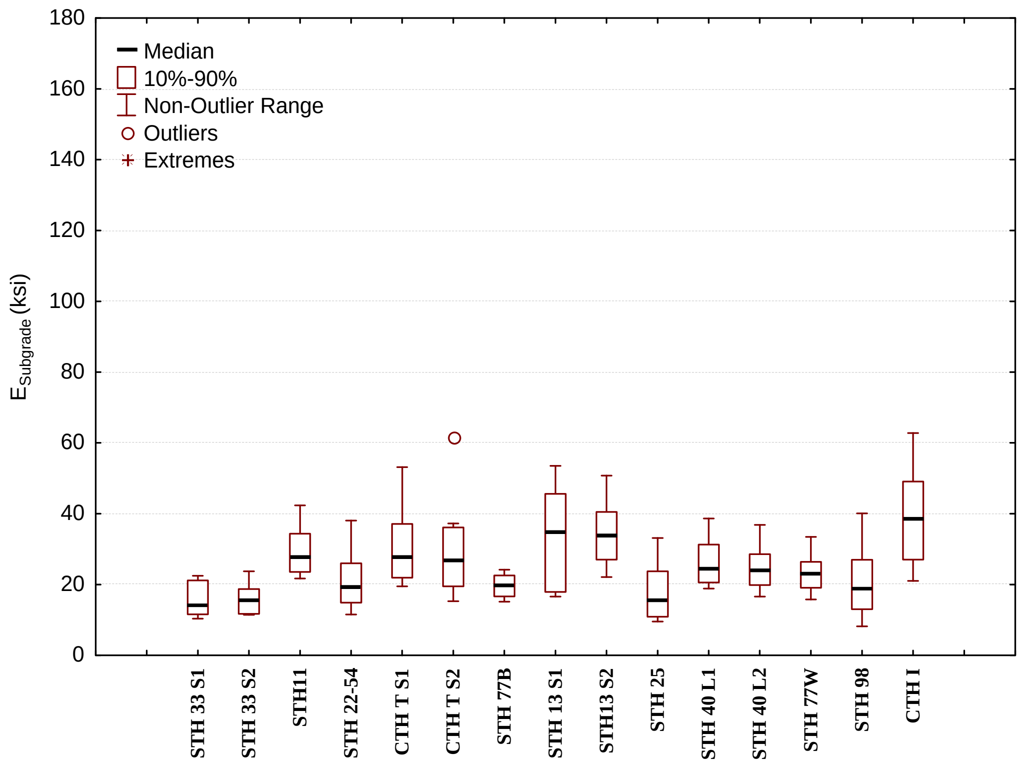

Figure 4.11: Whisker-box plot for 90 percentile of $E_{Subgrade}$ of the investigated projects.

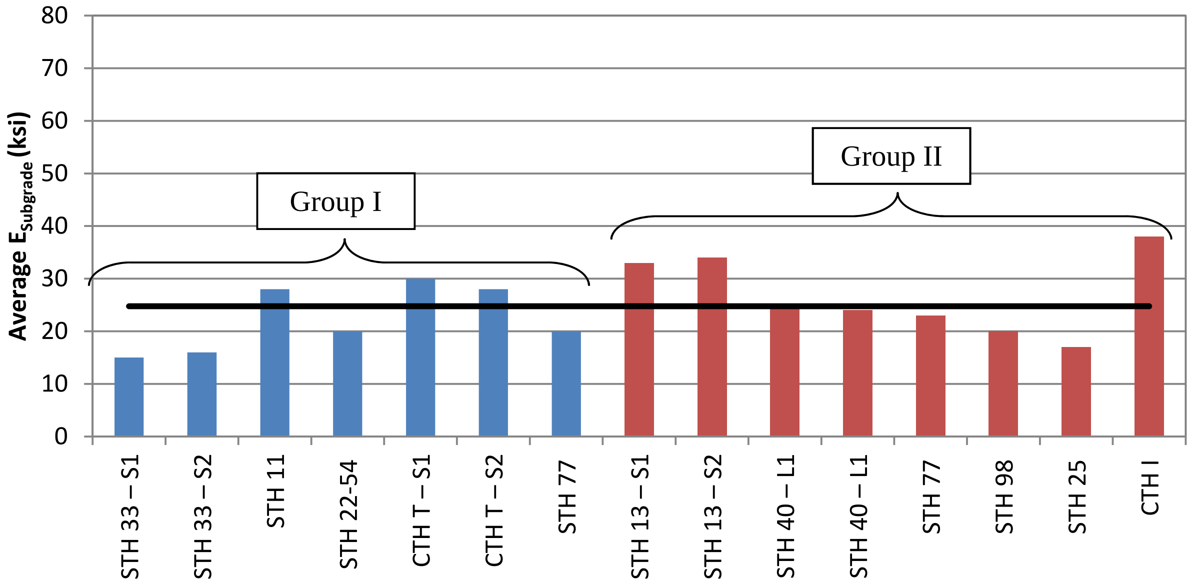

Figure 4.12: Average backcalculated subgrade modulus for the investigated HMA pavements.

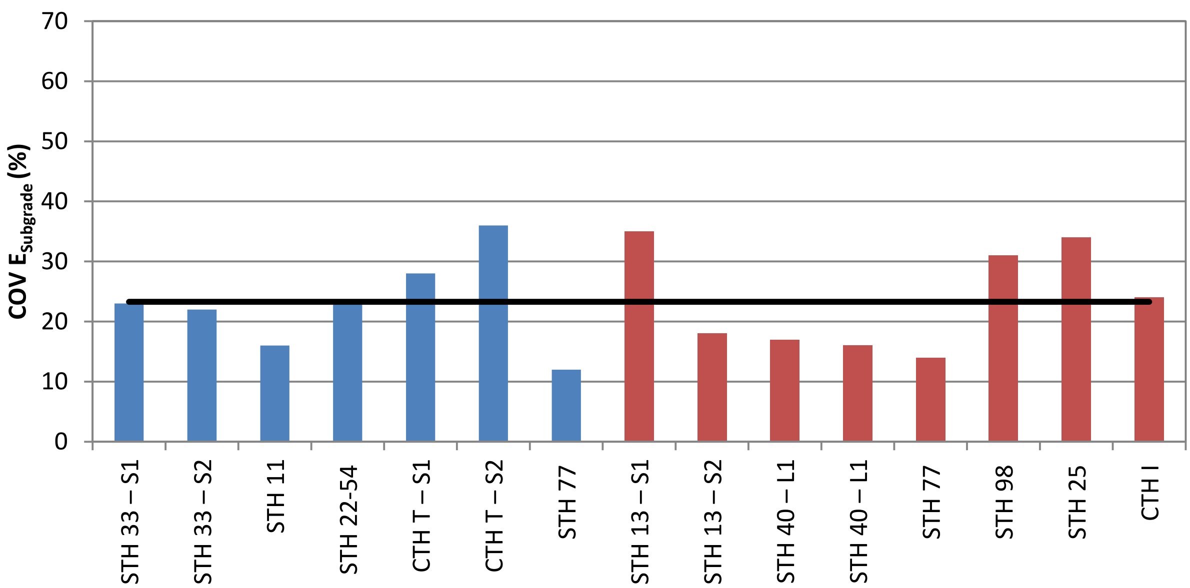

Figure 4.13: COV for backcalculated subgrade modulus for the investigated HMA pavements.

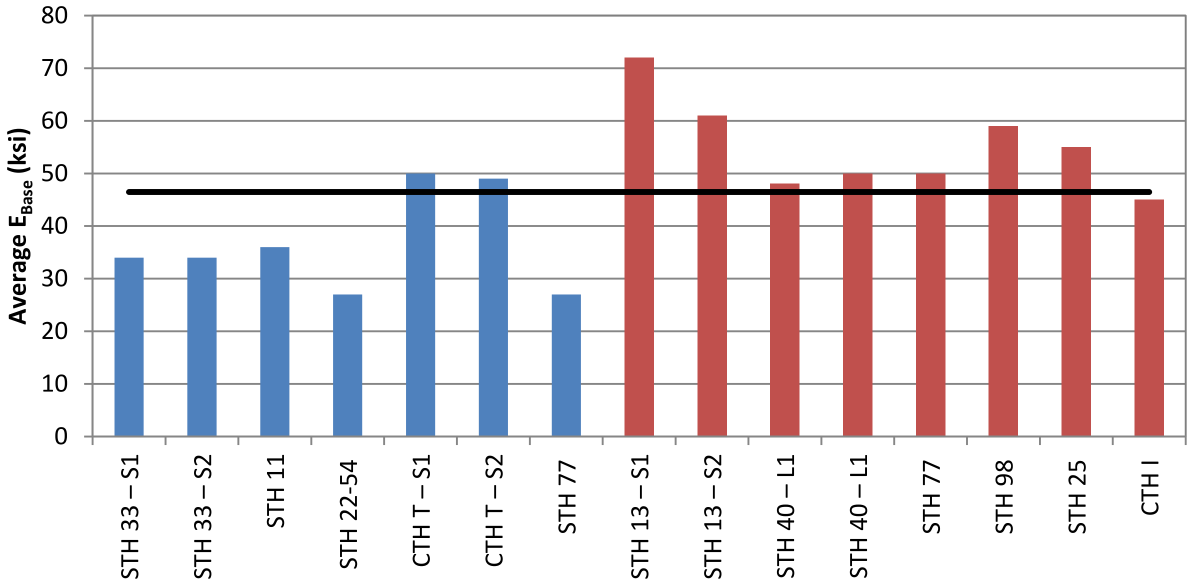

Figure 4.14: Average backcalculated base layer modulus for the investigated HMA pavements.

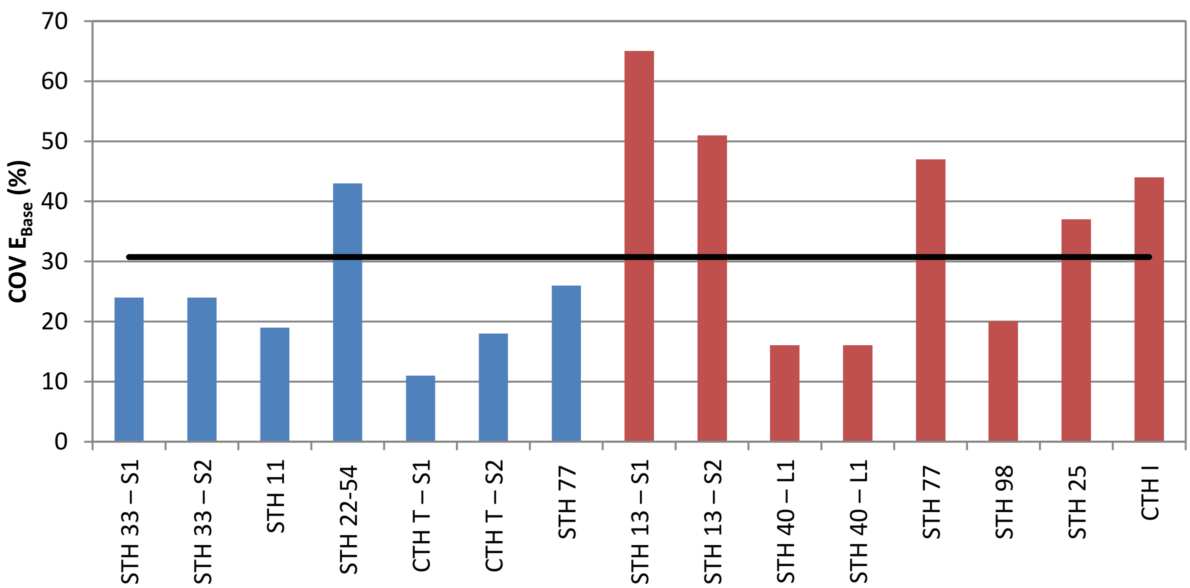

Figure 4.15: COV for backcalculated base layer modulus for the investigated HMA pavements.

The average aggregate base modulus of Group I projects is lower than that of Group II projects (36.7 ksi < 55 ksi), but the COV of E_{Base} for Group I is lower than that of Group II projects (23.6% < 37%). It is evident, based on this statistical information available, that the high variability of E_{Base} of Group II projects is an indication of the pavement performance, which is observed and quantified by the visual distress survey conducted in this research.

4.3 Visual Distress Survey Analysis

The research team conducted a visual distress survey analysis on all pavement sections included in this study. The target of this task is to calculate the pavement condition index (PCI) values for the pavement sections in order to investigate the potential influence of base compaction variability on the pavement condition. The authors realize that the PCI calculation protocol involves measuring distresses that may be attributed to factors other than base layer quality. Therefore, in the evaluation of the pavement surface distresses, the calculation of the PCI only involved distresses that are attributed to pavement foundation. For example, aggregate polishing, raveling, and bleeding are excluded from the process. On the other hand, depression, base related rutting (i.e., no lateral deformation is observed in the surface layer), and base-related cracking are included in the analysis. This is conducted in an attempt to isolate the effect of the base layer on final pavement condition. The results for the two groups of pavements are included in the following plot.

Figure 4.16 depicts three distressed pavements and one non-distressed pavement out of the investigated projects. The visual distress survey data were analyzed using the computer program MicroPAVER and PCI values were calculated. Table 4.3 presents the results of the analysis and the corresponding classification of the pavement condition.

Table 4.3: Results of the visual distress survey conducted on the investigated pavements.

Group	Project	PCI (%)	Pavement Condition	Remarks
I (Low performance variability of aggregate base)	STH 33 – LaCrosse	92	Good	
	STH 11 – Racine	97	Good	
	STH 22-54 – Waupaca	99	Good	
	CTH T – Grant	96	Good	
	STH 77 – Burnett	97	Good	
II (High performance variability of aggregate base)	STH 13 – Taylor	42	Poor	
	STH 40 – Rusk	94	Good	Ride Quality
	STH 77 – Washburn	68	Fair	
	STH 98 – Clark	26	Very Poor	
	STH 25 – Dunn	21	Serious	
	CTH I – Ozaukee	92	Good	Ride Quality

(a) STH 98

(b) STH 25

(c) STH 77 Burnett County

(d) STH 77 Washburn County

Figure 4.16: Pavement condition for selected number of the investigated HMA projects.

Pavements on STH 40 and CTH I exhibited profile irregularities that were observed in the first project and through a ride test on the second project. Figure 4.17 depicts the pavement profile irregularities observed on STH 40; therefore, the PCI index for these projects was modified to reflect the pavement profile irregularities. Figure 4.18 shows the modified PCI values for the investigated projects. Inspection of the figure indicates a cluster based on the pavement group. Group I pavements yielded a minimum PCI value of 92. For Group II, the PCI values range from 21 to 94. The trend demonstrated in Figure 4.18 indicates that the although on average Group II pavements demonstrated higher values of modulus as calculated using the FWD results, the higher variability may have created internal effects within the pavement where cracking has occurred. The more uniform Group I pavements are performing better compared with the Group II projects. To demonstrate the relationship between the measured surface distresses and the variability in the base quality, a damage indicator is calculated by subtracting the PCI value from 100 as depicted in Figure 4.19.

The damage index is calculated according to ASTM D6433, which allows pavement condition to be objectively rated on a scale of 0 to 100 based on the severity of distresses observed. According to ASTM D6433, there are 19 distress types identified for pavement evaluation. The severity of each distress is calculated using standard protocol. Then a deduct value is determined based on the extent and level of severity of distresses. The deduct values is subtracted from 100 to determine the PCI value for the pavement. The 19 distress types include distresses that are related to factors other than the base layer structural stability, such as raveling, utility cuts and patches, bleeding. For the purpose of this study, ASTM D6433 procedure is used considering only the following distresses:

1- Longitudinal Cracking
2- Rutting
3- Alligator Cracking
4- Depression
5- Bumps and sags
6- Lane/Shoulder Drop off
7- Potholes.

It is important to note that the projects surveyed for this research did not experience all the mentioned above distresses. Only the first three distresses were observed.

Figure 4.17: Pavement profile irregularities on STH 40.

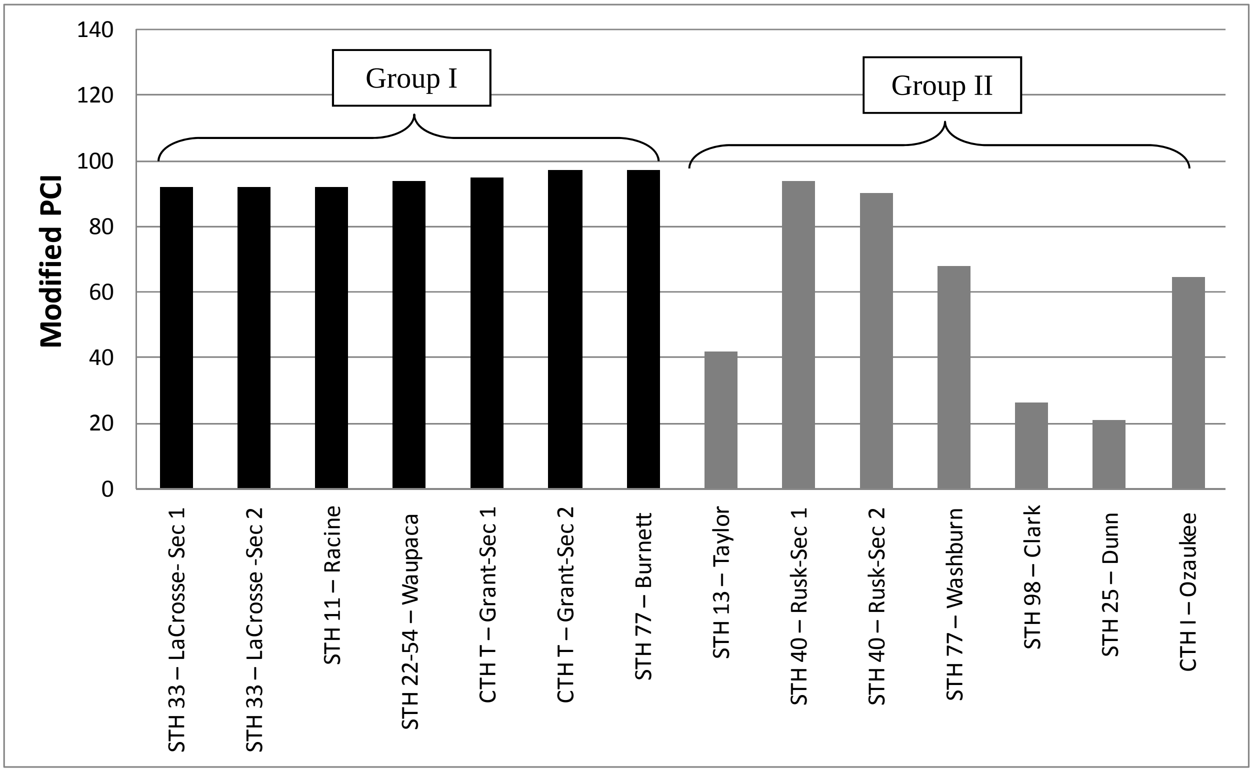

Figure 4.18: Calculated modified PCI for all pavement sections included in the study.

Figure 4.19 demonstrates a trend between the damage index and the calculated variability of base layer modulus. It is important to note that two projects exhibited significant damage. These projects were removed from the analysis/correlation since they sway the relationship. These projects are STH 98 and STH 25. The plot shows an exponential increase in damage as the variability of the base quality increases. This is an expected trend that follows engineering judgment. It is important to note that projects of Group II are showing the most damage and variability. Two of the projects in Group II are showing damage index value of 10 or less. These projects still fit well in the trend. This analysis demonstrates that although the average modulus as backcalculated from FWD testing can be higher than that for other projects, the variability in the constructed base layer can have serious effect on the service life of the pavement.

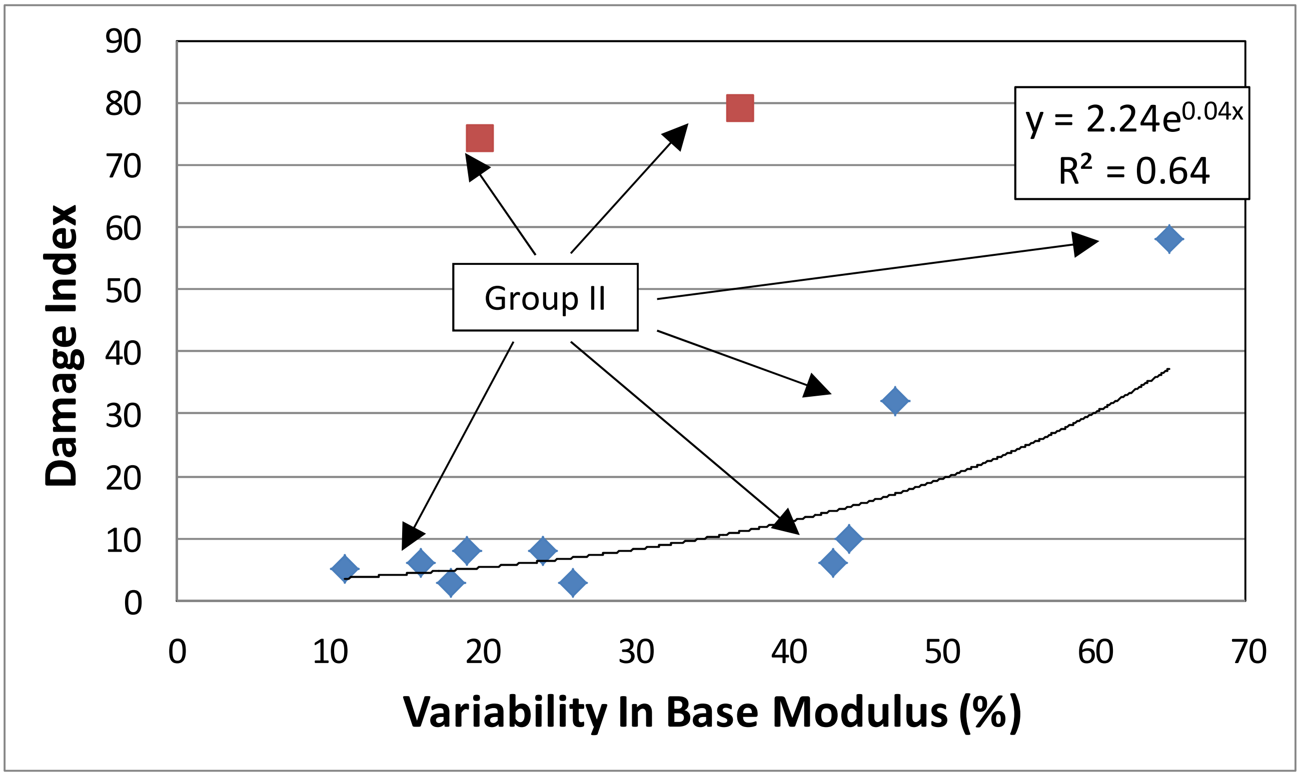

Figure 4.19: Relationship of damage index and base layer variability as measured by the coefficient of variation of calculated moduli for all projects.

It is important to note that the analysis of variance (ANOVA) was attempted on the collected data to conduct a thorough statistical analysis. This analysis is attempting to distinguish between the influence of modulus of the base measured and the variability of the measured modulus on the distress survey index values; however, since the data distribution did not show randomly normal distribution, the ANOVA could not be conduct.

Figure 4.20 shows the normal probability plot of the damage index measured from the PCI. The distribution of the data is clearly deviating from normality. Therefore, one way regression analysis was used to correlate the measured damage to variability in base modulus as shown in Figure 4.19. To validate that the relationship follows the basic regression assumption of normality, Figure 4.21 is presented. The plot demonstrates the normality of the residual error supporting the assumption.

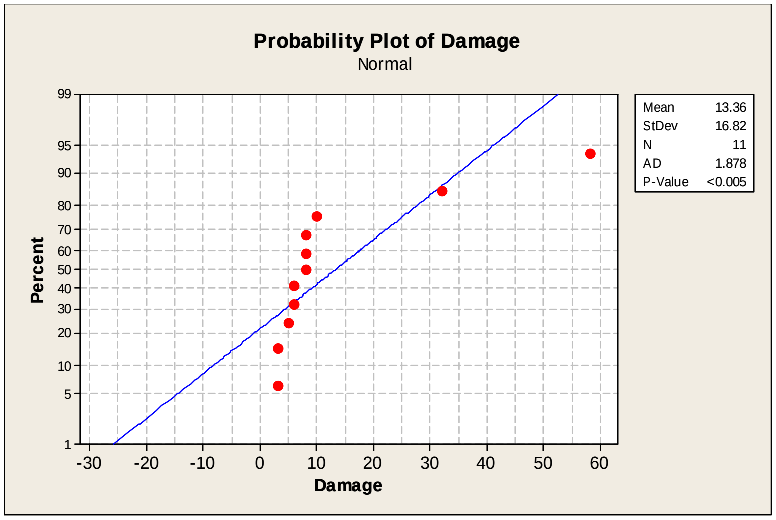

Figure 4.20: Normality test for damage index.

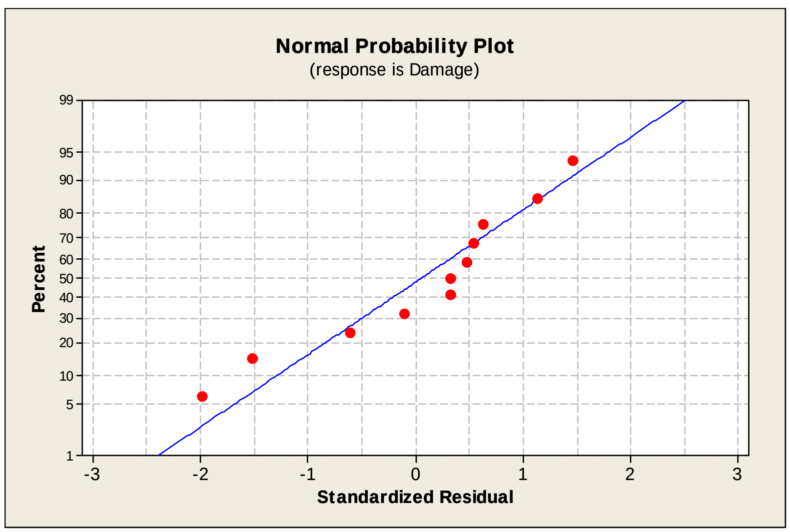

Figure 4.21: Normality test for regression analysis.

.

Chapter 5
Analyses of Field and Laboratory Test Results on Aggregate Base Materials during Construction

This chapter presents the results of the field and laboratory testing program on aggregate base materials conducted during construction. Field and laboratory test results for 10 projects are presented and analyzed. In addition, mechanistic-empirical pavement analyses are conducted to assess the effect of aggregate base layer modulus on long term pavement performance.

5.1 Field and Laboratory Testing Results

Pavements constructed in ten different construction projects were subjected to various tests in the field based on the availability of test equipment. Table 3.2 listed the investigated projects as well as their aggregate base layer thicknesses. Figure 3.4 presented the locations of these projects in Wisconsin. The research work plan called for three projects to be studied; however, more test sites were added for the benefit of the research. In this section, field and laboratory test results for CTH B only will be analyzed and presented because all the available test equipment were successfully used in this project. Detailed results for all individual projects are presented in Appendix B.

5.1.1 Aggregate Base Evaluation for CTH B – Woodville

Field and laboratory tests were conducted on the aggregate base layer during construction of CTH B near Woodville. The field testing program was executed after completing the construction of the aggregate base course layer on CTH B south of the intersection with I-94 as depicted in Figure 5.1. The constructed base course aggregate is 10-in. thick with the 7-in. asphalt surface layer to be paved. The finished pavement section, shown in Figure 5.2, includes the 10-in. thick aggregate base course layer constructed with 1.25-in. top size aggregate. Field tests on CTH B consisted of in place density measurements using sand cone method, LWD, GeoGauge, and DCP. Laboratory tests conducted on aggregate materials collected from the site included the following: grain size analysis, standard compaction test, and repeated load triaxial test to evaluate resilient modulus of aggregate compacted at maximum dry unit weight and optimum moisture content.

The results of grain size distribution for base aggregate materials of CTH B are depicted in Figure 5.3 along with WisDOT grain size specification limits. As indicated by the figure, the grain size distribution of the base aggregate is consistent with WisDOT specification requirements. Figure 5.4 presents the compaction curve for CTH B base aggregate materials. The figure shows the maximum dry unit weight (γ_{dmax}) to be 136.6 lb/ft^3 and the corresponding optimum moisture content w_{opt} is 8.75%, which is considered within typical values for base aggregate materials.

Figure 5.1: Location of field testing of the aggregate base layer during construction of CTH B near Woodville, WI.

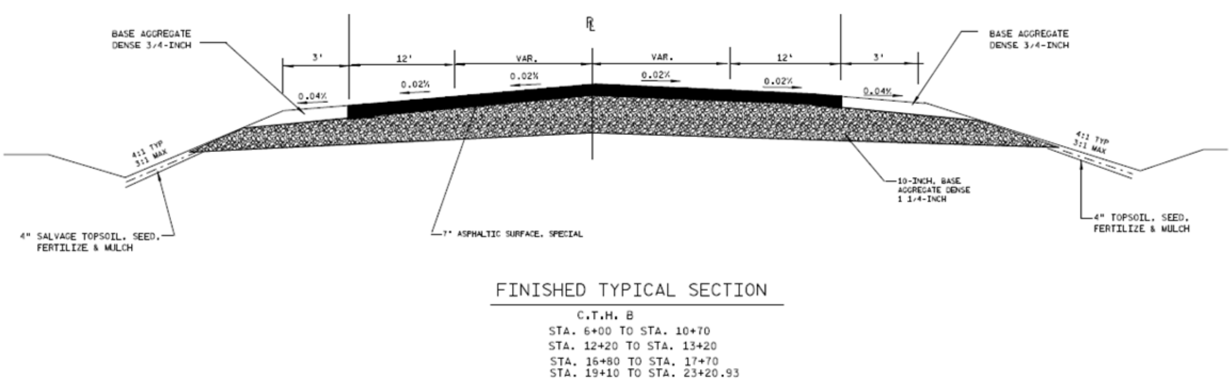

Figure 5.2: Finished typical pavement section for CTH B near Woodville, WI.

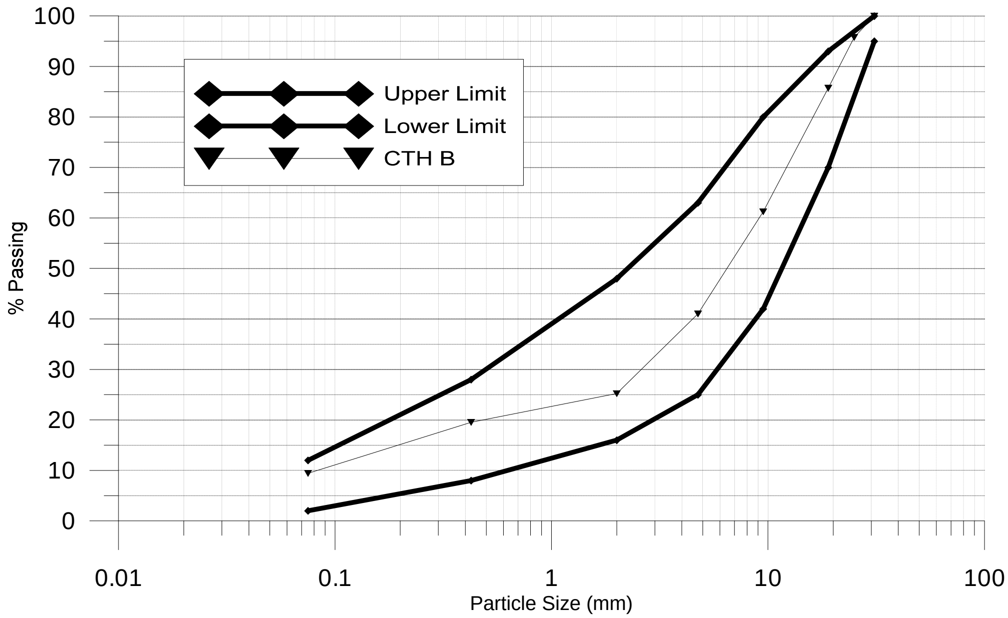

Figure 5.3: Grain size distribution for base aggregate material used at CTH B.

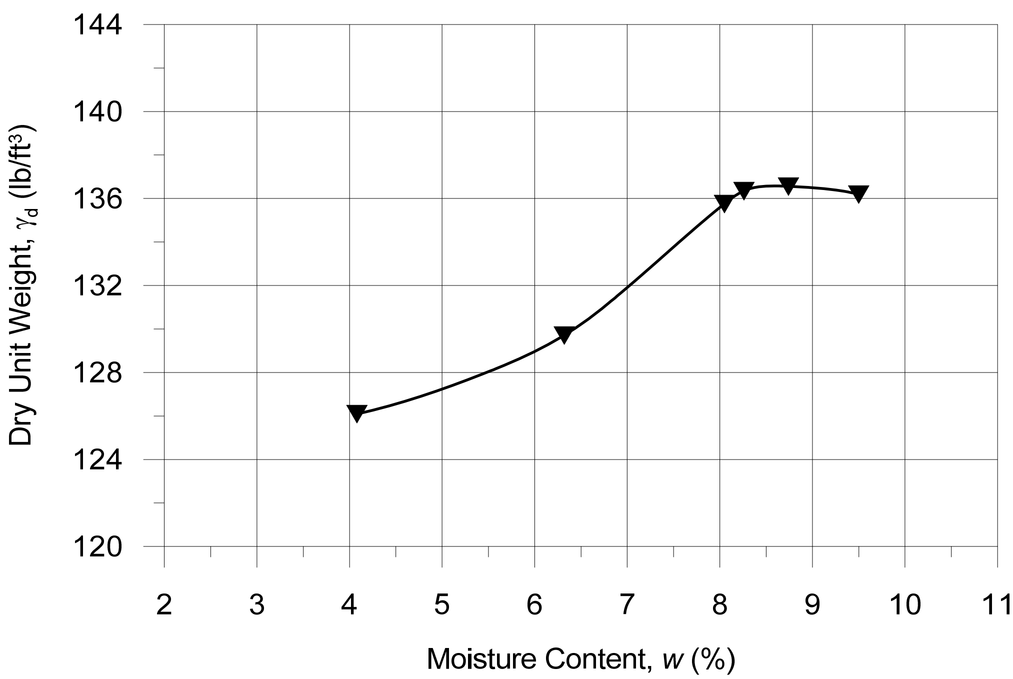

Figure 5.4: Compaction curve (AASHTO T 99) for base aggregate material used at CTH B.

The results of the repeated load triaxial test (AASHTO T 307) on the base aggregate collected from CTH B are shown in Figures 5.5. The aggregate specimen was subjected to repeated loading at average field density and average field moisture content. The resilient modulus values of CTH B base aggregate increase with the increase of bulk stress, which is consistent with typical unbound material behavior. Inspection of the figure indicates intermediate to high range of resilient modulus values were obtained. For example, for a confining pressure of 10 psi and bulk stress ranges between 40.5 and 60.8 psi, the resilient modulus varies from 35,740 to 41,945 psi.

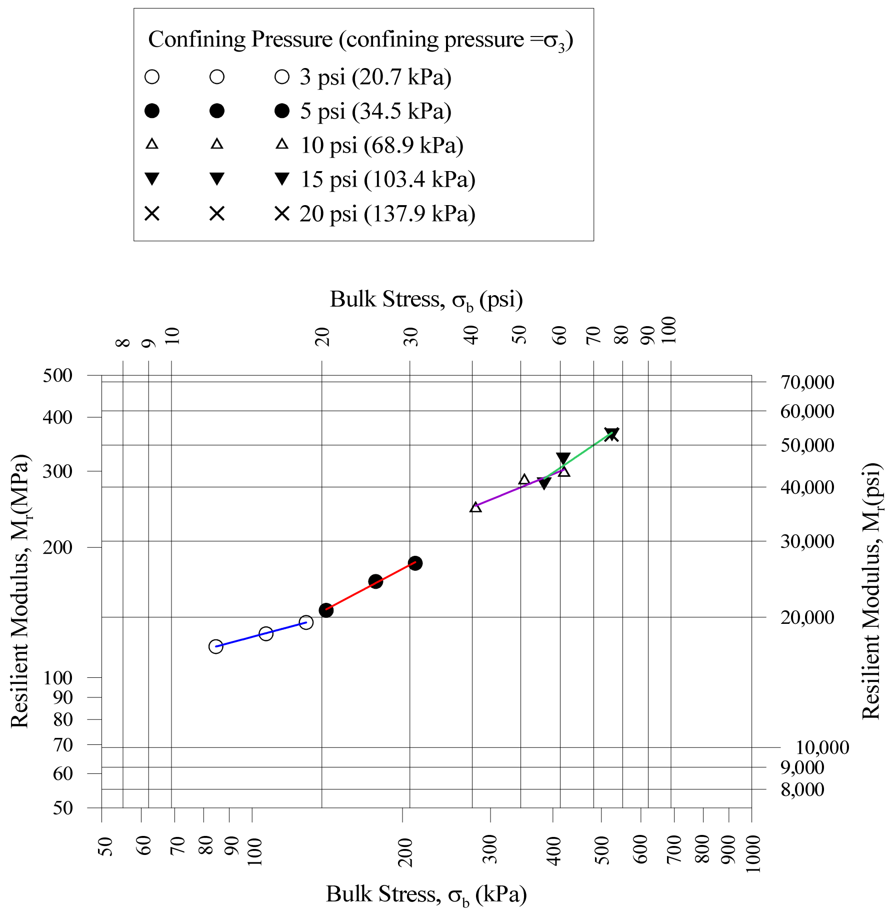

Figure 5.5: Results of repeated load triaxial test conducted on base aggregate specimen at average field density and moisture content from CTH B near Woodville, WI.

The field testing program in terms of number of test points and location varied from one project to another based on the availability of finished/constructed section of the aggregate base course layer. For CTH B, the field testing was conducted on 400-ft long section of the project south of the I-94 interchange. Figure 5.6 depicts the field testing plan executed on the aggregate base course layer on CTH B.

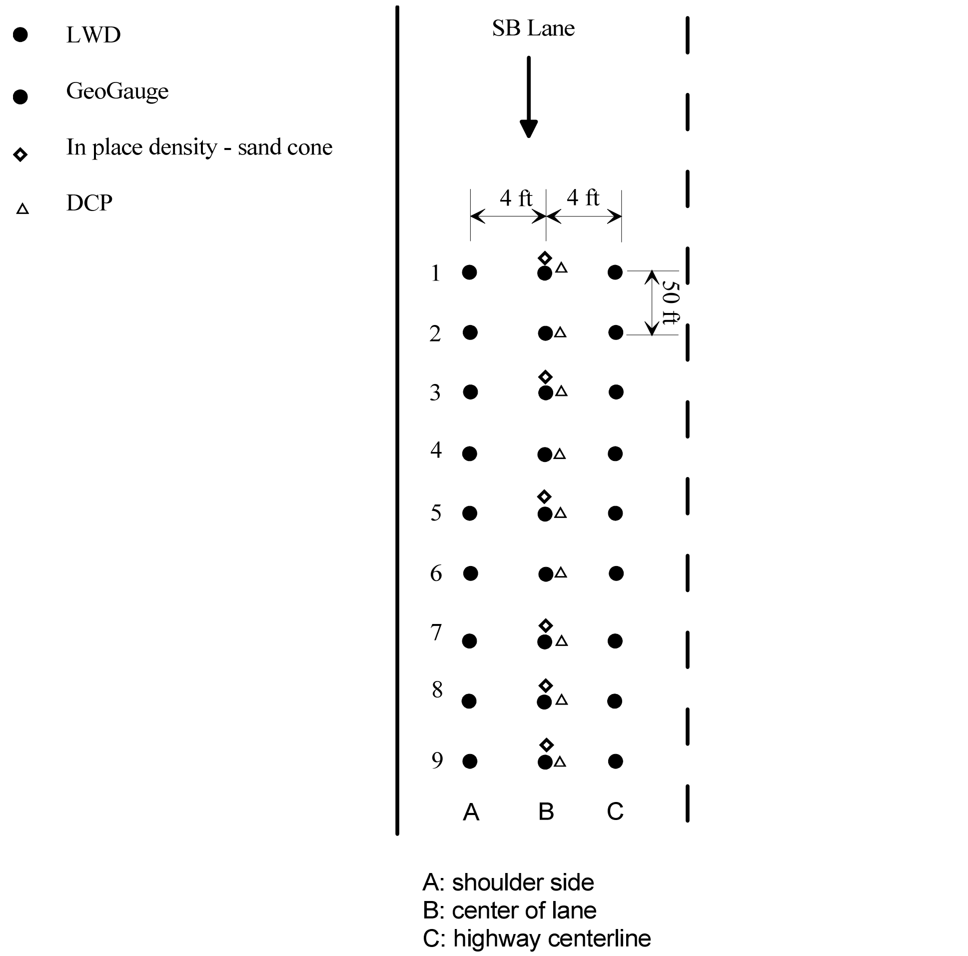

Figure 5.6: Field testing plan for the aggregate base course layer on CTH B.

In place density was evaluated at 6 test locations on the aggregate base course layer as shown in Figure 5.6. The dry unit weight (γ_d) and the corresponding field moisture content (w_{field}) were also determined. The field dry unit weight ranges from 121.81 to 134.93 lb/ft^3 while the field moisture content varies between 4.13 and 5.45%. Table 5.1 presents the results of the field unit weight measurements taken at the test points where the in-place density using the sand cone method was measured. The range of the dry unit weight is less than the maximum dry unit weight (γ_{dmax} =136.6 lb/ft^3 and w_{opt} = 8.75%) obtained from laboratory compaction test depicted in Figure 5.4. The relative compaction, R, was calculated for all test points using the following equation:

$$R = \frac{\gamma_{(d)field}}{\gamma_{dmax}} \times 100\% \qquad \textbf{(5.1)}$$

The calculated relative compaction values are presented in Table 5.1. Inspection of the test results show that the relative compaction varies between 89.2 and 98.8%. Figure 5.7 shows the variation of the relative compaction and field moisture content with distance along the center line of SB lane of CTH B. The relative compaction results indicate the variability of compaction for the aggregate base course layer.

Table 5.1: Summary of field unit weight testing at CTH B

Field Moisture Content, w_{field} (%)	In-place Dry Unit Weight $\gamma_{d(field)}$ (lb/ft^3)	Relative Compaction R (%)
4.71	134.93	98.8%
4.62	133.44	97.7%
4.13	124.07	90.9%
5.45	133.46	97.7%
4.80	121.81	89.2%
4.69	132.38	96.9%

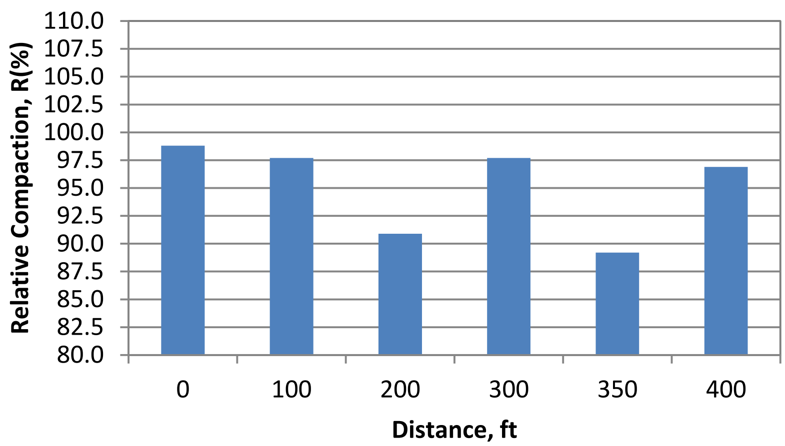

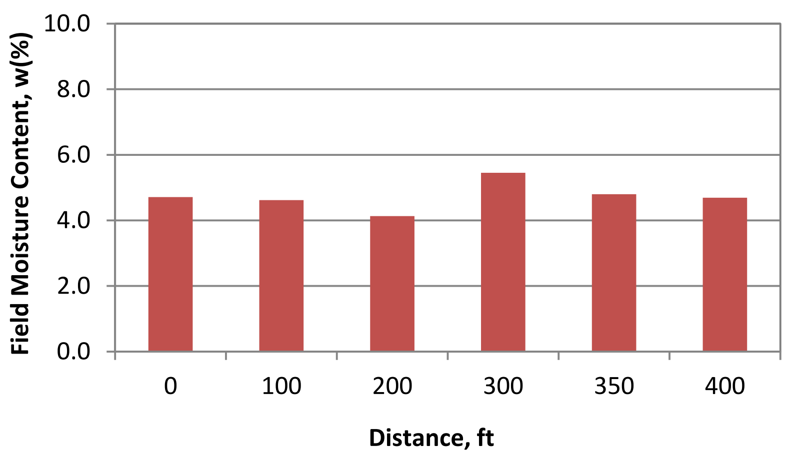

Figure 5.7: Variation of relative compaction and field moisture content with distance at test section on aggregate base layer on CTH B.

In-place density test results provided a density based characterization of the construction quality of the aggregate based course layer. The light weight deflectometer and the GeoGauge were used to provide a modulus based evaluation of the aggregate base course layer construction quality.

Table 5.2 presents the results of the LWD testing on aggregate base layer on CTH B. Analyses of the LWD tests were conducted using the Dynatest LWDmod software provided with the LWD equipment by Dynatest International. The average deflection under the loading plate D_0 varies from 6.1 to 16.58 mils. The calculated aggregate base layer modulus, E_o, ranges between 10.8 and 29.55 ksi. Since seven LWD tests were conducted at each test location, the COV was also calculated to evaluate the variation in LWD measurements. The coefficient of variation for these measurements ranges from 1.29 to 21.5%; the majority of the points with COV values were less than 5%, indicating good test repeatability at each location.

Table 5.2: Results of the LWD test on CTH B

Test Location	Test Position	Average Deflection D_o (mils)	COV (%)	Average Modulus E_o (ksi)	COV (%)
1	Center	13.07	8.70	13.62	8.30
	Right	11.16	2.31	15.80	3.13
	Left	10.59	3.45	16.50	3.43
2	Center	11.34	4.34	15.53	3.90
	Right	12.99	5.20	13.70	5.22
	Left	14.74	7.57	11.75	8.28
3	Center	11.25	3.52	15.65	3.42
	Right	13.83	3.77	12.71	3.78
	Left	13.15	4.94	13.33	5.27
4	Center	11.63	1.95	15.20	2.04
	Right	14.47	4.38	12.25	4.52
	Left	13.05	1.53	13.43	1.61
5	Center	11.30	25.60	16.46	14.10
	Right	11.89	4.02	14.60	6.28
	Left	10.82	2.33	16.71	21.50
7	Center	6.01	5.86	29.55	5.23
	Right	10.58	1.59	17.00	1.29
	Left	13.44	2.01	13.18	1.94
8	Center	10.29	1.05	17.40	1.58
	Right	11.35	5.92	15.75	5.76
	Left	13.80	4.50	12.83	4.82
9	Center	10.62	2.73	16.85	2.80
	Right	12.91	4.31	13.78	4.40
	Left	16.58	7.83	10.80	8.26

Figures 5.8 to 5.12 depict the range and average deflection under LWD loading plate, the range and average of calculated base layer modulus, and the corresponding coefficient of variation. The variability of stiffness of the aggregate base layer is evident from these figures, which demonstrate the variation of deflection and calculated modulus between test points.

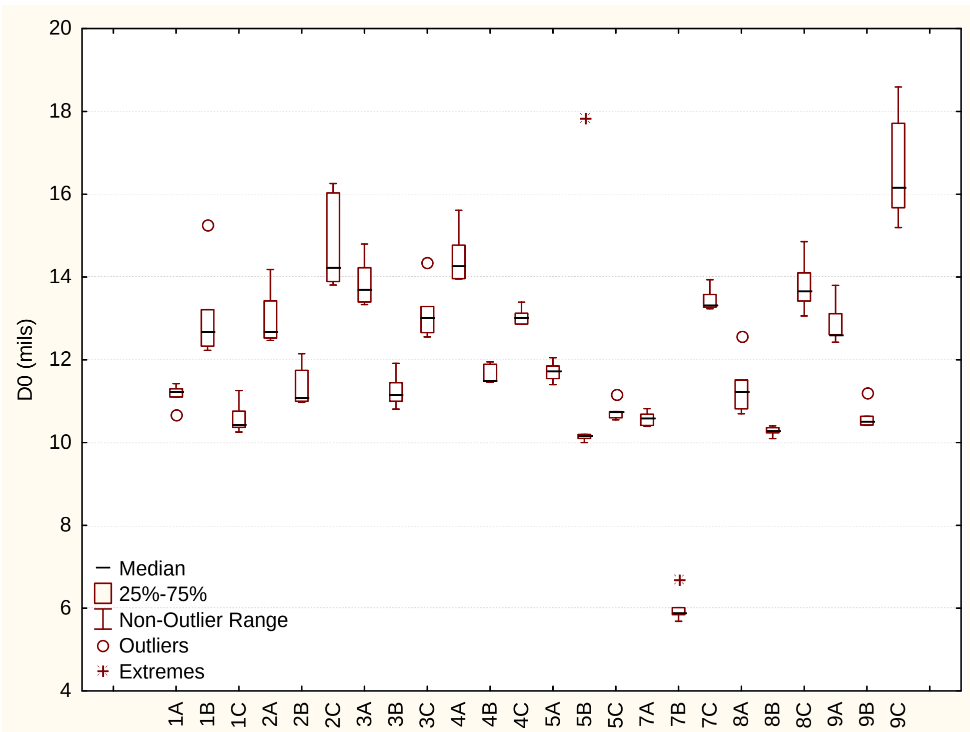

Figure 5.8: Whisker-box plot for the measured deflection under loading plate at LWD test points on the aggregate base layer, CTH B.

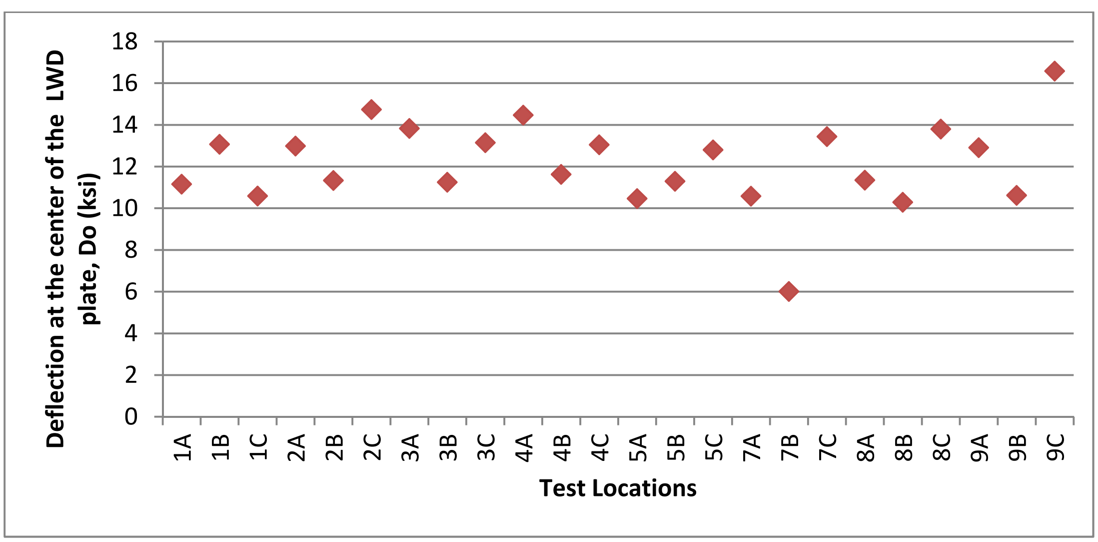

Figure 5.9: Distribution of average measured deflection under loading plate at LWD test points on the aggregate base layer, CTH B.

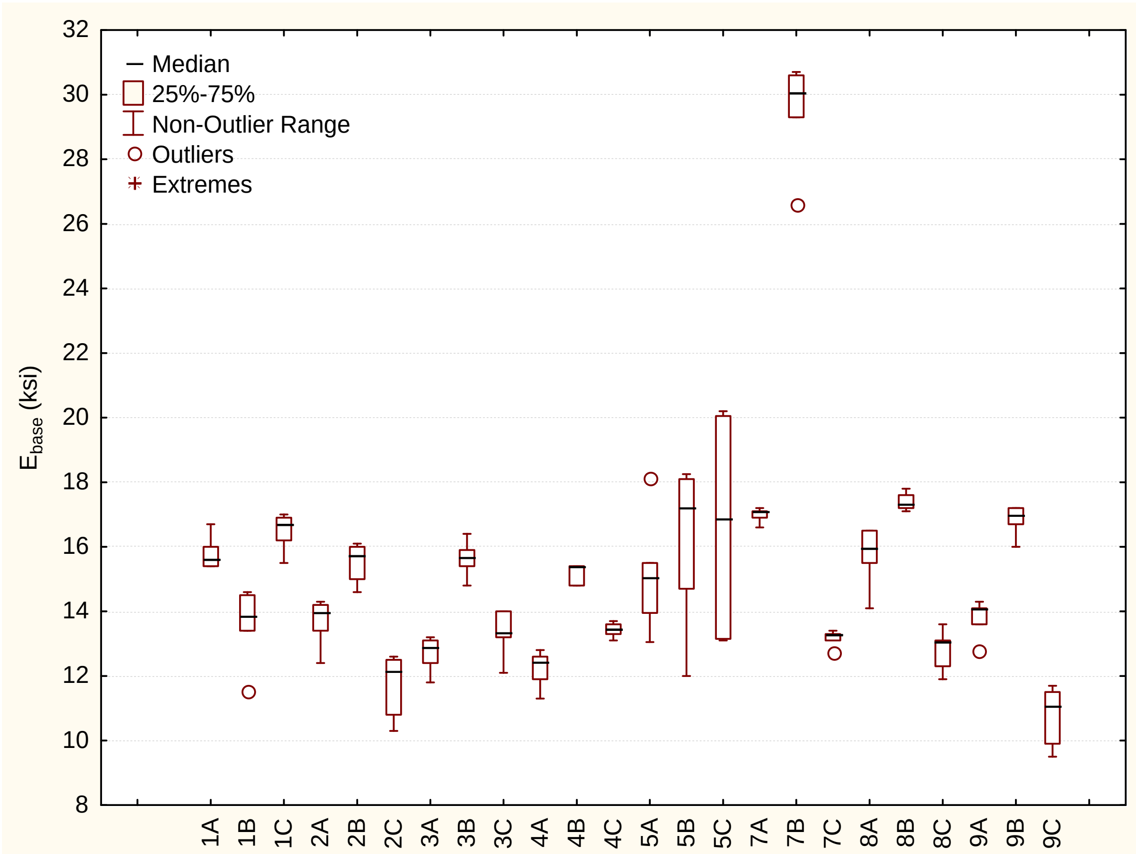

Figure 5.10: Whisker-box plot for the calculated aggregate base layer modulus from LWD tests at CTH B.

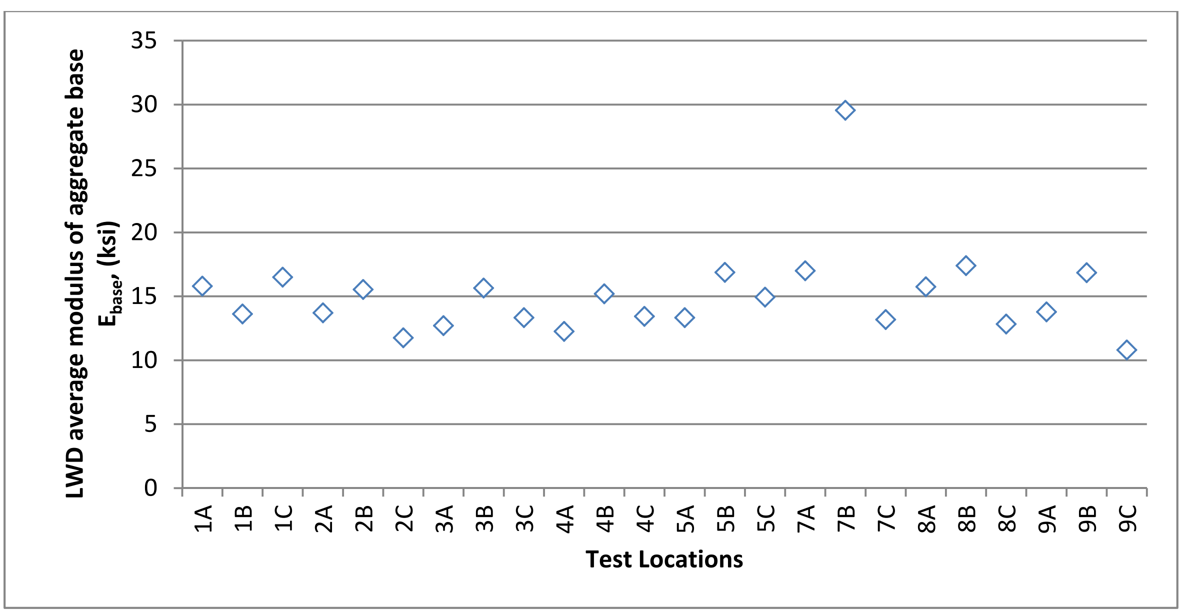

Figure 5.11: Distribution of average LWD calculated aggregate base layer modulus, CTH B.

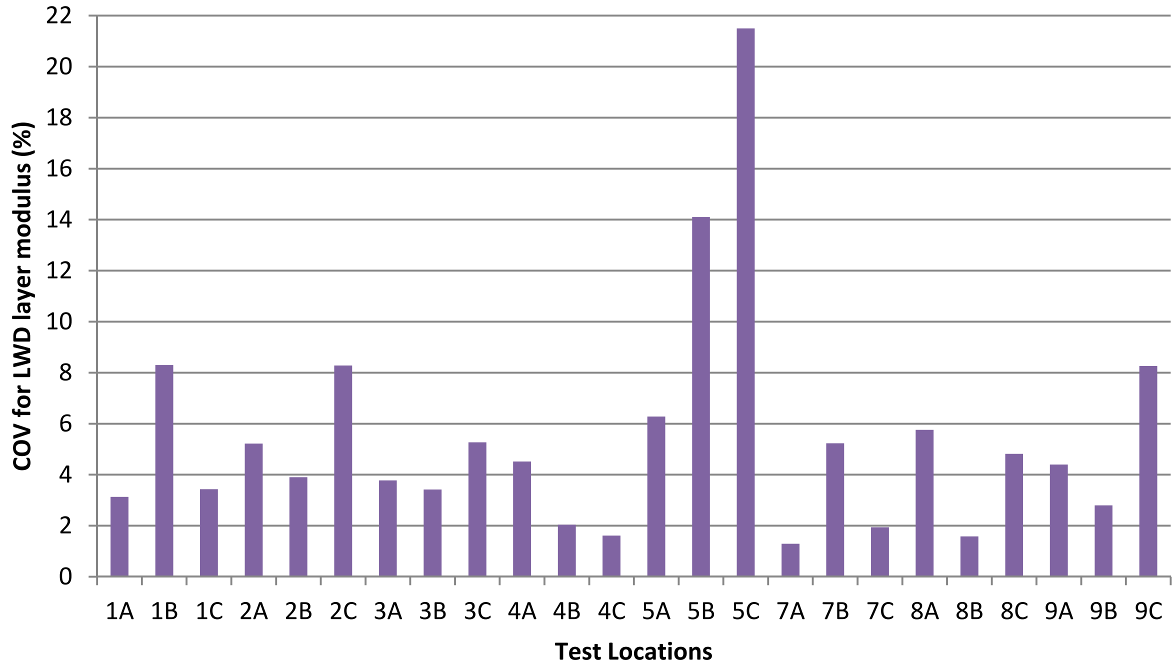

Figure 5.12: COV for the LWD calculated aggregate base layer modulus, CTH B.

The GeoGauge test was also used on CTH B to calculate the modulus of the aggregate base layer at different points after construction. The results are obtained directly from the device during measurement. Table 5.3 presents the calculated aggregate base layer modulus for the test points and the corresponding coefficient of variation. The aggregate base layer modulus varies between 7.82 and 19.92 ksi, which is lower than the range for the calculated values from the LWD test results due to only one test point. Figures 5.13 and 5.14 depict the average aggregate base layer modulus obtained by GeoGauge and the corresponding COVs, respectively. Inspection of Figures 5.13 and 5.14 shows that the distribution of base layer moduli calculated from LWD tests and measured by the GeoGauge is consistent and values show only "small variation." Figure 5.15 shows contour representation of the base layer moduli calculated from LWD and GeoGauge measurements. The maps indicate consistent results with ability of both devices to identify areas of higher layer moduli values around the distance of 300 ft. The area identified by LWD and GeoGauge with modulus values has also high density as shown by the relative compaction of the point tested at distance of 300 ft, which is 97.7%.

Table 5.3: Aggregate base layer elastic moduli obtained by GeoGauge measurement.

Test Location	Test Position	Average E (ksi)	COV (%)
1	Center	15.13	0.05
	Right	12.44	2.56
	Left	17.92	1.14
2	Center	9.86	2.08
	Right	7.82	2.17
	Left	12.98	2.23
3	Center	11.33	2.87
	Right	11.78	7.87
	Left	15.01	2.64
4	Center	12.11	7.71
	Right	15.55	6.78
	Left	14.05	8.96
5	Center	10.33	0.27
	Right	13.86	2.65
	Left	15.81	3.80
6	Center	14.89	7.17
	Right	13.73	14.42
	Left	15.54	5.69
7	Center	14.07	1.71
	Right	18.34	0.12
	Left	19.92	0.60
8	Center	15.47	3.75
	Right	12.34	14.21
	Left	15.88	18.22
9	Center	10.52	6.45
	Right	10.81	18.05
	Left	14.47	19.05

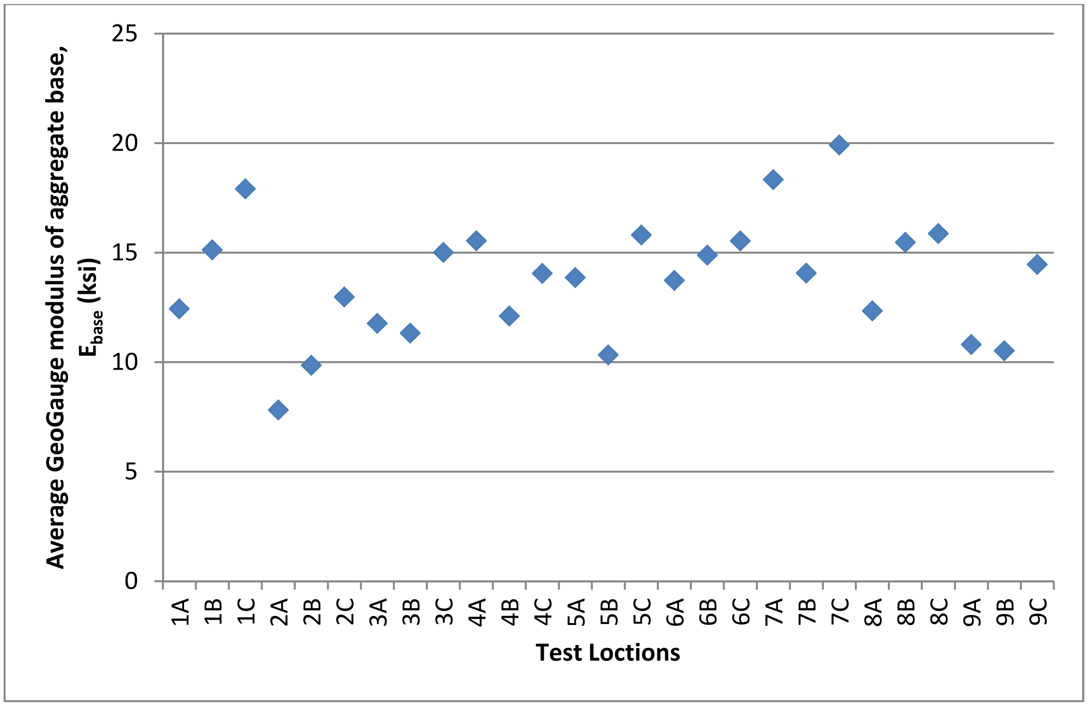

Figure 5.13: Distribution of average GeoGauge measured aggregate base layer modulus, CTH B.

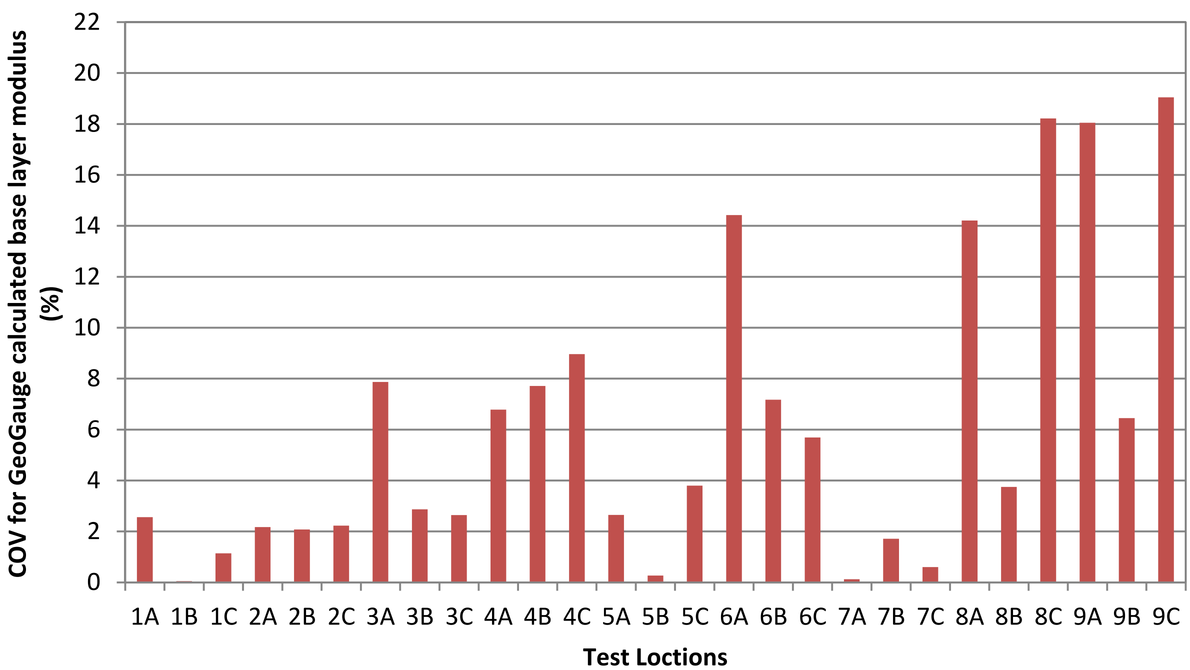

Figure 5.14: COV for the GeoGauge calculated aggregate base layer modulus, CTH B.

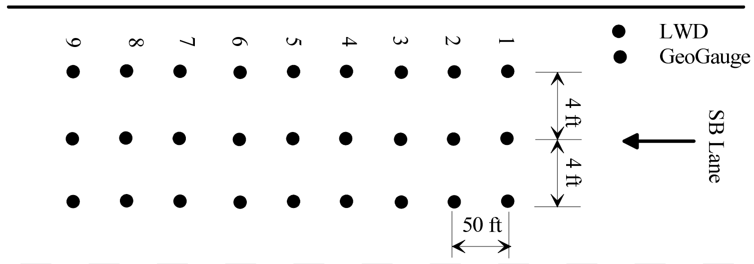

(a) Locations of test points

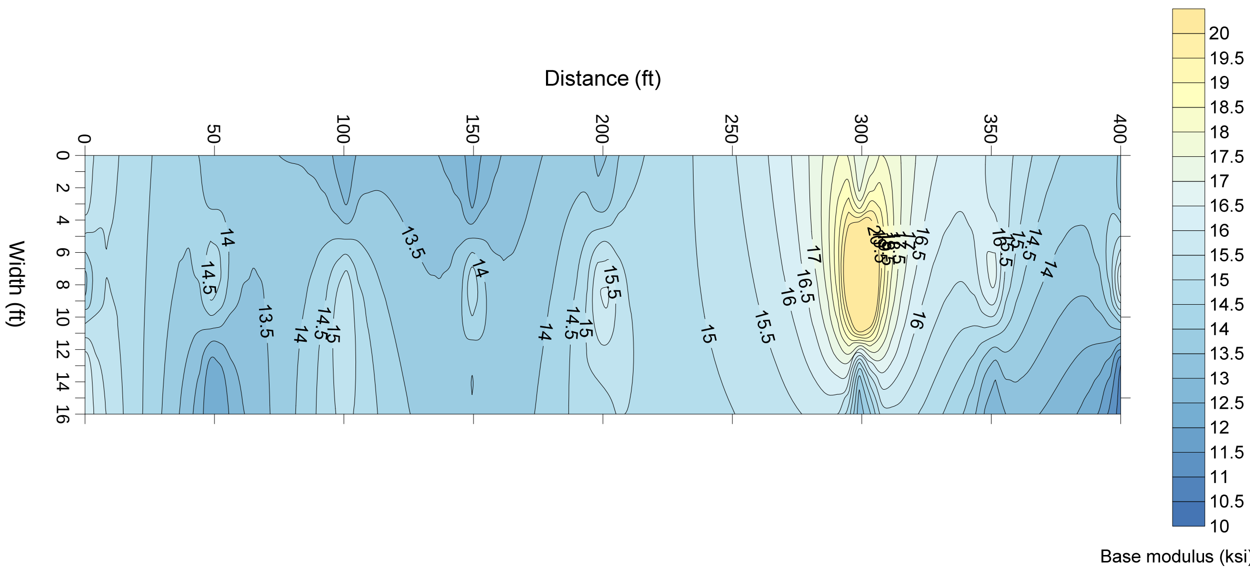

(b) LWD

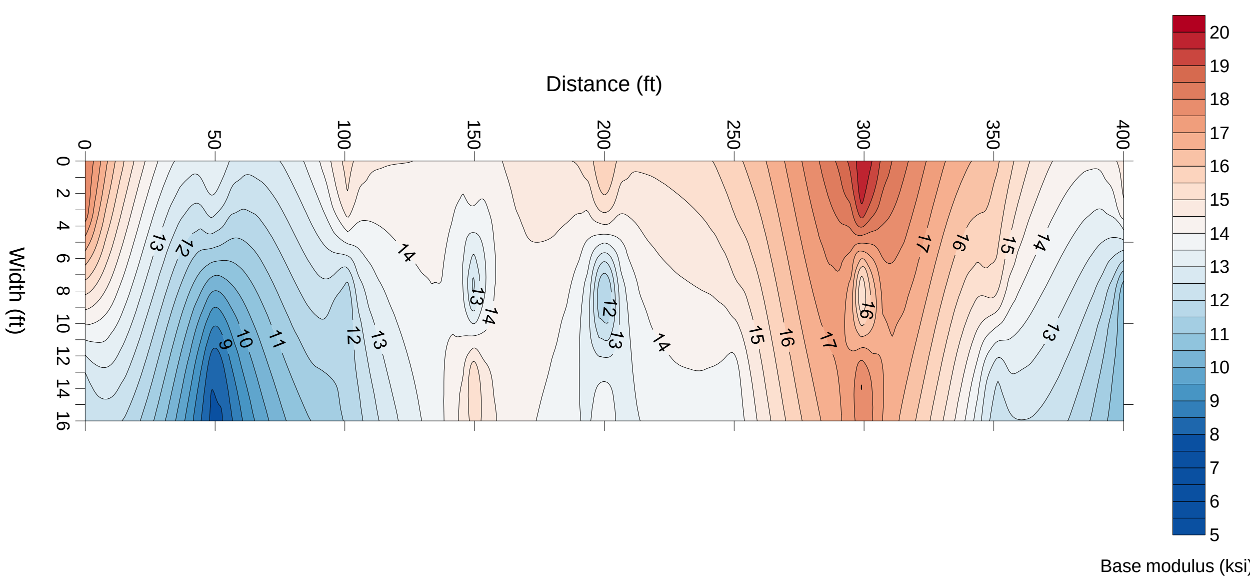

(c) GeoGauge

Figure 5.15: Contours of the calculated base layer modulus (E_{base}) based on LWD and GeoGauge measurements.

The results of the dynamic cone penetration tests on the aggregate base layer are shown in Figure 5.16. The penetration rate profile in inch/blow is presented with depth. The figure indicates the variability of the base aggregate material resistance to penetration and therefore, spatial variability in density and uniformity of the base materials in addition to the variability in density with depth. The resistance to penetration is low on the upper-part of the aggregate base layer, with an average penetration rate of about 0.4 in./blow for the upper 2.5-in. of the layer. Then, the penetration resistance increases with depth with an average penetration rate of about 0.22 in./blow, indicating the lower part of the base course layer is denser.

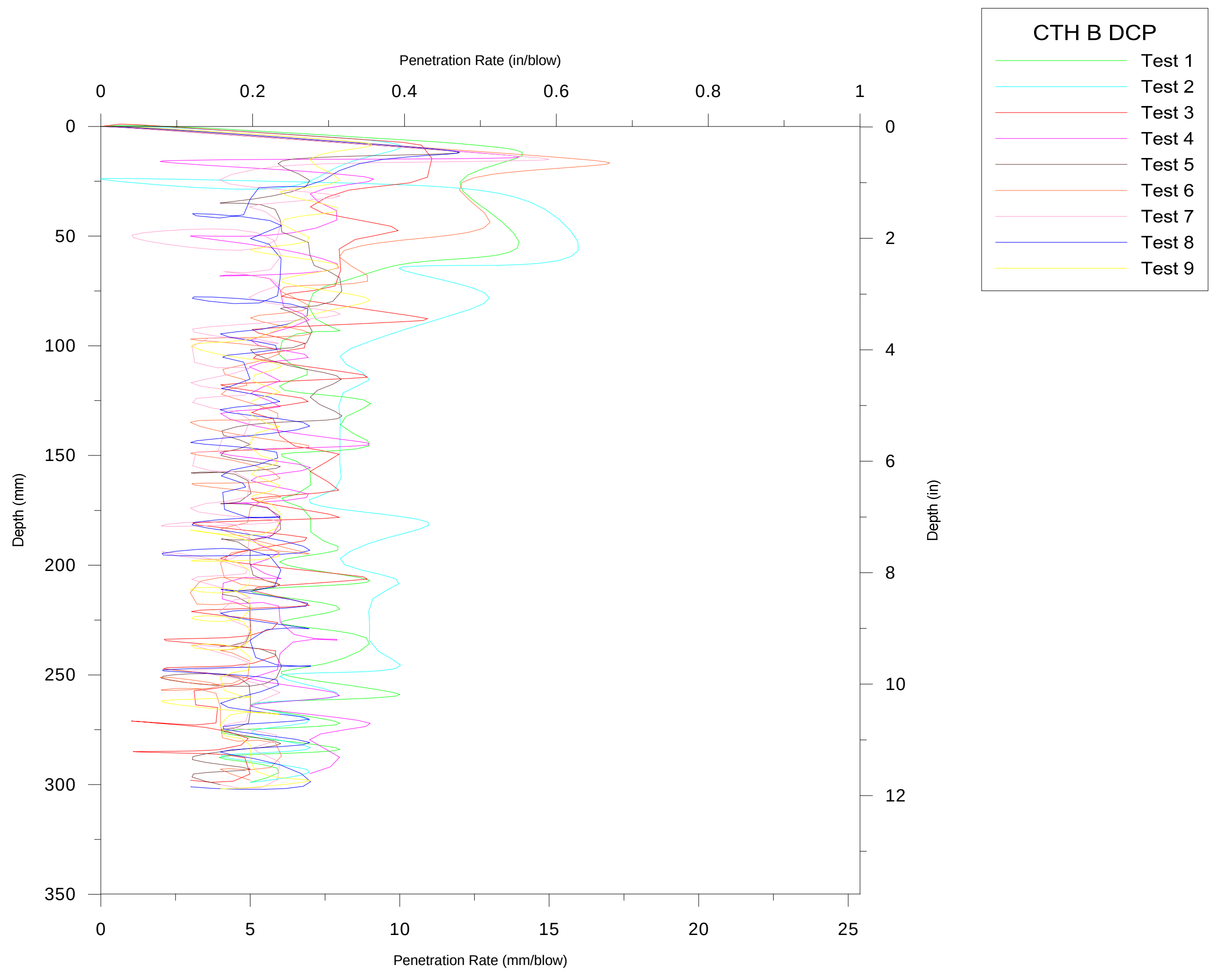

Figure 5.16: Penetration resistance with depth from DCP test at different point on the aggregate base layer on CTH B.

The dynamic cone penetration tests on the aggregate base layer were used to estimate the California Bearing Ratio (CBR) variation with depth using the U.S. Army Corps of Engineers formula. The estimated values of CBR are then averaged over three inches of aggregate base layer thickness to provide a profile of CBR with depth. Estimated CBR profiles with depth for DCP tests 1, 3, and 6 are shown in Figure 5.17. Examination of the figure demonstrates the variability in uniformity of base aggregate materials with depth. The upper-part of the base layer possessed lower CBR values of 23 and 27% for tests 1 and 3, respectively. The CBR values increased slightly with depth for test point 1 to reach 40% at the bottom of the layer, while the increase was significant and reached 95% at the bottom of the base layer at test point 3. For test point 6, the variation with depth of CBR was low, with 27% CBR at the upper-part of the base layer, increasing to about 56% in the middle of the layer, and increasing to 66% at the bottom of the base. This demonstrates the spatial variability of the aggregate base constructability in terms of density (state of compactness) and modulus and the variability of these parameters with depth.

5.1.2 Aggregate Base Evaluation for All Investigated Projects

The testing program described for CTH B was conducted on nine other projects but the scope of the tests varied. For example, LWD tests were conducted on five projects while GeoGauge tests were performed on two projects. The number of test points and the length of the test sections varied depending on the circumstances associated with each individual projects; however, the number of test points and the length of test sections were considered satisfactory for the purposes of this work. In all cases, the length of the test sections ranged between 400- and 1,200-ft.

The results of grain size distribution for base aggregate materials for all investigated projects are depicted in Figure 5.18 along with WisDOT grain size specification limits. As indicated by the figure, the grain size distributions of the base aggregate for all projects are within WisDOT specification limits.

The results of the laboratory compaction test on the aggregates collected from all investigated projects are depicted in Figure 5.19. Inspection of the figure shows large variations of the maximum dry unit weight (γ_{dmax}) and optimum moisture content w_{opt} among the investigated projects. The range of γ_{dmax} is between 133.8 lf/ft^3 (for STH 33 in Port Washington/Saukville) and 149.2 lb/ft^3 (for CTH I – USH 45 in Larsen). The optimum moisture content also varies between 6.2 and 8.75%. The results of the laboratory and field compaction tests on all projects materials and sites are summarized in Table 5.4. The relative compaction, which quantifies the quality of construction in terms of achieved state of compactness of aggregate particles within the base layer, is also presented. The relative compaction for the investigated projects varies between 82.6 and 109.1% indicating spots/areas that were lightly compacted and areas that were heavily compacted. The relative compaction spatial variability along the investigated projects is shown in Figure 5.20.

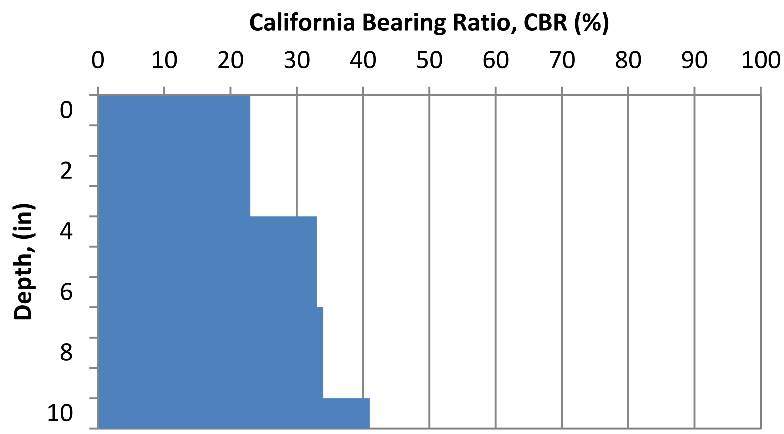

Test 1

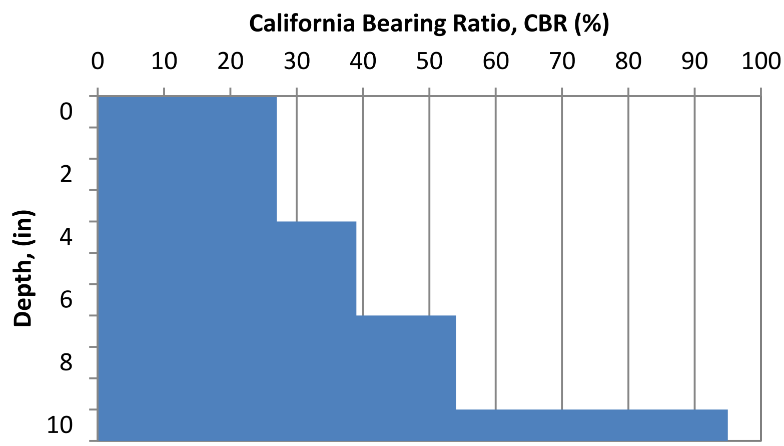

Test 3

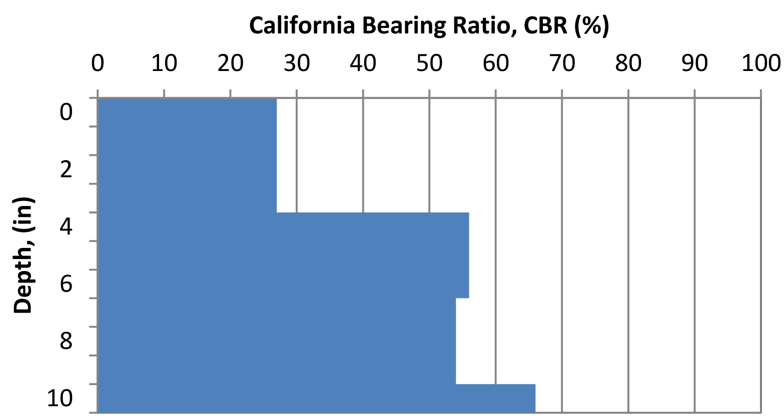

Test 6

Figure 5.17: Distribution with depth of estimated CBR from DCP test for the aggregate base layer on CTH B.

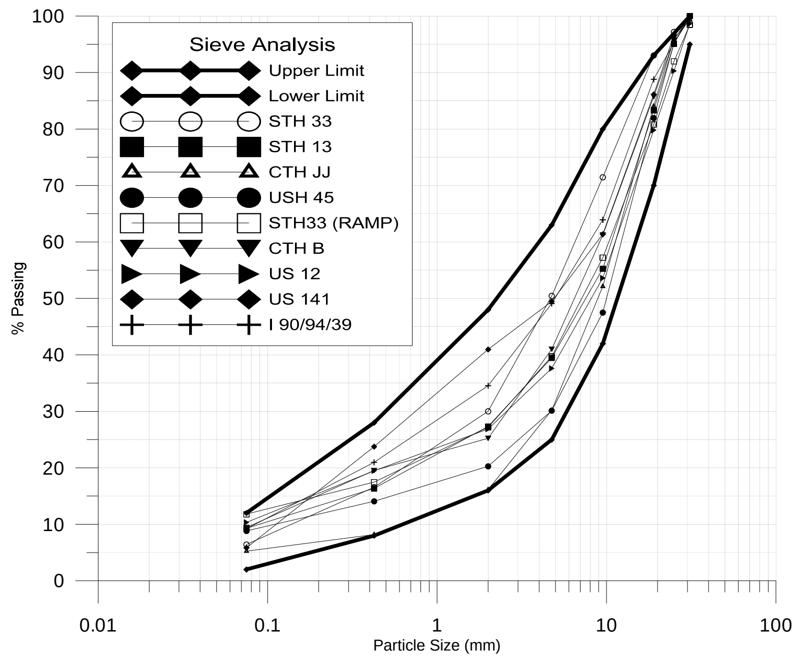

Figure 5.18: Grain size distribution for base aggregate materials collected from the investigated project sites.

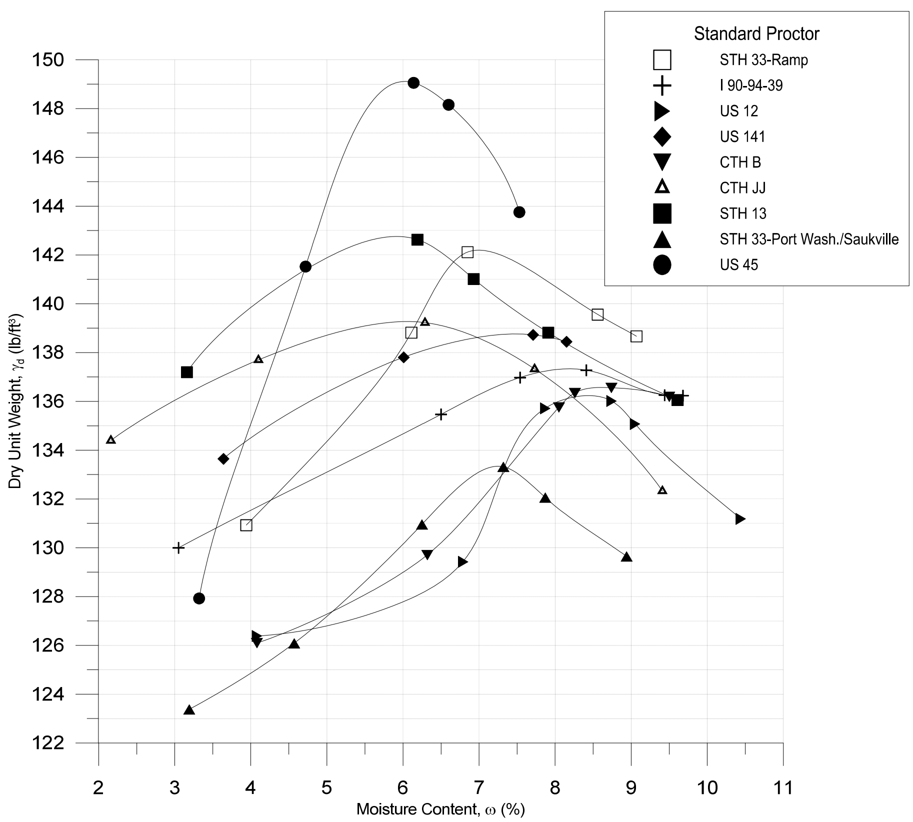

Figure 5.19: Results of the laboratory compaction tests (AASHTO T 99) on the investigated base aggregates materials.

Table 5.4: Result of the laboratory and field compaction test on the base aggregate materials.

Project	Laboratory Compaction Test		Field Compaction		
	γ_{dmax} (lb/ft^3)	w_{opt} (%)	Point	Relative Compaction %	Moisture Content (%)
STH 13 (Spencer)	142.6	6.35	1	86.9	7.18
			3	96.9	9.21
USH 45 (Larsen, Appleton)	149.2	6.30	1	97.5	4.10
			3	85.7	4.43
			5	82.6	4.05
			7	91.2	4.26
			9	87.5	4.65
			11	90.1	3.69
CTH JJ (Appleton)	139.2	6.20	1	90.3	7.41
			2	86.9	4.5
			3	101	6.49
			4	100.8	6.19
			5	103.9	6.92
			6	95.2	7.92
			7	93.8	3.75
			8	91.5	4.9
			9	101.2	5.57
			10	96.7	5.73
			11	92.8	3.89
			12	100.3	4.61
STH 33 (Port Washington)	133.6	7.35	1	94.3	7.94
			3	93.2	7.80
			5	94.8	7.66
			7	91.5	7.24
			9	86.6	7.00
			11	94.7	6.76
STH 33 Saukville	133.6	7.35	1	89.8	5.06
			3	94.6	5.91
			5	98.2	6.31
			7	101.8	7.51
			8	102.1	8.24
			9	90.4	6.48

Table 5.4 (cont.): Result of the laboratory and field compaction test on the base aggregate materials.

Project	Compaction Test		Field Compaction		
	γ_{dmax} (lb/ft³)	w_{opt} (%)	Point	Relative Compaction %	Moisture Content (%)
US 12 (Gammon)	136.15	8.3	1	90.9	4.79
			3	94.0	5.93
			5	90.3	5.9
			7	89.2	5.34
			9	97.1	2.85
			11	90.3	3.69
CTH B (Woodville)	136.56	8.75	1	98.8	4.71
			3	97.7	4.62
			5	90.9	4.13
			7	97.7	5.45
			9	89.2	4.8
			8	96.9	4.69
USH 151 I-39/90/94 (Two Projects)	137.3	8.2	1	98.0	3.49
			3	96.8	2.34
			5	92.2	2.87
			1B	97.0	2.7
			3B	94.0	3.65
			5B	102.0	2.9
STH 33 Saukville (ramp)	142.12	6.85	1	94.8	2.2
			3	90.9	2.99
			5	93.4	2.66
			7	89.4	3.17
			9	84.9	2.98
US 141 (Beecher)	138.8	7.8	1	104.7	3.58
			3	105.6	2.5
			5	109.1	2.48
			7	108.2	2.3
			9	100.3	2.49

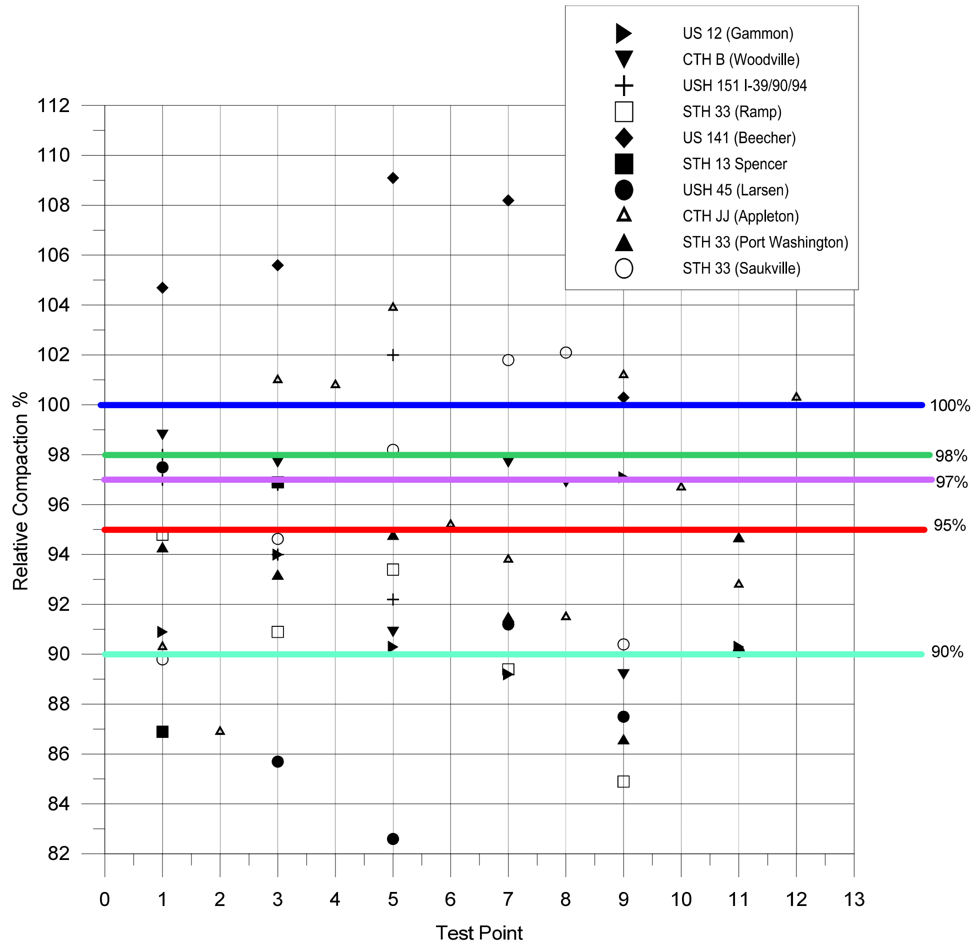

(a) Variation of field compaction within typical specification limits

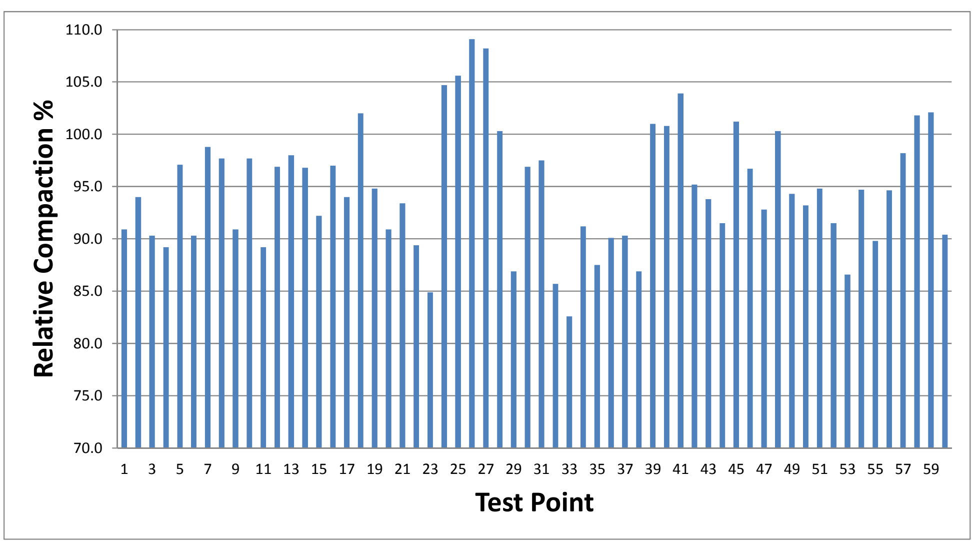

(b) Relative compaction for all investigated test points

Figure 5.20: Spatial variability of field compaction as indicted by the relative compaction.

The construction quality/uniformity of aggregate base course layers of the investigated projects varies significantly, as indicated by the various test results. A density-based evaluation provided evidence of this spatial variability/non-uniformity of the investigated aggregate base layers. In addition, layer moduli values calculated using different test methods led to the same conclusion. The spatial variability of the base layer construction quality can be evaluated using the widely used method of evaluating the field compaction/density.

Inspection of Figure 5.20 indicates that the results from all projects vary significantly. Imposing relative compaction limits on the test results can quantify the construction quality of the base layers. For example, within all test points in all projects, 17% exhibited relative compaction of less than 90%, which is considered insufficient. On the other hand, 54% of the test points possessed relative compaction values above 95%, indicating good compaction quality. This demonstrates the presence of high variability in the constructed base and therefore the significant need to establish/implement measures to assess and evaluate the quality of constructed aggregate base course layers. The base compaction survey conducted by the research team showed that 93% of the state highway agencies in the U.S. and Canada that implement density-based specifications require minimum of 95% γ_{dmax} for aggregate base acceptance. This percentage decreases to 49% when 98% γ_{dmax} is required. It should be noted that spatial variability of density of the constructed base layers is affected by many factors, including aggregate characteristics, compaction energy, moisture content, and lift thickness. The spatial variability of the field moisture content along the investigated test points is presented in Figure 5.21.

Modulus-based characterization of construction quality of aggregate base layers is also evaluated for five of the investigated projects. Figure 5.22 depicts the spatial variation of the calculated layer modulus from LWD tests. It should be noted that these points are located in different projects. Inspection of the figure demonstrates the variability of the calculated layer modulus with the individual project and among the investigated projects, with most of the values falling in a range between 10 and 30 ksi. The range of base layer moduli calculated values from LWD tests is between 7.95 and 65.37 ksi with an average of 19.7 ksi. Repeatability of the tests was also investigated for all projects, which showed results that are consistent with the results presented for CTH B. All test results for all investigated projects are presented in Appendix B. It should be noted that the results of the calculated base layer moduli based on LWD tests are somewhat in line with the results of the resilient moduli obtained from the repeated load triaxial testing when considering typical stress levels.

The results of DCP tests on the investigated aggregate base layers demonstrated the spatial variability in penetration resistance within the individual project and among all projects. The results also demonstrated the variability in penetration resistance with depth at the same test point. Resistance to penetration is influenced significantly by the state of compactness of aggregate particles and therefore, DCP results reflect the density/uniformity of the aggregate base construction. Figure 3.23 depicts the estimated CBR values at various points at the investigated projects. Inspection of Figure 5.23 shows wide range of CBR values with depth. Base layer construction can be evaluated from these results in which DCP test points demonstrated adequate compaction achieved at locations USH 12 and USH 141. On the other hand, base layer construction is considered inadequate at the test location for STH 33.

The discussion/test results presented earlier demonstrate the existence of variability and non-uniformity in aggregate base layers. It should be noted that all investigated materials used in all projects conform to material specifications of WisDOT; however, test results demonstrated that aggregate layers ended up being constructed with a wide range of achieved field densities and modulus values i.e., variability and non-uniformity in aggregate base compaction.

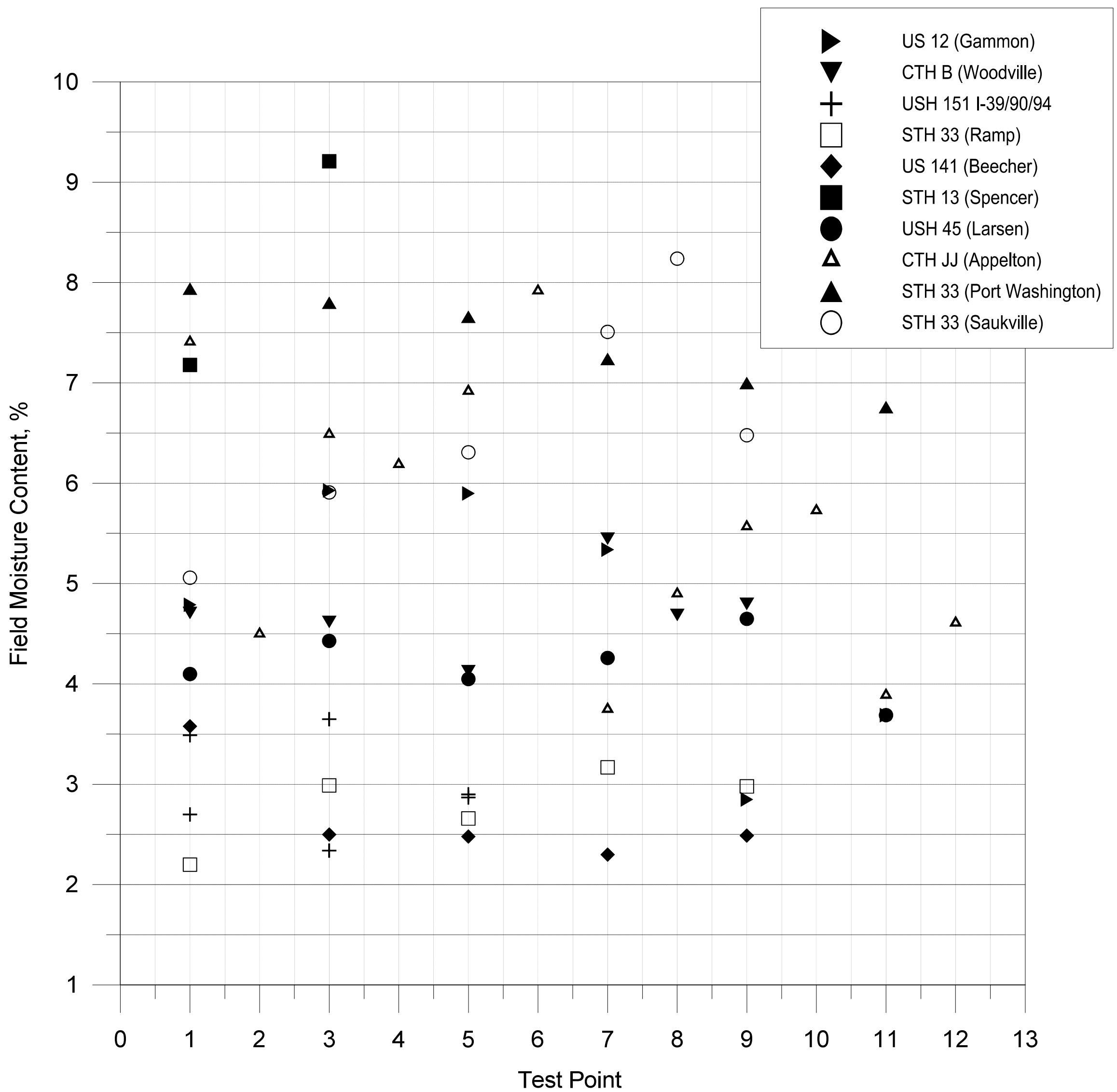

Figure 5.21: Spatial variability of field moisture content along the investigated projects.

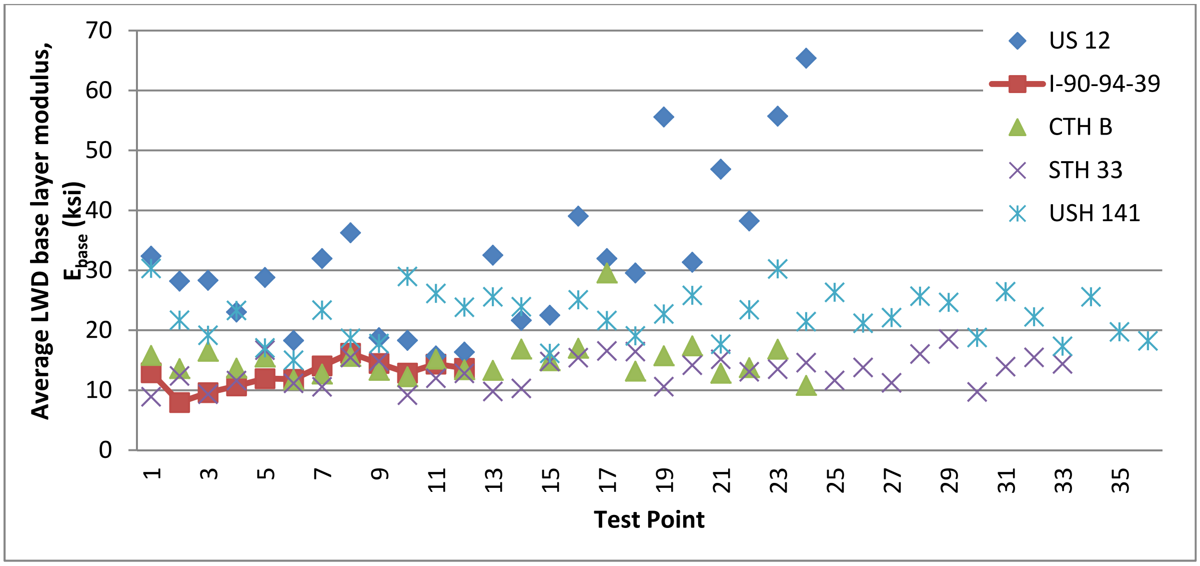

Figure 5.22: Variation of calculated base layer modulus with test points along the investigated projects.

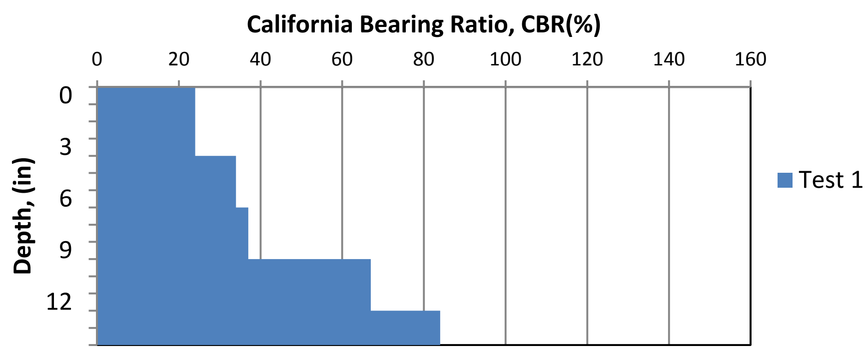

(a) Base layer for I-90/94/39

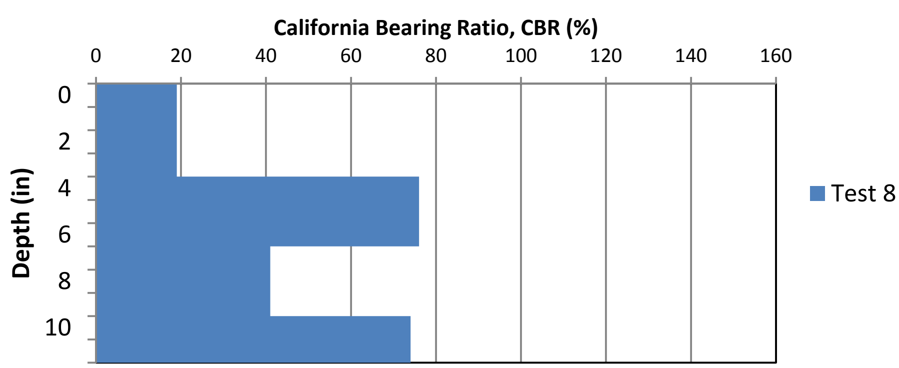

(b) CTH-I /US 45 Larsen

Figure 5.23: Variability of CBR with depth for various investigated projects.

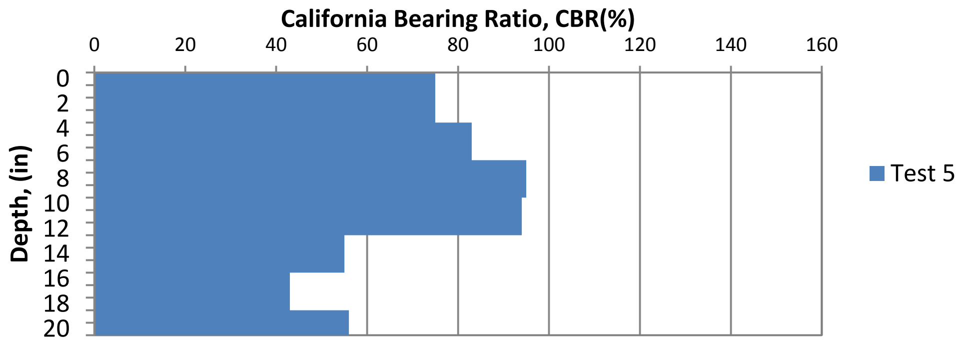

(c) USH 141

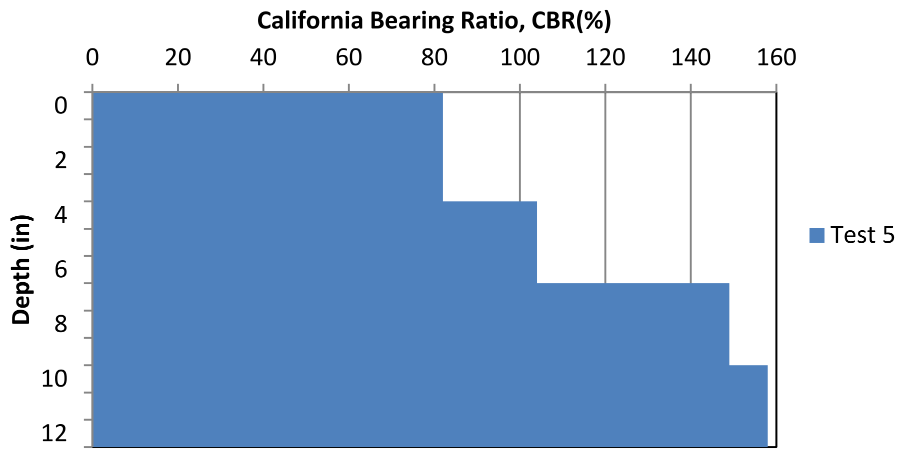

(d) US 12

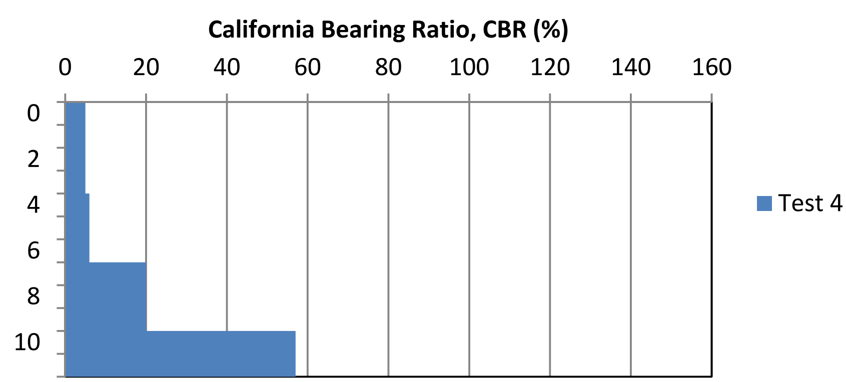

(e) STH 33

Figure 5.23 (cont.): Variability of CBR with depth for various investigated projects.

5.2 Mechanistic-Empirical Analyses of Aggregate Base Characteristics Impact on Pavement Performance

Aggregate base layer is an important structural component of a flexible pavement. Appropriate design and construction of the aggregate base layer has significant influence on structural stability and performance of pavements. Factors affecting the quality of constructed aggregate base layers include: gradation, particle shape, texture and angularity, density (state of compactness of particles) and uniformity. Density, moisture content and aggregate particles interlocking are among the factors affecting the stiffness of the aggregate base layers.

The influence of aggregate base characteristics (layer modulus) on pavement performance is investigated using the Mechanistic-Empirical (M-E) pavement design software DARWin-ME. The pavement designed and constructed at STH 33 in Port Washington – Saukville was selected for the analysis. The various input parameters needed for the analysis were obtained from project plans, via communication with project engineers, from laboratory tests on the aggregates materials and using assumed typical values in case of information/data was not available. Tables 5.5 to 5.7 present the input parameters obtained and used for M-E pavement analysis for the HMA layer, aggregate base layer, and subgrade soil, respectively.

M-E sensitivity analysis was conducted to assess the influence of aggregate base modulus on pavement performance. Base modulus values ranging from 10 to 50 ksi were used with increments of 5 ksi. Pavement performance in terms of fatigue cracking, ride quality (International Roughness Index, IRI), and rutting was investigated for pavement life of 20 years. The results of the M-E analysis are presented in Figure 5.24 to 5.26. The influence of base layer modulus on fatigue cracking is more significant than its influence on ride quality and rutting at 90% reliability levels. For example, after 20 years of pavement life, bottom up cracking of HMA surface layer propagated to 0.83% for base layer modulus of 40 ksi and to 3% for base layer modulus of 10 ksi, as shown in Figure 5.24. On the other hand, the influence of base layer modulus on the ride quality (IRI) is insignificant at reliability level 90% and for this particular pavement with the presented input parameter, as shown in Figure 5.25. The analysis also indicated that the base layer modulus has influence on rutting as presented in Figure 5.26. For base layer modulus of 10 ksi, a rut depth value of 0.75 in. was reached in 13.6 years, while it took 16.5 years for rutting to reach 0.75 in for base layer with modulus of 15 ksi. The pavement base layer with elastic modulus of 40 ksi did not reach the rutting threshold during the 20-year service life. This analysis demonstrates the influence of a strong, rut resistant aggregate base layer on pavement performance; therefore, it is essential to implement quantitative measures to assess the quality of constructed aggregate base layers to ensure a consistent and adequate platform is provided for better performing pavements.

Table 5.5: Properties of the HMA surface layer constructed at STH 33, Port Washington – Saukville.

Hot Mix Asphalt Layer	
Thickness (in.)	6.5
Unit Weight (pcf)	143.0
Poisson's Ratio	0.35
Reference Temperature (F)	70
Effective Binder Content (%)	12
Air Voids (%)	6
Thermal Conductivity (BTU/hr-ft-^{0}F)	0.67
Heat Capacity (BTU/lb-^{0}F)	0.23
Hot Mix Asphalt Dynamic Modulus (Input level: 3)	
Sieve Size	*% Passing*
¾ in. sieve	98
⅜ in. sieve	62
No. 4 sieve	50
No. 200 sieve	4
Asphalt Binder	
Parameter	*Value*
Grade	Superpave Performance Grade
Binder Type	64-22
A	10.98
VTS	-3.68

Note: Gradation and Asphalt Binder data was obtained from HMAC Mix Design Data given by contractor

Table 5.6: Properties of the aggregate base course layer constructed at STH 33, Port Washington – Saukville.

Unbound Aggregate Base Course Layer	
Thickness (in.)	13.5
Maximum Dry Unit Weight (pcf)	133.6
Poisson's Ratio	0.35
Coefficient of Lateral Earth Pressure (k_o)	0.5
Resilient Modulus (psi) Input level: 3	30,000 – 50,000
Liquid Limit	6.0
Plastic Index	1.0
Saturated Hydraulic Conductivity (ft/hr)	5.05×10^{-02}
Specific Gravity of Solids	2.7
Optimum Gravimetric Water Content (%)	7.4

Table 5.7: Properties of the subgrade soil at STH 33, Port Washington – Saukville.

Subgrade (A-7-6)	
Thickness (in)	Semi-infinite
Maximum Dry Unit Weight (pcf)	95.3
Poisson's Ratio	0.35
Coefficient of Lateral Earth Pressure (k_o)	0.5
Resilient Modulus (psi) Input level: 3	5,000
Liquid Limit	51.0
Plastic Index	40.0
Saturated Hydraulic Conductivity (ft/hr)	1.029e-05
Specific Gravity of Solids	2.7
Optimum Gravimetric Water Content (%)	23.4
Subgrade (A-7-6) - Gradation	
Sieve Size	*% Passing*
3 ½ in. sieve	99.9
2 in. sieve	99.6
1 ½ in. sieve	99.3
1 in. sieve	98.8
¾ in. sieve	98.3
½ in. sieve	97.5
⅜ in. sieve	96.9
No. 4 sieve	94.9
No. 10 sieve	93.0
No. 40 sieve	88.8
No. 80 sieve	84.9
No. 200 sieve	79.1

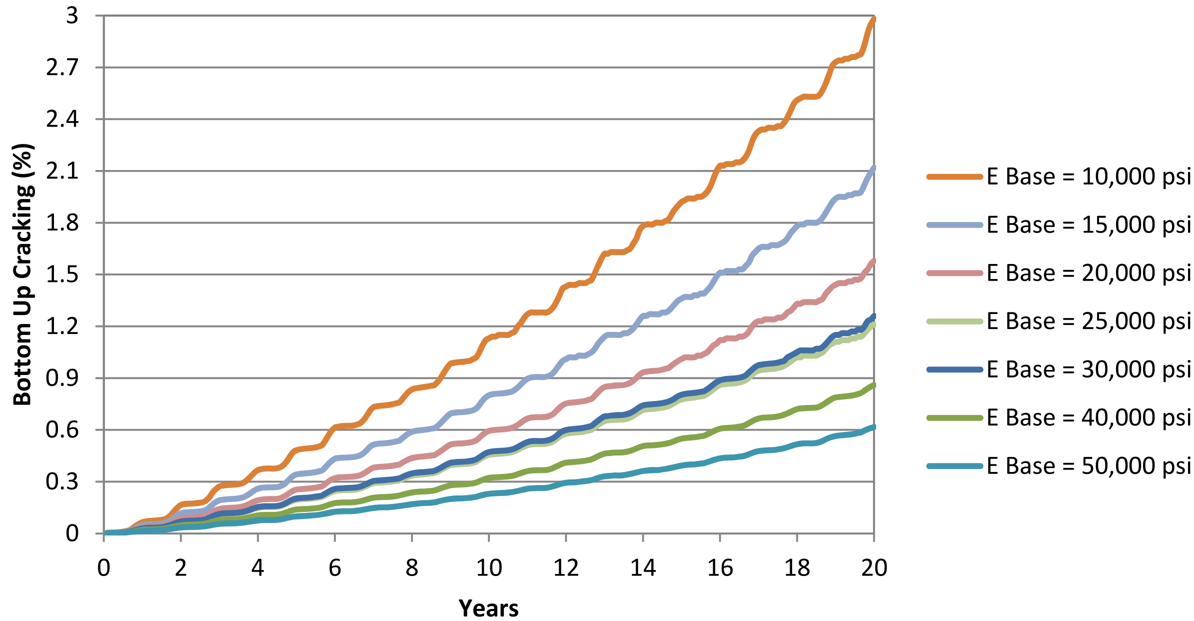

Figure 5.24: Propagation with time of bottom up fatigue cracking for various base layer moduli.

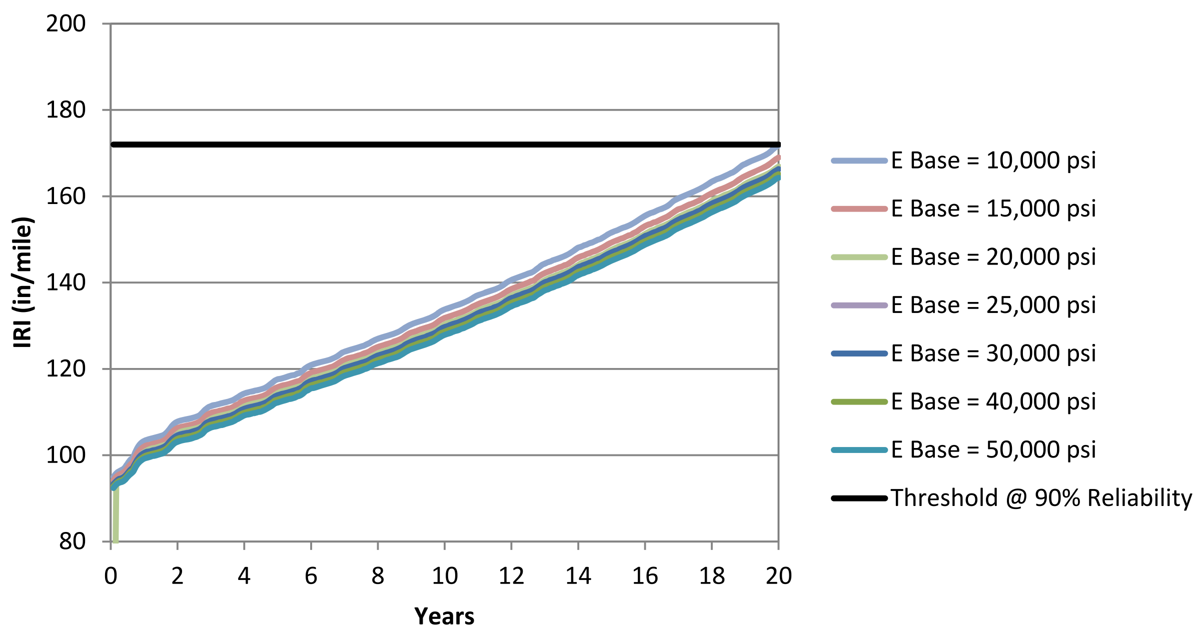

Figure 5.25: Effect of aggregate base layer moduli on the ride quality pavement.

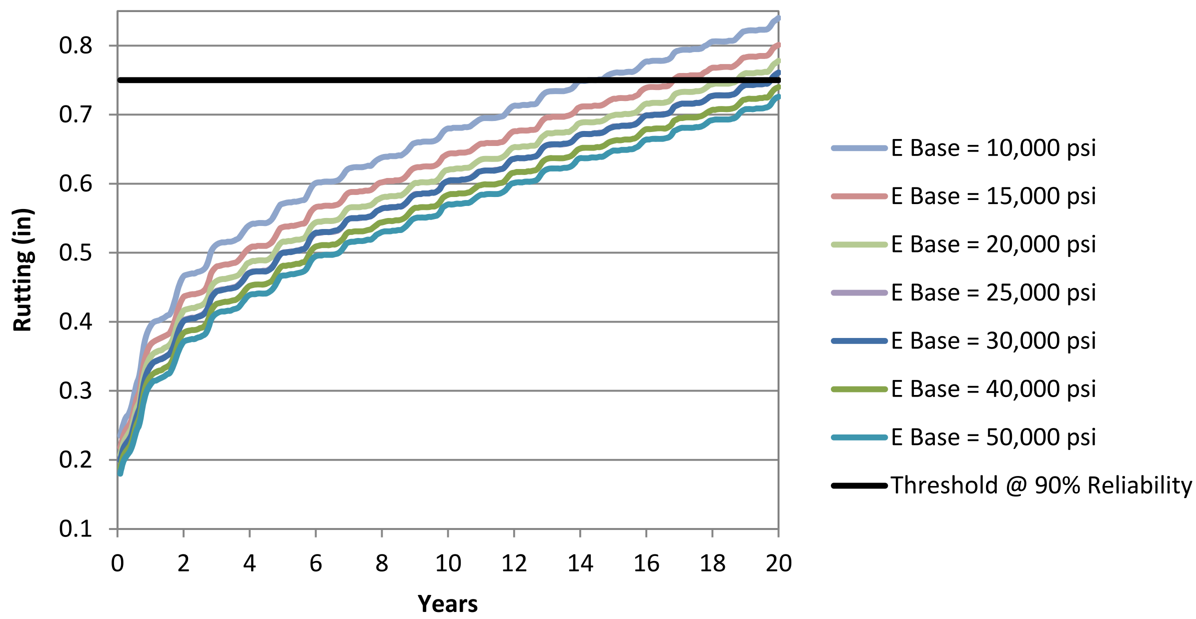

(a) Total rutting

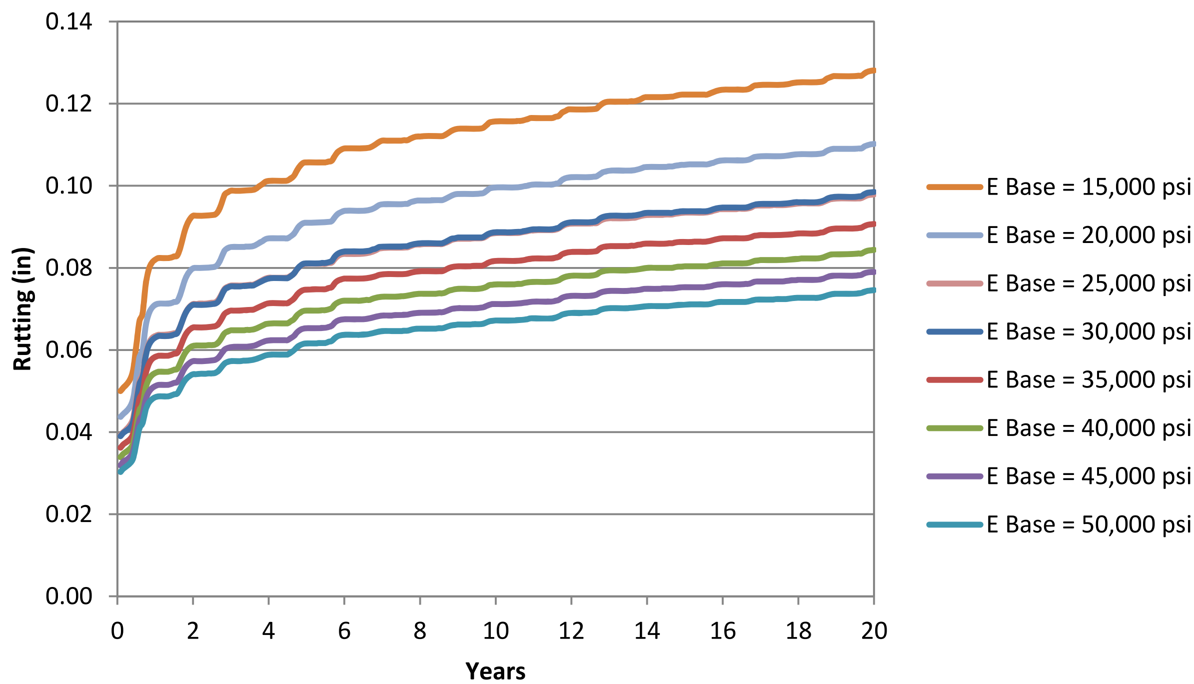

(b) Base layer rutting

Figure 5.26: Effect of aggregate base layer moduli on pavement rutting.

Chapter 6
Framework for Evaluating Aggregate Base Construction

This chapter presents a framework for evaluating the quality of constructed aggregate base course layer in flexible pavements. Density-based as well as modulus-based methods and their role in quality control/quality assurance (QC/QA) of aggregate base layers are emphasized. Draft proposed base compaction specifications as well as cost estimates are presented.

6.1 General

Construction of aggregate base course layers consists of spreading the aggregate materials in lifts and the subsequent compaction, under specified moisture content, using rollers. Compaction is defined as the process of densification of aggregate materials by reducing void space between aggregate particles through the application of mechanical energy. Water will act as lubricant in the compaction as it facilitates the relative movement/reorientation of aggregate particles and sliding to achieve more packed state of aggregation. Compaction leads to a dense state of compactness (dense aggregate matrix) with strong particle to particle interlocking/ interaction that affects the performance of the aggregate base layers in terms of: (1) reducing deformation/settlements, (2) increasing the shear strength, and thereby improving structural stability, (3) improving the bearing capacity of granular base layers, and (4) controlling undesirable volume change caused by frost action, swelling, and shrinkage (Holtz, 1990).

Various methods exist to evaluate the quality of constructed aggregate base layers to insure that the product is within acceptable limits and will lead to long lasting and better performing pavements. These methods are either density-based or modulus-based.

6.2 Density-Based Methods

Density-based methods for QC/QA of constructed aggregate base layers consist of measuring the field density of constructed aggregate base (γ_{field}) at test locations and comparing the results with target density (maximum dry unit weight γ_{dmax}). The target density is established by laboratory and/or field testing of the same material (representative material sample) used in the field. The field density is reported as a percentage of the target density, which is termed as the relative compaction (R).

The minimum acceptable relative compaction value is established by the base layer construction specifications. It should be noted that the materials tested in the laboratory should be the same materials as those used in the construction of the base course layer and both should be subjected to similar compactive energy. Marek and Jones (1974) emphasized this point and stated that for the relative compaction to be valid, the materials tested in the laboratory and in the field must be similar and compacted under similar compactive energy.

The target density (γ_{dmax}) can be established in the laboratory or obtained from field measurements. Laboratory based target density (γ_{dmax}) is obtained by performing standard or modified Proctor tests, which use a drop hammer to compact the aggregate in the compaction mold. In addition, the drop-hammer methods are commonly used to compact the aggregate materials in the laboratory. Vibratory-based compaction of the aggregate in the mold is the best practice although not very commonly used. Table 6.1 presents ASTM and AASHTO standard test methods used to establish target density in the laboratory based on the use of drop hammer. It should be noted that all state highway agencies have gradation requirements for base aggregates (upper and lower limits for particle size distribution), which includes minimum amount of fines (percent passing No. 200 sieve or sizes smaller than 0.075 mm). For aggregate materials with low amount of fines or with no fines (e.g., open graded), the drop hammer compaction (impact compaction) may not be effective in establishing the maximum state of compactness and therefore target density for these types of aggregates. For these cases, the vibratory compactors are used to establish the target density according to ASTM D7382: Standard Test Methods for Determination of Maximum Dry Unit Weight and Water Content Range for Effective Compaction of Granular Soils Using a Vibrating Hammer.

Direct field density measurement of constructed aggregate base layers includes the use of: (1) sand cone method (ASTM D1556, AASHTO T 191), (2) rubber balloon method (ASTM D2167, AASHTO T 205), and (3) the sand replacement method (ASTM D4914). It should be noted that AASHTO T 205 was withdrawn from the latest specifications. Direct measurement methods for moisture content include the oven dry method (ASTM D2216, AASHTO T 265), the microwave method (ASTM D4643), and the calcium carbide gas pressure test (ASTM D 4944, AASHTO T 217). Methods of directly measuring both field density and moisture content include the nuclear density gauge (ASTM D3017 for moisture and ASTM D2922 for density, AASHTO T 310).

The base compaction survey conducted for this research project showed that 90% of state highway agencies use density-based methods for quality control of constructed aggregate base layers. These methods are based on ASTM and AASHTO even though 29% of the surveyed agencies use their own modified methods.

Another method used for QC/QA of constructed aggregate base layer is the control strip method, which is used to establish target density for compaction control of aggregate base layers. A test section using the aggregate to be characterized is constructed and density is evaluated in the field after specified number of compaction passes by roller. The target density is established after no further densification is achieved with more roller passes. Field compaction is evaluated as a percentage of this target density. Consideration of previously established compaction should be taken when using the control strip method as the target density may not reflect the densest state of compactness. When materials from new sources are used or materials from the same source change, a new control strip test is often required. According to the survey conducted, Kentucky, New Hampshire, and Ohio use the control strip method in base course construction (NH and OH use also AASHTO T 99).

Density-based QC/QA of constructed aggregate base layers is commonly used by state highway agencies in the U.S. and Canada. However, these are spot test based methods and do not provide continuous characterization of the aggregate base in terms of density and uniformity. In addition, some of these measurements are labor intensive and time consuming (e.g., in-place density using sand cone method and moisture content determination by the oven dry method). Development of QC/QA specifications that are performance based requires evaluation of base layer compaction using rapid and reliable techniques. Continuous characterization to identify uniformity and consistency of aggregate base layers is of great importance. Personal communication indicated that research at the University of Illinois-Urbana Champaign (UIUC) and Iowa State University (FHWA DTFH 61-06-H-00011; Chavan, 2012; and Brand and Roesler, 2012), currently under review by FHWA, demonstrated that non-uniformity in aggregate base/subbase layers under concrete slabs developed more severe distresses/cracks in concrete pavements compared with weaker/softer base layers with uniformity. Both field measurements and modeling analysis supported this conclusion.

6.3 Modulus-Based Evaluation

The mechanistic-empirical pavement design requires fundamental material properties, such as the layer modulus for base course layers, as input for pavement design and for evaluating pavement performance. Therefore, it is important to establish methodologies that characterize the required inputs such as the modulus based on both field and laboratory test methods. Among these methods, the falling weight deflectometer is commonly used to calculate layer moduli based on backcalculation algorithms. Base course layer modulus can also be measured using portable devices such as the Light Weight Deflectometer (LWD) and GeoGauge. All mentioned methods are based on spot testing evaluation of layer modulus. Continuous compaction control and characterization of layer modulus can also be achieved in the field using intelligent compaction technology (IC). Table 6.2 summarizes methods available for field measurements of pavement layer moduli.

Modulus based characterization and evaluation of base course layers was recently investigated a great deal by many state highway agencies including Texas, Louisiana, Minnesota, and Indiana. In-place measurements of modulus were successfully reported by these studies (e.g., Chen et al., 1999; Nazzal, 2003; Siekmeier, 2010; Mishra et al., 2012).

Various studies established relationships/trends between field density and layer modulus for aggregate base layers. However, layer modulus is influenced by the state of compactness (density) as well as moisture content of aggregates. In the field, moisture content could fluctuate in a constructed aggregate base layer without any change to the field density. Such changes will be reflected in a modulus-based measurement but not in density-based evaluation. This is one of the most difficult aspects of establishing modulus-based compaction control specifications.

Modulus-based QC/QA for aggregate base layers consist of identifying technology/device to use for field measurements (such as FWD, LWD, GeoGauge) and parameters associated with using such device including level of induced stress, depth of influence/layer thickness, variable conditions of moisture state, and methods of analysis/backcalculation to find the modulus.

In comparing backcalculated pavement layer moduli with laboratory resilient or dynamic moduli, it is important to keep in mind what is being compared. The laboratory test result is appropriately termed a material property—a measurable characteristic of the material. In contrast, the backcalculated layer modulus from field measurement is more correctly thought of as a parameter—an estimate of the "average" material characteristic of the base layer, which does not fully account for spatial variations in moisture and stress states (Richter, 2006). Furthermore, the interpretation process used to obtain the estimate (backcalculated modulus) is based on theory that approximates, but does not match, reality. Key theoretical assumptions that are violated to one degree or another are the assumptions of homogeneity, isotropy, and linearity.

A field modulus measurement should be accompanied by both moisture and suction measurement in the field since increased moisture contents (above optimum) tend to decrease resilient modulus and vice versa. Even though the applied stresses on a constructed layer of aggregate base are measured by field test devices such as LWD, moisture sensitivity of the base course aggregates will vary depending on specific gradations and the amount and plasticity (PI) of the minus No. 200 material.

An essential feature of a modulus-based construction specification framework is to evaluate long term performance of a constructed base layer. The premise behind this approach is that field control of moisture and modulus is necessary and sufficient to ensure long term pavement performance (permanent deformation, fatigue). The modulus-based specification is therefore tightly conjoined with mechanistic-empirical design philosophy and the principles of unsaturated soil mechanics. One simple way for QC/QA of constructed layers in the field can be accomplished through controlling the base deflections using LWD measurements as in the approach taken by Siekmeier and colleagues in Minnesota (2010). Current state of practice and research in the U.S. is focused on the modulus-based specifications and developing such specifications for QC/QA. This is demonstrated by the Indiana DOT's move to use/implement the LWD tests for base layer characterization, and by a major National Cooperative Highway Research Program (NCHRP) project 10-84 (Modulus-Based Construction Specification for Compaction of Earthwork and Unbound Aggregate) and NCHRP Synthesis 20-05/Topic 43-03 (Practices for Unbound Aggregate Pavement Layers) on modulus-based characterization of aggregate base layers.

Table 6.1: Standard tests for establishing laboratory target density.

Equipment/ Test Parameter	ASTM						AASHTO							
	Standard (D698)			Modified (D1557)			Standard T 99				Modified T 180			
	A	B	C	A	B	C	A	B	C	D	A	B	C	D
Mold Diameter (in)	4	4	6	4	4	6	4	6	4	6	4	6	4	6
Mold Volume (ft^3)	0.033	0.033	0.075	0.033	0.033	0.075	0.033	0.075	0.033	0.075	0.033	0.075	0.033	0.075
Weight of Hammer (lb.)	5.5	5.5	5.5	10	10	10	5.5	5.5	5.5	5.5	10	10	10	10
Number of Blows/Layer	25	25	56	25	25	56	25	56	25	56	25	56	25	56
Number of Layers	3	3	3	5	5	5	3	3	3	3	5	5	5	5
Material Specification*	3/16	3/8	3/4	3/16	3/8	0.19	3/16	3/16	3/4	3/4	3/16	3/16	3/4	3/4

*Material finer than sieve opening size (in)

Table 6.2: Different methods available for in-situ modulus measurement of constructed pavement layers (Tutumluer, 2012)

Test Category	Underlying Principle	Corresponding Devices
Surface Deformation	Static Load	• Benkelman Beam • Briaud Compaction Device (BCD, based on measuring the bending strain on a loading plate in cotact with the ground)
	Steady State Vibratory	Soil Stiffness Gauge (e.g. Humboldt GeoGauge™)
	Impact Load	• Falling Weight Deflectometer (FWD) • Portable Falling Weight Deflectometer (PFWD) or Light Weight Deflectometer (LWD)
	Sinusoidal Load	• Dynaflect • Road Rater
	Continuous Load	• Rolling Wheel Deflectometer (RWD)
Geophysical	Wave Propagation	• Ultrasonic Body Waves • Ultrasonic Surface Waves • Spectral Analysis of Surface Waves (SASW) • Multi-channel analysis of surface waves • Free-Free Resonant Column Tests • Seismic Pavement Analyzer (SPA) • Portable Seismic Pavement Analyzer (PSPA)

6.4 Proposed Aggregate Base Layer Construction Specifications

Based on the results of this research study, which included experimental work (field and laboratory), literature review, and comprehensive survey of 62 highway agencies in the U.S. and Canada, the following aggregate base course layer specifications are proposed:

<u>Definition</u>

The following AASHTO standard test procedures are listed to provide a quick reference to the proposed/draft specification document:

1. AASHTO T 99: Standard Method of Test for Moisture-Density Relations of Soils Using a 2.5-kg (5.5-lb) Rammer and a 305-mm (12-in.) Drop
   i. Method A—A 101.60-mm (4-in.) mold: Soil material passing a 4.75-mm (No. 4) sieve Sections 4 and 5.
   ii. Method B—A 152.40-mm (6-in.) mold: Soil material passing a 4.75-mm (No. 4) sieve Sections 6 and 7.
   iii. Method C—A 101.60-mm (4-in.) mold: Soil material passing a 19.0-mm (3/4-in.) sieve Sections 8 and 9.
   iv. Method D—A 152.40-mm (6-in.) mold: Soil material passing a 19.0-mm (3/4-in.) sieve Sections 10 and 11.
2. AASHTO T 180: Standard Method of Test for Moisture-Density Relations of Soils Using a 4.54-kg (10-lb) Rammer and a 457-mm (18-in.) Drop
   i. Method A—A 101.60-mm (4-in.) mold: Soil material passing a 4.75-mm (No. 4) sieve Sections 4 and 5.
   ii. Method B—A 152.40-mm (6-in.) mold: Soil material passing a 4.75-mm (No. 4) sieve Sections 6 and 7.
   iii. Method C—A 101.60-mm (4-in.) mold: Soil material passing a 19.0-mm (¾-in.) sieve Sections 8 and 9.
   iv. Method D—A 152.40-mm (6-in.) mold: Soil material passing a 19.0-mm (¾-in.) sieve Sections 10 and 11.
3. AASHTO T 272: Standard Method of Test for Family of Curves—One Point Method
4. AASHTO T 191: Standard Method of Test for Density of Soil In-Place by the Sand-Cone Method
5. AASHTO T 310: Standard Method of Test for In-Place Density and Moisture Content of Soil and Soil-Aggregate by Nuclear Methods (Shallow Depth)
6. ASTM D6938: Standard Test Method for In-Place Density and Water Content of Soil and Soil-Aggregate by Nuclear Methods (Shallow Depth)
7. AASHTO T 255: Standard Method of Test for Total Evaporable Moisture Content of Aggregate by Drying

8. ASTM D2216: Standard Test Methods for Laboratory Determination of Water (Moisture) Content of Soil and Rock by Mass
9. ASTM D4643 - 08 Standard Test Method for Determination of Water (Moisture) Content of Soil by Microwave Oven Heating
10. ASTM E2583: Standard Test Method for Measuring Deflections with a Light Weight Deflectometer (LWD)

<u>Proposed Draft Base Compaction Specification</u>

The following AASHTO/ASTM test methods may be added to WisDOT SS 301.2.3 Sampling and Testing

In-place density and moisture content …… AASHTO T 310

In-place density and moisture content ……. AASHTO T 272

Aggregate Moisture Content ….. AASHTO T 255

Base layer surface deflection ….. ASTM E2583

The following may replace <u>301.3.4.2 Standard Compaction and 301.3.4.3 Special Compaction</u>

<u>301.3.4.2 Compaction</u>

Aggregate placement, spreading, and compaction in a lift are noted as base layer herein. Compact the base layer to field density values not less than 98% of the target density established by field and/or laboratory tests on representative material of the base aggregate. The target density is the maximum dry density determined according to AASHTO T 180 Method C or D or the maximum dry density measured in the field by constructing a test strip (control section) as specified in 301.3.4.2(a). Determine the optimum moisture content according to AASHTO T 180 or from test strip described in 301.3.4.2(a). The field density is determined by either AASHTO T 310, AASHTO T 191 or by combination of both methods. Determine the field moisture content of the aggregate base in accordance with AASHTO T 310, AASHTO T 191 or combination of both methods.

301.3.4.2(a) Test Strip (Control Section) – Density

Construct a 300-ft aggregate base test strip in accordance with 301.3.1 and 301.3.2. The width of the test strip shall be the plan width of the base layer. The moisture content at which the control strip aggregate materials will be compacted is recommended by the project engineer. Compact the test strip with minimum of 4 passes and measure the field density and moisture content using AASHTO T 310 or AASHTO T 191 or combination of both methods. Field density and moisture content shall be measured at 5 different locations that are evenly spaced along the test strip. The average value of the five measurements is calculated as the field density and moisture content. Continue base compaction with two additional passes and measure field density and moisture content. To determine the target dry density value, plot the dry density versus number of passes. Continue base layer compaction with additional passes as necessary until the peak density value on the curve is reached. Field density and moisture content measurements shall be measured every other pass during base compaction to establish the target density. The average moisture content is set as the target field moisture content from field density measurement locations.

301.3.4.2(b) Test Strip (Control Section) – Deflection

Preform deflection measurement using Light Weight Deflectometer, LWD on the compacted aggregate base test strip. Compaction of the base layer to the required density shall be performed in accordance with 301.3.4.2 and 301.3.4.2 (a).

Using the test strip described in 301.3.4.2 (a), select 10 different test locations per 100-ft of the test strip. Figure 301.3.4.2(b)-1 can be used as a guide for selecting test points. Perform LWD deflection measurement according to ASTM E2583 test procedure. Record the maximum deflection for each test. Calculate the average of the 10 LWD test values. The maximum allowable deflection is the average value.

301.3.4.2(c) Compaction Acceptance and QC/QA

The acceptable average field density after compacting base layers shall be equal to or more than 98% of the target dry density with no individual measured field density shall be less than 95% of the target density. The field moisture content shall be controlled within -3 and -1 percentage points of the optimum moisture content determined by AASHTO T 180 or test strip. The average deflection shall be equal to or less than the maximum allowable deflection determined by LWD deflection tests on the test strip.

The frequency of testing for field density and moisture content shall be five tests performed by the contractor for each 1,000 ton of compacted aggregate with a minimum of five tests per day. The frequency of testing for field density and moisture content shall be five tests performed by the engineer for each 4,000 ton of compacted aggregate with a minimum of five tests per project.

The frequency of testing for LWD deflection shall be 10 tests performed by the contractor for each 1,000 ton of compacted aggregate with a minimum of five tests per day. The frequency of testing for LWD deflection shall be 10 tests performed by the engineer for each 4,000 ton of compacted aggregate with a minimum of 10 tests per project.

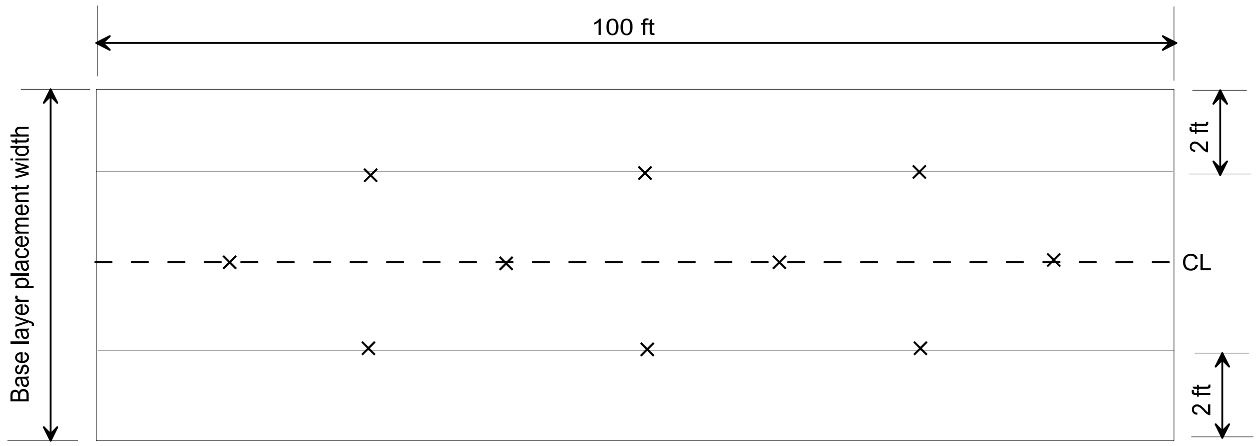

Figure 301.3.4.2(b)-1: LWD test pattern for measurements of maximum deflection.

6.5 Cost Effectiveness and Feasibility of Implementing Base Layer Construction Specifications

Based on the results of this research study, which included experimental work (field and laboratory), literature review, and comprehensive survey of 62 highway agencies in the U.S. and Canada, the following points are presented to support the need for QC/QA of base layer construction specifications from cost effectiveness point of view:

1. Based on the results of the conducted comprehensive survey, implementing base layer QC/QA construction specifications has no significant impact on the schedule and activities of a project. About 62.9% of the surveyed highway agencies reported no impact on project timelines versus 12.9% who stated that QC/QA will cause delays in project timelines (Figure 2.18). In terms of impact on project budgets and cost, 53.2% of the surveyed highway agencies reported that implementing QC/QA for base layer construction has no impact on the project budget (no increase in cost), while 21% stated that the project budget will increase to account for such implementation (Figure 2.19).
2. Field and laboratory tests and analyses demonstrated that variability in base layer properties and non-uniformity resulted in early distressed HMA pavements, which require rehabilitation measures. Early deteriorated HMA pavements due to base layer performance problems will result in increased rehabilitation cost and will strain the agency’s budget.
3. The cost of implementing base layer QC/QA construction specifications (density-based and modulus-based) is considered low and is affordable by contractors and highway agencies. The following is approximate cost estimates of acquiring density based and modulus based test equipment:

    a. Density-based: manual Proctor test apparatus (mold and hammer) will cost $250; automated compactor will cost $6,000 (high production rate); sand cone apparatus will cost $150; standard sand will cost $50 per 25 lb. bag; drying oven will cost $2,500 (microwave will cost $200); high precision balances will cost $2,000; nuclear density gauge cost ranges between $6,000 and $12,500; in addition to low cost for disposable supplies.
    b. Modulus based: light weight deflectometer will cost $24,000.
4. The proposed QC/QA base layer construction specifications call for five density tests per 1,000 ton of constructed base to be conducted by the contractor. This will produce about 1,800 ft long of 12-ft wide and 8-inch thick constructed base layer. The following is a cost estimate for the contractor:
    a. Initial density-based apparatus will cost between $2,600 (manual apparatus, sand cone, scales, and microwave) and $23,000 (automated Proctor, nuclear density gauge, drying oven, scales).
    b. Disposable supplies (sand, plastic bags, etc.) $60.
    c. Initial modulus-based apparatus cost $24,000 (LWD only)
    d. Labor hours are estimated to be between 5 and 8 hours for both density and modulus based tests.

Chapter 7
Conclusions and Recommendations

This research investigated the performance of aggregate base layers for existing HMA pavements and for HMA pavements under construction through field and laboratory tests of pavements and pavement materials. In addition, comprehensive survey of aggregate base layer construction quality acceptance was conducted by contacted highway agencies in the U.S. and Canada.

Eleven existing HMA pavement projects with aggregate base course layers constructed in the past few years were selected for FWD testing and visual distress surveys. In six of these projects, issues with aggregate base performance in terms of stability and uniformity were observed and reported during paving of the HMA surface layer. Later, these pavements exhibited various levels of early distresses, including cracking (longitudinal, transverse, and alligator), aggregate base failure, and pavement surface roughness/irregularities (in terms of ride quality). The remaining five HMA pavement projects, in which no issues related to aggregate base layer behavior during construction were reported, performed well after construction. These projects were subjected to FWD testing of approximately one-mile test section/sections per project. Field and laboratory tests were also conducted on 10 projects during base course layer construction to evaluate the quality and uniformity of the constructed base layers. The mechanistic-empirical analyses were conducted to assess the effect of the aggregate base layer modulus on long-term pavement performance.

A comprehensive survey was conducted to obtain the current state of practice on base compaction and acceptance criteria by highway agencies in the U.S. and Canada. The survey showed that 58 out 62 agencies surveyed are using quantifying test methods (density-based and performance-based) for quality control/quality assurance (QC/QA) of constructed aggregate base layers. The survey also showed that modulus-based specifications are being investigated/ considered and are of interest for future implementation.

Based on the results of this research, the following conclusions are reached:

1. The existing HMA pavements that showed early distresses exhibited high levels of spatial variability and non-uniformity in aggregate base course layers, as demonstrated by FWD testing and backcalculated base layer modulus values and distributions. Current research at UIUC and ISU showed that non-uniformity of base layers caused more distresses/cracks in PCC pavements compared with PCC pavements with more uniform bases that are even “softer.”
2. The existing HMA pavements that performed well exhibited low levels of spatial variability and good uniformity in aggregate base course layers, as shown by the

FWD test results and the backcalculated base layer modulus values and distributions.
3. High spatial variability in field density and moisture content exists in base course layers under construction, as demonstrated by the relative compaction test results.
4. High variability exists along the depth of base course layers, as demonstrated by the DCP test results and the estimated profiles of CBR along the depth of the investigated base layers.
5. Spatial variability and non-uniformity were also demonstrated by the results of the LWD and GeoGauge results, in which the layer moduli vary within a large range of values.
6. Mechanistic-empirical sensitivity analyses on the effect of the base course layer modulus on pavement performance demonstrated that pavement with a lower base layer modulus exhibited earlier fatigue bottom-up cracking and developed more rutting at earlier time. The analyses were conducted using Wisconsin data, STH 33, and DARWin-ME software.
7. The survey conducted to obtain the current state of practice on the QC/QA of constructed aggregate base layers showed that four highway agencies out of 62 in the U.S. and Canada use subjective observation methods for accepting constructed aggregate base layers.
8. The survey also indicated that 42% of the highway agencies exploring new methodologies such as modulus-based specifications to replace/complement their current density-based specifications.
9. The current state of practice and research in the U.S. is focused on the modulus-based specifications and developing such specifications for QC/QA. This is demonstrated by the Indiana DOT's recent move to use/implement the LWD tests for base-layer characterization and by a major National Cooperative Highway Research Program (NCHRP) project 10-84 (Modulus-Based Construction Specification for Compaction of Earthwork and Unbound Aggregate) and NCHRP Synthesis 20-05/Topic 43-03 (Practices for Unbound Aggregate Pavement Layers) on modulus-based characterization of aggregate base layers.

Based on the results of this research, the research team recommends the following:

1. Switching from the subjective visual observation-based method of acceptance to a quantitative method that is based on testing and evaluation.
2. Using density-based or modulus-based methods, with more weight/consideration for the modulus-based methods, as analyzed in Chapter Six.
3. Using portable devices such as LWD, GeoGauge, and DCP to provide spatial quantification for base layer moduli and to estimate base layer strength variation with depth.

4. Using/implementing methods/techniques for characterizing the uniformity of aggregate base layers such as continuous compaction control and intelligent compaction techniques.
5. Executing research projects to establish acceptance criteria and levels, bias, and accuracy for selected modulus-based devices; and to determine how these measured values correlate with laboratory/field measurements.

References

1. Adu-Osei, A., Little, D. N., Tutumluer, E., and Lytton, R. L. (2000). “Effect of Compaction on Orthotropic Properties of Aggregates,” Proceedings of the European Workshop on Compaction of Soils and Granular Materials, ISSMGE, Paris, France.
2. Adu-Osei, A., Little, D. N., Lytton, R. L. (2001). “Structural Characteristics of Unbound Aggregate Bases to Meet AASHTO 2002 Design Requirements,” International Center for Aggregates Research (ICAR) Report 502-1, Texas Transportation Institute, The Texas A&M University System, College Station, Texas.
3. American Association of State Highway and Transportation Officials (1990), *Construction Manual for Highway Construction*, Washington, D.C.
4. American Association of State Highways and Transportation Officials (2002). Standard Specifications for Transportation Materials and Methods of Sampling and Testing, 2002 Edition and AASHTO Provisional Standards, 2002 Edition.
5. Arnold, G. K. (2004). *Rutting of Granular Pavements*, PhD Thesis, University of Nottingham, Nottingham.
6. Arnold, G., Werkmeister, S., and Alabaster, D. (2007). “The Effect of Grading on the Performance of Basecourse Aggregate,” Land Transport New Zealand Research Report 325, Technical Report, ISBN 0–478–28737–2, ISSN 1177–0600.
7. Asphalt Institute, *Soils Manuals for the Design of Asphalt Pavement Structures*, MS-10, 5th Edition, 1997.
8. Ayers, M., Thompson, M., Uzarski, D. (1989). “Rapid Shear Strength Evaluation of In Situ Granular Materials”. *Transportation Research Record 1227*. TRB, Washington D.C., pp. 134-146.
9. Barksdale, R. D. (1972). “Laboratory Evaluation of Rutting in Basecourse Materials,” Proceedings of the 3rd International Conference on the Structural Design of Asphalt Pavements, London. pp. 161–174.
10. Barksdale, R. D. (1991). *The Aggregate Handbook*, National Stone Association, Washington, DC.
11. Barksdale, R. D. (2001). *The Aggregate Handbook*. National Stone, Sand and Gravel Association, 4th Ed.
12. Barksdale, R. D., J. Alba, P. N. Khosla, R. Kim, P. C. Lame, and M. S. Rahman (1997). “Laboratory Determination of Resilient Modulus for Flexible Pavement,” NCHRP Web Document 14 (Project 1-28), NCHRP, Transportation Research Board, Washington, D. C., 486 pp.
13. Baus, R.L. and Li, T. (2006). “Investigation of Graded Aggregate Base (GAB) Courses.” South Carolina Department of Transportation, Report FHWA-SC-06-03.
14. Bennert, T., and Maher, A. (2003), “The Development of a Performance Specification for Granular Base and Sub-base Materials,” Piscataway, Department of Civil and Environmental Engineering, NJ State University.

15. Brand, A., Roesler, J. (2012). "Effect of Nonuniform Foundation Support on Concrete Slab Responses." 10th International Conference on Concrete Pavements. Québec, Canada. July 8-12, pp. 54-67.
16. Chavan, H. L. (2012). *Field Investigation of Subgrade Non-Uniformity Effects on Concrete Pavement*. Master Degree Thesis. University of Illinois at Urbana-Champaign.
17. Chen, D. H., Wang, J-N., and Bilyeu, J. (2001). "Application of Dynamic Cone Penetrometer in Evaluation of Base and Subgrade Layers," *Journal of the Transportation Research Board*, No. 1764, Transportation Research Board, Washington, D.C.
18. Choubane, B. and McNamara, R. L. (2000) "Flexible Pavement Embankment Moduli Using Falling Weight Deflectometer (FWD) Data," Research Report FL/DOT/SMO/00-442. State Materials Office, Florida Department of Transportation, Tallahassee.
19. Chua, K.M. and Tenison, J. (2003). "Explaining the Hveem Stabilometer Test: Relating R-value, S-value, and the Elastic Modulus," *ASTM Journal of Testing and Evaluation*. West Conshohocken PA: ASTM International. (Vol. 31, No. 4).
20. Dodds, A., Logan, T., McLachlan, M., and Patrick, J. (1999). "Dynamic Load Properties of New Zealand Basecourse," Transfund New Zealand Research Report 151.
21. Eggen, P., Brittnacher, D. (2004). "Determination of Influences on Support Strength of Crushed Aggregate Base Course Due to Gradational, Regional, and Source Variations," Wisconsin Highway Research Program (WHRP). Wisconsin Department of Transportation (WisDOT).
22. Ese, D., Myre, J., Magne, P., and Vaernes, E. (1995). "The Use of the Dynamic Cone Penetrometer (DCP) for Road Strengthening Design in Norway." Proc., Int. Conf. on Bearing Capacity of Rd. and Airfield, p. 3-22.
23. Fiedler, S., Nelson, C., Berkman, F., and DiMillio, A. (1998). "Soil Stiffness Gauge for Soil Compaction Control." Public Road Magazine, Vol. 61, No. 5, pp. 5-11.
24. Gabr, M. A., Hopkins, K., Coonse, J., and Hearne, T. (2000). "DCP Criteria for Performance Evaluation of Pavement Layers." *Journal of Performance and Constructed Facilities*, ASCE, Vol. 4, No. 4. p. 141-148.
25. Harison, J. A. (1987). "Correlation between California Bearing Ratio and Dynamic Cone Penetrometer Strength Measurement of Soils." Proc. Instn. Civ. Engrs, Part 2, Technical Note 463. p. 833-844.
26. Heukelom, W., and Klomp, A. J. G. (1962). "Dynamic Testing as Means of Controlling Pavements during and After Construction," Proc., 1st International Conference on Structural Design of Asphalt Pavement, University of Michigan.
27. Holtz, R. D. (1990). *Compaction Concepts, Chapter 3, Guide to Earthwork Compaction,* State of the Art Report 8, Transportation Research Board (TRB), Washington, D.C.
28. Holubec, I. (1969). "Cyclic Creep of Granular Materials," Report No. RR147, Department of Highways, Ontario, Canada.
29. Huang, Yang H. (2004). *Pavement Analysis and Design*, 2nd Edition, Prentice Hall.

30. Humboldt Mfg. Co. (2007). *GeoGauge User Guide*. Model H-4140 Soil Stiffness/Modulus Gauge (patent pending).” Version 4.1, June 2007.
31. Irwin, L. H., (1983). *User’s Guide to MODCOMP2*. Version 2.1. Local Roads Program, Cornell University, Ithaca, N.Y.
32. Jones, D., Harvey, J. (2005). “Relationship between DCP, Stiffness, Shear Strength and R-Value.” Technical Memorandum: UCPRC-TM-2005-12.
33. Kaya, Z., A. Cetin, B. Cetin, and A. H. Aydilek (2012). “Effect of Compaction Method on Mechanical Behavior of Graded Aggregate Base Materials”, Proceedings of the 2012 GeoCongress, Oakland, California, pp. 1486-1494.
34. Kleyn, E.G., (1975). “The Use of the Dynamic Cone Penetrometer (DCP).” Report 2/74, Transvaal Roads Department, Pretoria, South Africa.
35. Kleyn, E. G., Maree, J. H., and Savage, P. F. (1982). “The Application of a Portable Pavement Dynamic Cone Penetrometer to Determine in situ Bearing Properties of Road Pavement Layers and Subgrades in South Africa.” The European Symposium on Penetration Testing, Amsterdam, Netherlands, May.
36. Lay, M. (1984). “*Handbook of Road Technology*,” Vol. 1. Planning and Pavements. New York: Gordon and Breach Science Publishers.
37. Lenke, L. R., McKeen, R. G., and Grush, M. P. (2003). “Laboratory Evaluation of GeoGauge for Compaction Control.” *Journal of the Transportation Research Board*, No. 1849, TRB, National Research Council, Washington, D.C., pp. 20-30.
38. Livneh, M., Ishai, I., (1987). “Pavement and Material Evaluation by a Dynamic Cone Penetrometer.” Sixth International Conference, Structural Design of Asphalt Pavements, Vol. I. p. 665-676.
39. Nazarian, S., Baker, M. and Crain, K. (1995). “Use of Seismic Pavement Analyzer in Pavement Evaluation,” Transportation Research Record 1505, Transportation Research Board, National Research Council, Washington, D. C., pp. 1-8.
40. Nazarian, S., Yuan, D., Tandon, V., and Arellano, M. (2003). “Quality Management of Flexible Pavement Layers with Seismic Methods,” Research Report 0-1735-3F, Center for Transportation Infrastructure System, University of Texas at El Paso. El Paso.
41. Nazarian, S., Yuan, D., and Tandon, V. (2005). “Quality Management of Flexible Pavement Layers with Seismic Methods,” Research Report 0-1735-S, Center for Transportation Infrastructure System, University of Texas at El Paso.
42. Powell, W. D., Potter, J. F., Mayhew, H. C., and Nunn, M. E. (1984). “The Structural Design of Bituminous Roads.” TRRL Report LR 1132, 62 pp.
43. Pen, C. K. (1990). “An assessment of the available methods of analysis for estimating the elastic moduli of road pavements.” Proc., 3rd Int. Conf. on Bearing Capacity of Roads and Airfields, Trondheim, Norway.
44. Puppala, A. (2008). “Estimating Stiffness of Subgrade and Unbound Materials for Pavement Design,” National Cooperative Highway Research Program (NCHRP)

Synthesis 382, Transportation Research Board, National Research Council, Washington, D.C.

45. Rohde, G. (1994). “Determining Pavement Structural Number from FWD Testing.” *Transportation Research Record 1448*, Transportation Research Board, National Research Council, Washington, D. C., pp. 61-68.
46. Saeed, A., Hall, J., and Barker, W. (2001). “Performance-Related Test of Aggregates for Use in Unbound Pavement Layers,” National Cooperative Highway Research Program (NCHRP) Report 453, Transportation Research Board, National Research Council, Washington, D.C.
47. Seyhan, U., and Tutumluer, E. (2002). “Anisotropic Modular Ratios as Unbound Aggregate Performance Indicators.” *Journal of Materials in Civil Engineering*, 14 (5), pp. 409-416.
48. Siekmeier, J., Pinta, C., Merth, S., Jensen, J., Davich, P., Camargo, F., and Beyer, M. (2009). “Using the Dynamic Cone Penetrometer and Light Weight Deflectometer for Construction Quality Assurance,” Report Number MN/RC 2009-12, Minnesota Department of Transportation.
49. Siekmeier, J., (2010). “Implementation of Deflection Testing during Construction to Support Modulus-based Pavement Design,” Presentation, Great Lakes Geotechnical Geo-environmental Conference Milwaukee, Wisconsin.
50. Smith, R., and Pratt, D., (1983). “A Field Study of In Situ California Bearing Ratio and Dynamic Cone Penetrometer Testing for Road Subgrade Investigations,” *Australian Road Research*, 13 (4), Dec., pp. 285-294.
51. Theyse, H. (2002). “Stiffness, Strength, and Performance of Unbound Aggregate Material: Application of South African HVS and Laboratory Results to California Flexible Pavements,” University of California Pavement Research Center. Davis, California.
52. Thom, N. H., and Brown, S. F. (1988). “The Effect of Grading and Density on The Mechanical Properties of a Crushed Dolomitic Limestone,” Proceedings of the 14th ARRB Conference, Part 7: 94–100.
53. Thom, N. H., and Brown, S. F. (1989). “The Mechanical Properties of Unbound Aggregates from Various Sources,” UNBAR 3. Nottingham. pp. 130–142.
54. Thompson, M. R., and Smith, K. L. (1990). “Repeated Triaxial Characterization of Granular Bases,” *Transportation Research Record 1278*, Dynamic Testing of Aggregates and Soils and Lateral Stress Measurements, TRB, Washington D.C.
55. Titi, H., Druckrey, A., and Bautista, E. (2012). “Resilient Modulus Testing of Steel Slag and Steel Slag-Aggregate Mixtures,” Research Report, Bureau of Technical Services, Wisconsin Department of Transportation, Project ID: 0657-45-14.
56. Tutumluer, E. (2012). “Practice for Unbound Aggregate Pavement Layers,” National Cooperative Highway Research Program (NCHRP) Synthesis Topic 43-03, Transportation Research Board, National Research Council, Washington, D.C.

57. Tutumluer, E. (2009). "State of the Art: Anisotropic Characterization of Unbound Aggregate Layers in Flexible Pavements," ASCE Geotechnical Special Publication No. 184, Pavements and Materials – Modeling, Testing and Performance, Edited by Z. You, A. R. Abbas, and L. Wang, pp. 1-16.
58. Van Niekerk, A., Molenaar, A., and Houben, L. J. M. (2002). "Effect of Material Quality and Compaction on the Mechanical Behavior of Base Course Materials and Pavement Performance." Proc., 6th Int. Conf. on Bearing Capacity of Roads, Railways and Airfields, Taylor & Francis, Lisbon, Portugal.
59. Van Vuuren, D. J., (1969). "Rapid Determination of CBR with the Dynamic Cone Penetrometer." Rhod. Engr. p. 852-854.
60. Von Quintus, H. L., Rao, C., Minchin, R. E., Nazarian, S., Maser, K. R., and Prowell, B. (2009). "NDT Technology for Quality Assurance of HMA Pavement Construction," National Cooperative Highway Research Program (NCHRP) Report 626, Transportation Research Board (TRB), Washington, D.C.
61. Walaa, E. I. K., and El Hussein, M. (2004). "Novel Approach for Characterization of Unbound Materials," *Journal of the Transportation Research Board*, No. 1874, TRB, Washington D.C., p 38–46.
62. Webster. S. L., Grau, R. H., and Williams, R. P. (1992). "Description and Application of Dual Mass Dynamic Cone Penetrometer." U.S. Army Engineer Waterways Experiment Station, Instruction Report, No. GL-92-3.
63. Wu, S. and Sargand, S. (2007). "Use of Dynamic Cone Penetrometer in Subgrade and Base Acceptance," Ohio Research Institute for Transportation and the Environment (ORITE), Report Number FHWA/ODOT-2007/01.

Appendix A

Base Compaction Survey

Survey on Base Aggregate Construction

1. What is your involvement in base aggregate construction?
   a) Production
   b) Construction
   c) Testing
   d) Specifications

2. Which test method do you use to determine laboratory maximum density and optimum moisture content?
   a) AASHTO T99 - Standard Proctor
   b) AASHTO T180 - Modified Proctor
   c) ASTM D698- Standard Proctor
   d) Agency modified method:_________________
   e) Other (Please Specify):____________________

3. Method used for evaluating degree of compaction in the field?
   a) Observation based
   b) Density based
   c) Performance based

4. What method do you use to determine in-place Density?
   a) AASTHO T191 – Sand Cone
   b) AASHTO T310 – Nuclear Method
   c) AASHTO T238 – Nuclear Method
   d) Agency modified method:_________________
   e) Other: _____________________, _________________________, ____________________

5. What is the acceptance limit for Compaction?
   a) 90% maximum density
   b) 95% maximum density
   c) 97% maximum density
   d) 98% maximum density
   e) 100% maximum density
   f) No further displacement

6. What method do you use to determine in-place Stiffness?
   a) Dynamic Cone Penetrometer
   b) Geogauge
   c) Falling Weight Deflectometer
   d) Light Weight Deflectometer
   e) None
   f) Other: _____________________, _________________________, ____________________

7. What is the acceptable variation from optimum moisture content for aggregate bases?
____
____
____

8. Is there a need for new field test(s) to measure degree of compaction?

a) Yes [Please provide field test(s) you suggest]

i. ____________________

ii. ____________________

iii. ____________________

b) No

9. Do you think that requiring a field test to measure the degree of compaction will:

a) Delay construction schedule

b) Bring forward

c) No effect

d) Not applicable

e) Depends on tests

10. Do you think that requiring a field test to measure the degree of compaction will:

a) Increase project cost

b) Reduce project cost

c) No effect

d) Not applicable

e) Depends on tests

11. List compaction equipment type used for compaction of aggregate bases?

a) ________________________

b) ________________________

c) ________________________

d) ________________________

e) ________________________

12. Is there a certain aggregate type (s), your agency use, difficult to compact in the field?

a) Yes, [Please provide aggregate type (s)]

i. ___________________

ii. ___________________

iii. ___________________

b) No

13. If you face difficulties in compacting your base aggregate layer, what measures do you follow to meet the state DOT requirements?

____

____

____

14. What is the maximum Lift Thickness allowed by your agency for aggregate base compaction?

a) Less than 6 in.

b) 6 in.

c) 8 in.

d) 10 in.

e) 12 in.

f) More than 12 in.

15. What requirement(s) does your agency have for subgrade preparation for aggregate base construction?

____
____
____

16. Does your agency have gradations requirements for the aggregate(s) used in the base course?

a) Yes, Specify:____

b) No

Appendix B

Laboratory and Field Test Results for Constructed Aggregate Base Projects

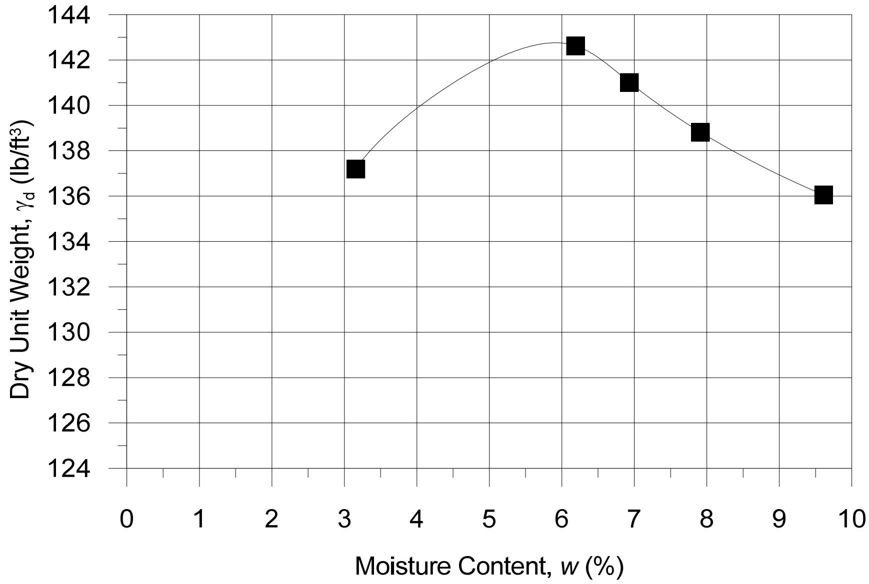

Figure B1: Compaction curve (AASHTO T 99) for base aggregate material used at STH 13, Spencer.

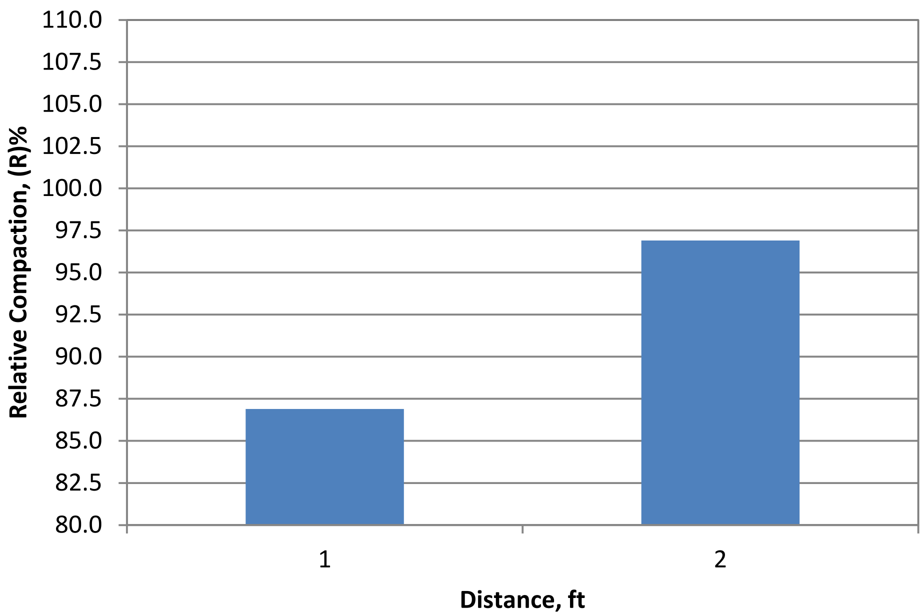

Figure B2: Variation of relative compaction with distance at test section on aggregate base layer, STH 13, Spencer.

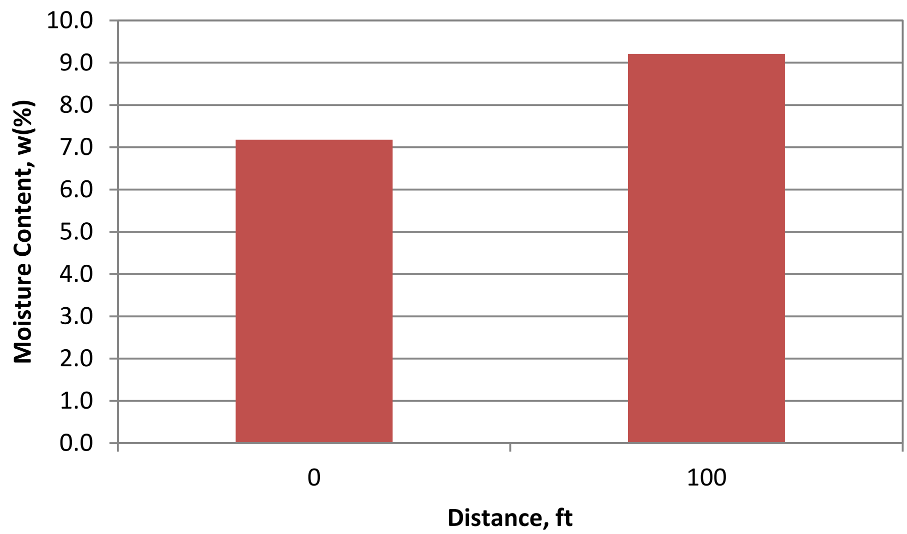

Figure B3: Variation of field moisture content with distance at test section on aggregate base layer, STH 13, Spencer.

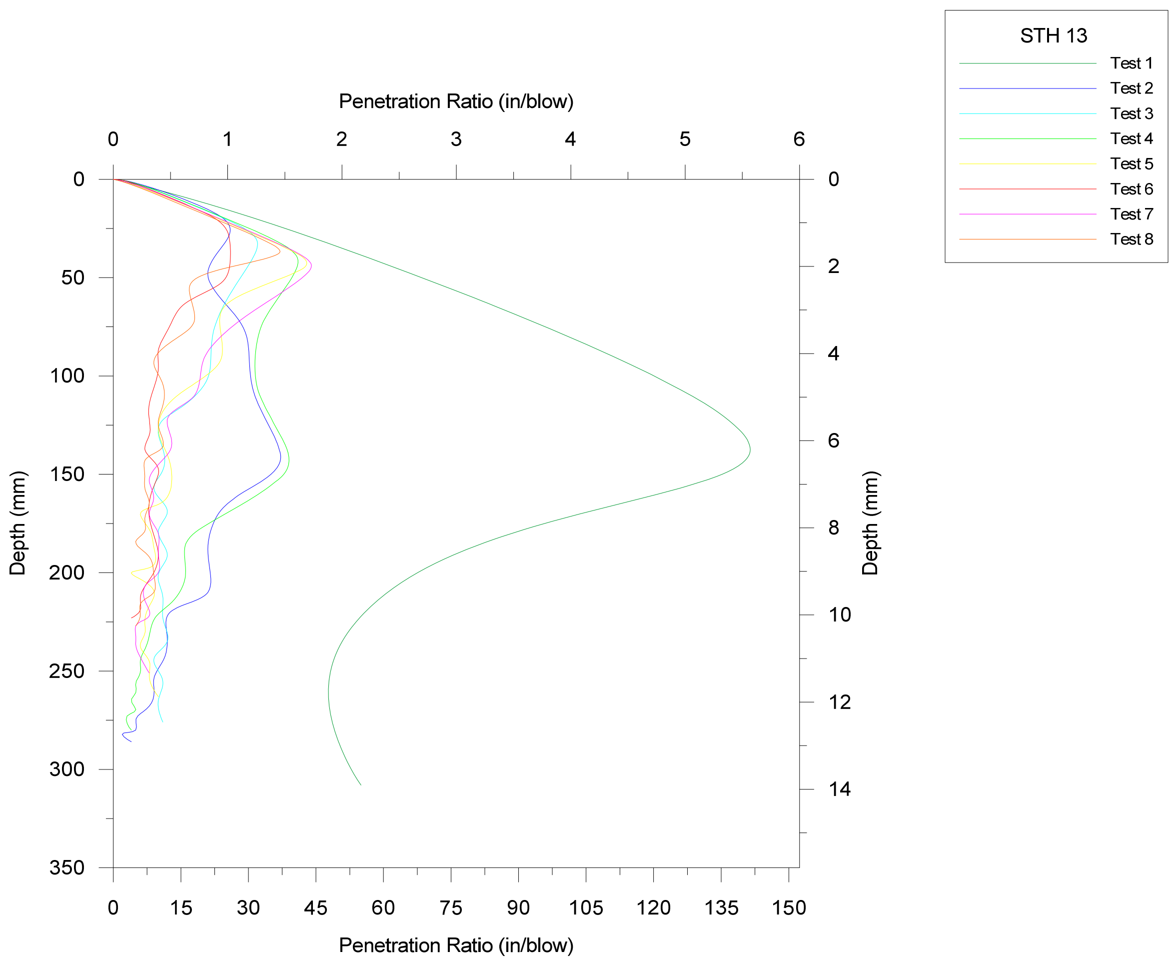

Figure B4: Penetration resistance with depth from DCP test at different points on the aggregate base layer, STH 13, Spencer.

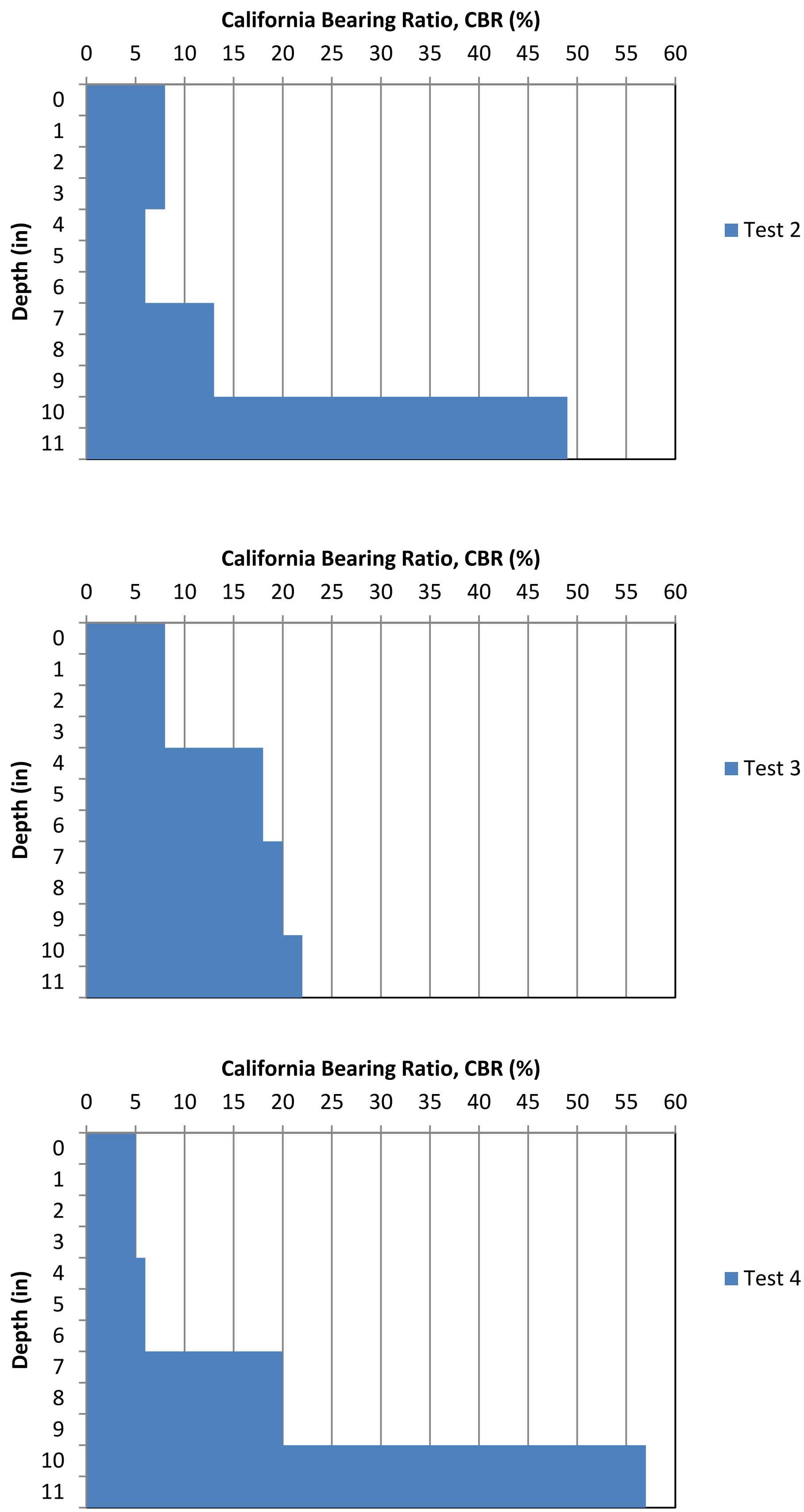

Figure B5: Variability of CBR with depth for aggregate base at STH 13, Spencer.

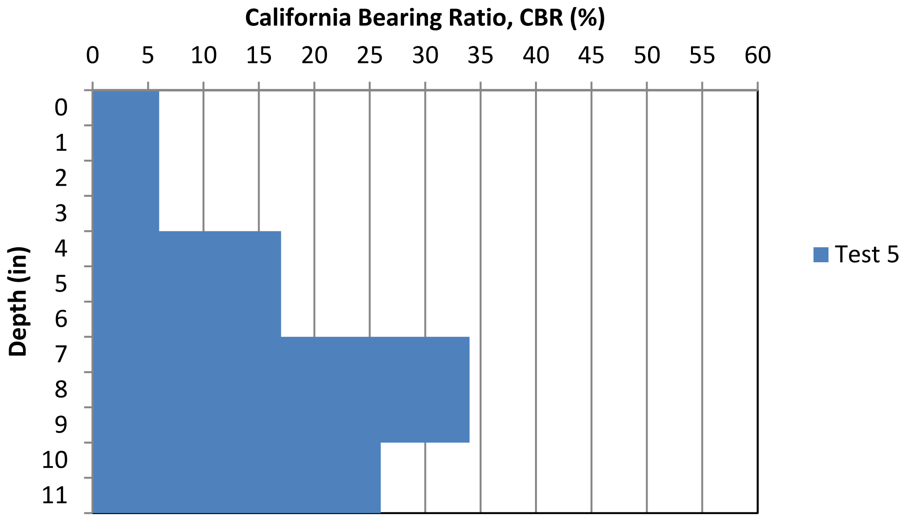

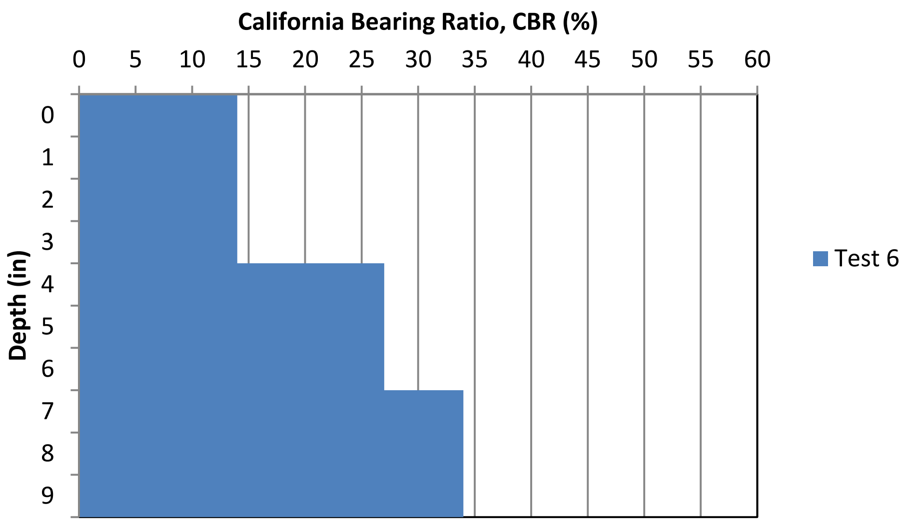

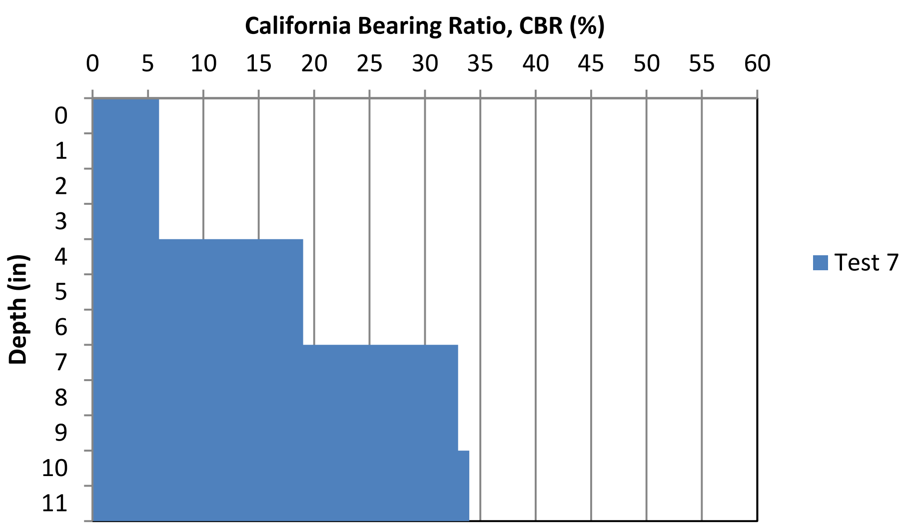

Figure B5 (cont.): Variability of CBR with depth for aggregate base at STH 13, Spencer.

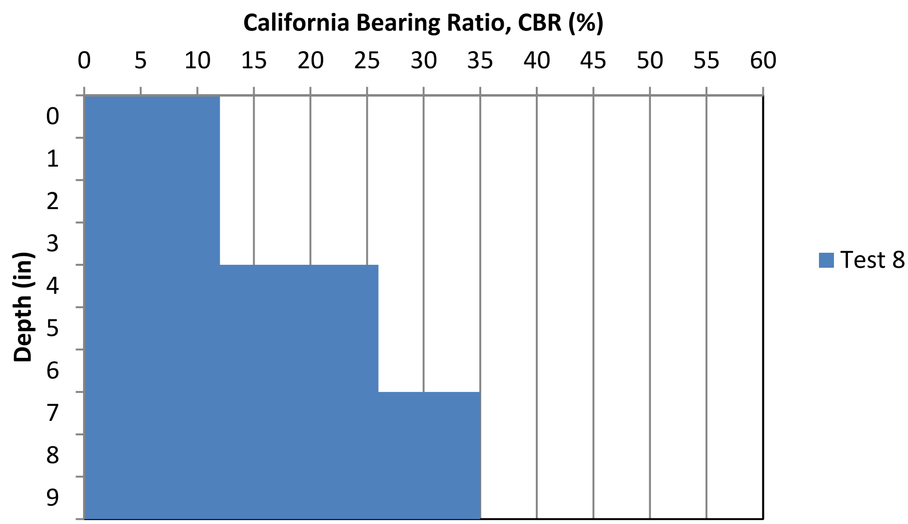

Figure B5 (cont.): Variability of CBR with depth for aggregate base at STH 13, Spencer.

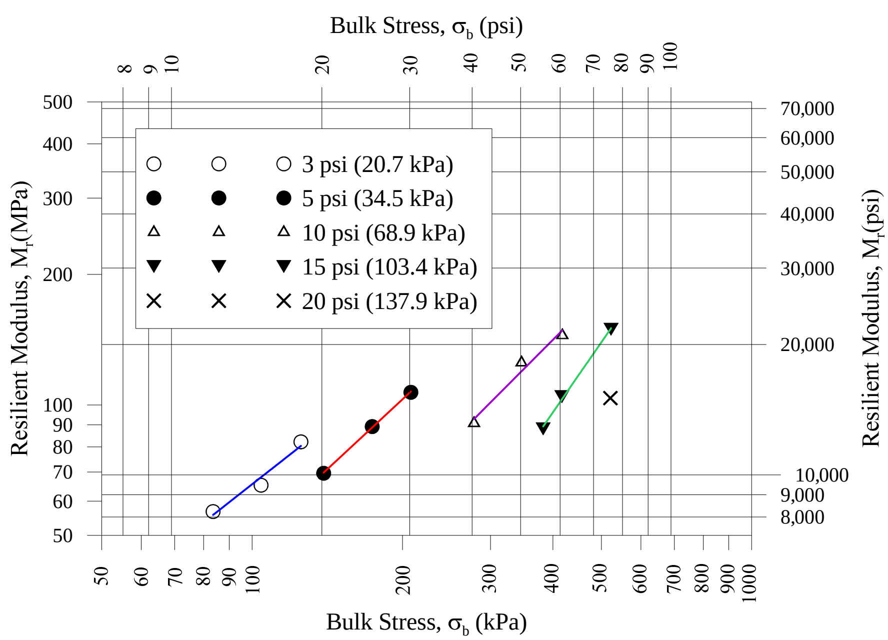

Figure B6: Results of repeated load triaxial test conducted on base aggregate specimen at maximum dry density and optimum moisture, STH 13, Spencer.

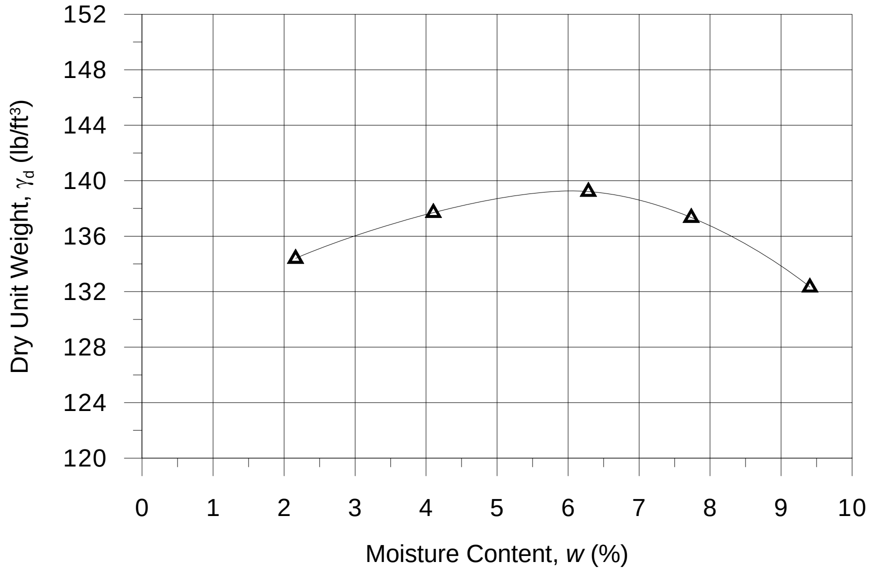

Figure B7: Compaction curve (AASHTO T 99) for base aggregate material used at CTH JJ, Appleton.

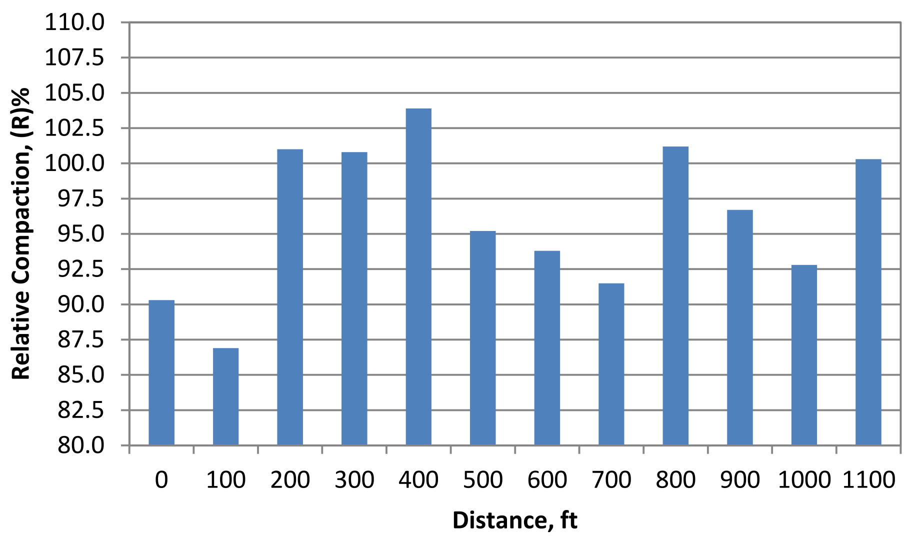

Figure B8: Variation of relative compaction with distance at test section on aggregate base layer, CTH JJ, Appleton.

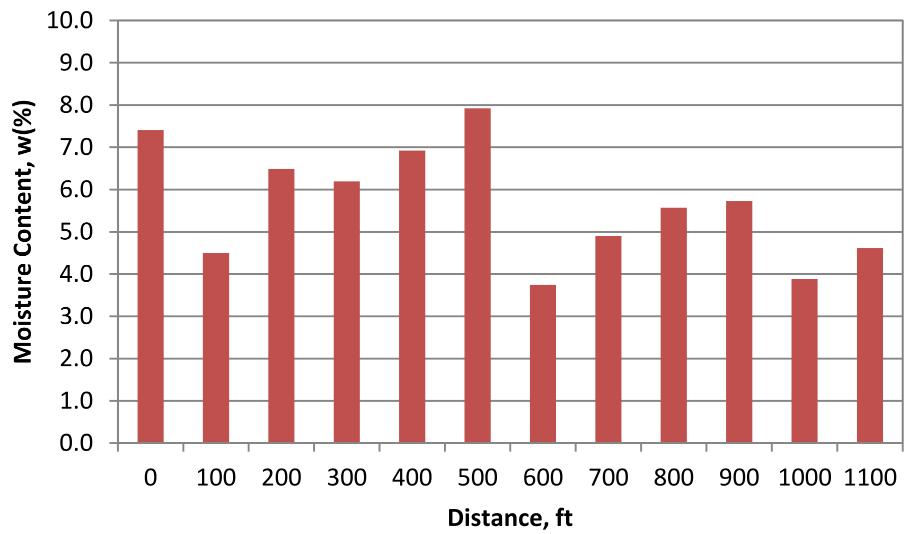

Figure B9: Variation of moisture content with distance at test section on aggregate base layer, CTH JJ, Appleton.

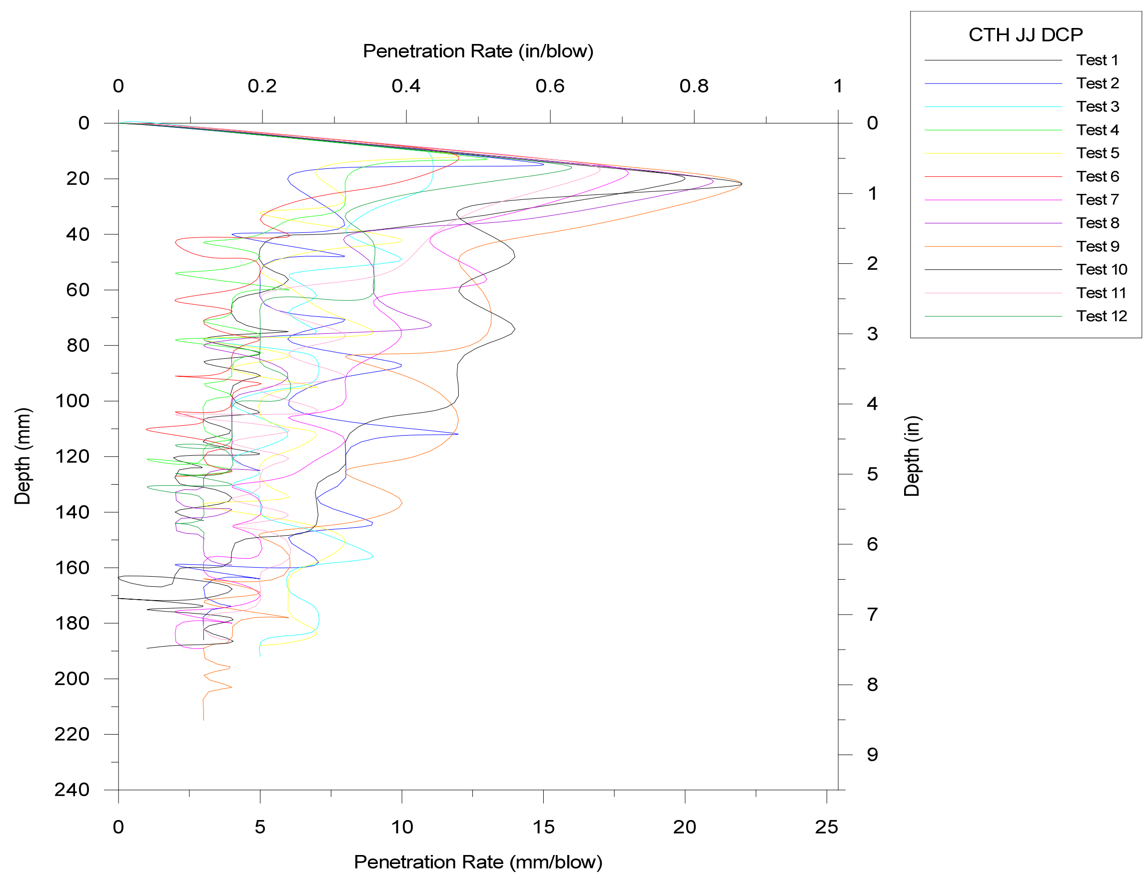

Figure B10: Penetration resistance with depth from DCP test at different points on the aggregate base layer, CTH JJ, Appleton.

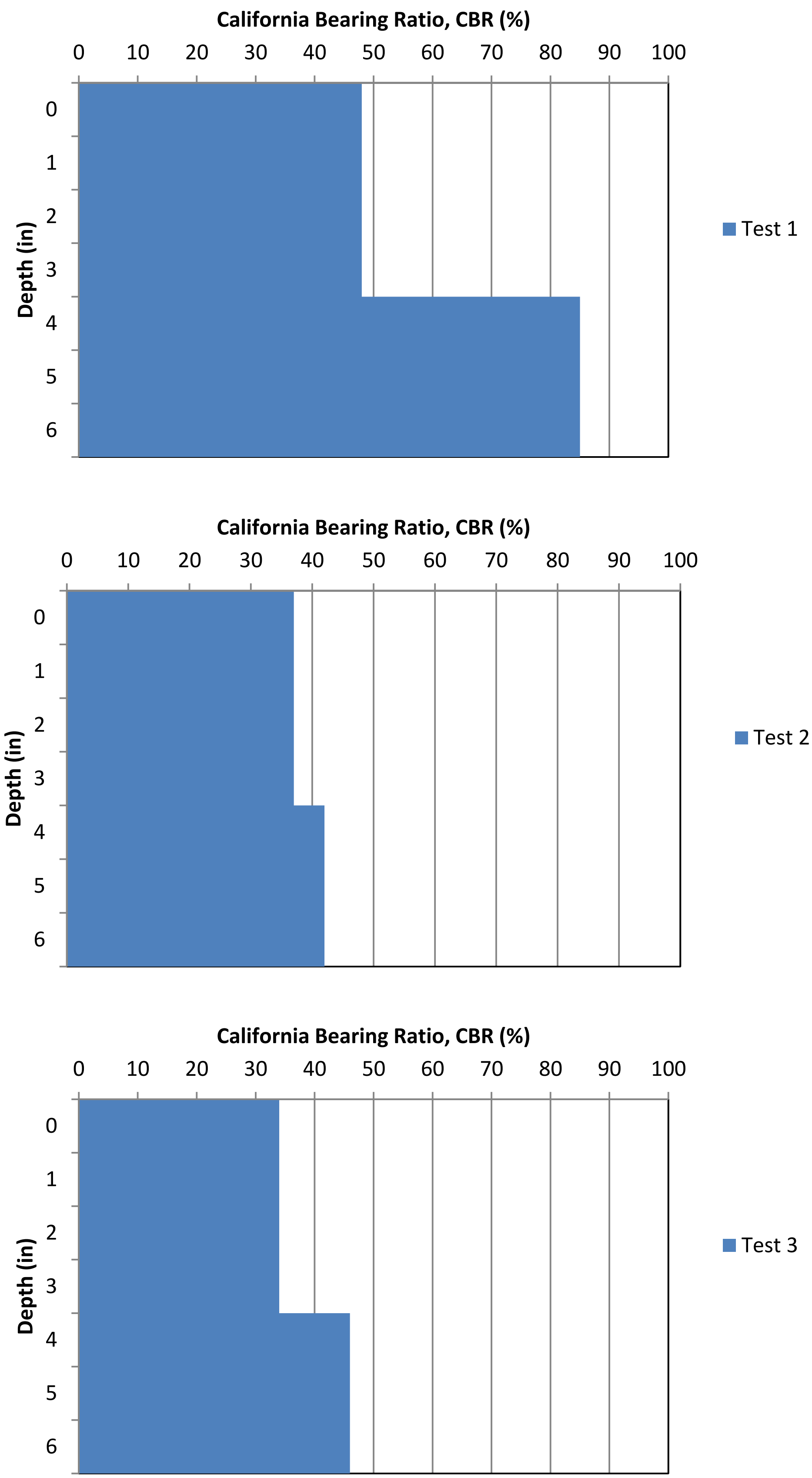

Figure B11: Variability of CBR with depth for aggregate base at CTH JJ, Appleton.

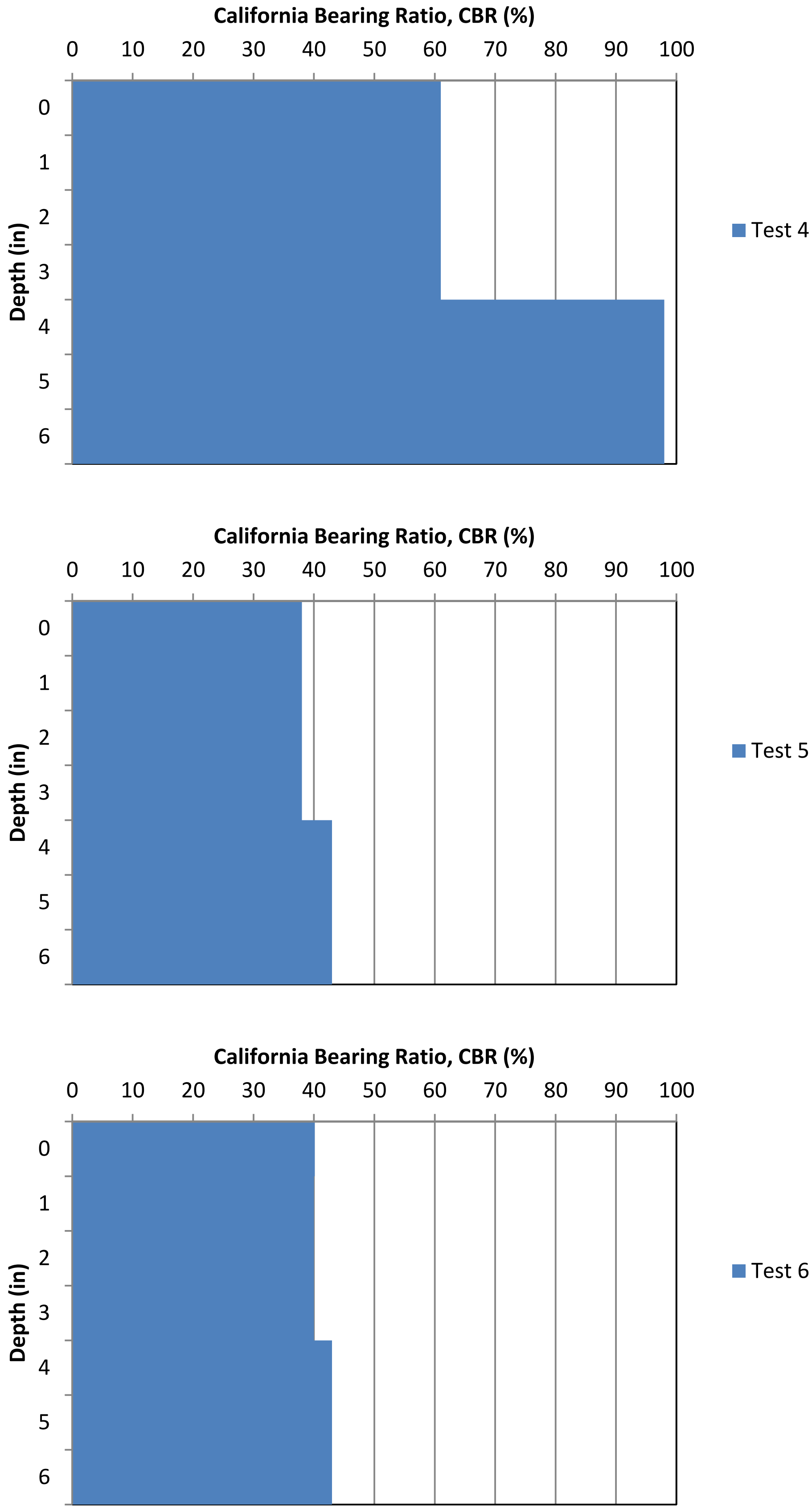

Figure B11 (Cont.): Variability of CBR with depth for aggregate base at CTH JJ, Appleton.

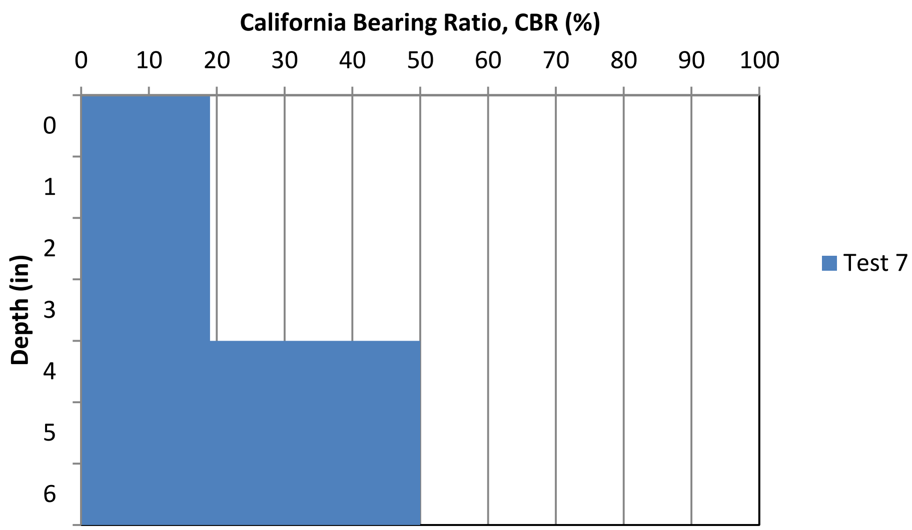

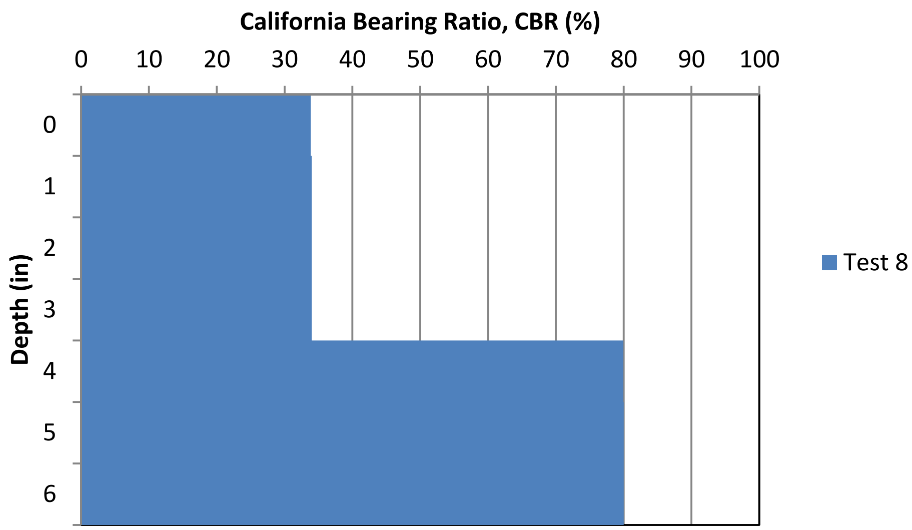

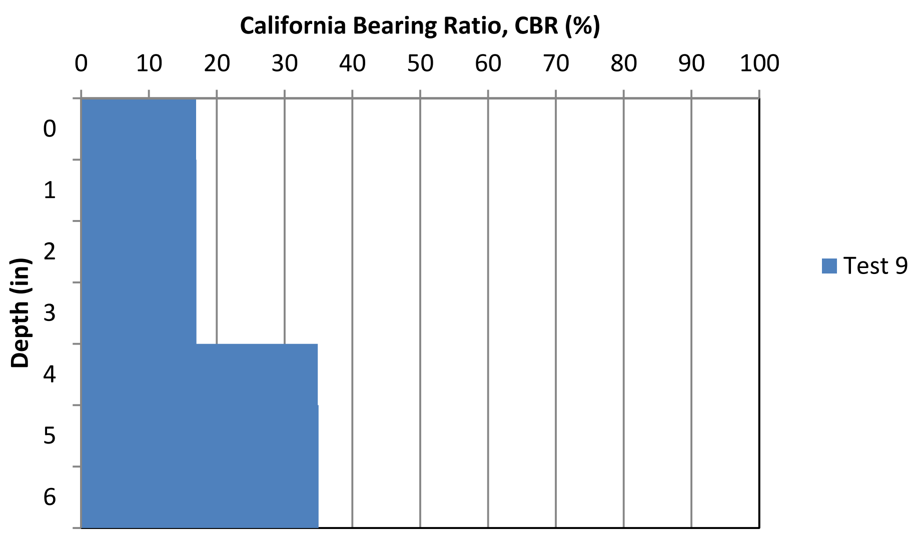

Figure B11 (Cont.): Variability of CBR with depth for aggregate base at CTH JJ, Appleton.

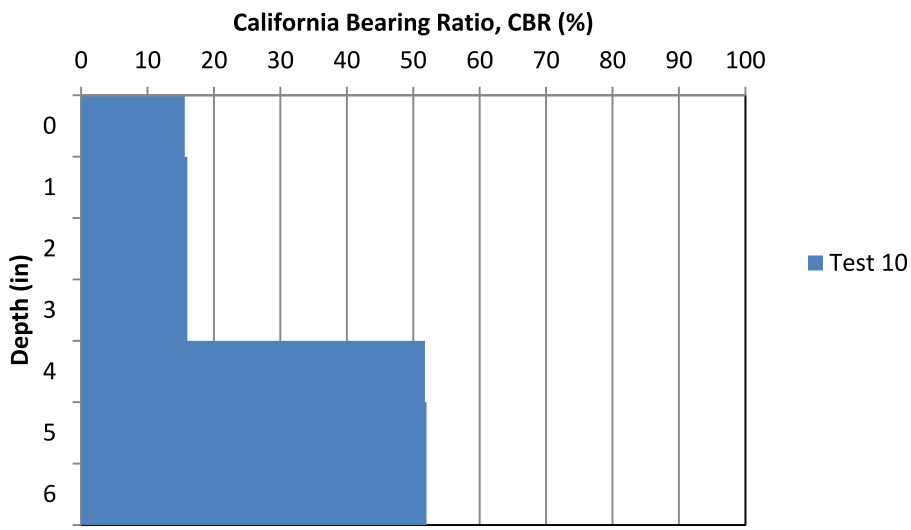

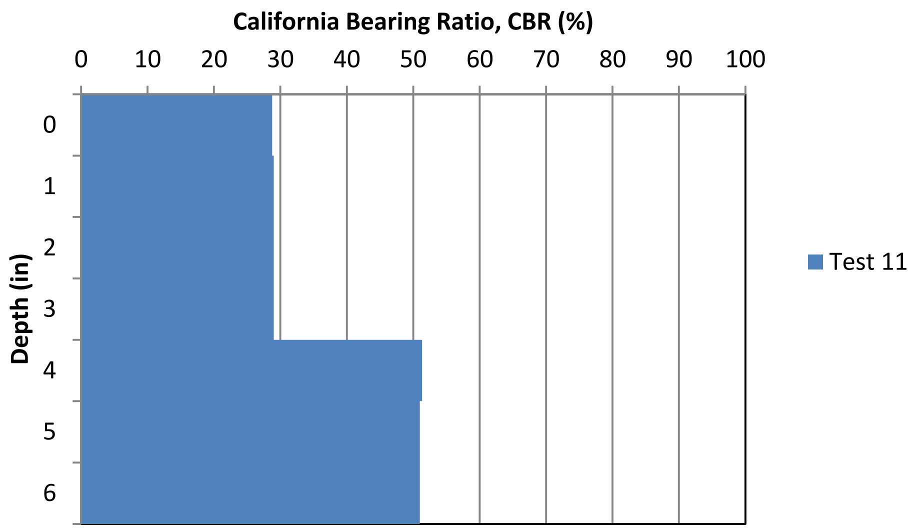

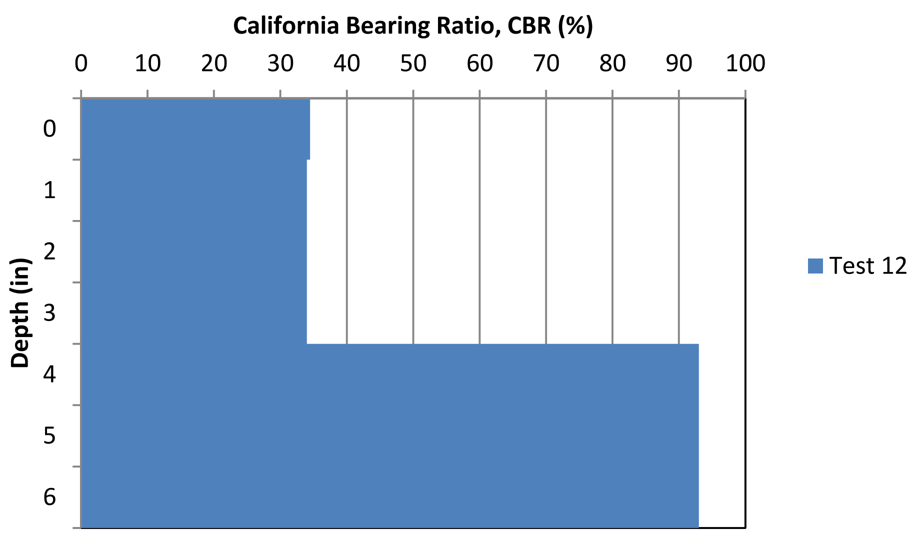

Figure B11 (Cont.): Variability of CBR with depth for aggregate base at CTH JJ, Appleton.

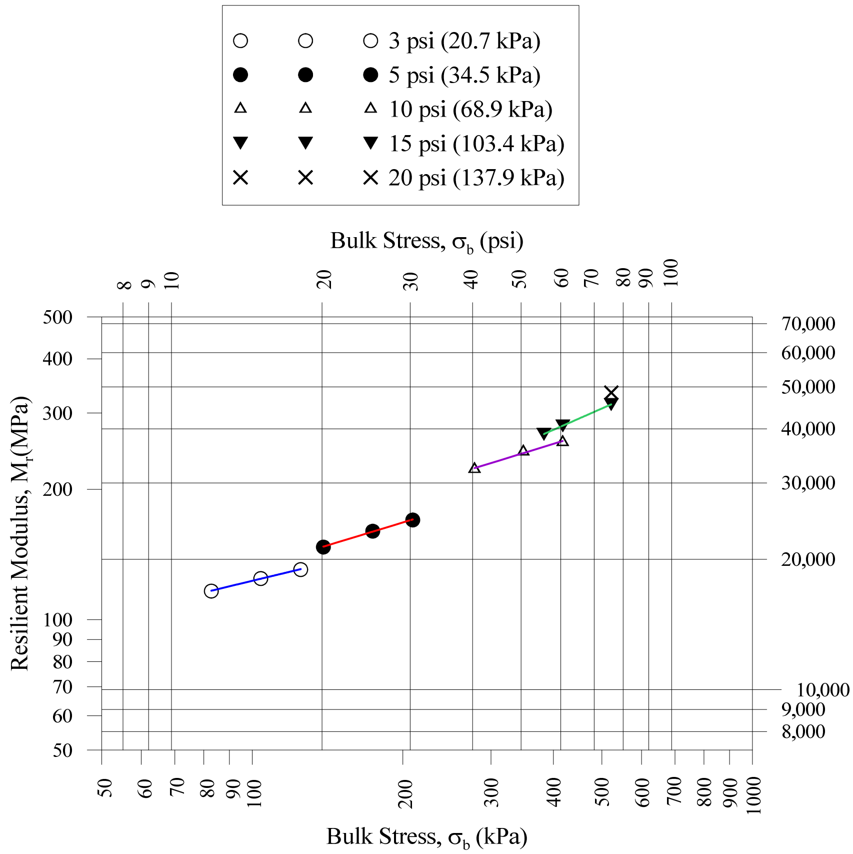

Figure B12: Results of repeated load triaxial test conducted on base aggregate specimen at maximum dry density and optimum moisture content, CTH JJ, Appleton.

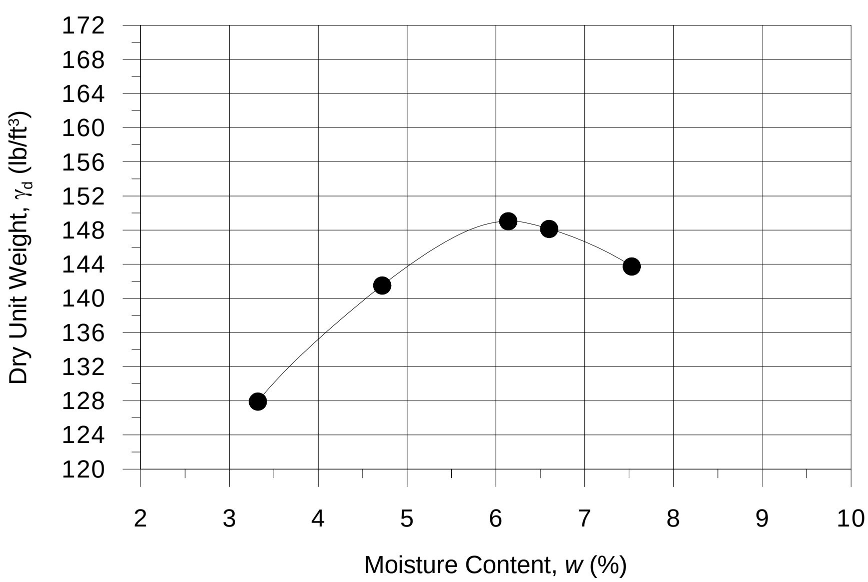

Figure B13: Compaction curve (AASHTO T 99) for base aggregate material used at USH 45, Larsen.

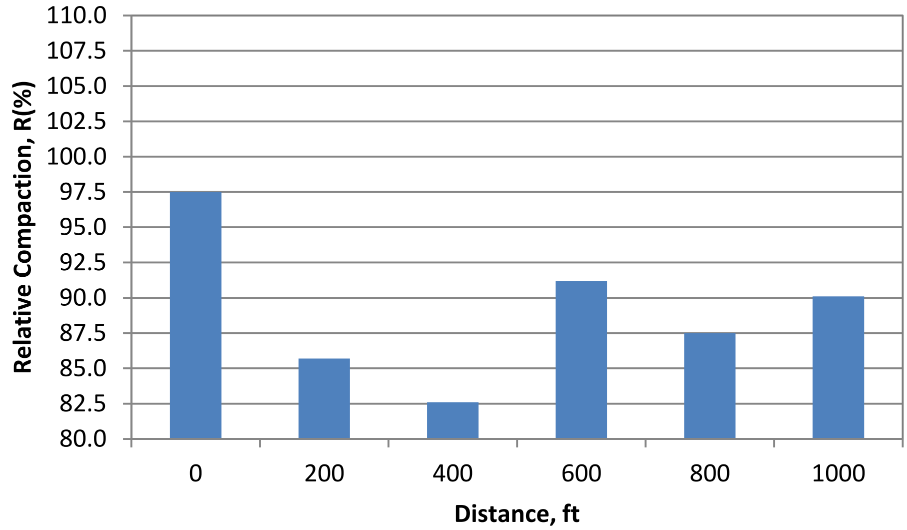

Figure B14: Variation of relative compaction with distance at test section on aggregate base layer, USH 45, Larsen.

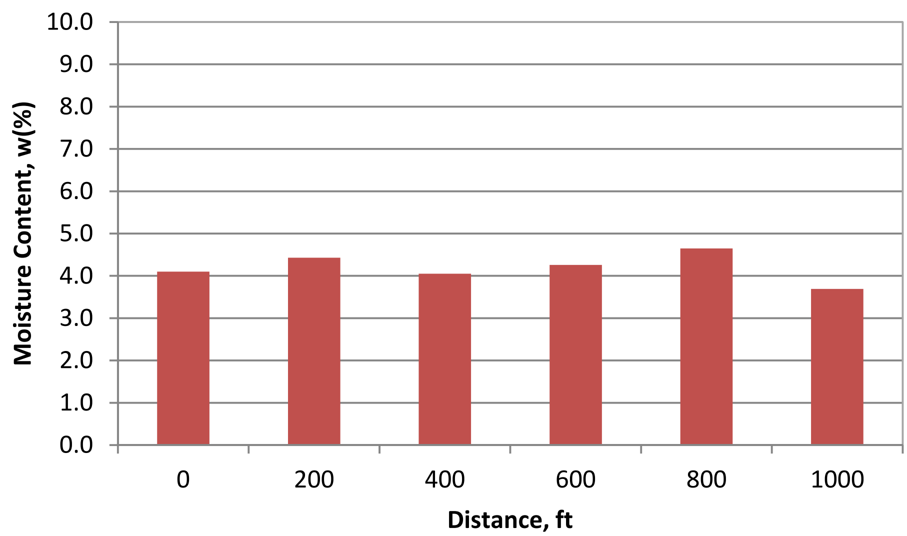

Figure B15: Variation of moisture content with distance at test section on aggregate base layer, USH 45, Larsen.

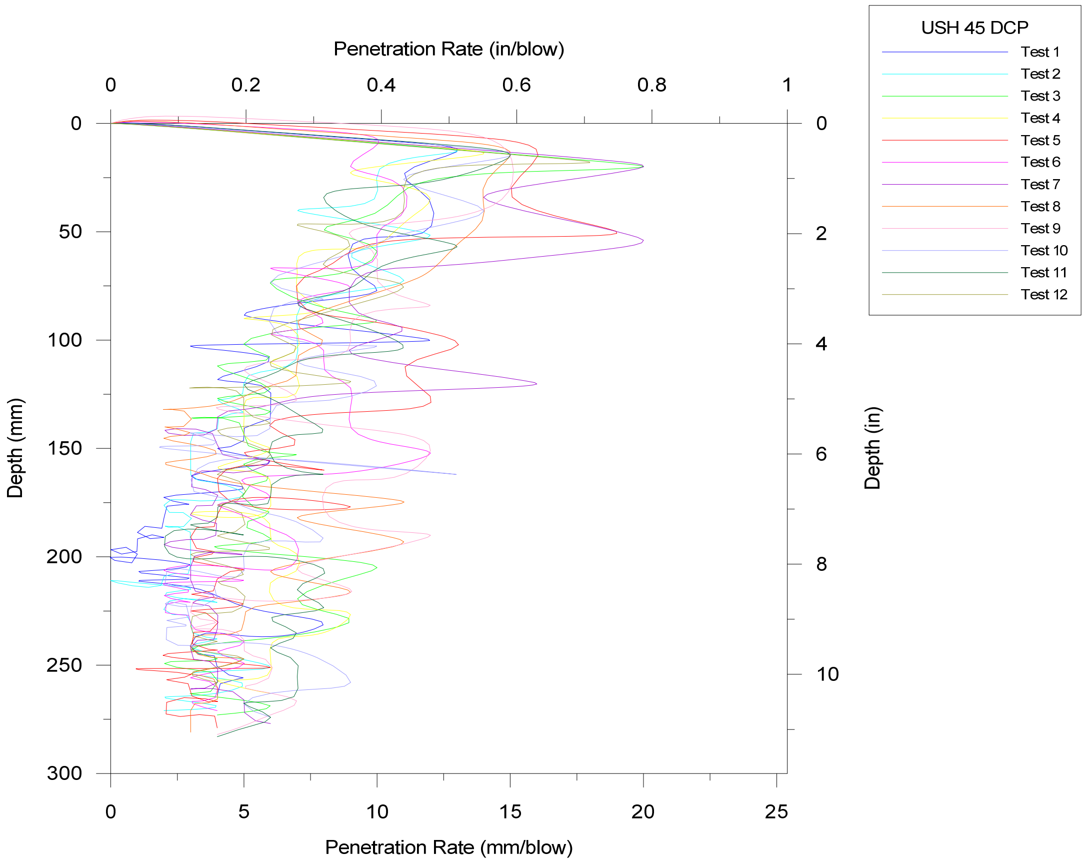

Figure B16: Penetration resistance with depth from DCP test at different points on the aggregate base layer, USH 45, Larsen.

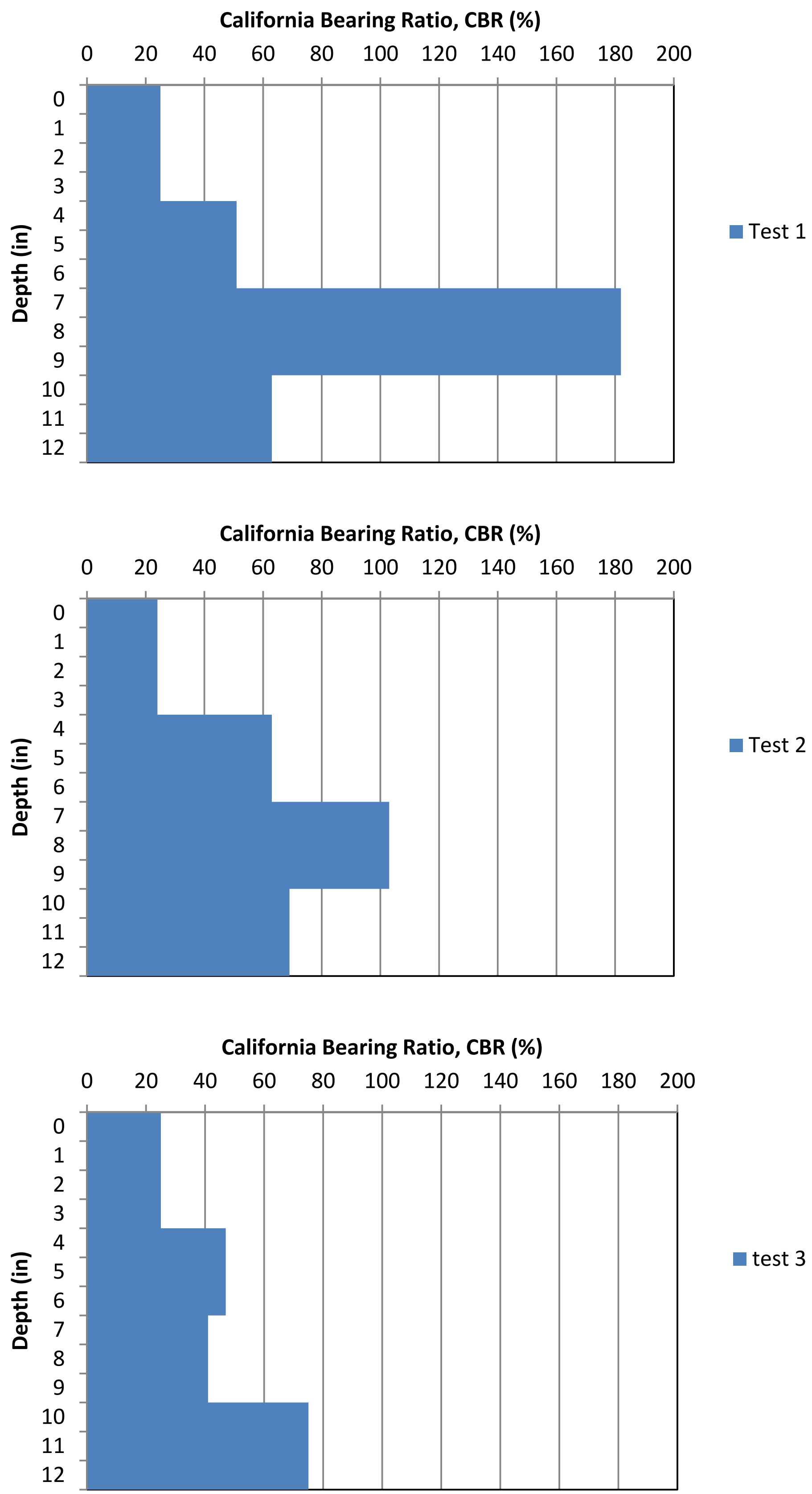

Figure B17: Variability of CBR with depth for aggregate base at USH 45, Larsen.

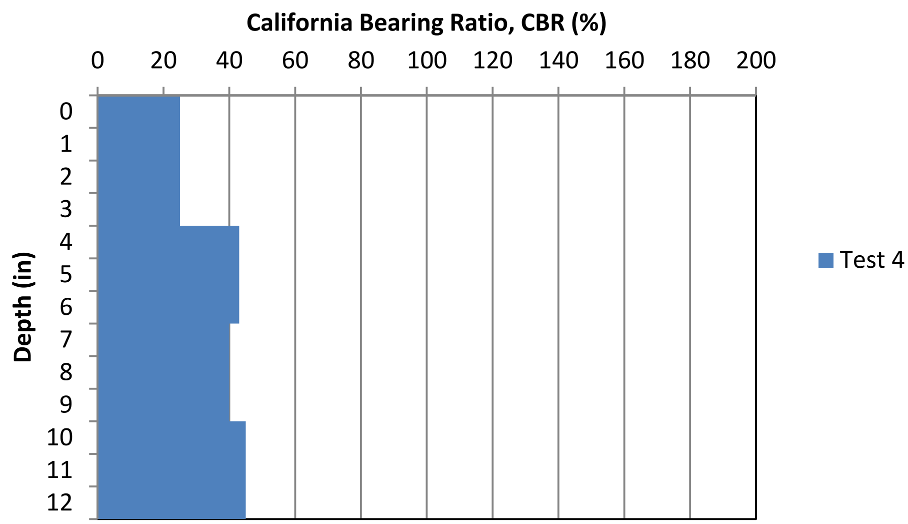

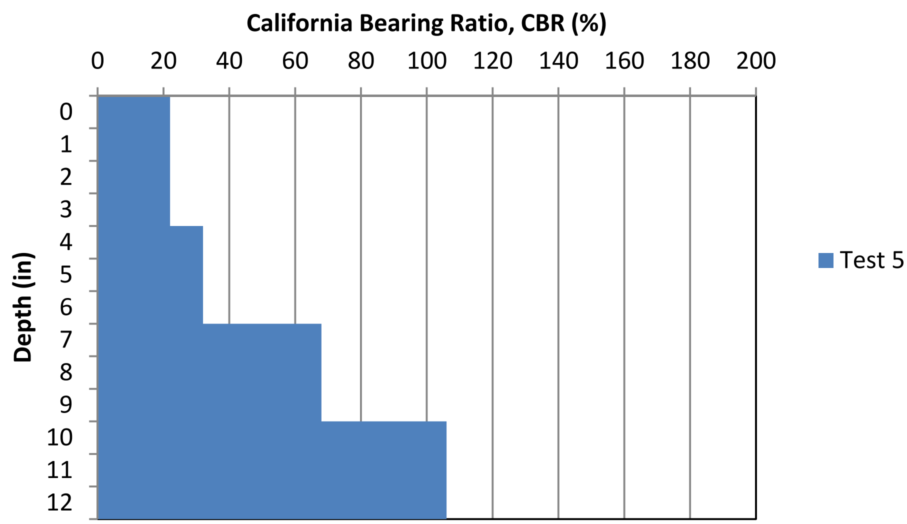

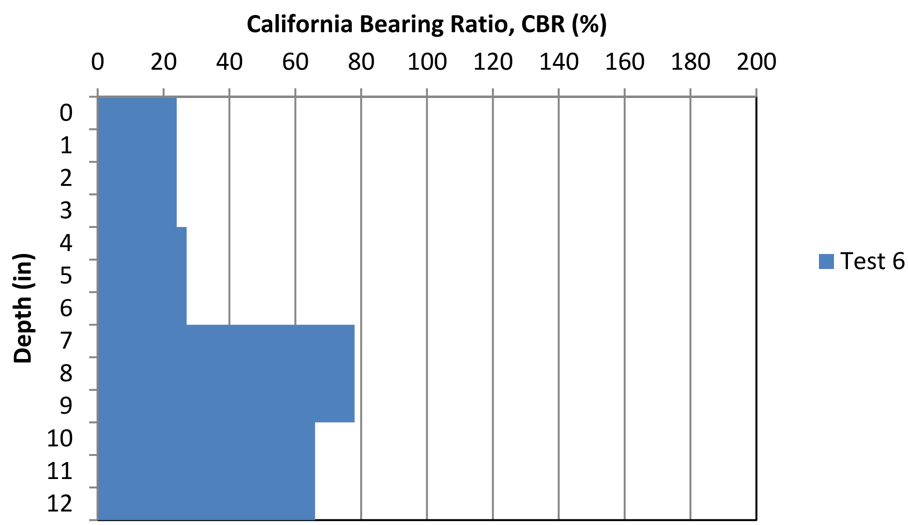

Figure B17 (Cont.): Variability of CBR with depth for aggregate base at USH 45, Larsen.

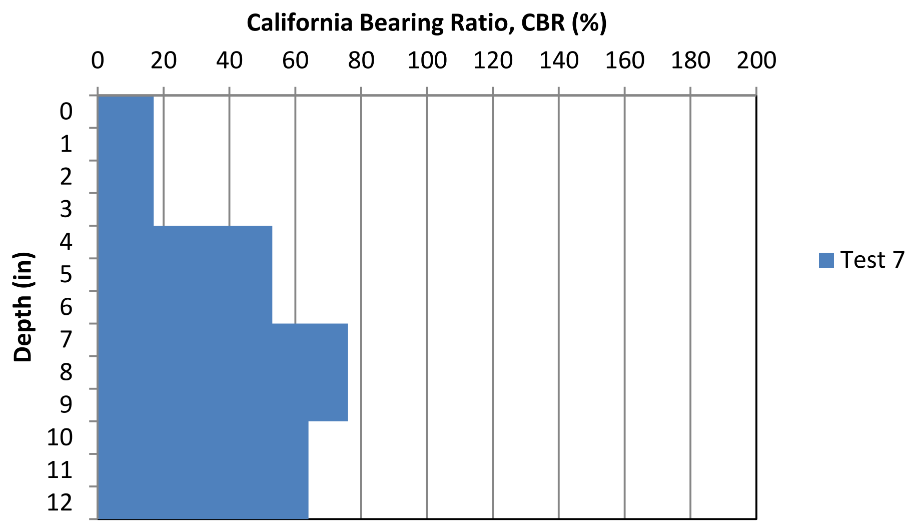

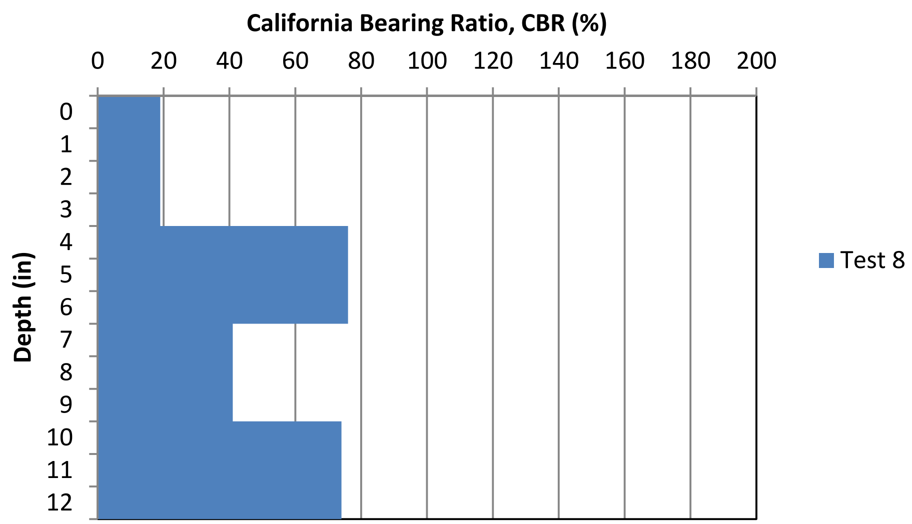

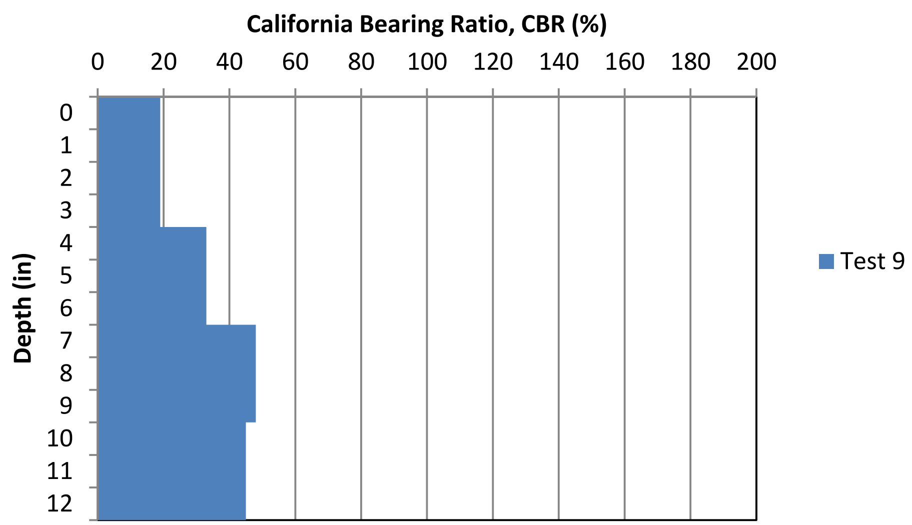

Figure B17 (Cont.): Variability of CBR with depth for aggregate base at USH 45, Larsen.

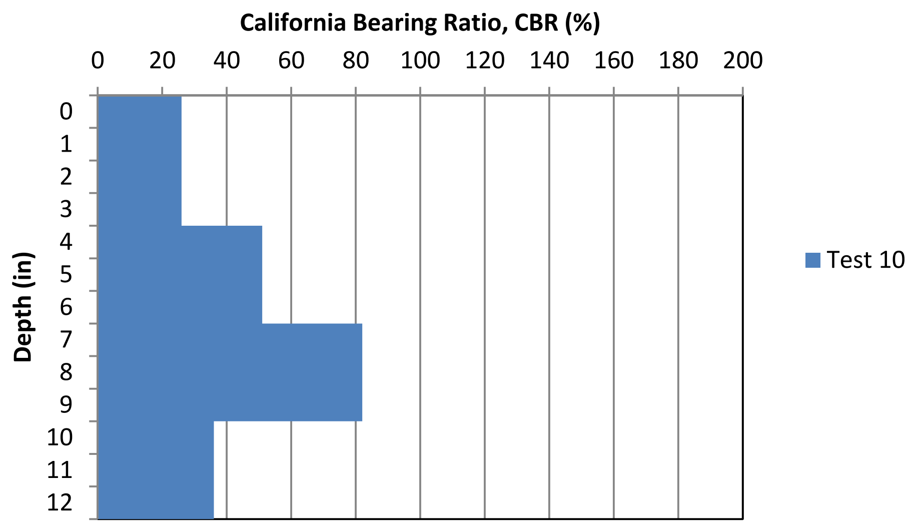

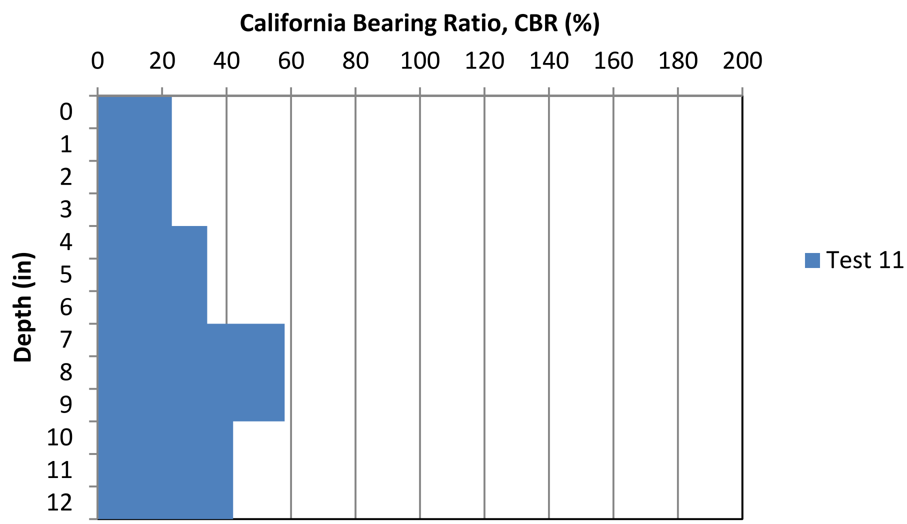

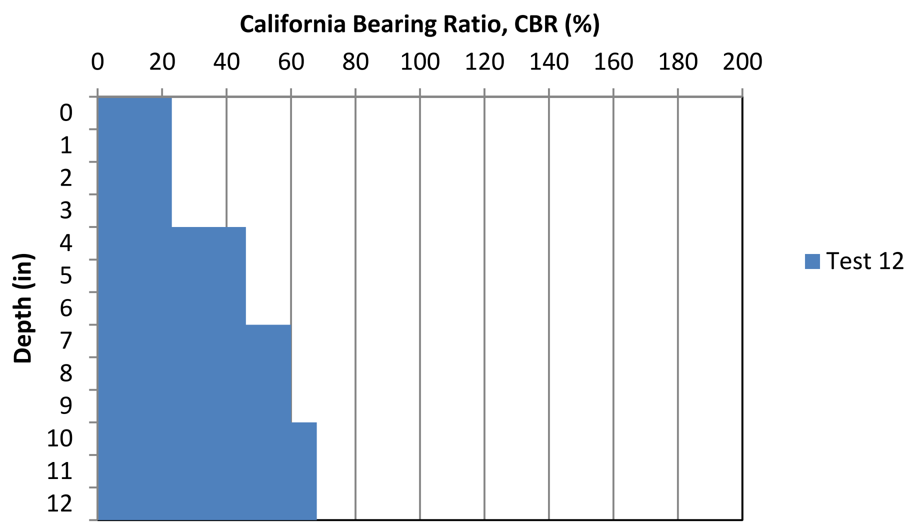

Figure B17 (Cont.): Variability of CBR with depth for aggregate base at USH 45, Larsen.

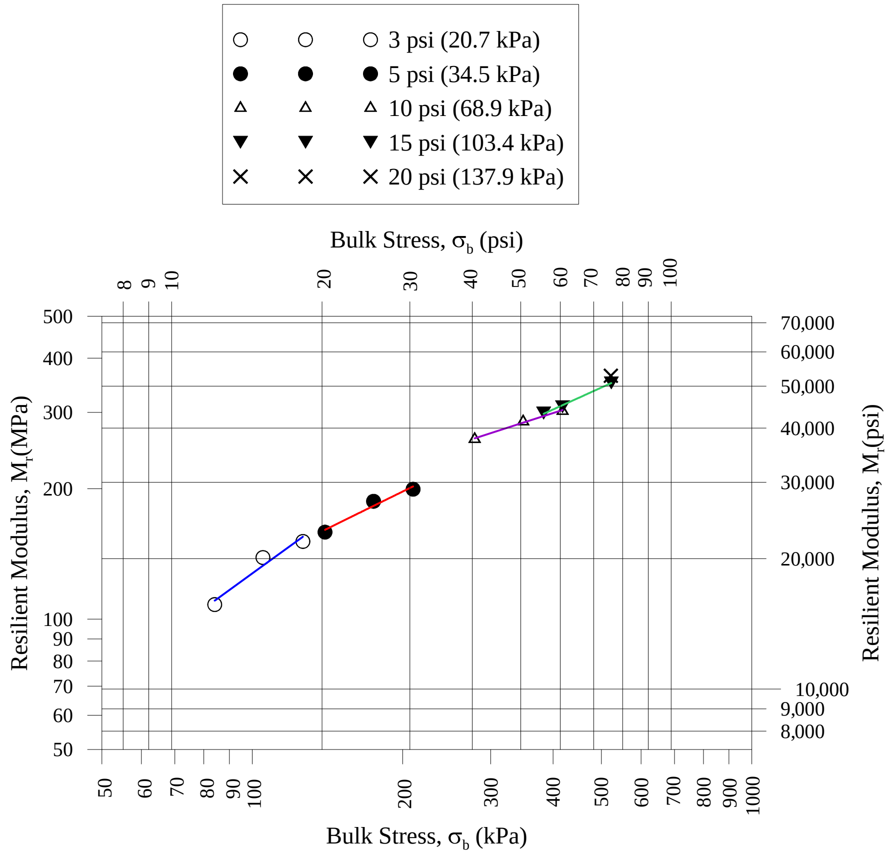

Figure B18: Results of repeated load triaxial test conducted on base aggregate specimen at maximum dry density and optimum moisture content, USH 45, Larsen, WI.

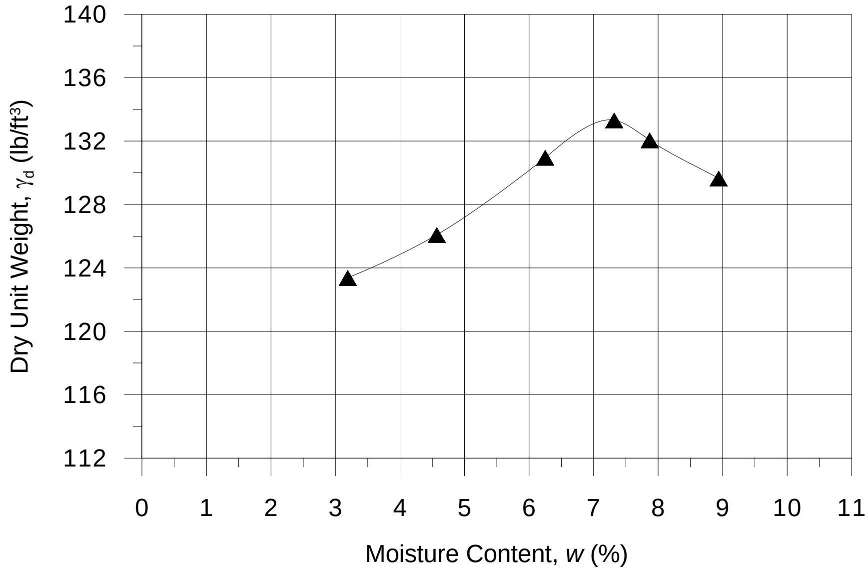

Figure B19: Compaction curve (AASHTO T 99) for base aggregate material used at STH 33, Port Washington.

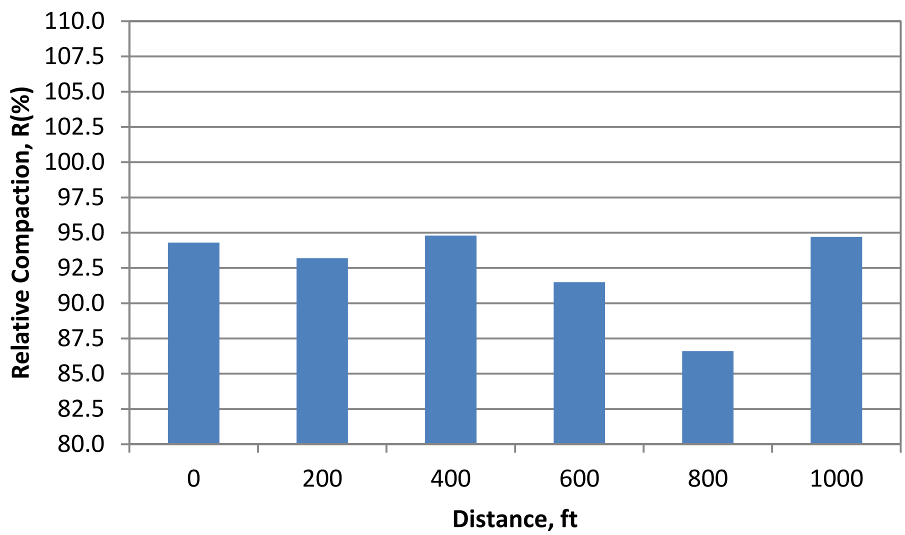

Figure B20: Variation of relative compaction with distance at test section on aggregate base layer, STH 33, Port Washington.

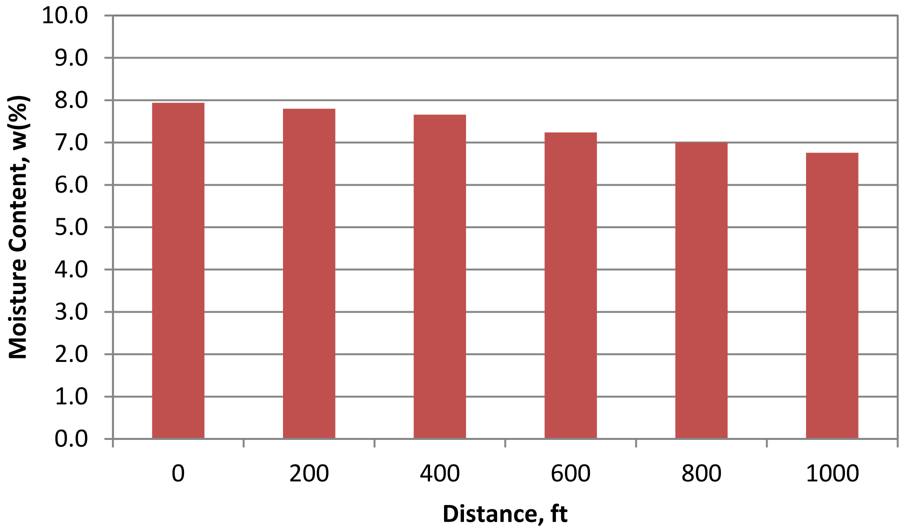

Figure B21: Variation of moisture content with distance at test section on aggregate base layer, STH 33, Port Washington.

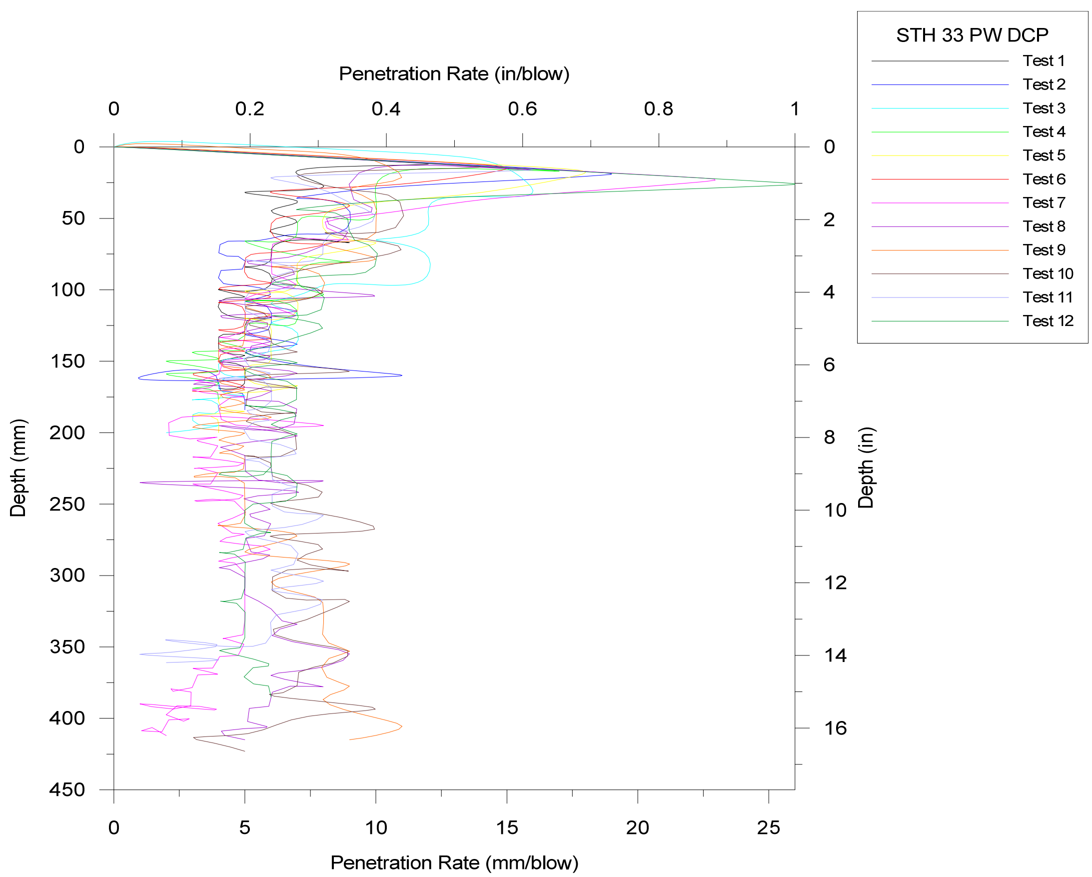

Figure B22: Penetration resistance with depth from DCP test at different points on the aggregate base layer, STH 33, Port Washington.

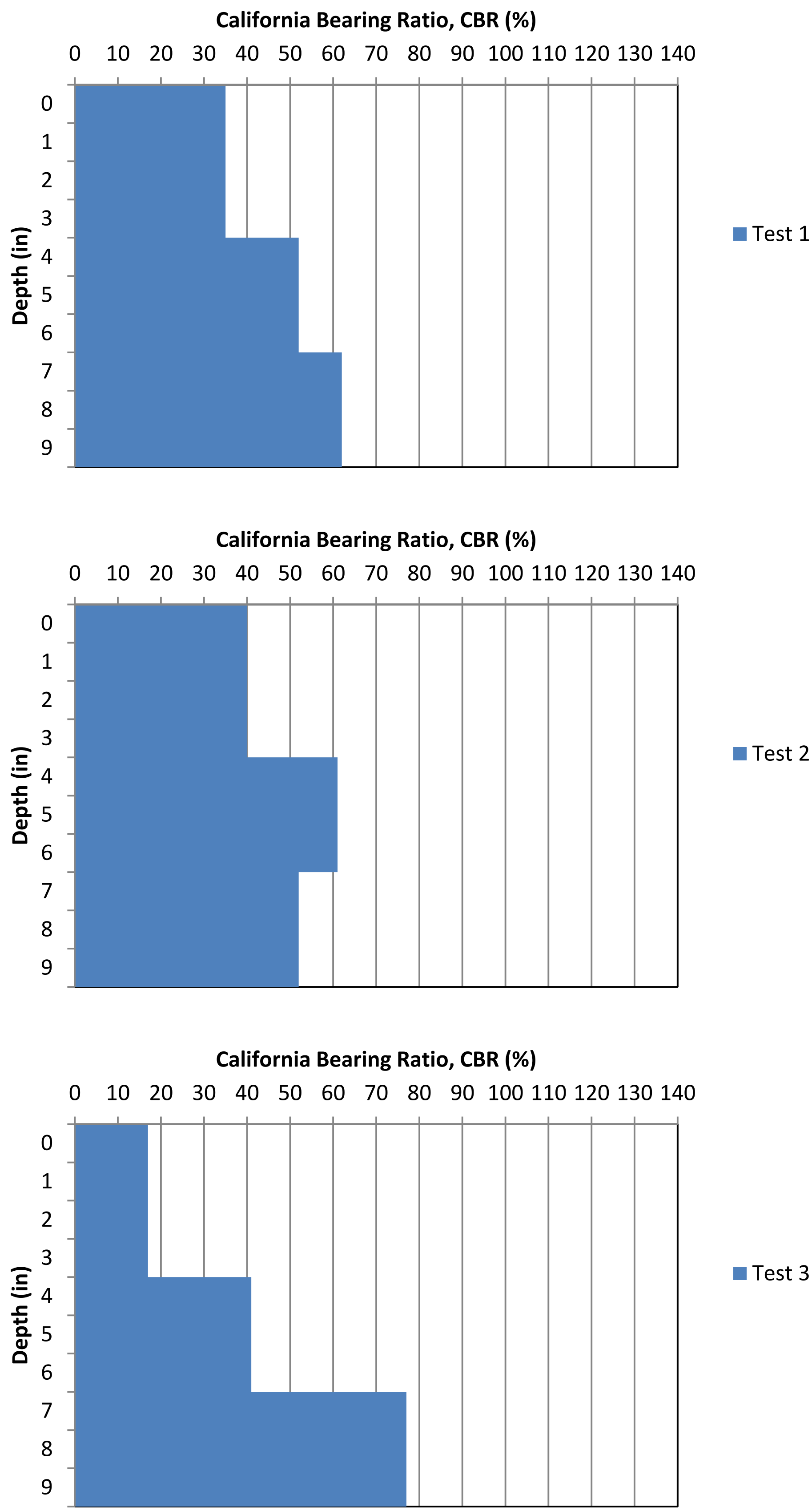

Figure B23: Variability of CBR with depth for aggregate base at STH 33, Port Washington.

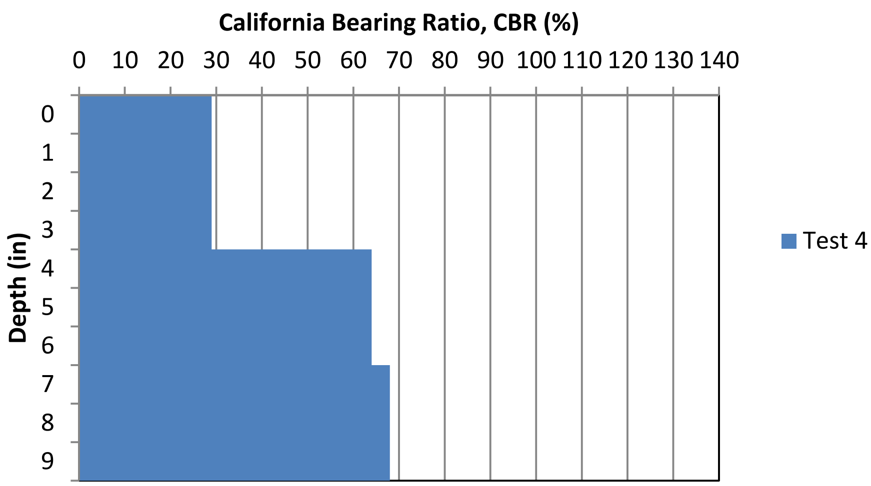

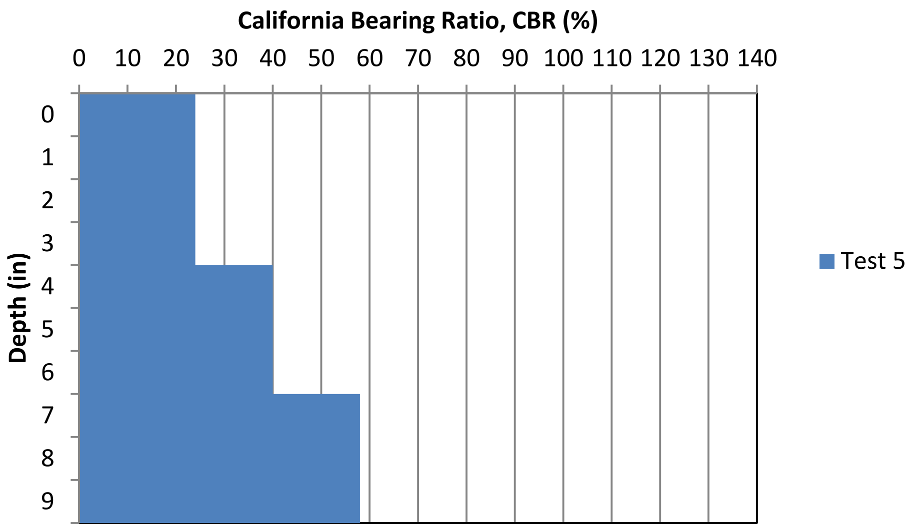

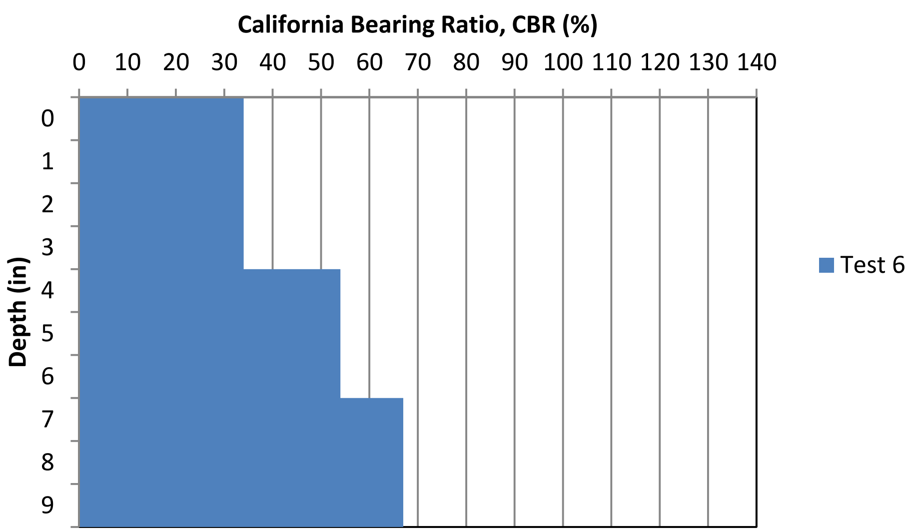

Figure B23 (Cont.): Variability of CBR with depth for aggregate base at STH 33, Port Washington.

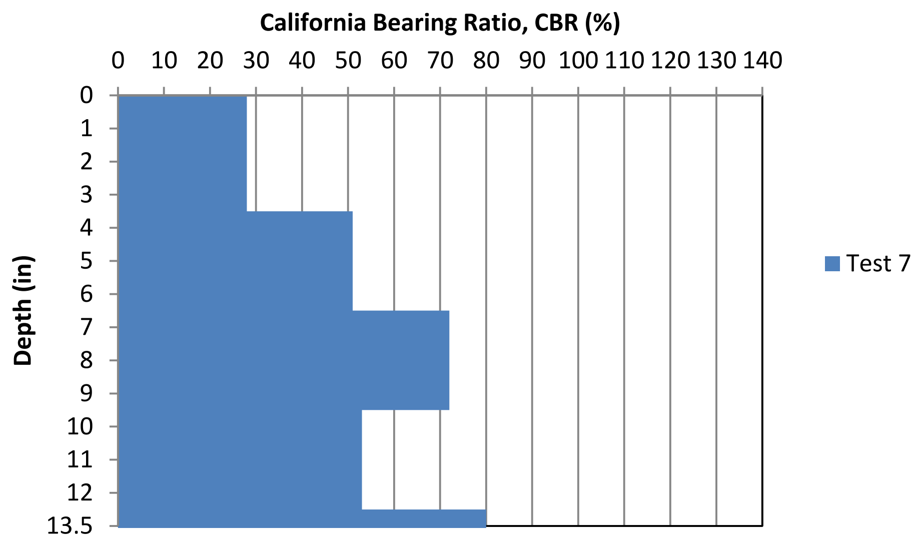

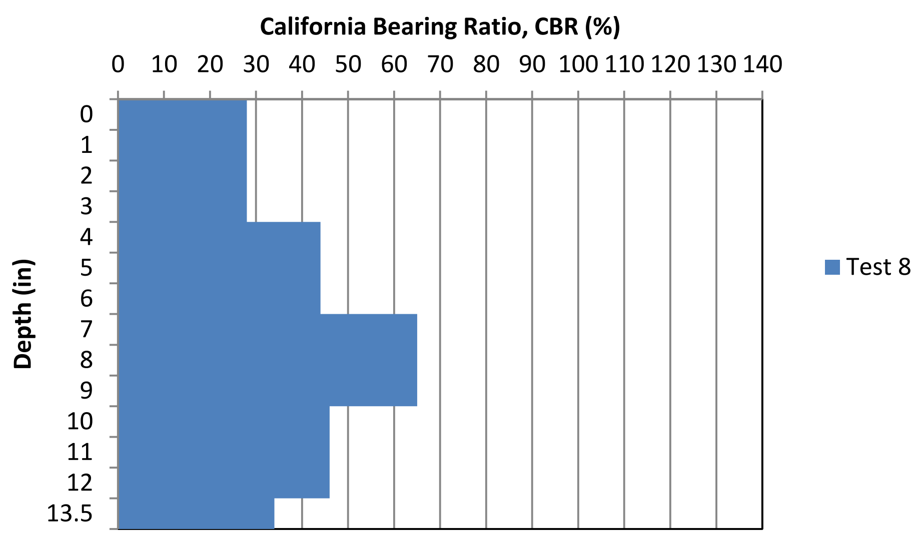

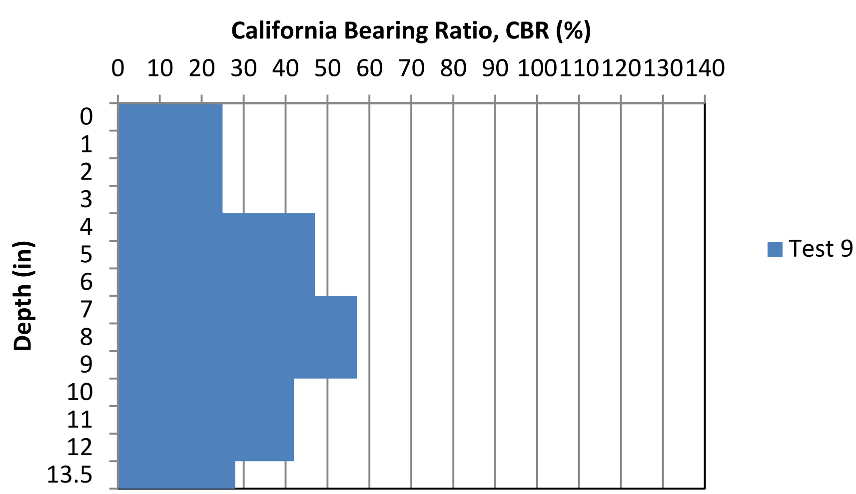

Figure B23 (Cont.): Variability of CBR with depth for aggregate base at STH 33, Port Washington.

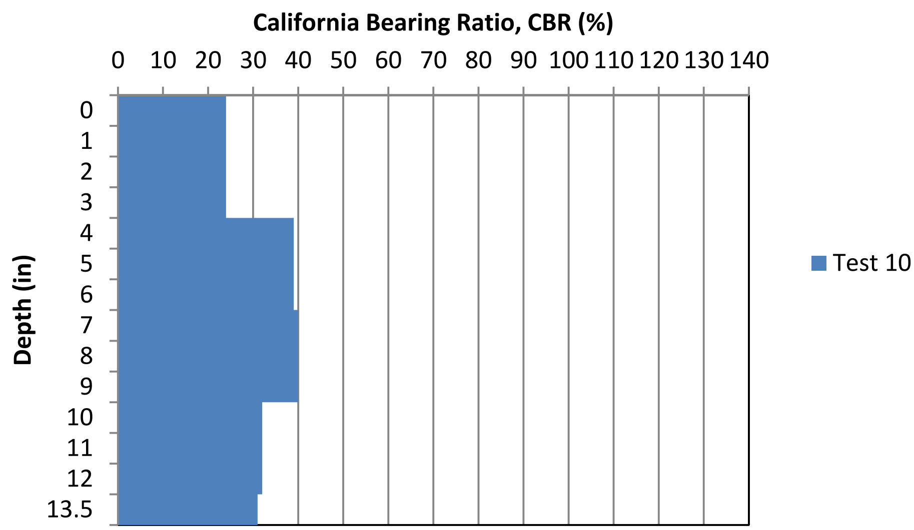

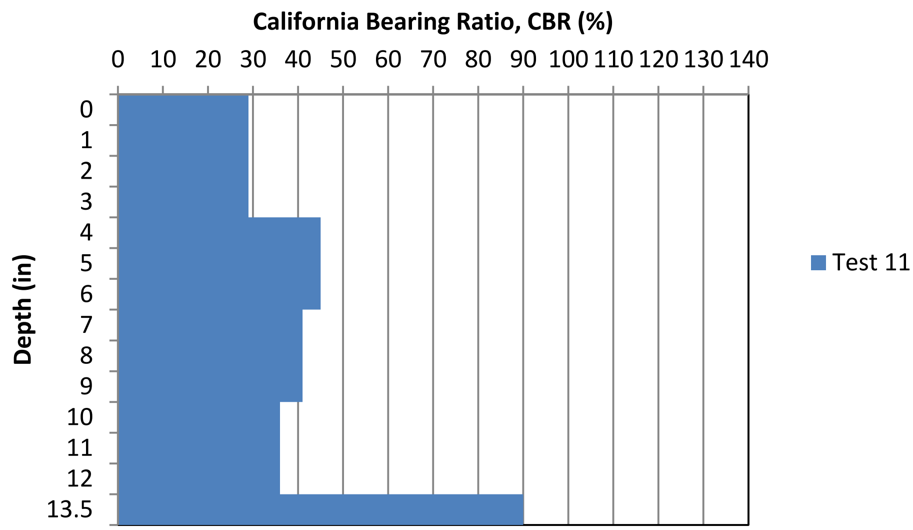

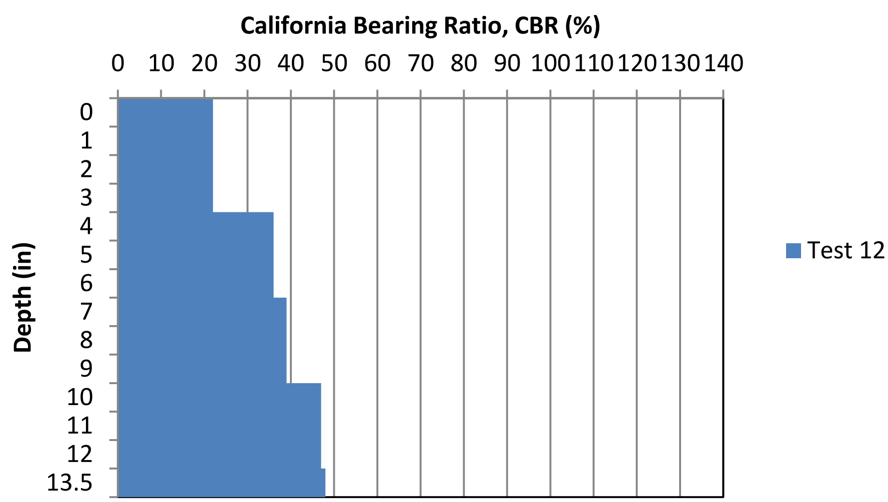

Figure B23 (Cont.): Variability of CBR with depth for aggregate base at STH 33, Port Washington.

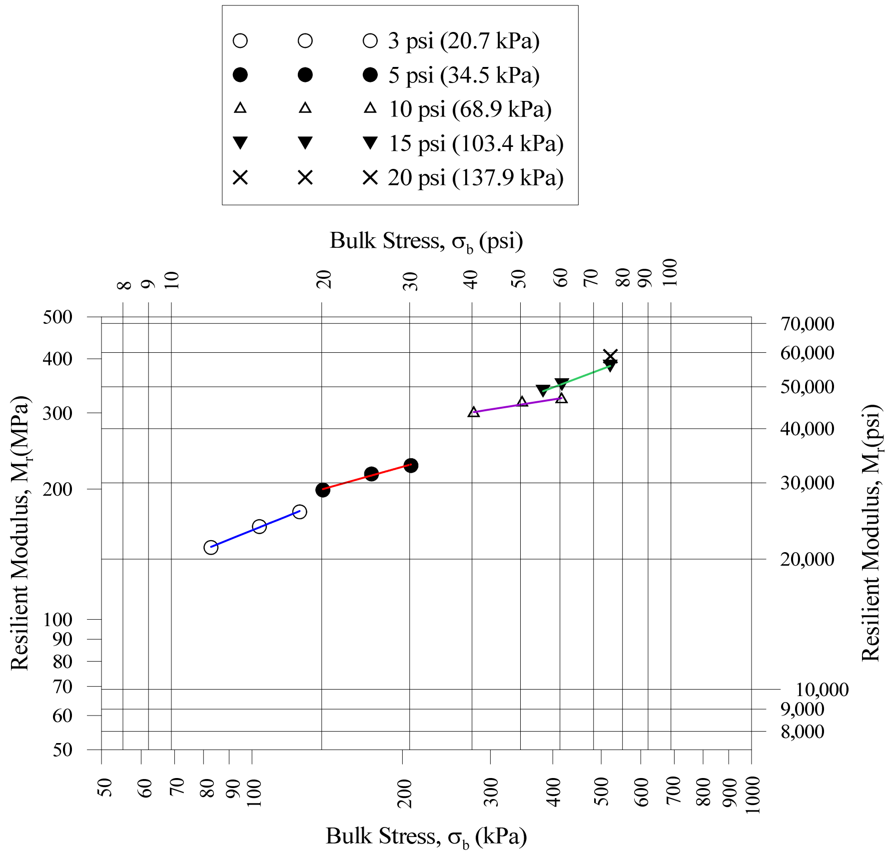

Figure B24: Results of repeated load triaxial test conducted on base aggregate specimen at maximum dry density and optimum moisture content, STH 33, Port Washington, WI.

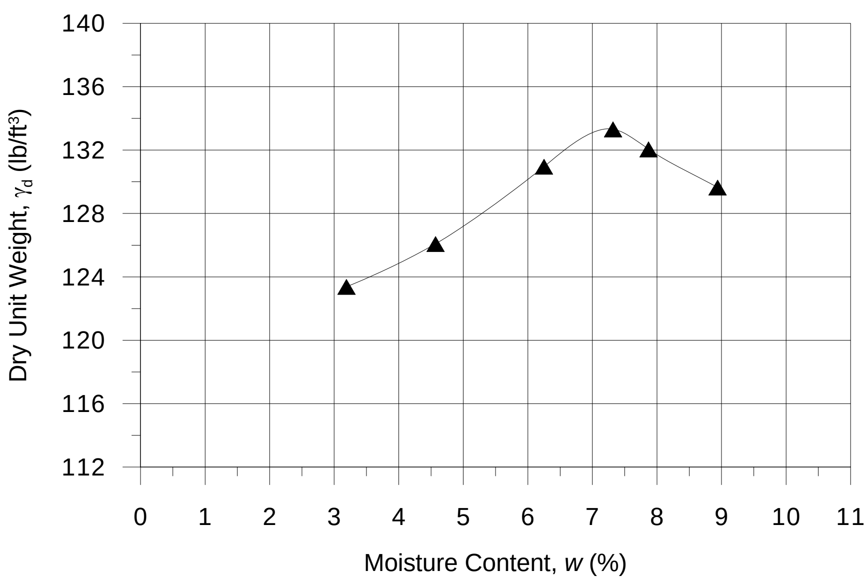

Figure B25: Compaction curve (AASHTO T 99) for base aggregate material used at STH 33, Saukville.

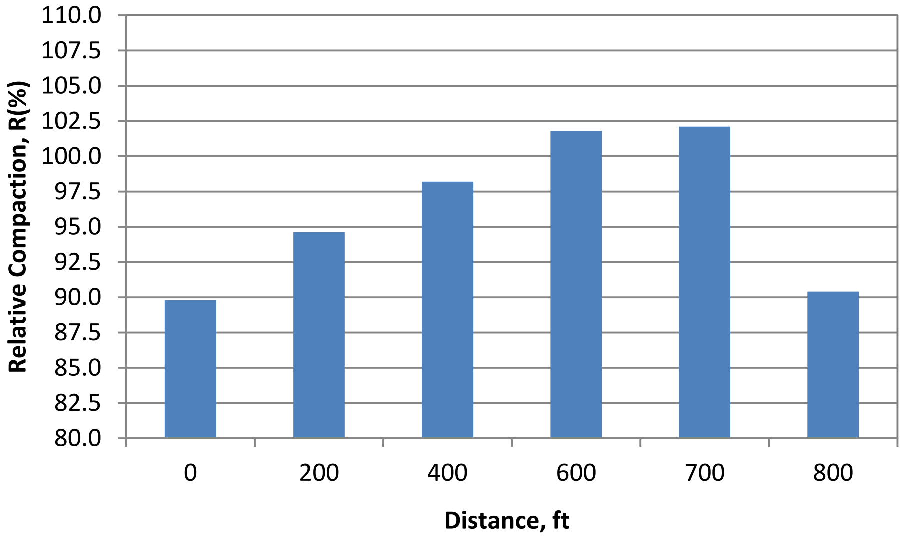

Figure B26: Variation of relative compaction with distance at test section on aggregate base layer, STH 33, Saukville.

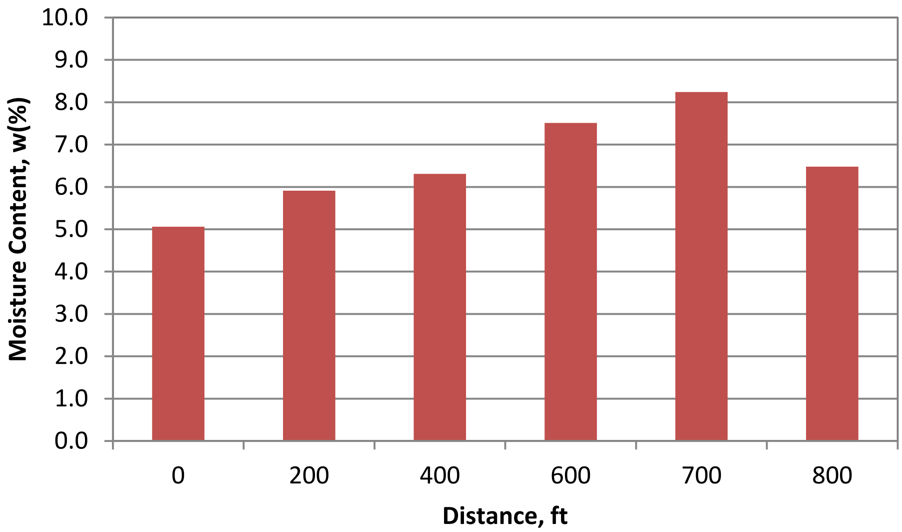

Figure B27: Variation of moisture content with distance at test section on aggregate base layer, STH 33, Saukville.

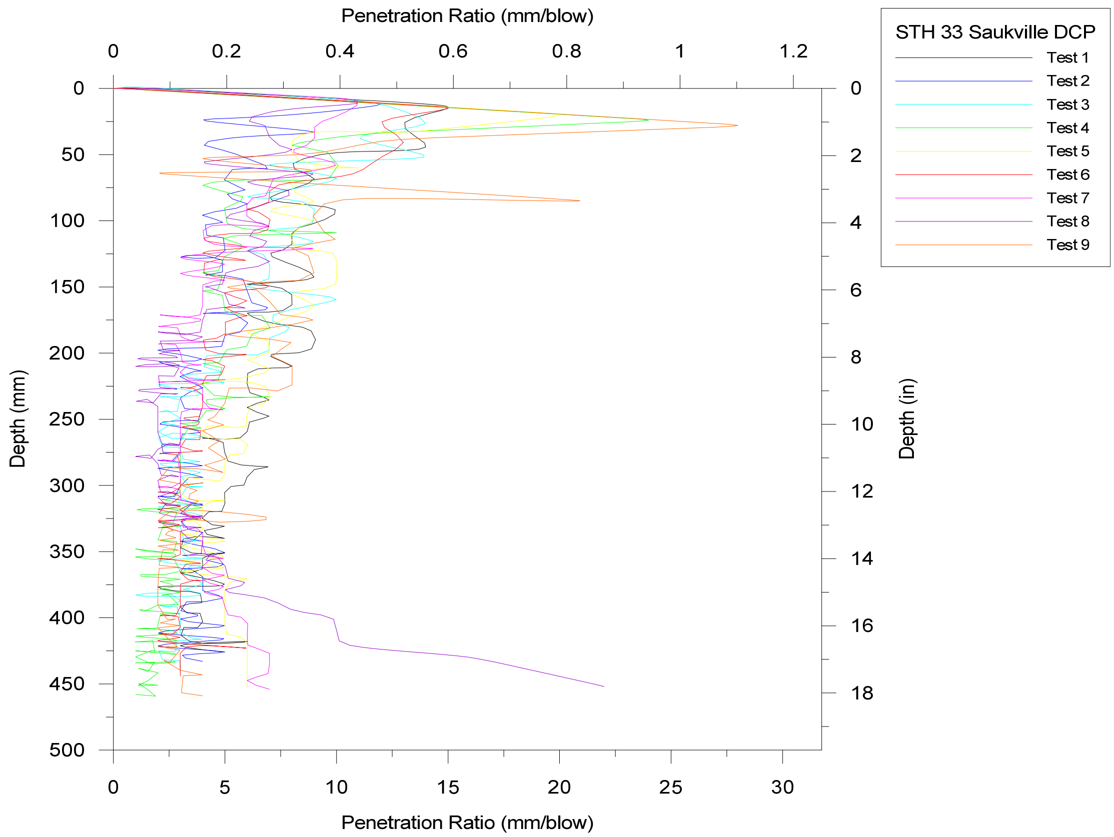

Figure B28: Penetration resistance with depth from DCP test at different points on the aggregate base layer, STH 33, Saukville.

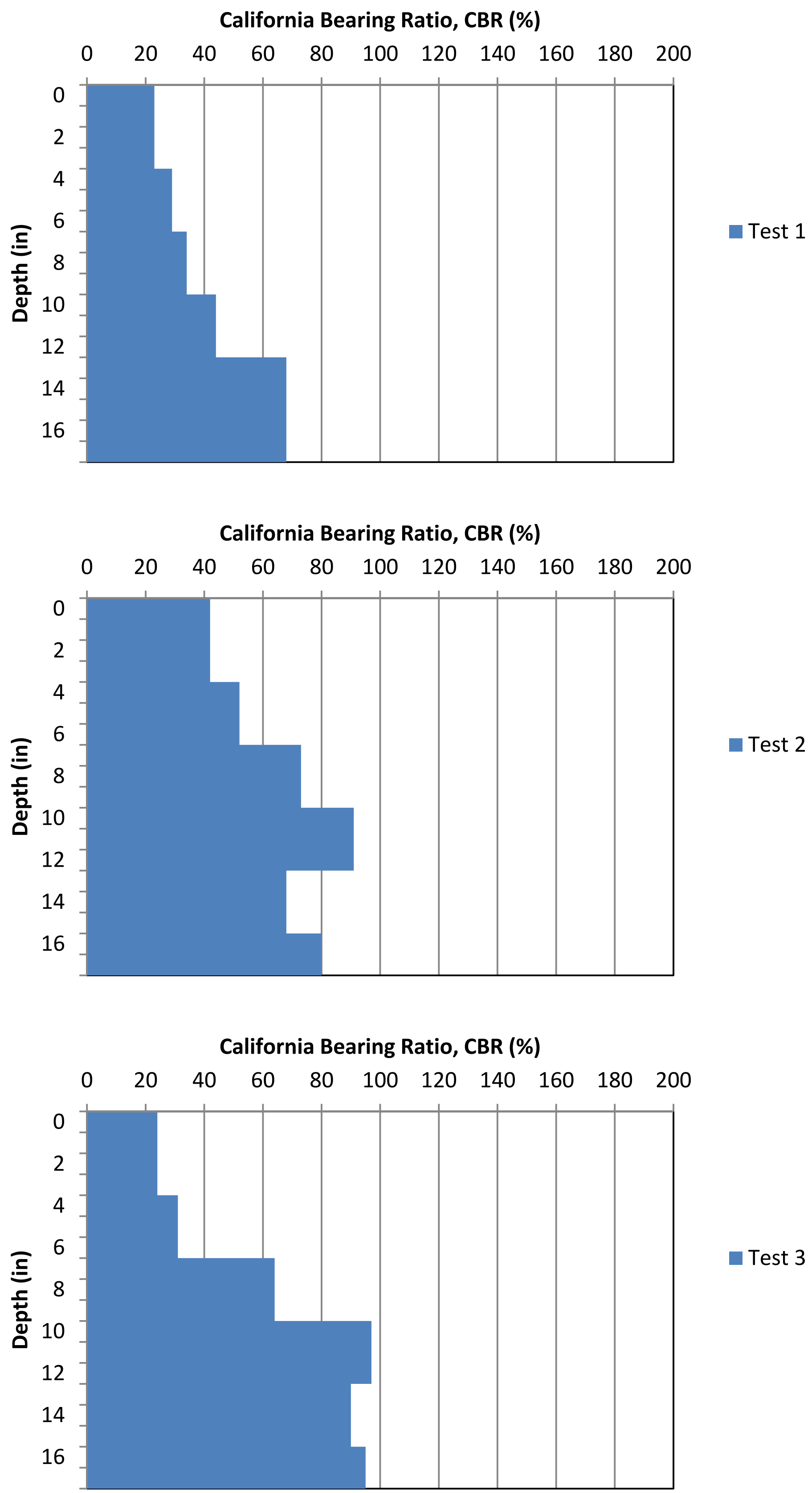

Figure B29: Variability of CBR with depth for aggregate base at STH 33, Saukville.

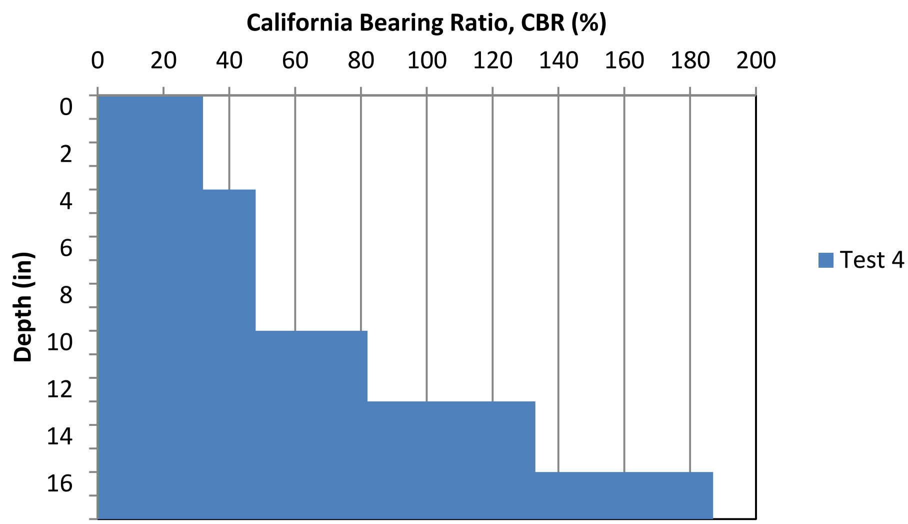

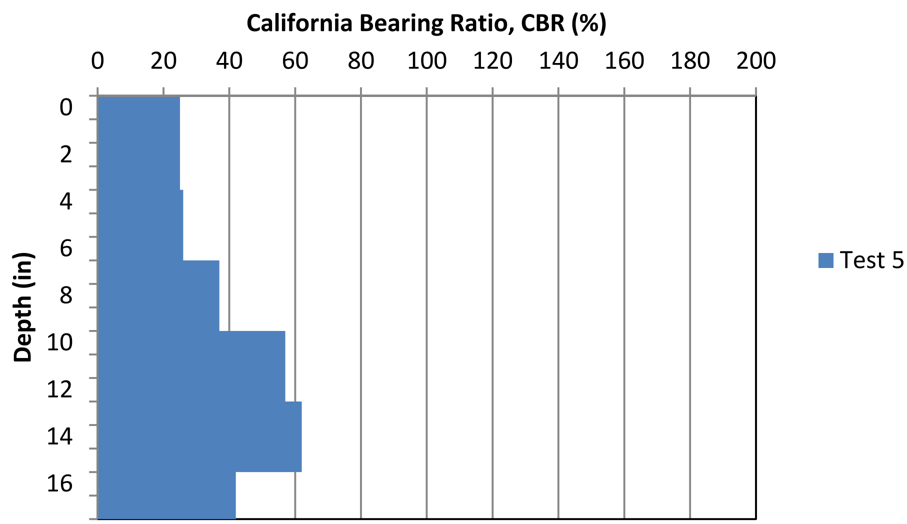

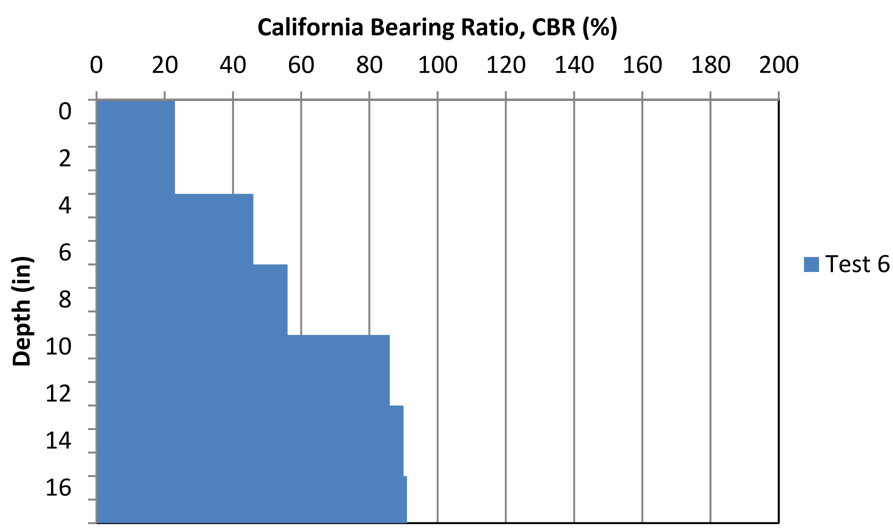

Figure B29 (Cont.): Variability of CBR with depth for aggregate base at STH 33, Saukville.

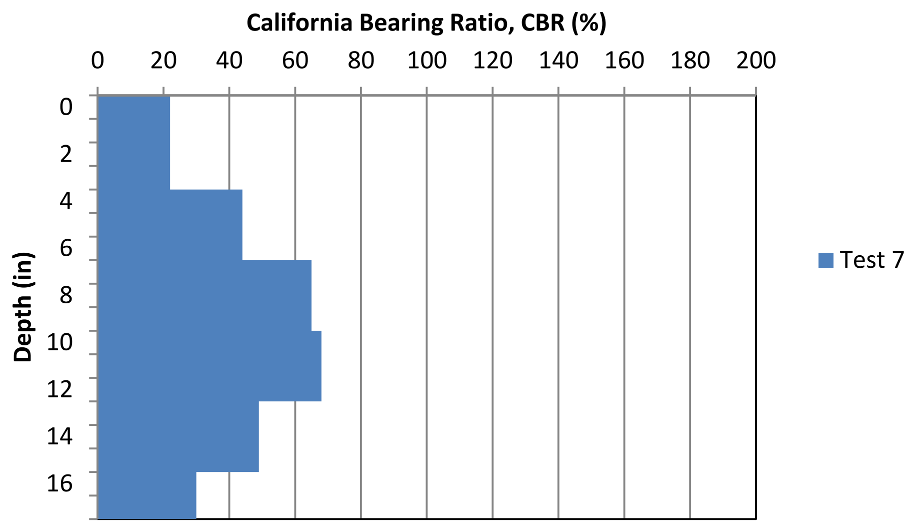

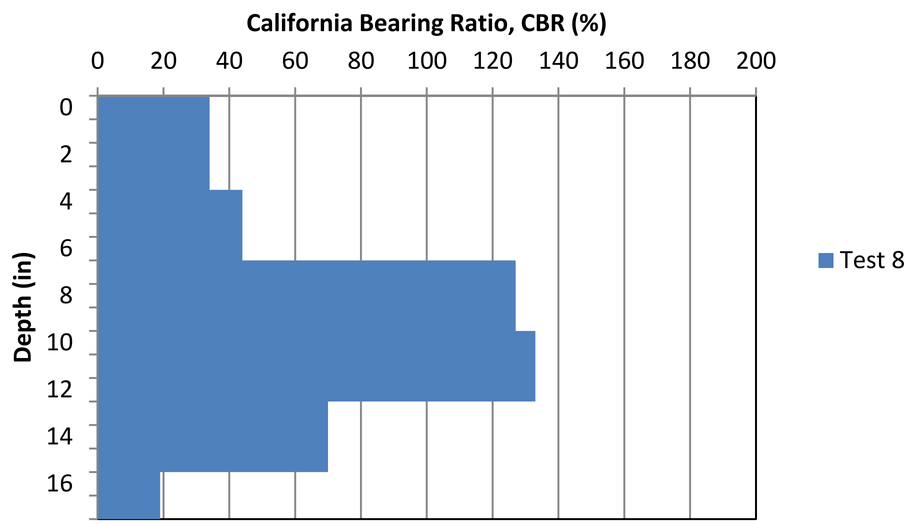

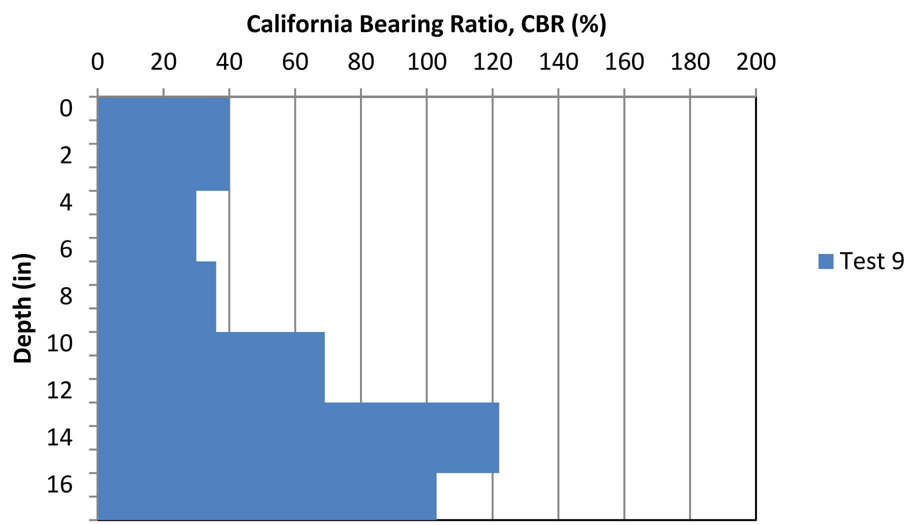

Figure B29 (Cont.): Variability of CBR with depth for aggregate base at STH 33, Saukville.

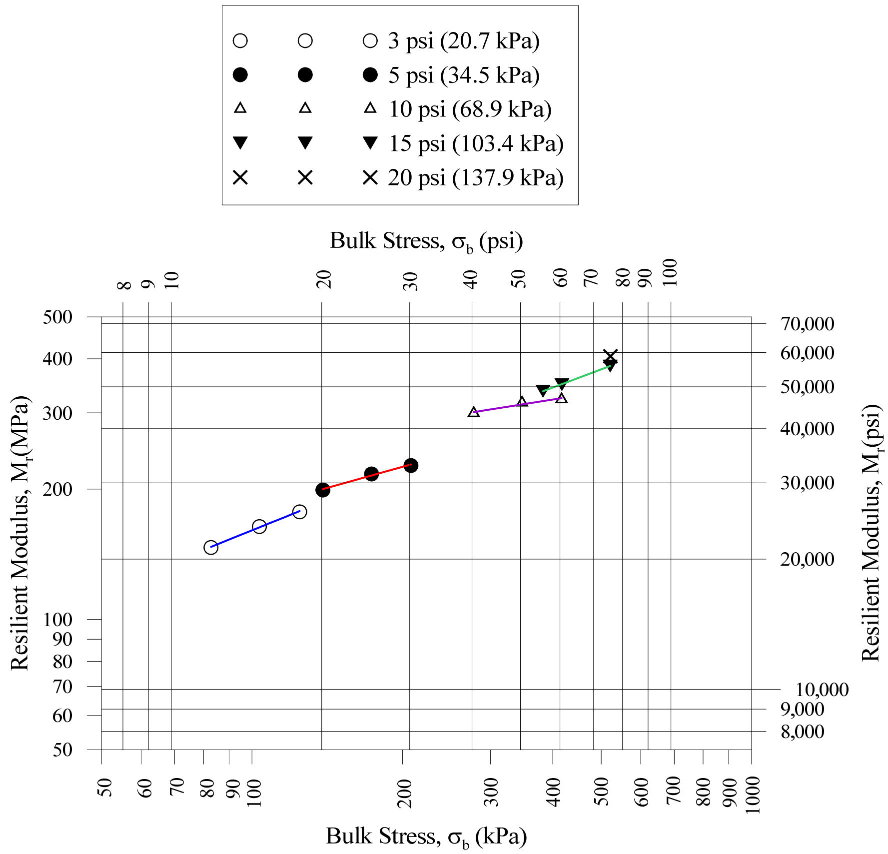

Figure B30: Results of repeated load triaxial test conducted on base aggregate specimen at maximum dry density and optimum moisture content, STH 33, Saukville.

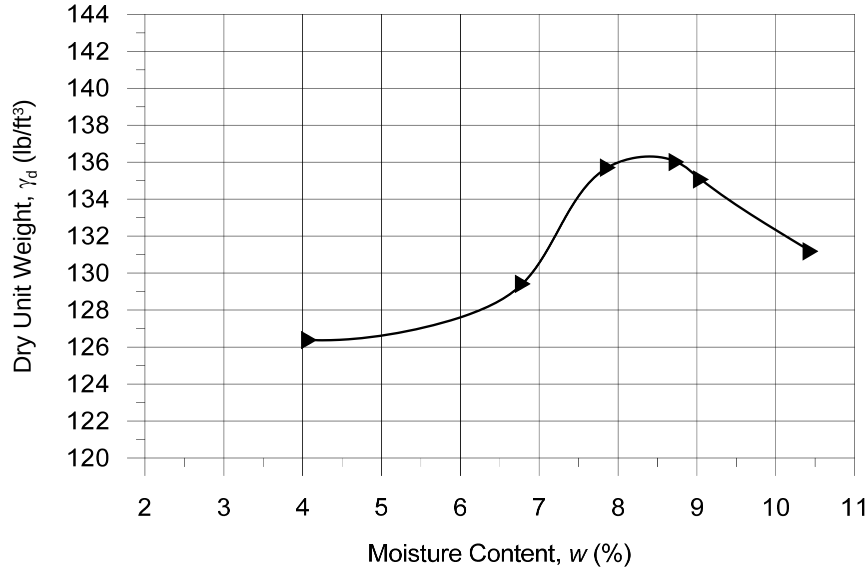

Figure B31: Compaction curve (AASHTO T 99) for base aggregate material used at USH 12, Madison.

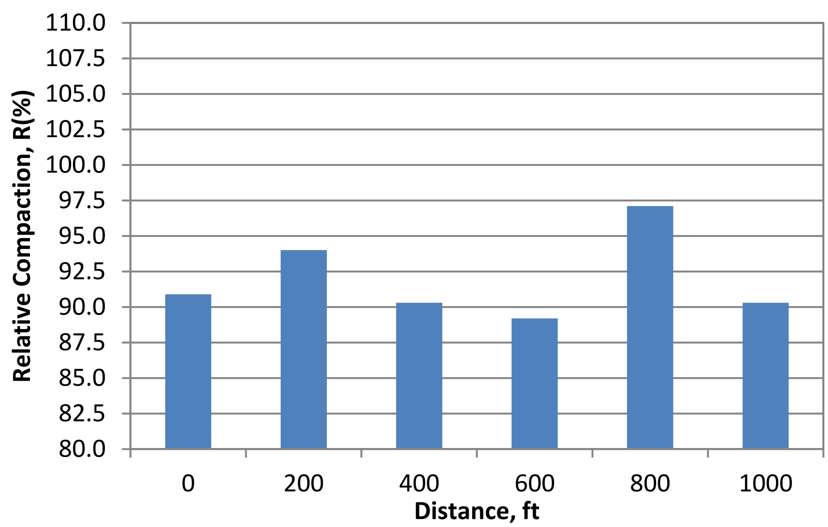

Figure B32: Variation of relative compaction with distance at test section on aggregate base layer, USH 12, Madison.

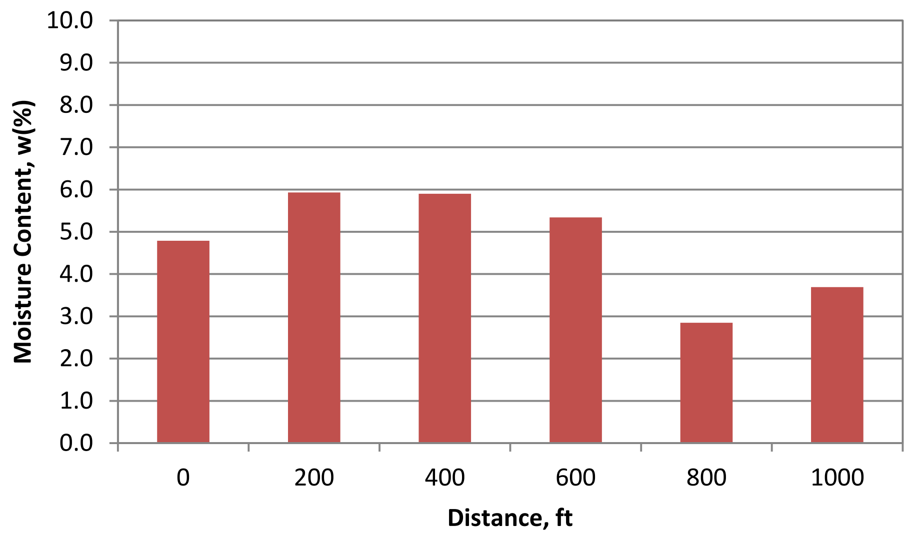

Figure B33: Variation of moisture content with distance at test section on aggregate base layer, USH 12, Madison.

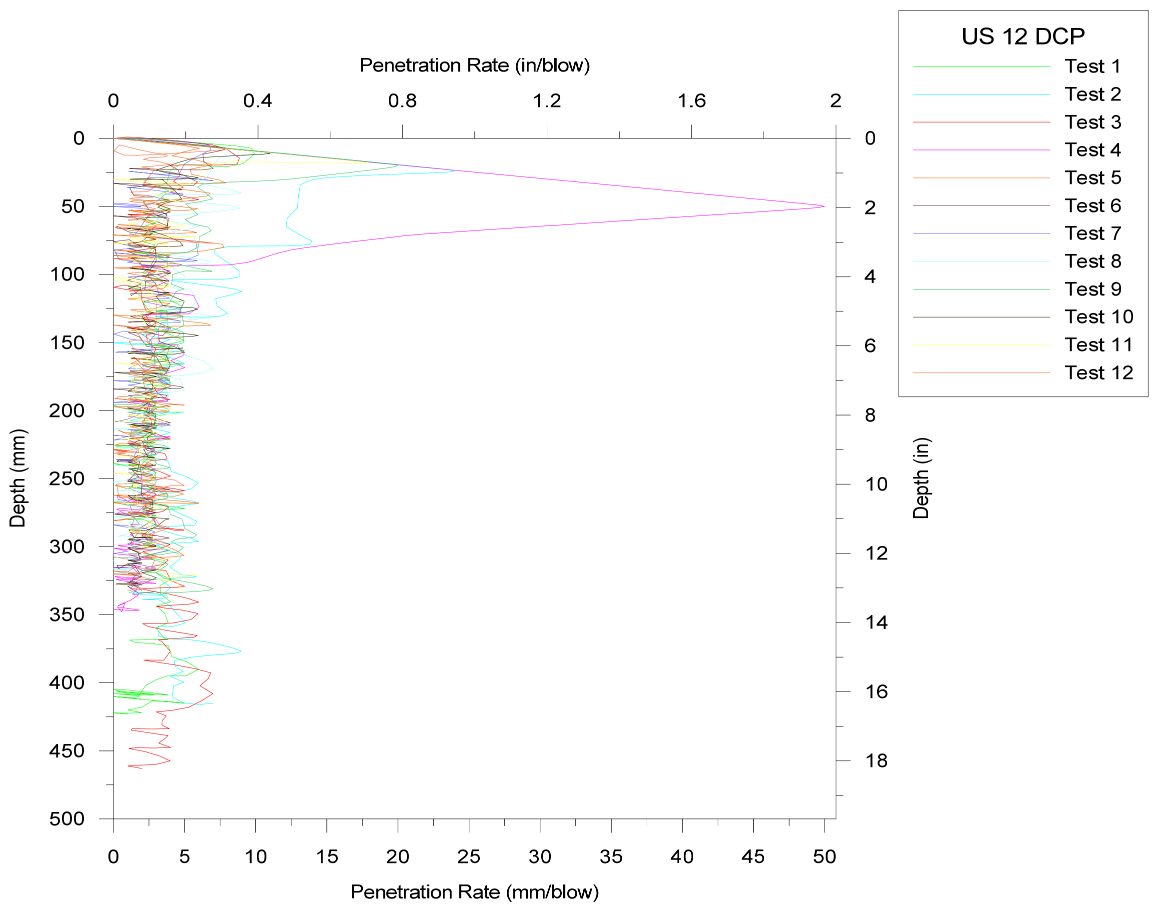

Figure B34: Penetration resistance with depth from DCP test at different points on the aggregate base layer, USH 12, Madison.

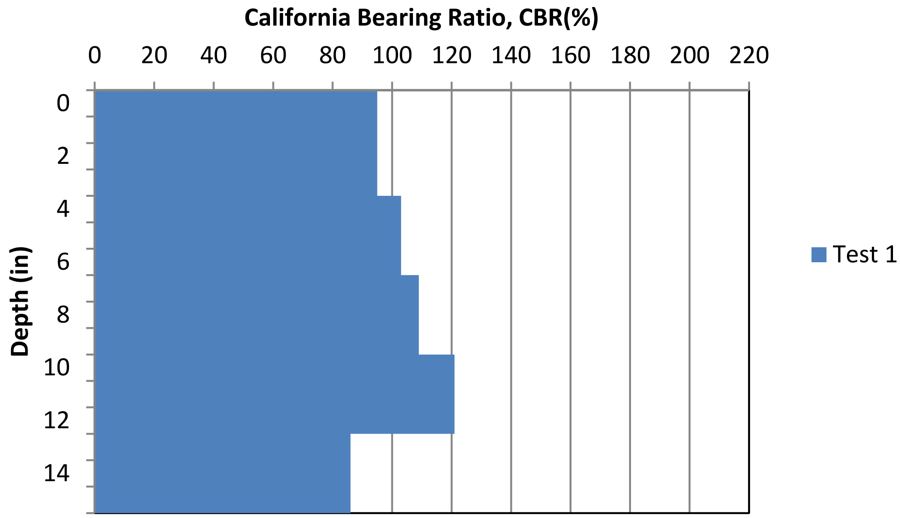

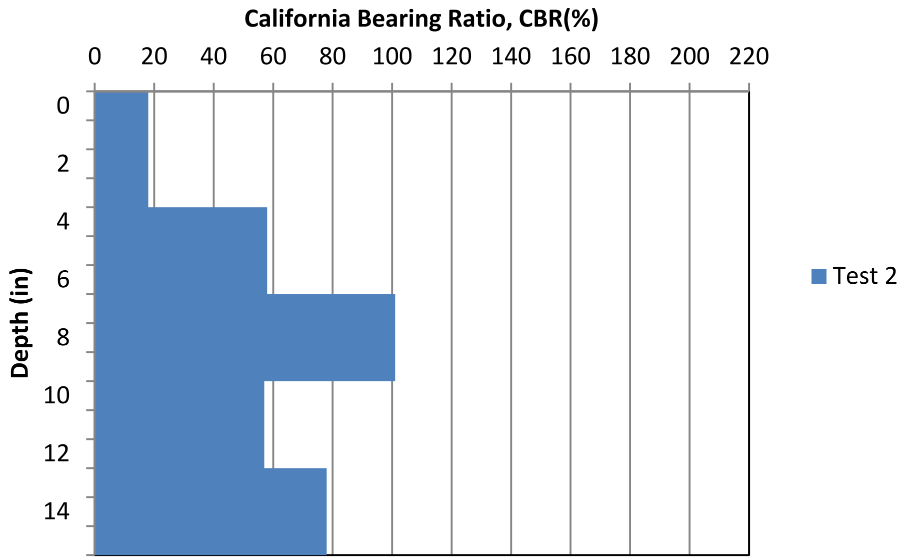

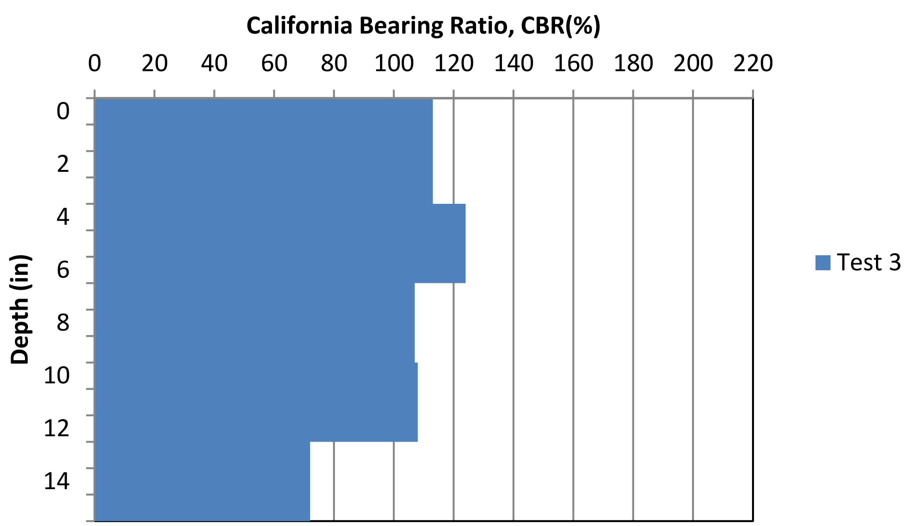

Figure B35: Variability of CBR with depth for aggregate base at USH 12, Madison.

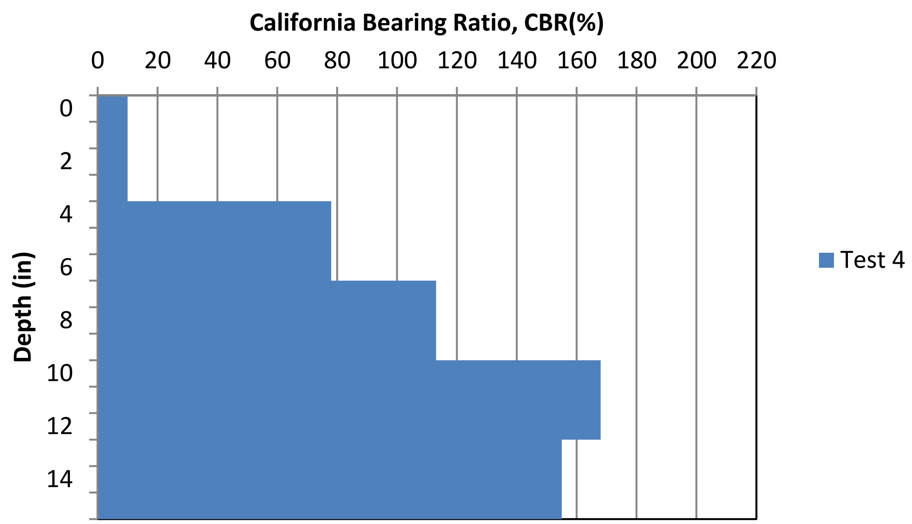

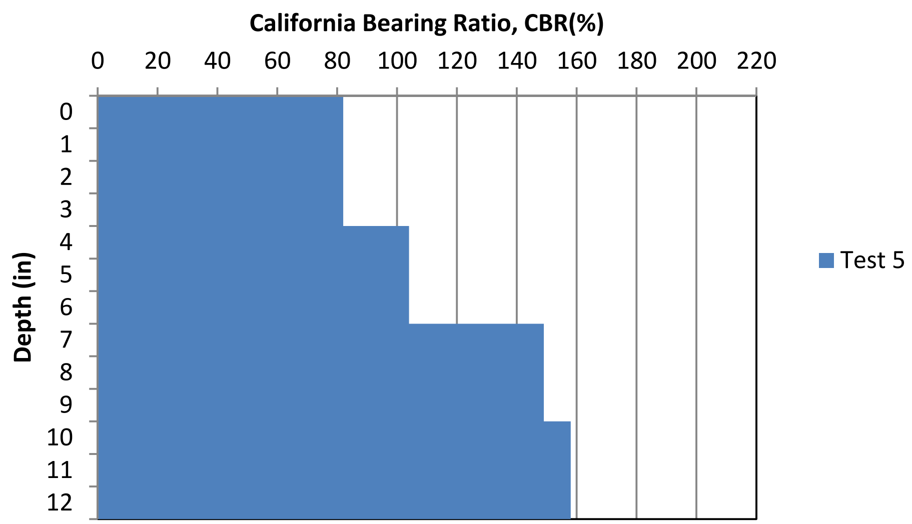

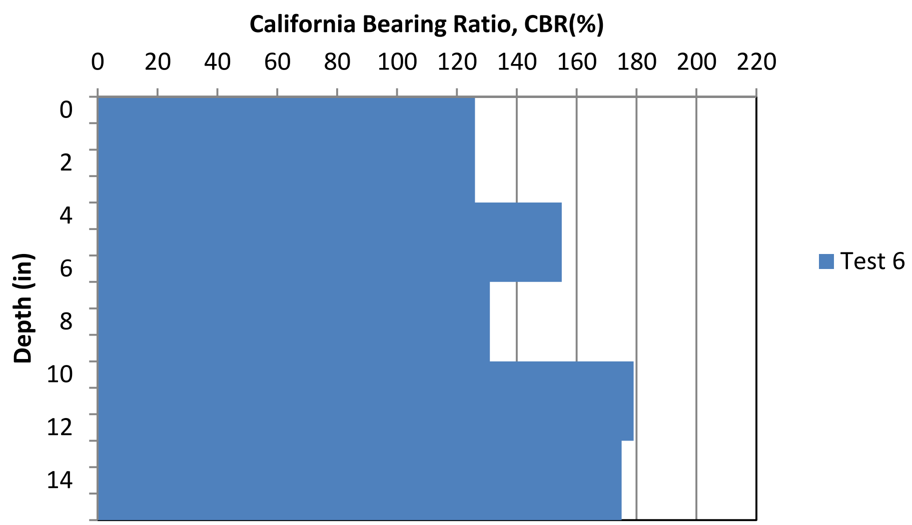

Figure B35 (Cont.): Variability of CBR with depth for aggregate base at USH 12, Madison.

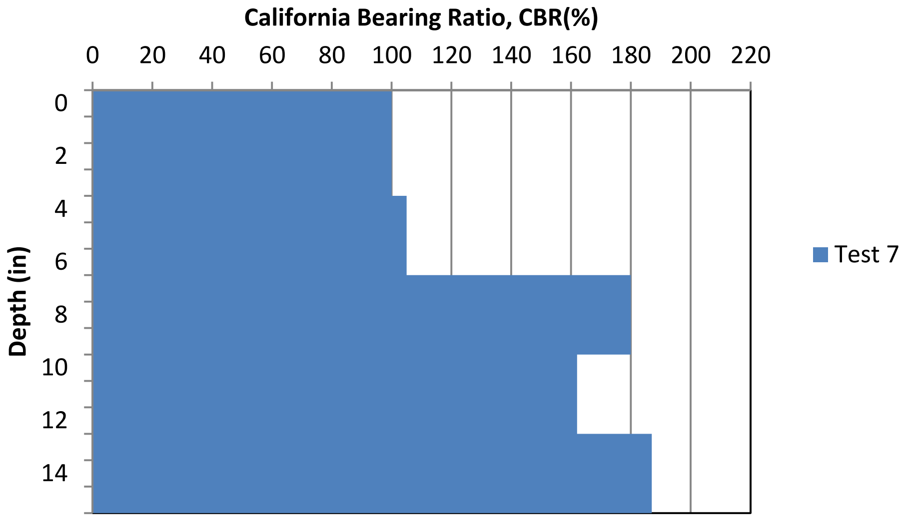

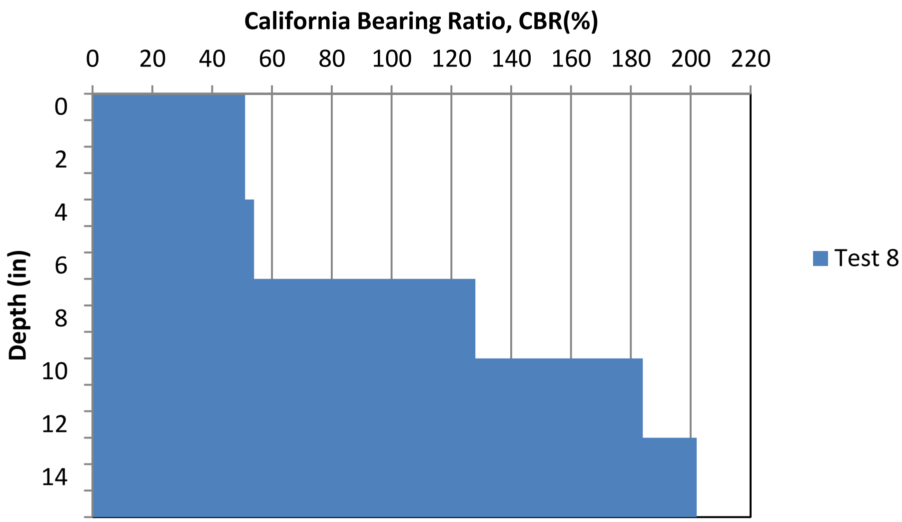

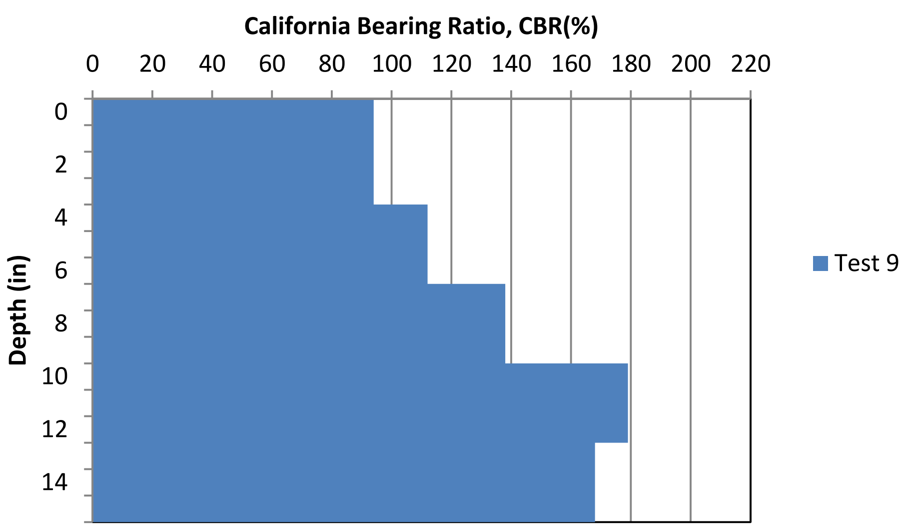

Figure B35 (Cont.): Variability of CBR with depth for aggregate base at USH 12, Madison.

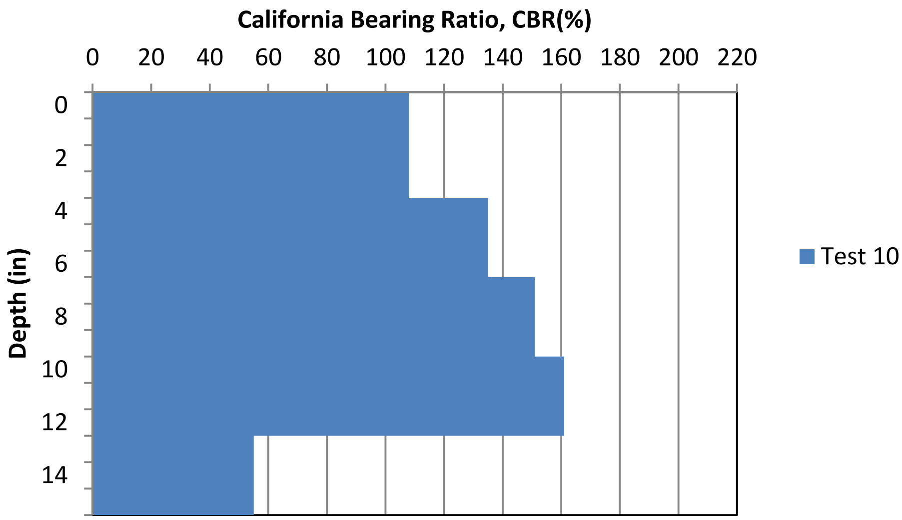

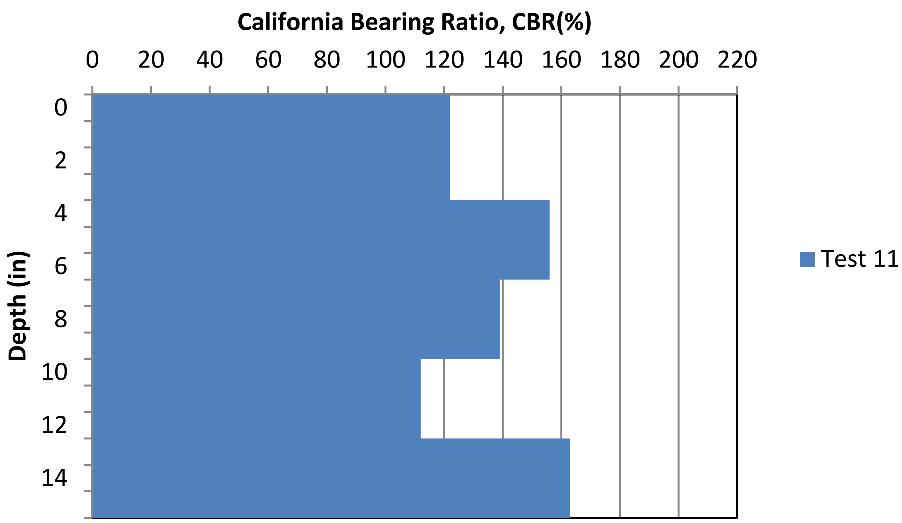

Figure B35 (Cont.): Variability of CBR with depth for aggregate base at USH 12, Madison.

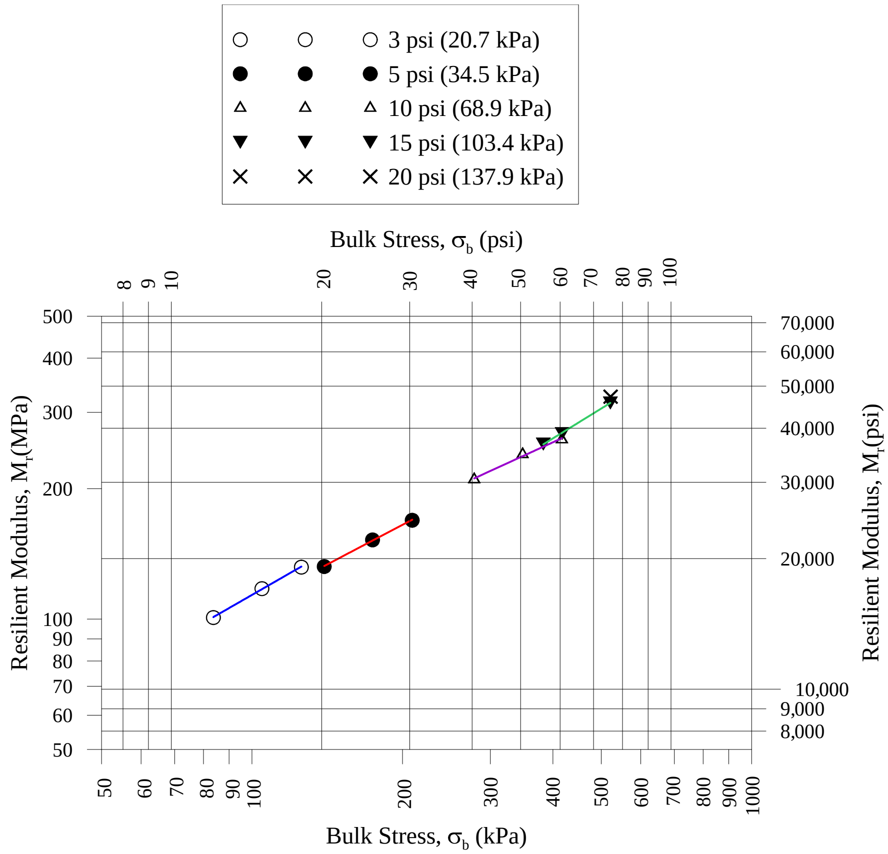

Figure B36: Results of repeated load triaxial test conducted on base aggregate specimen at maximum dry density and optimum moisture content, USH 12, Madison.

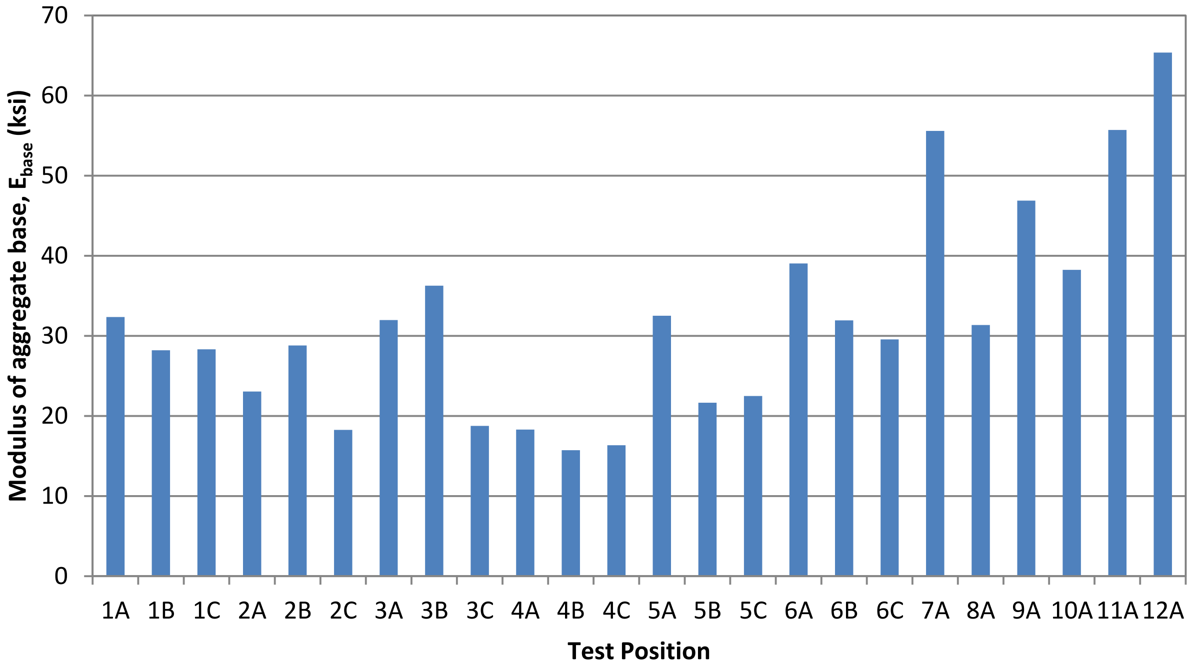

Figure B37: Distribution of average aggregate base layer modulus from LWD tests at USH 12, Madison.

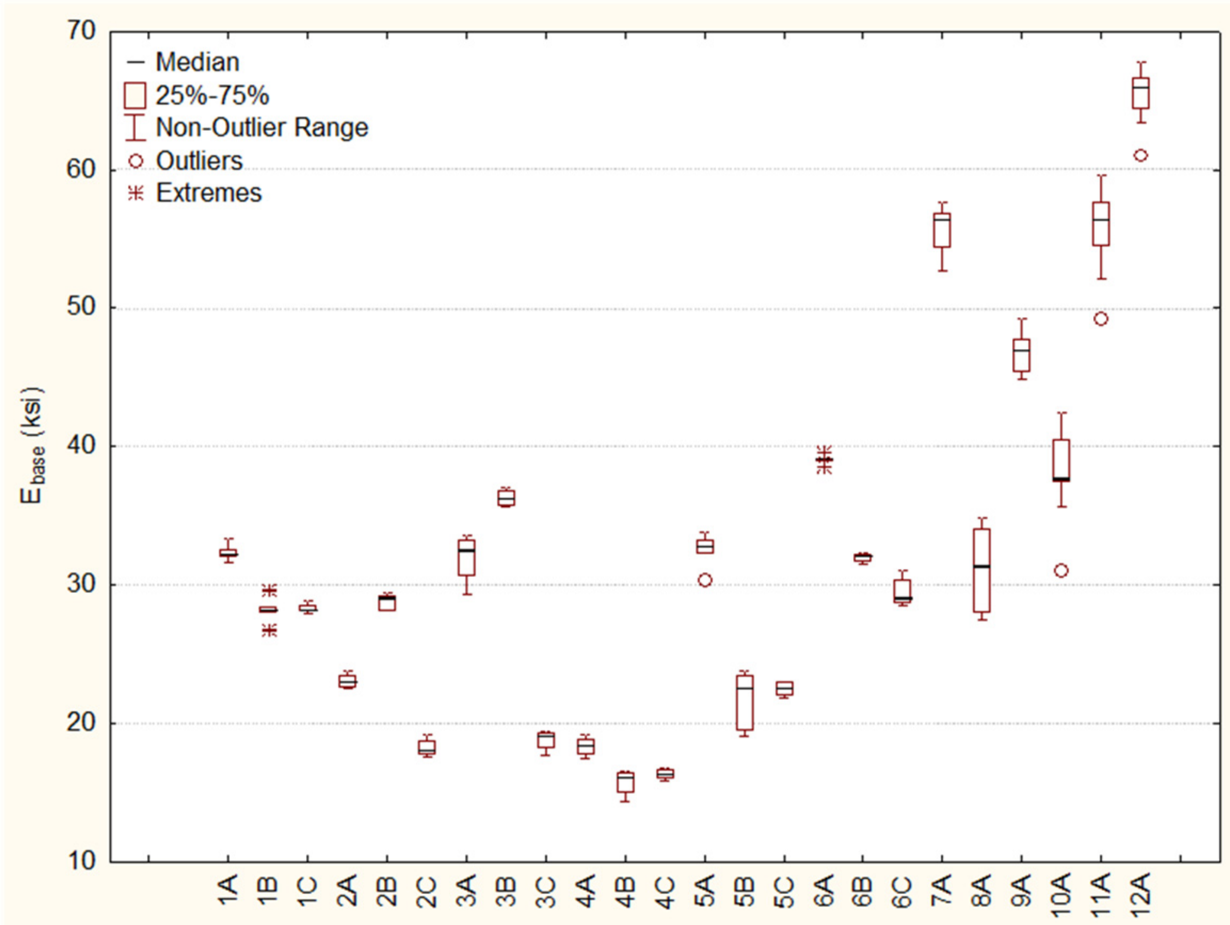

Figure B38: Whisker-box plot for the calculated aggregate base layer modulus from LWD tests at USH 12, Madison.

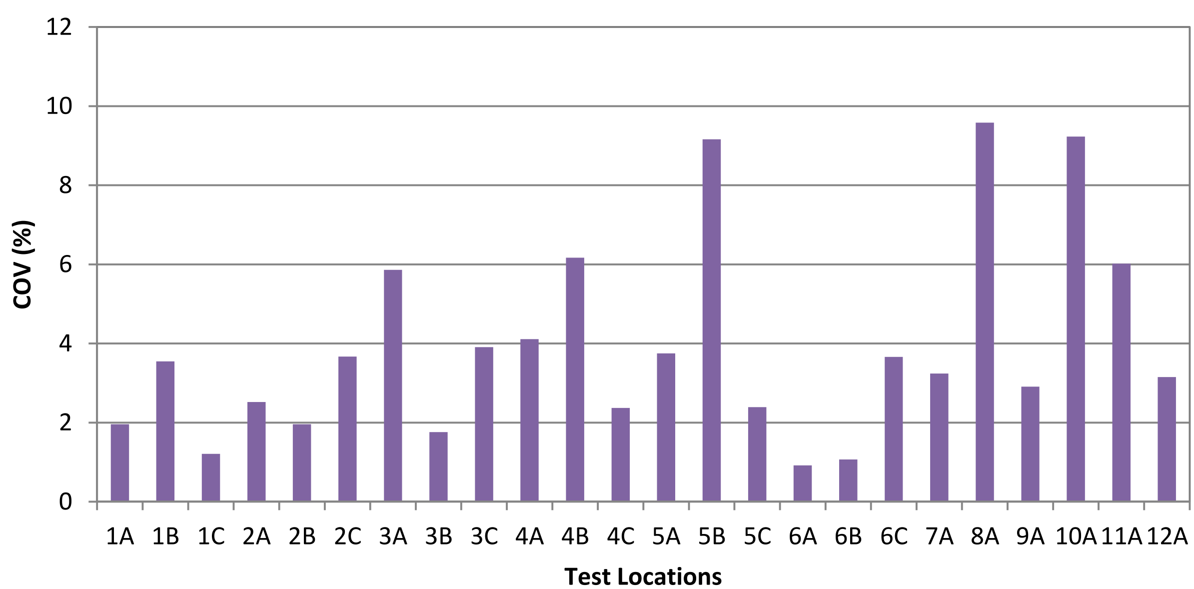

Figure B39: COV for the LWD calculated aggregate base layer modulus, USH 12, Madison.

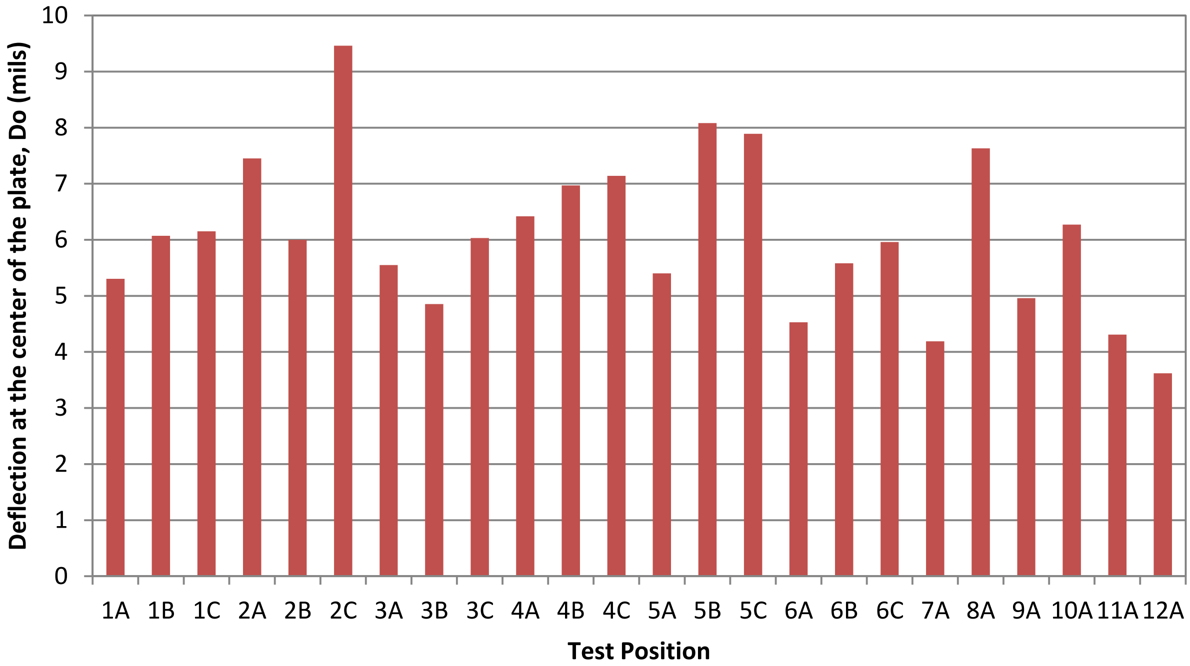

Figure B40: Distribution of average measured deflection under loading plate at LWD test points on the aggregate base layer, USH 12, Madison.

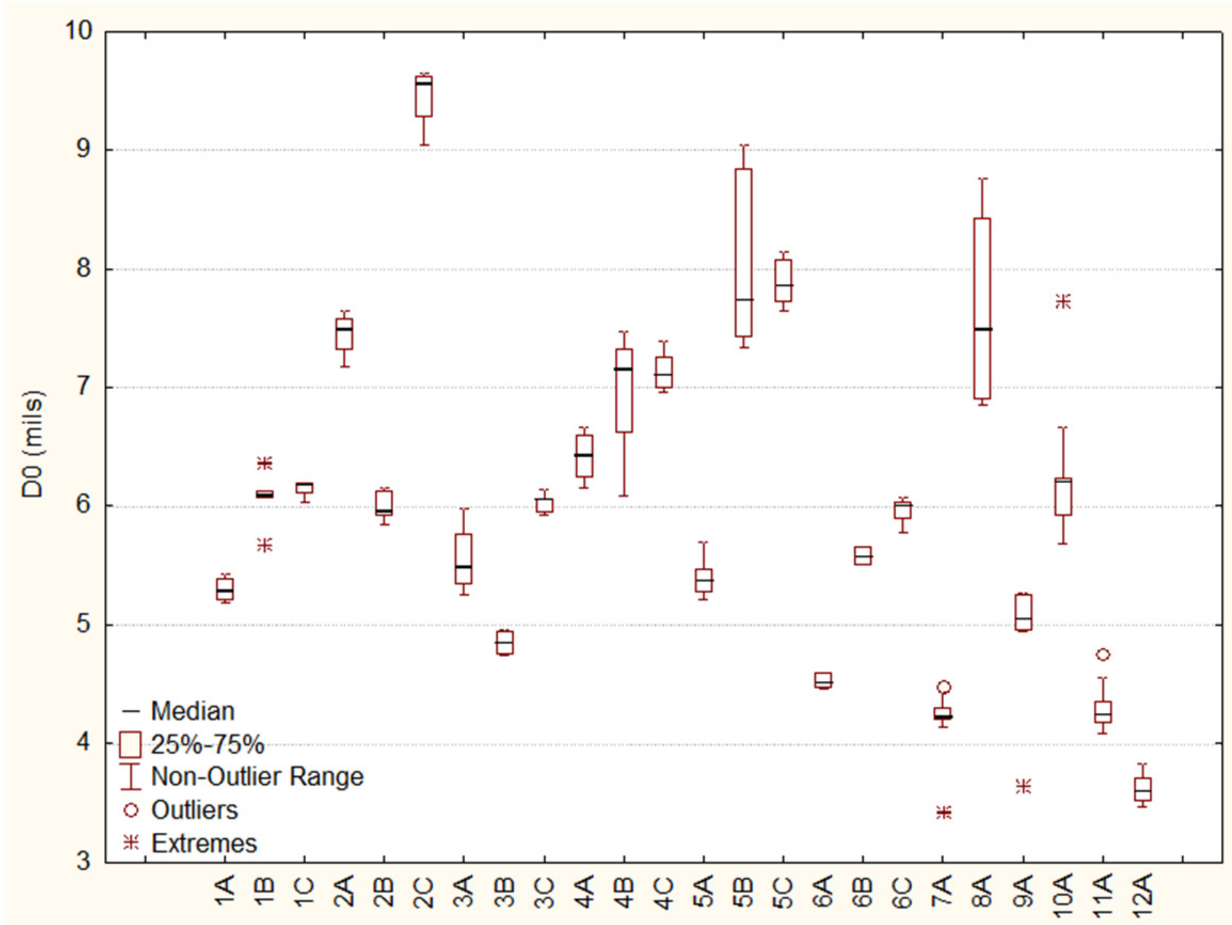

Figure B41: Whisker-box plot for the measured deflection under loading plate at LWD test points on the aggregate base layer, USH 12, Madison.

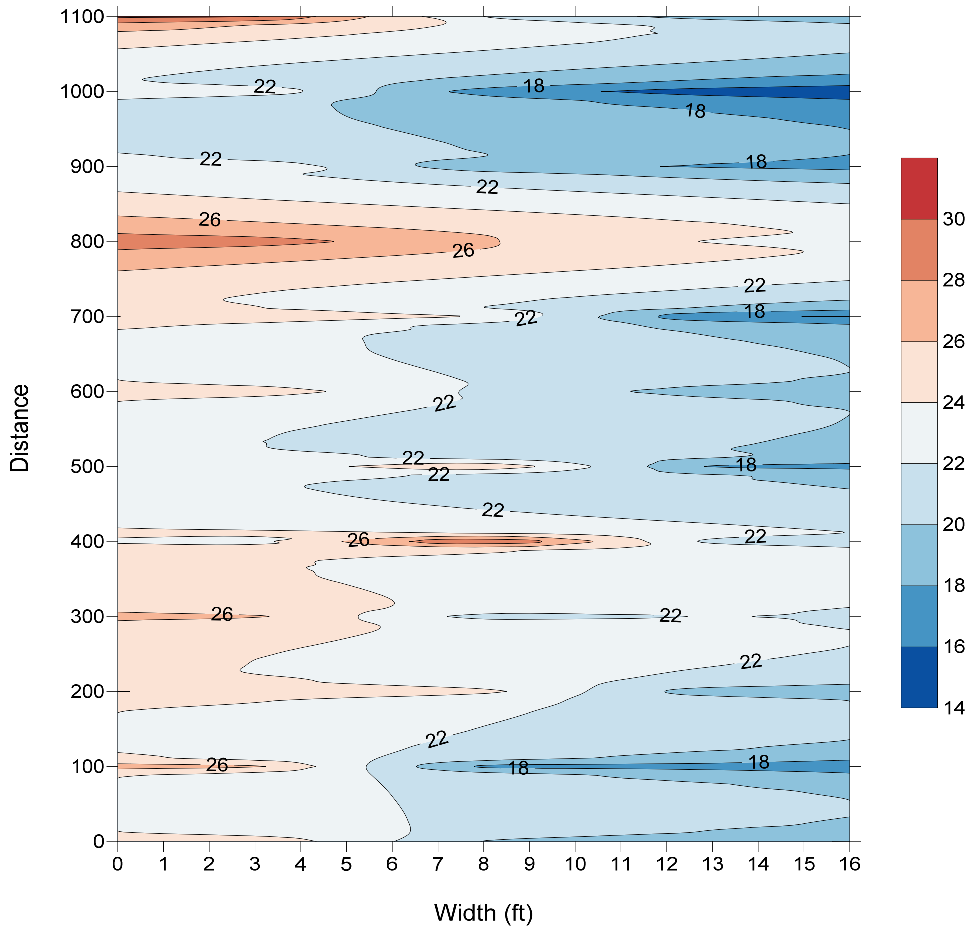

Figure B42: Contours of the calculated base layer modulus (E_{base}) based on LWD measurements, USH 12, Madison.

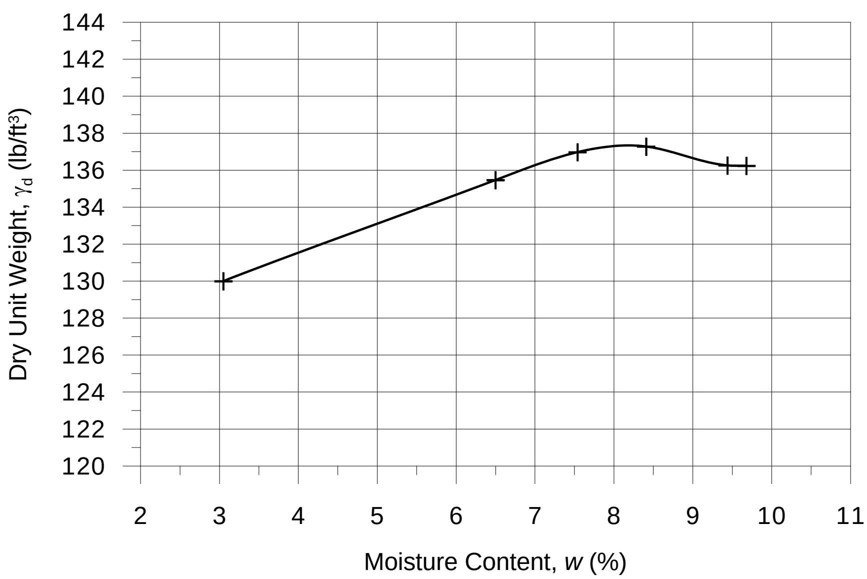

Figure B43: Compaction curve (AASHTO T 99) for base aggregate material used at I 90-94-39, Madison.

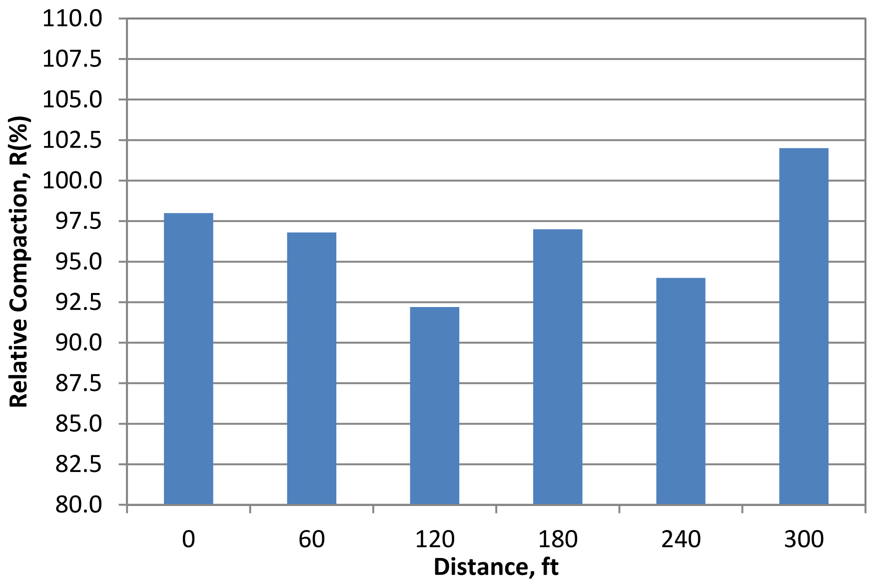

Figure B44: Variation of relative compaction with distance at test section on aggregate base layer, I 90-94-39, Madison.

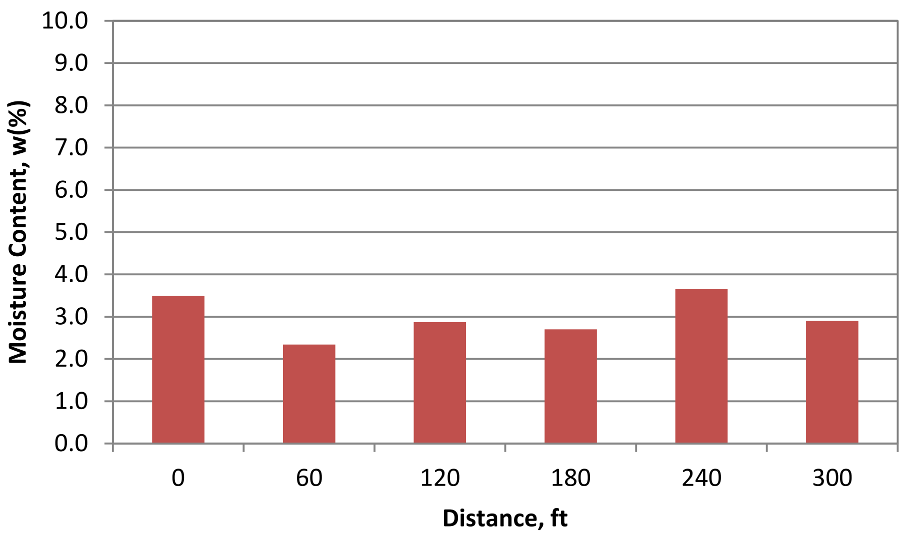

Figure B45: Variation of moisture content with distance at test section on aggregate base layer I 90-94-39, Madison.

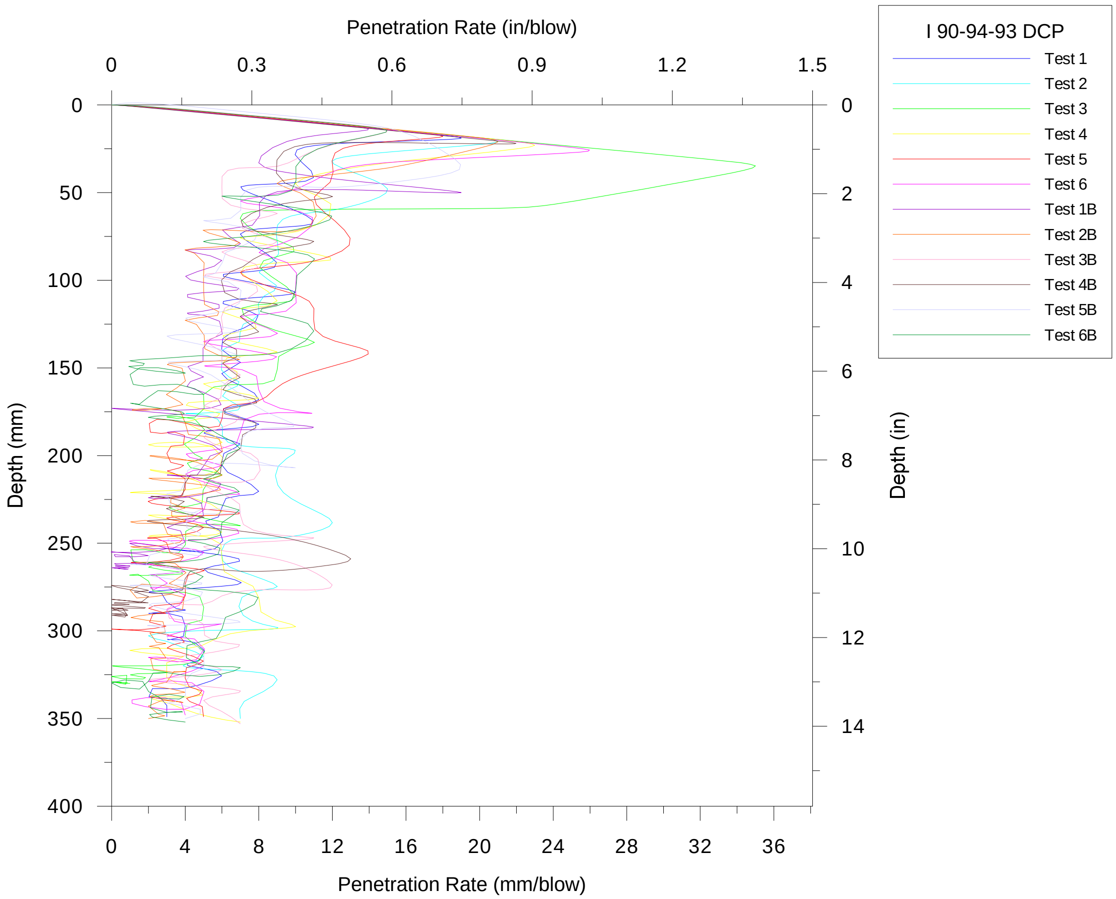

Figure B46: Penetration resistance with depth from DCP test at different points on the aggregate base layer, I 90-94-39, Madison.

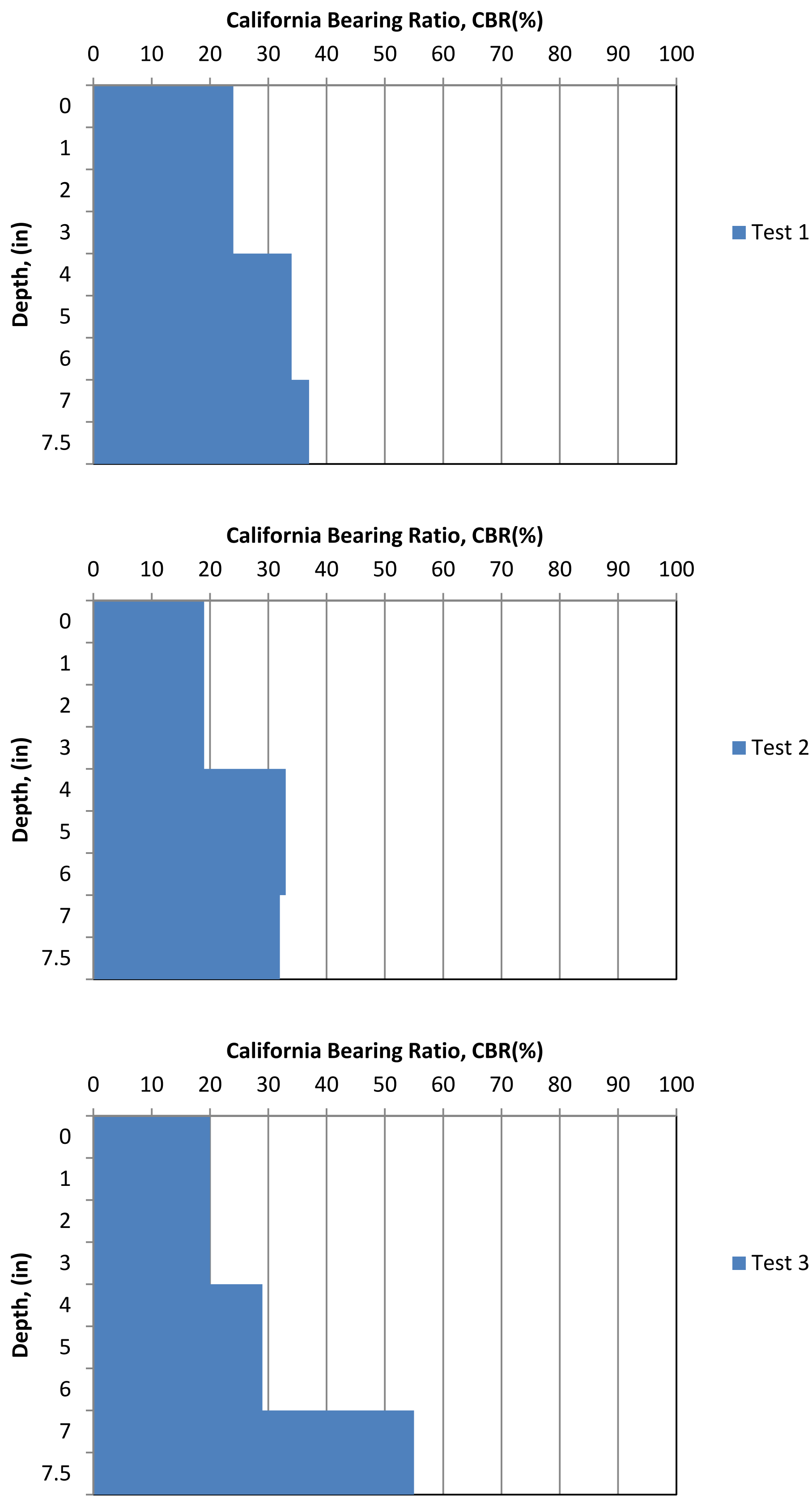

Figure B47: Variability of CBR with depth for aggregate base at I 90-94-39, Madison.

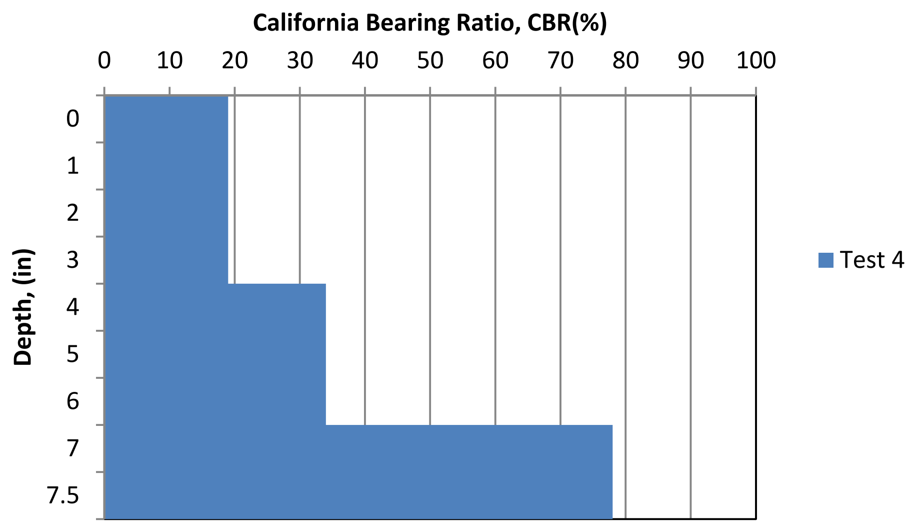

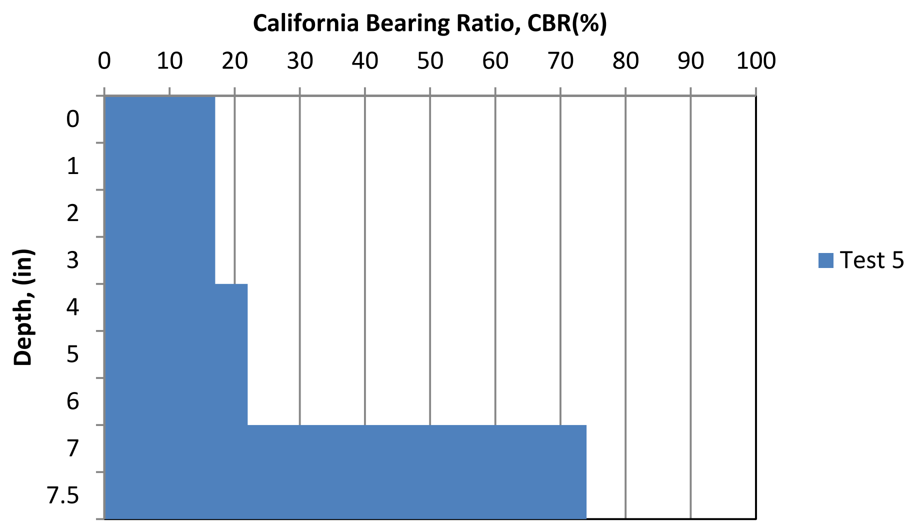

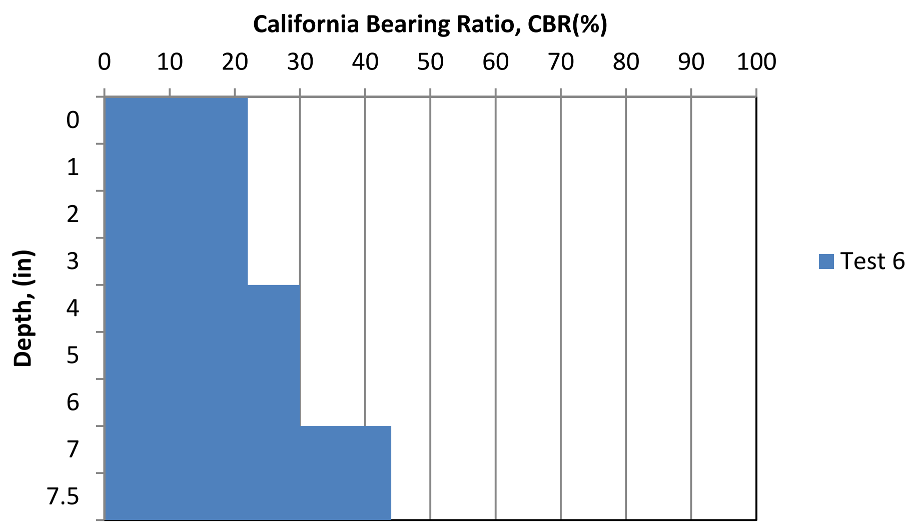

Figure B47 (Cont.): Variability of CBR with depth for aggregate base at I 90-94-39, Madison.

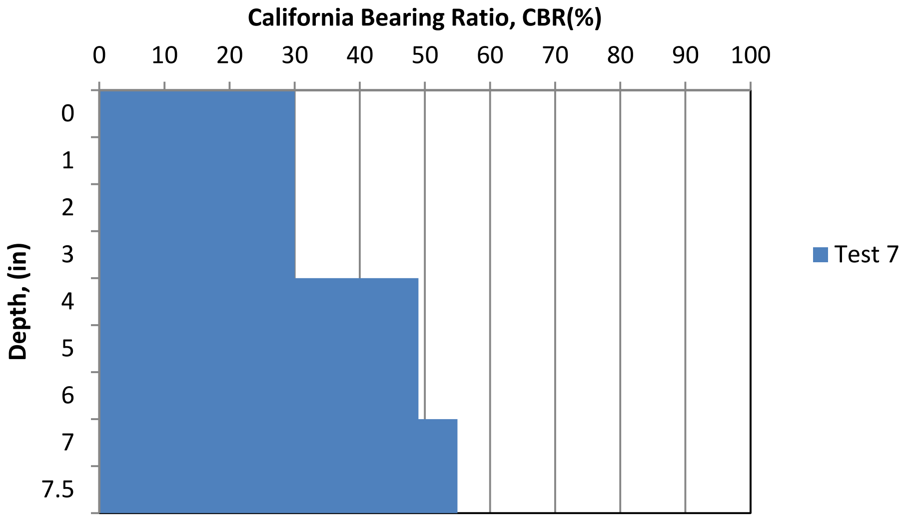

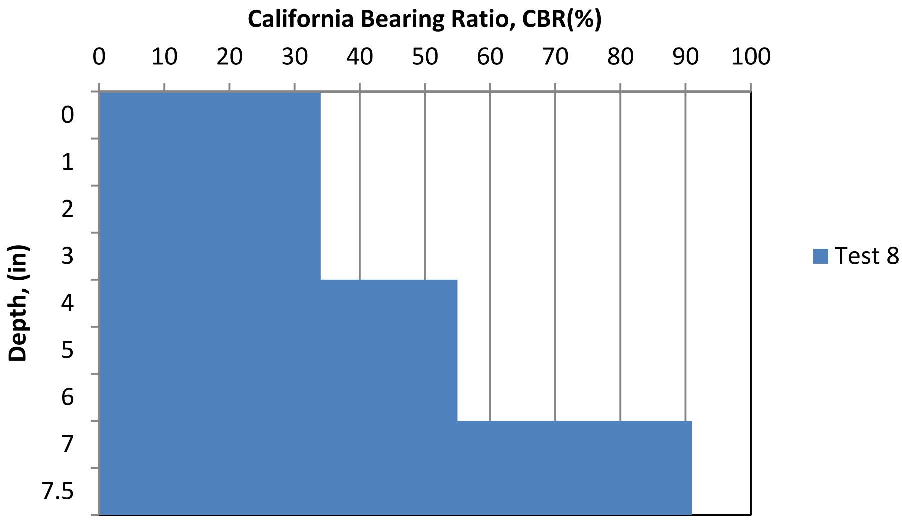

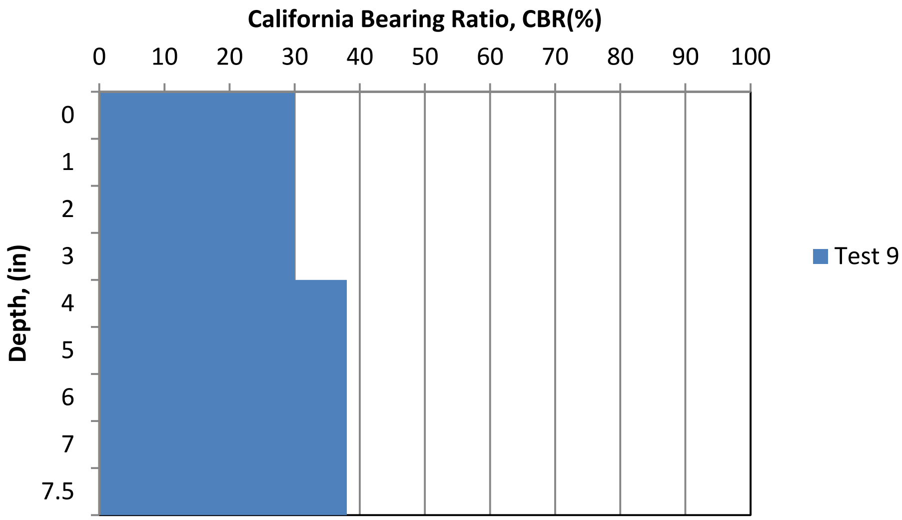

Figure B47 (Cont.): Variability of CBR with depth for aggregate base at I 90-94-39, Madison.

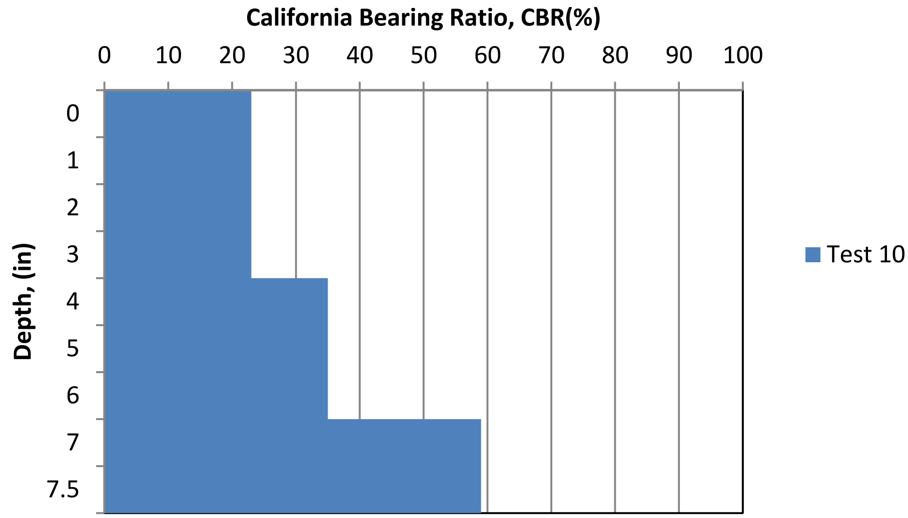

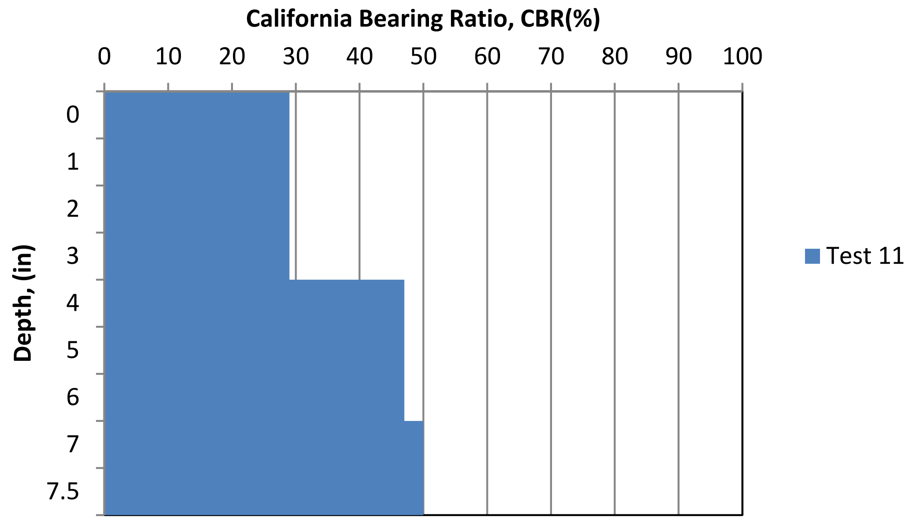

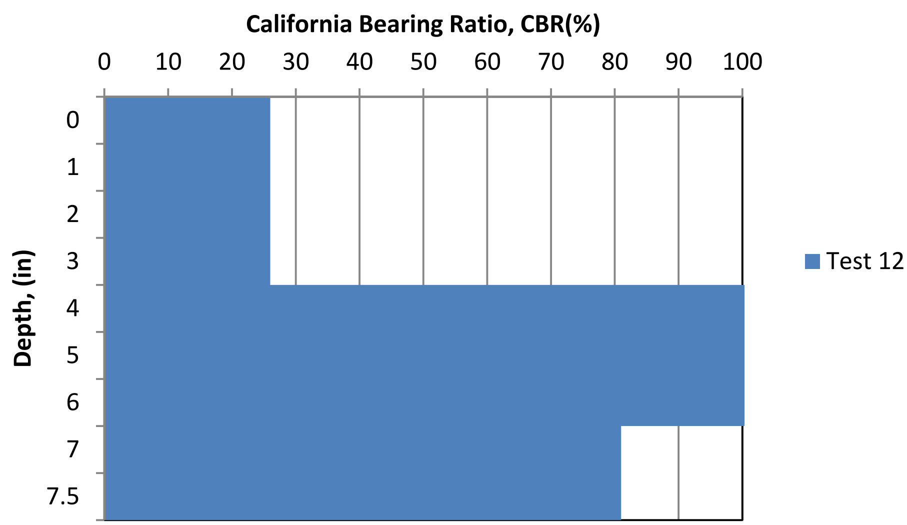

Figure B47 (Cont.): Variability of CBR with depth for aggregate base at I 90-94-39, Madison.

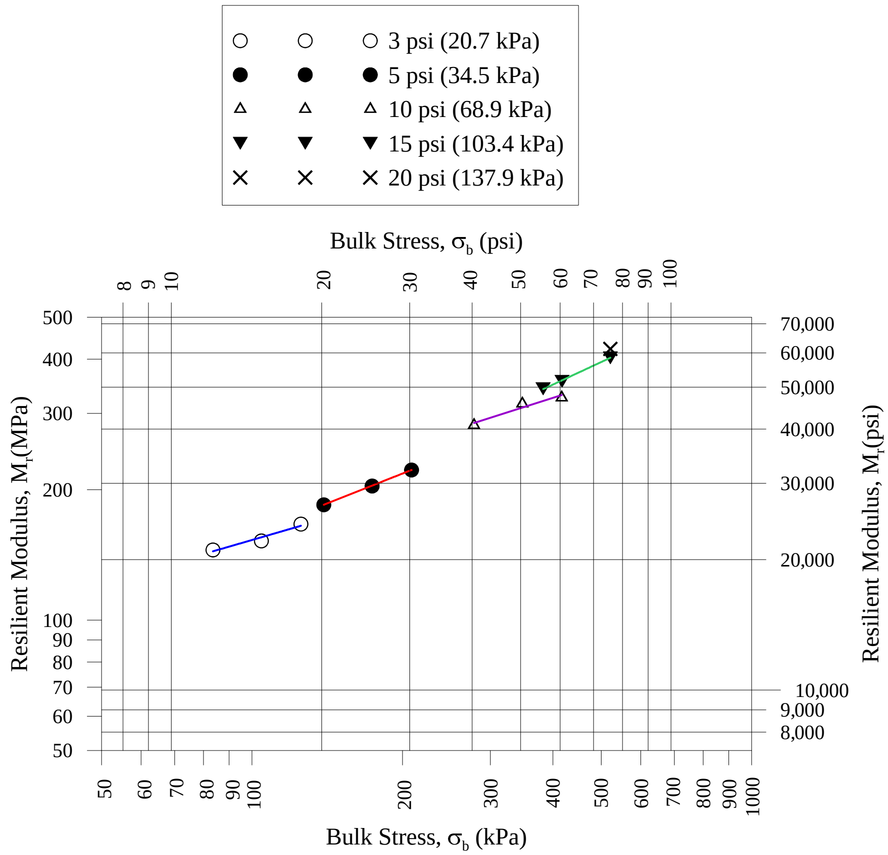

Figure B48: Results of repeated load triaxial test conducted on base aggregate specimen at maximum dry density and optimum moisture content, I 90-94-39, Madison.

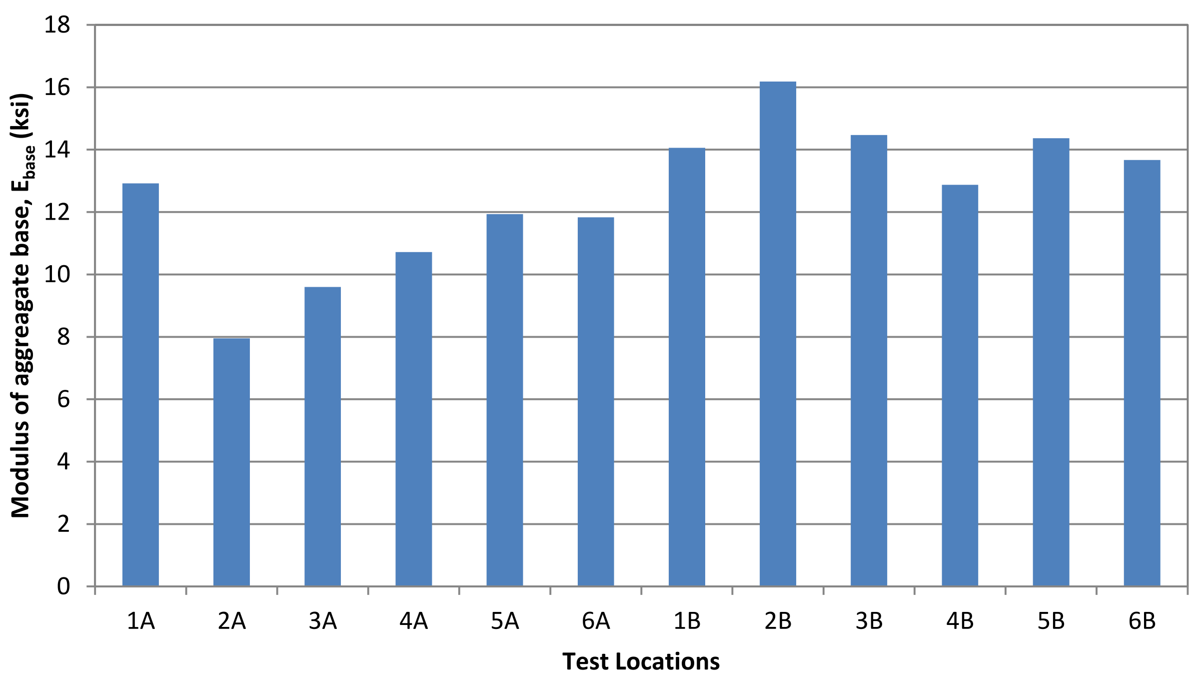

Figure B49: Distribution of average aggregate base layer modulus from LWD tests at I90-94-39, Madison.

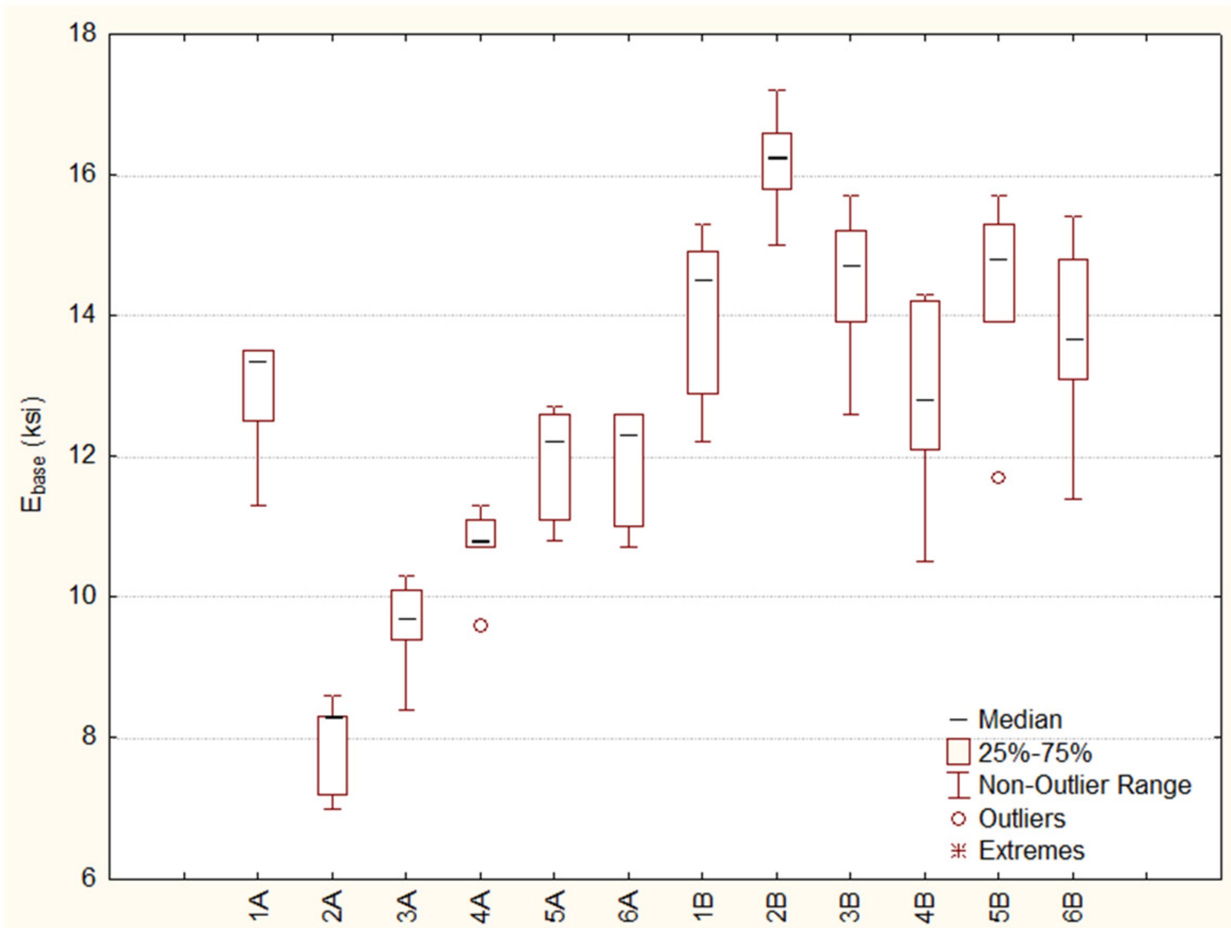

Figure B50: Whisker-box plot for the calculated aggregate base layer modulus from LWD tests at I90-94-39, Madison.

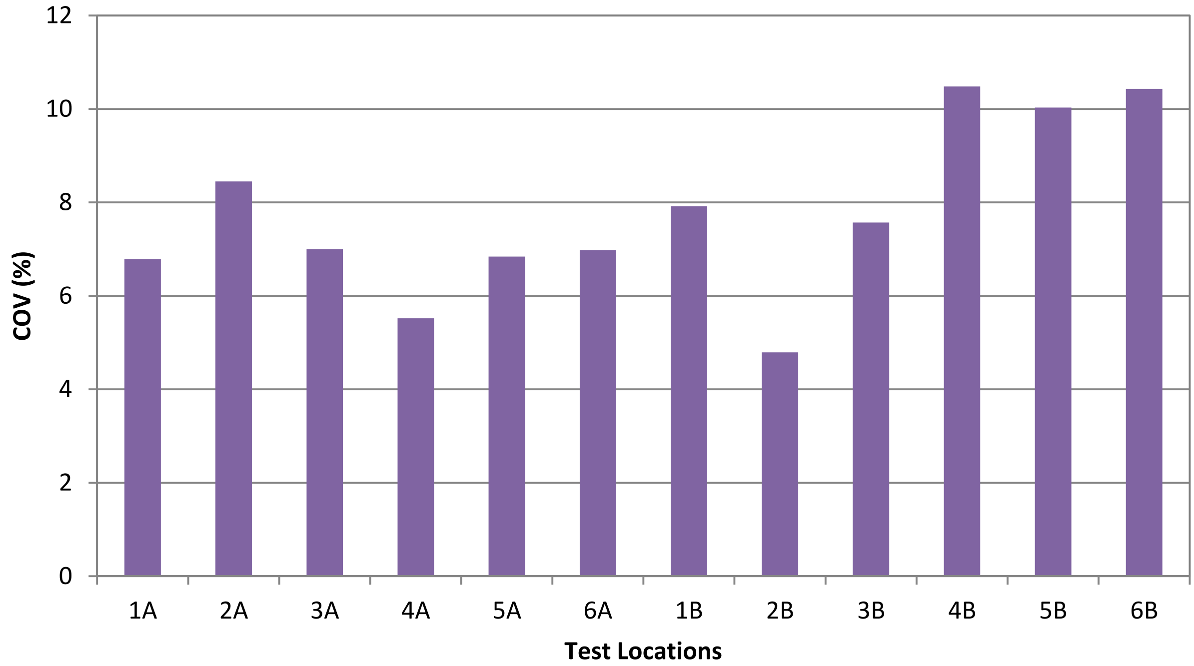

Figure B51: COV for the LWD calculated aggregate base layer modulus, I90-94-39, Madison.

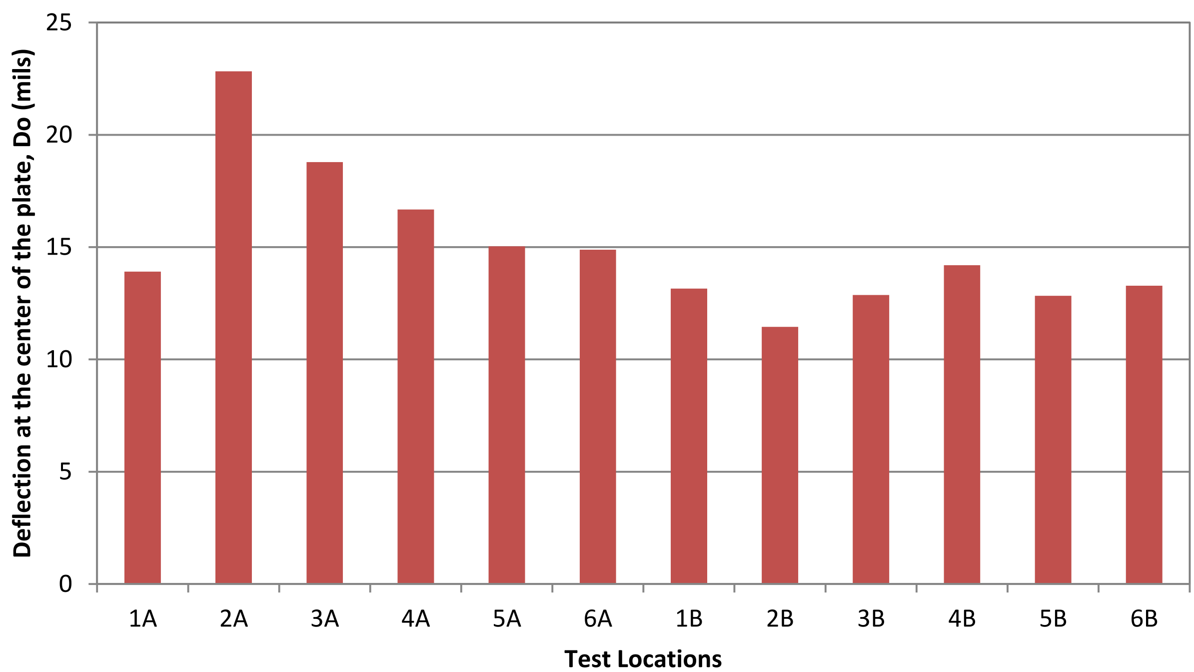

Figure B52: Distribution of average measured deflection under loading plate at LWD test points on the aggregate base layer, I90-94-39, Madison.

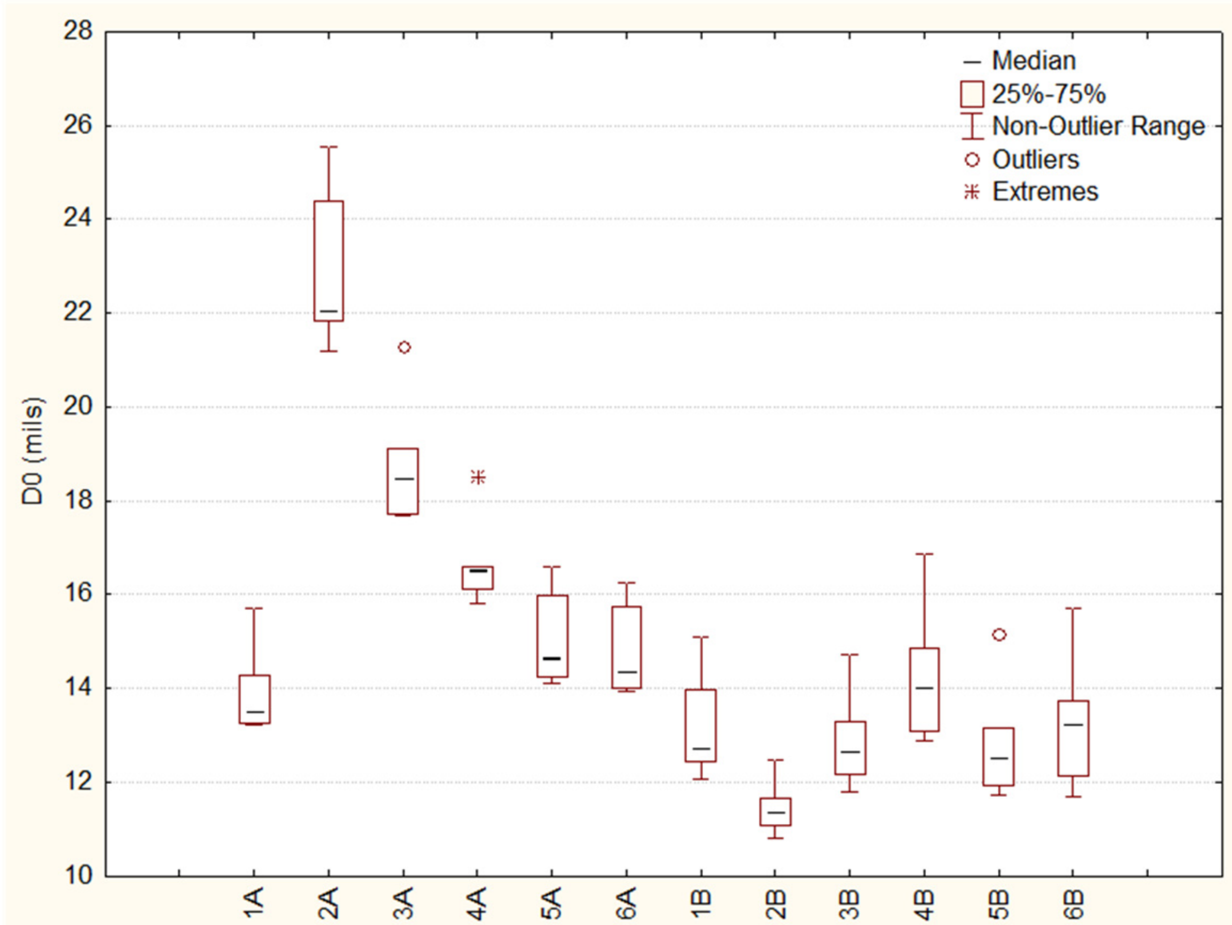

Figure B53: Whisker-box plot for the measured deflection under loading plate at LWD test points on the aggregate base layer, I90-94-39, Madison.

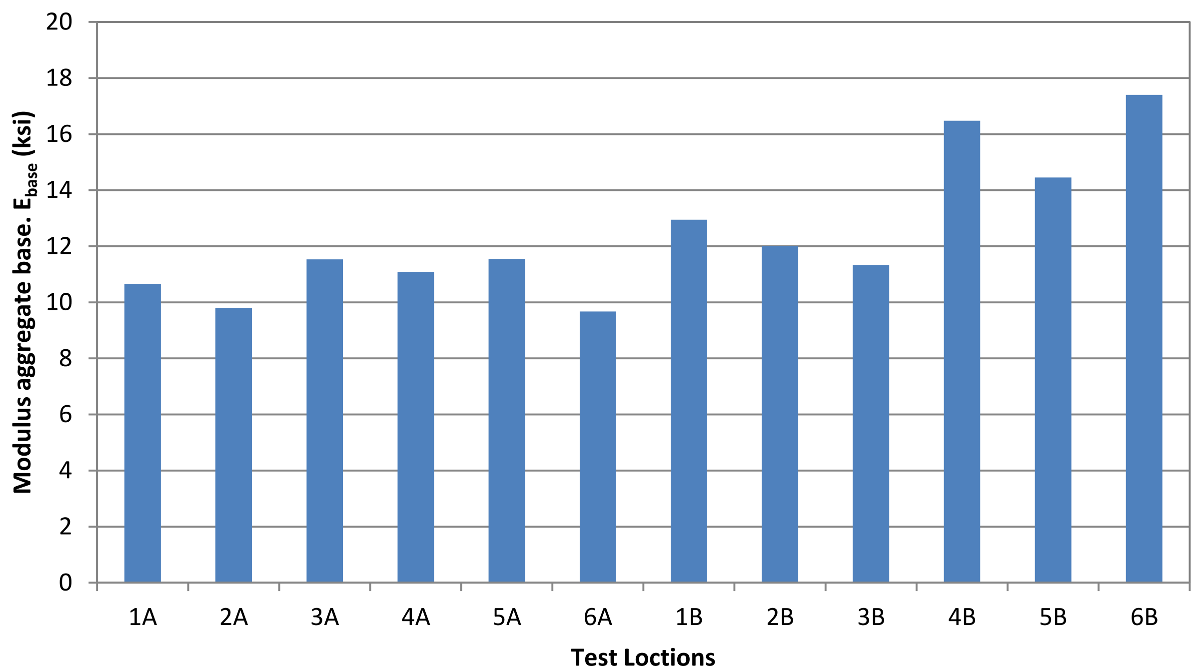

Figure B54: Distribution of average aggregate base layer modulus from GeoGauge tests at I90-94-39, Madison.

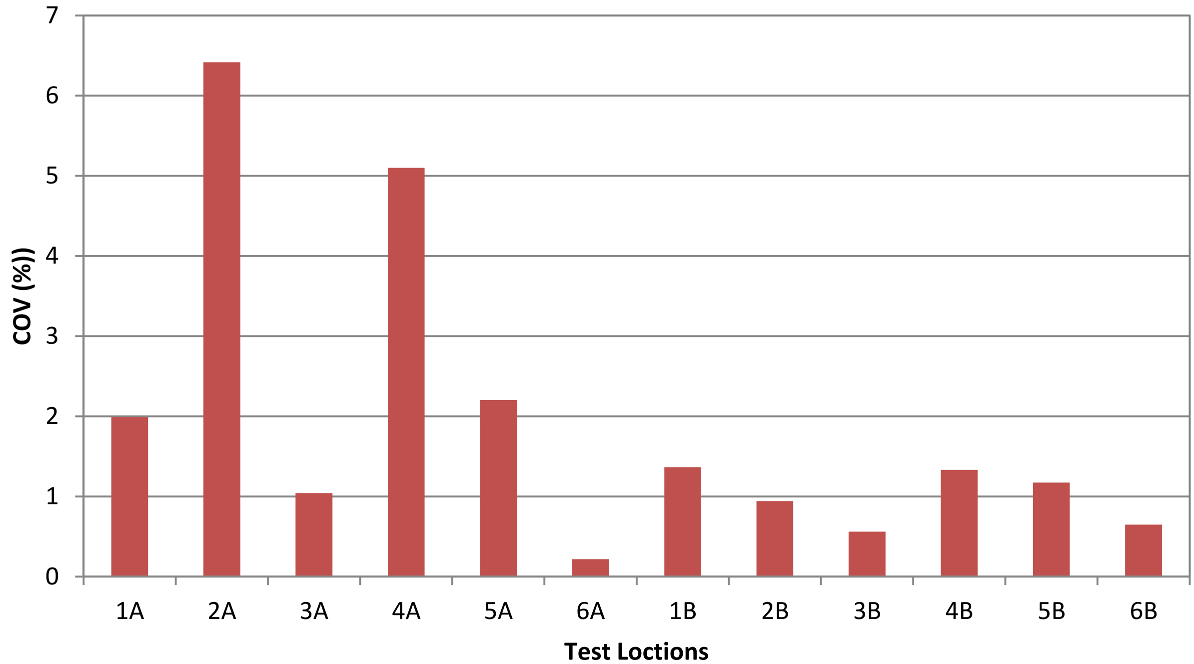

Figure B55: COV for the GeoGauge calculated aggregate base layer modulus, I90-94-39, Madison.

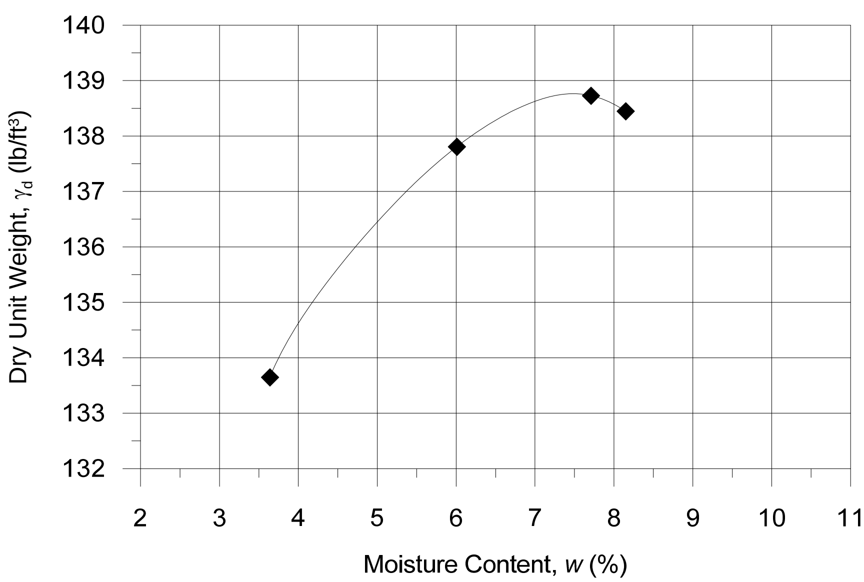

Figure B56: Compaction curve (AASHTO T 99) for base aggregate material used at USH 141, Beecher.

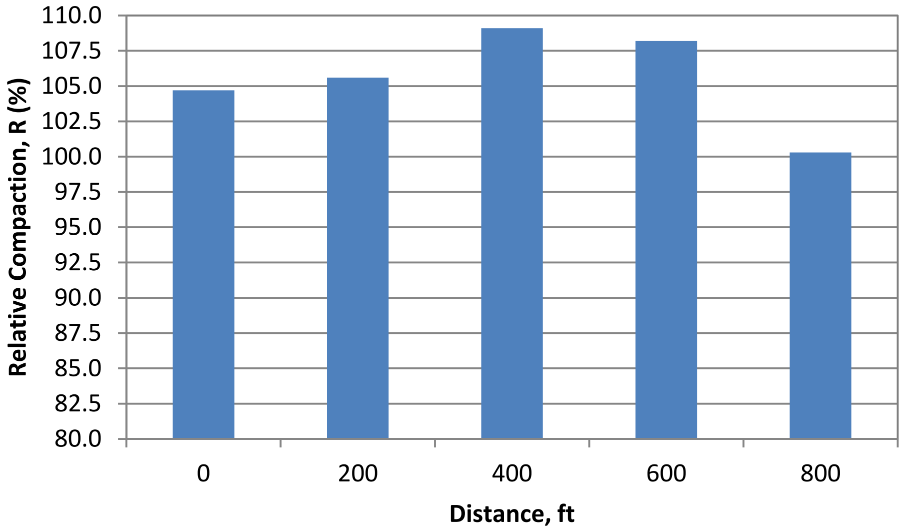

Figure B57: Variation of relative compaction with distance at test section on aggregate base layer, USH 141, Beecher.

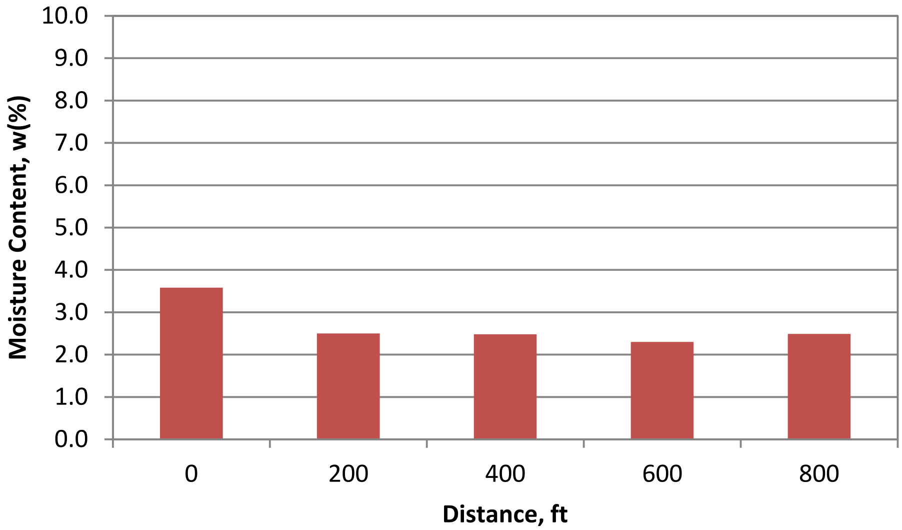

Figure B58: Variation of moisture content with distance at test section on aggregate base layer, USH 141, Beecher.

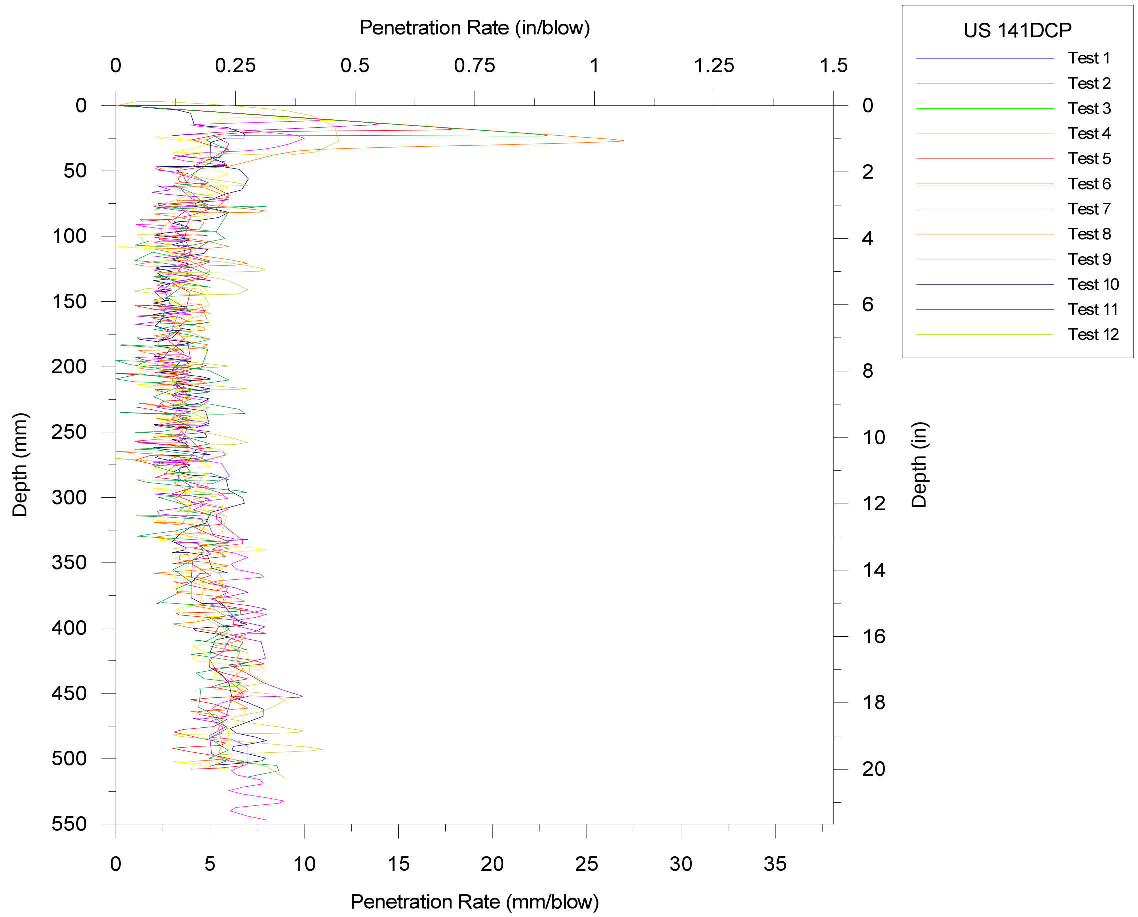

Figure B59: Penetration resistance with depth from DCP test at different points on the aggregate base layer on USH 141, Beecher.

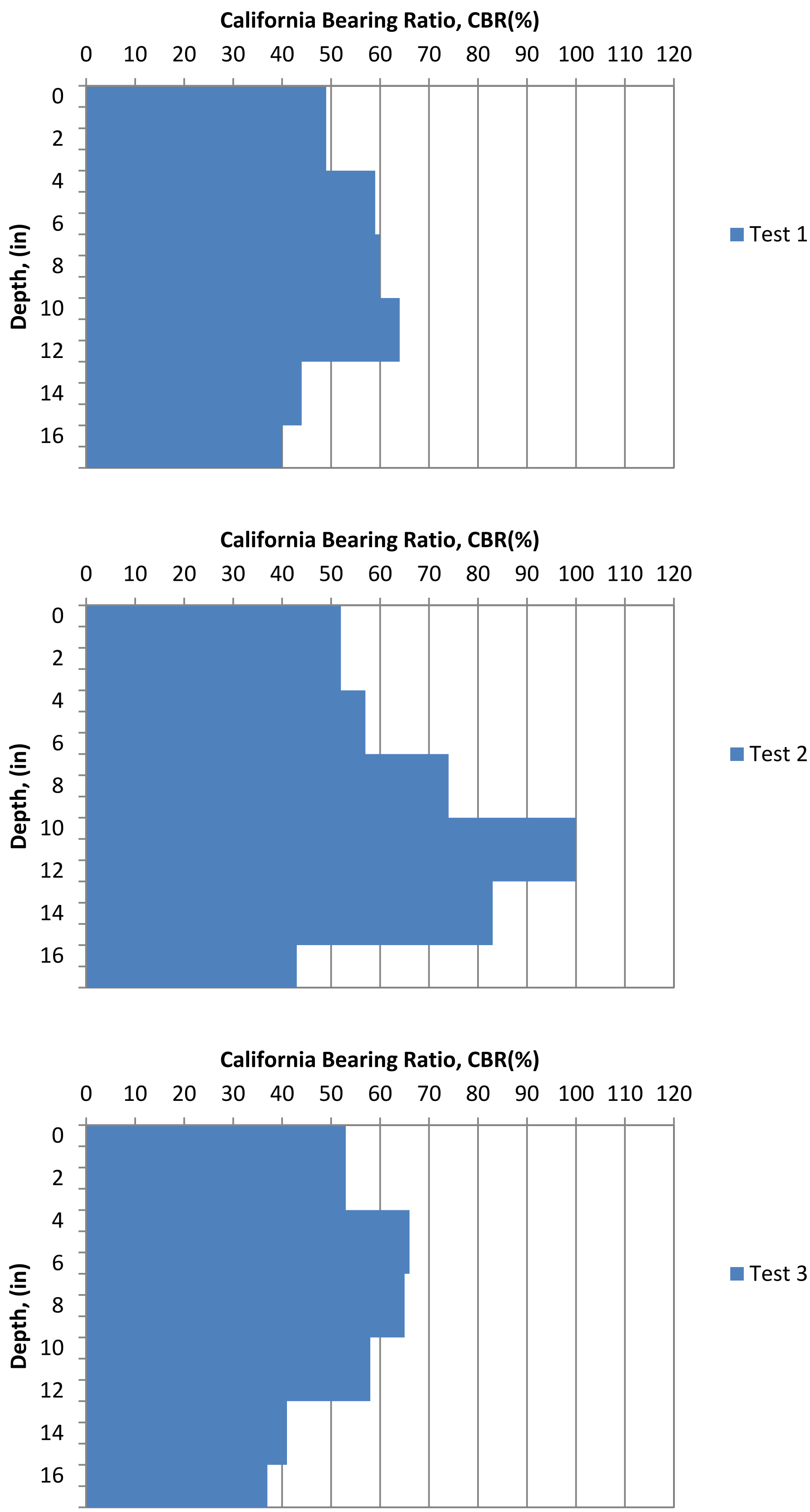

Figure B60: Variability of CBR with depth for aggregate base at USH 141, Beecher.

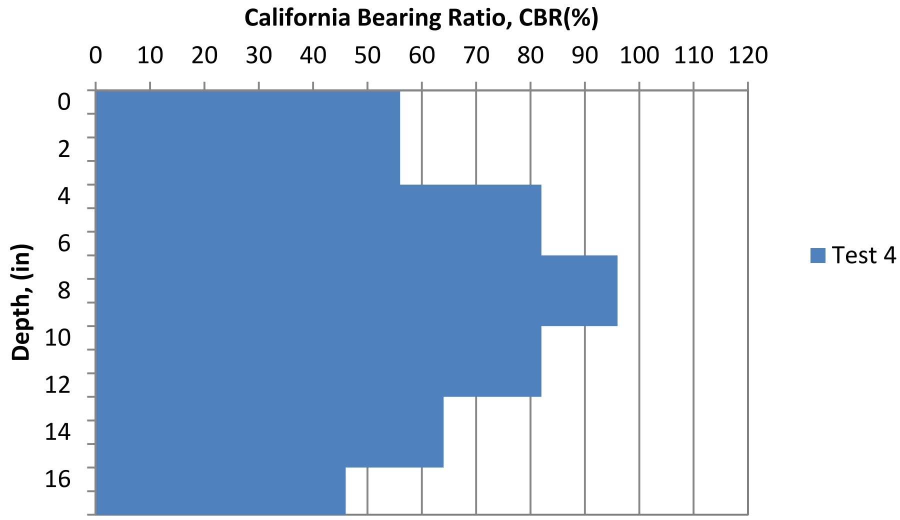

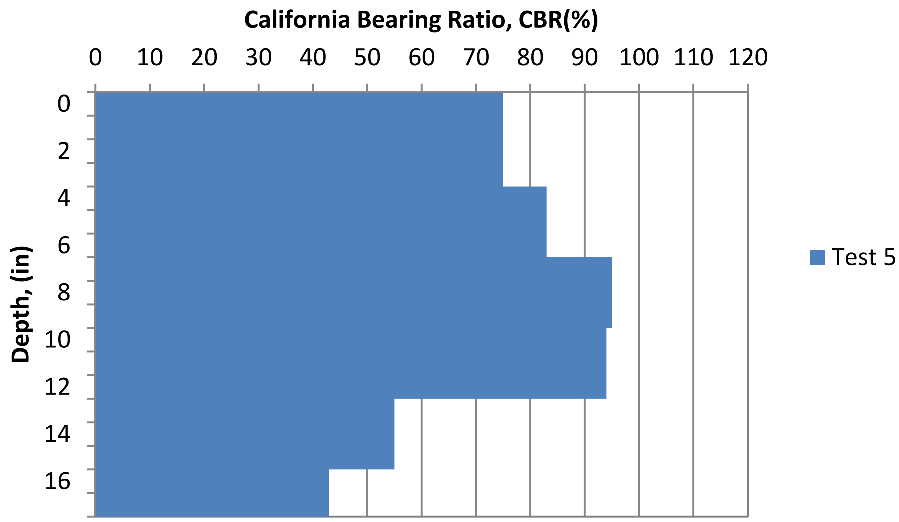

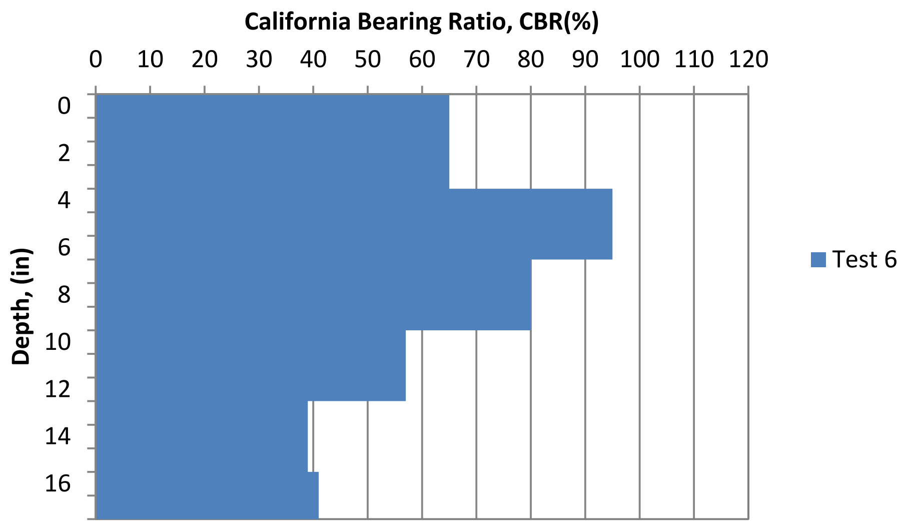

Figure B60 (Cont.): Variability of CBR with depth for aggregate base at USH 141, Beecher.

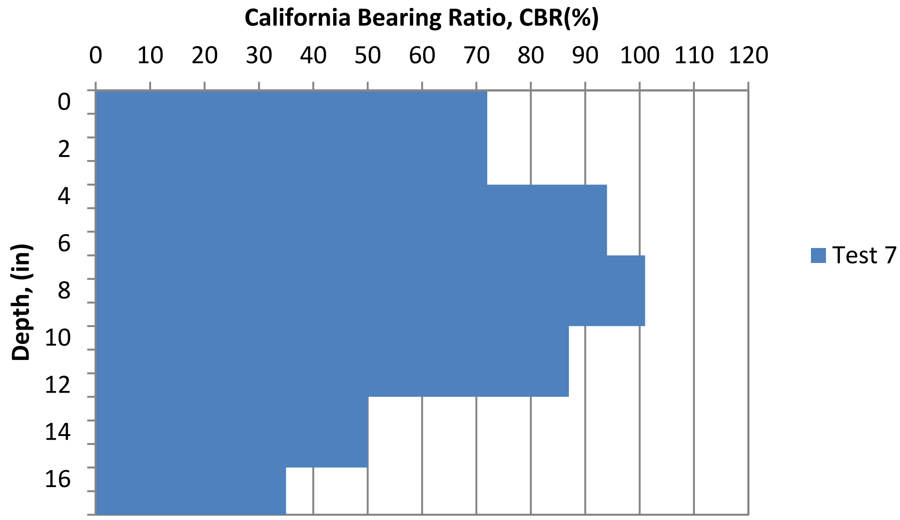

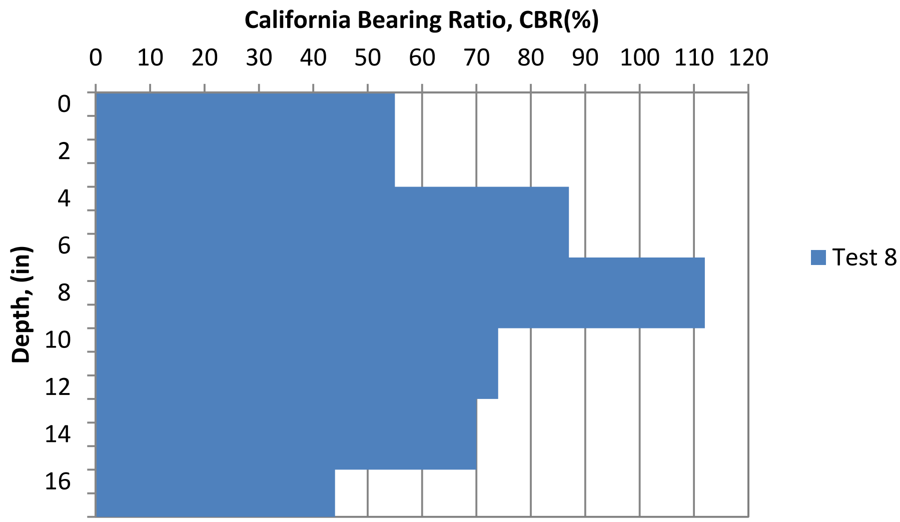

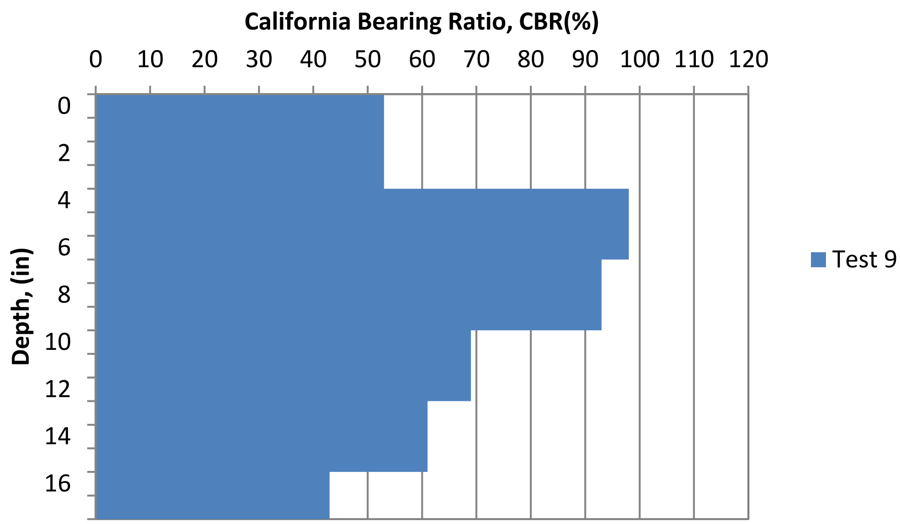

Figure B60 (Cont.): Variability of CBR with depth for aggregate base at USH 141, Beecher.

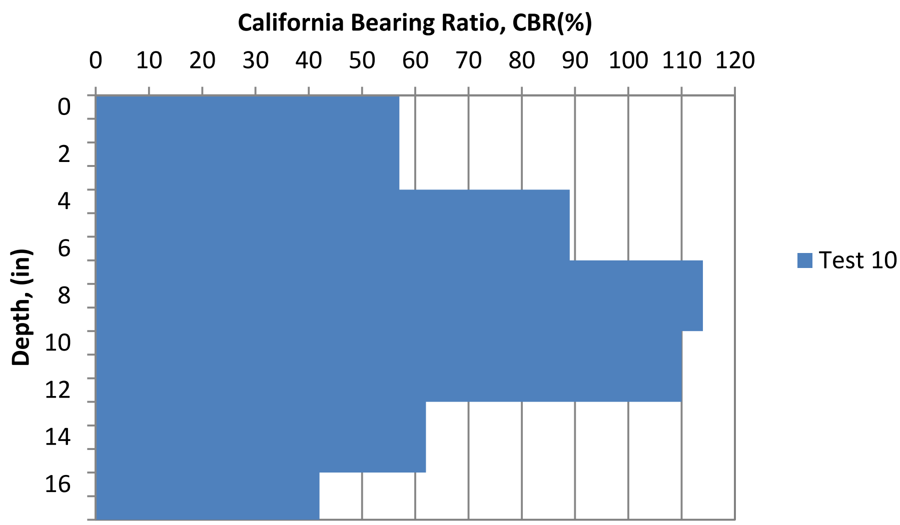

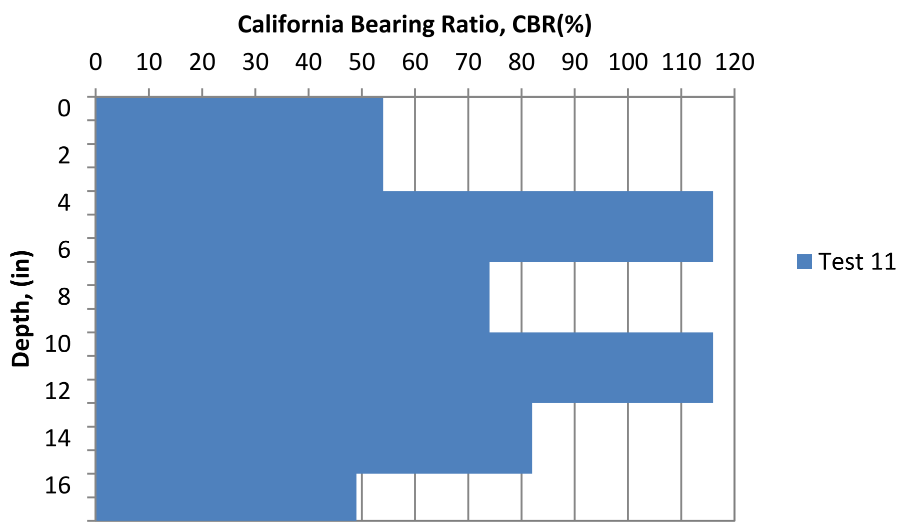

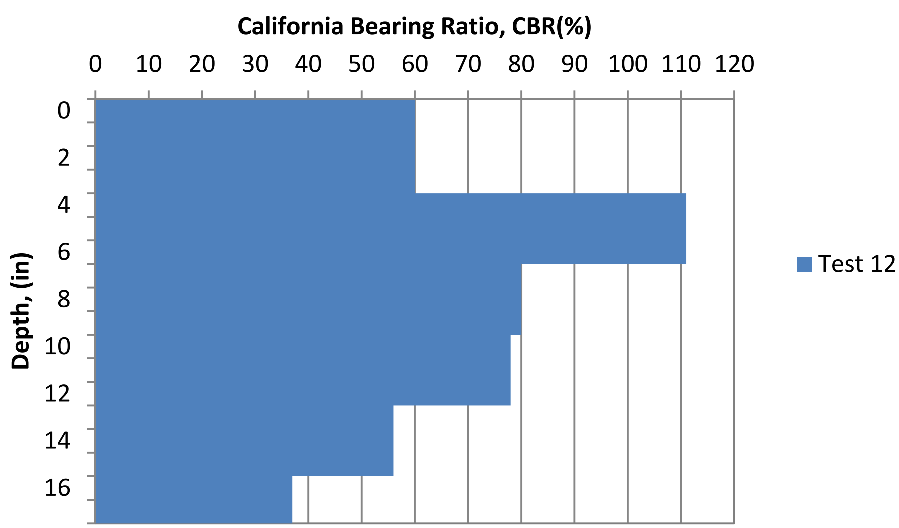

Figure B60 (Cont.): Variability of CBR with depth for aggregate base at USH 141, Beecher.

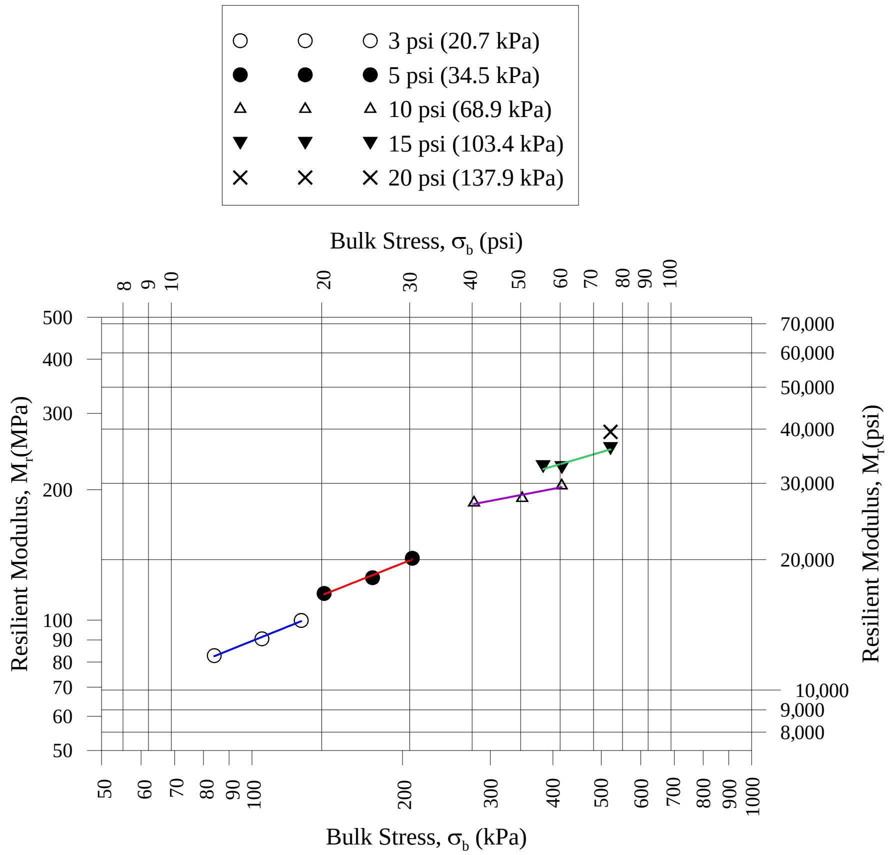

Figure B61: Results of repeated load triaxial test conducted on base aggregate specimen at maximum dry density and optimum moisture content, USH 141, Beecher.

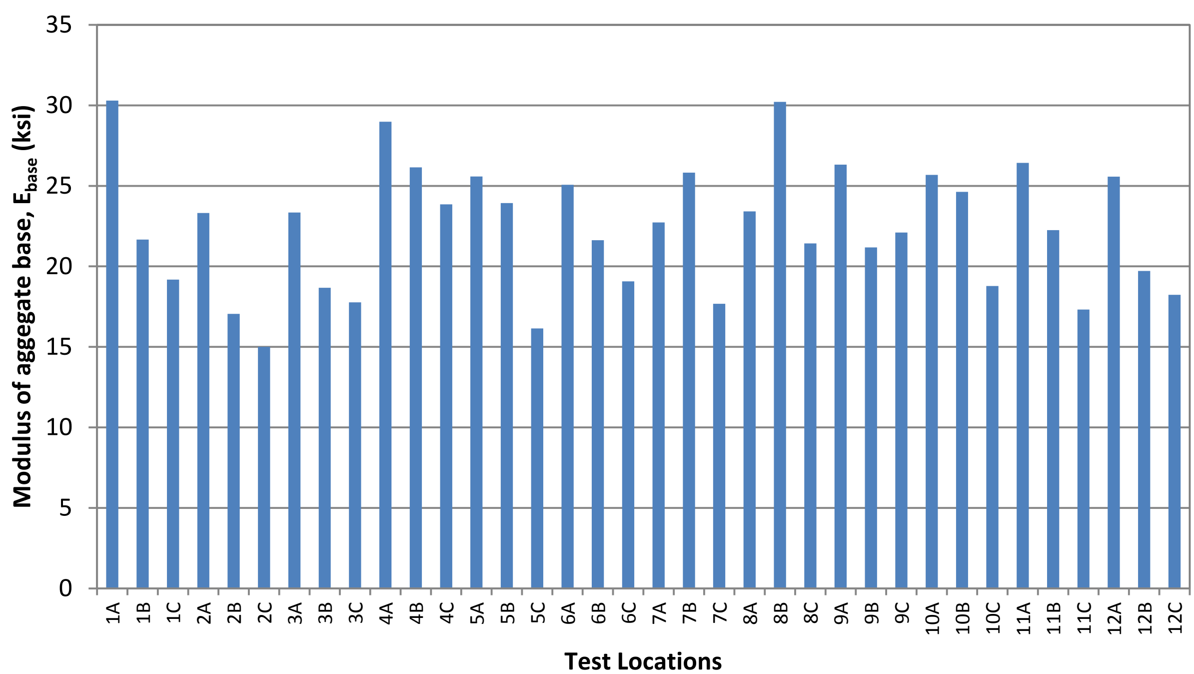

Figure B62: Distribution of average aggregate base layer modulus from LWD tests at USH 141, Beecher.

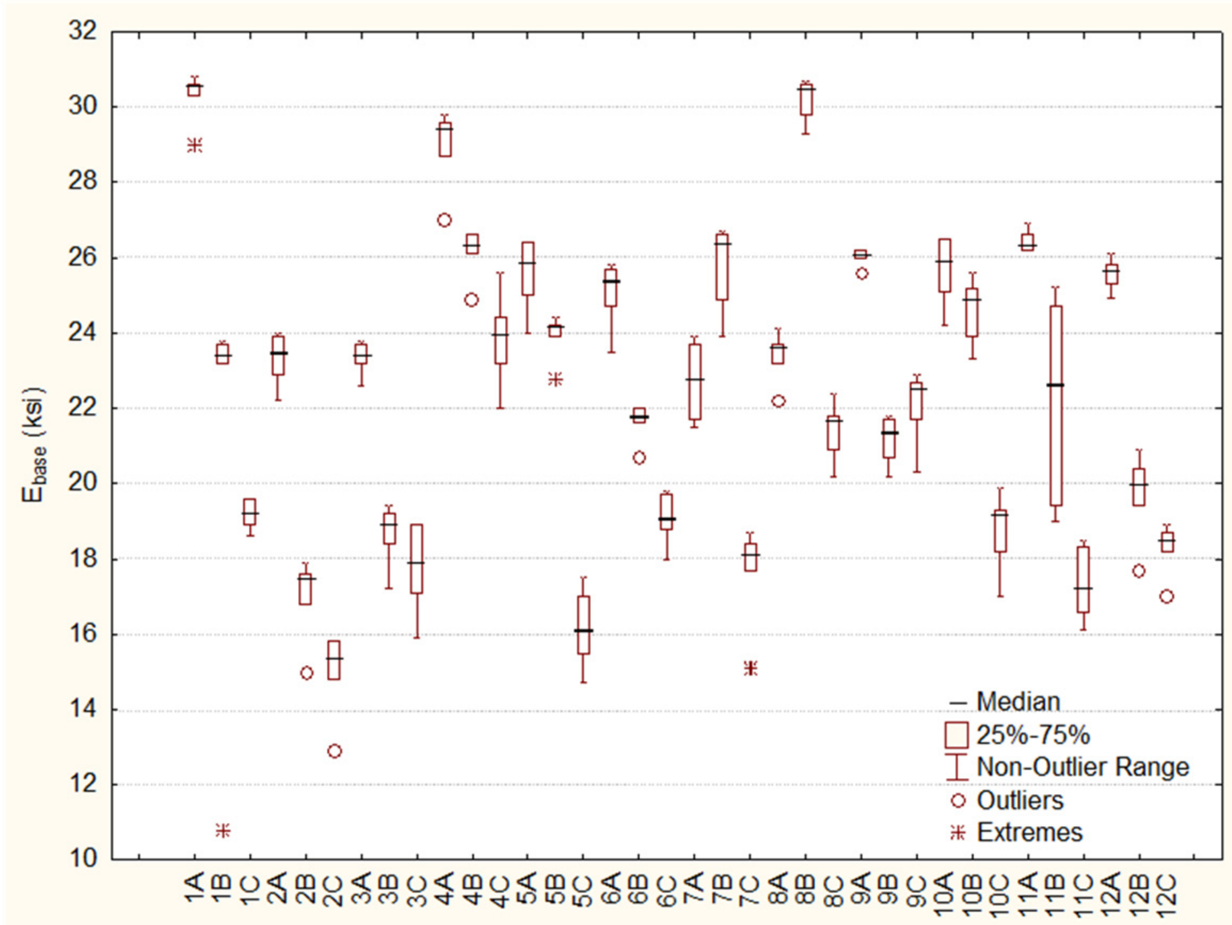

Figure B63: Whisker-box plot for the calculated aggregate base layer modulus from LWD tests USH 141, Beecher.

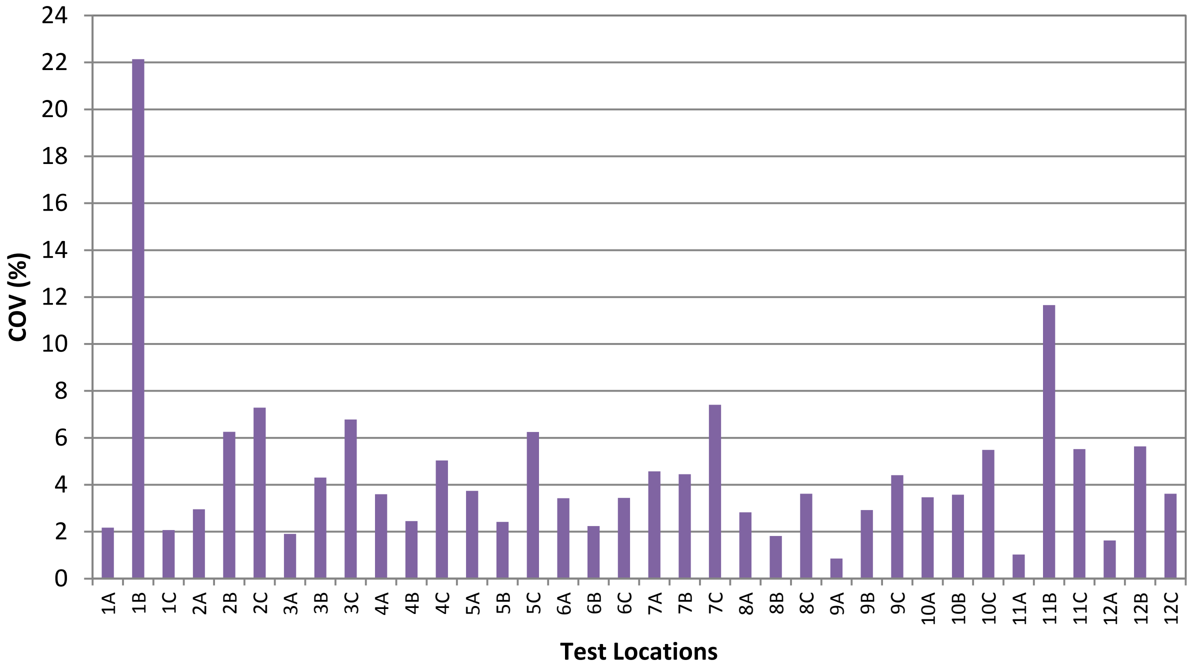

Figure B64: COV for the LWD calculated aggregate base layer modulus, USH 141, Beecher.

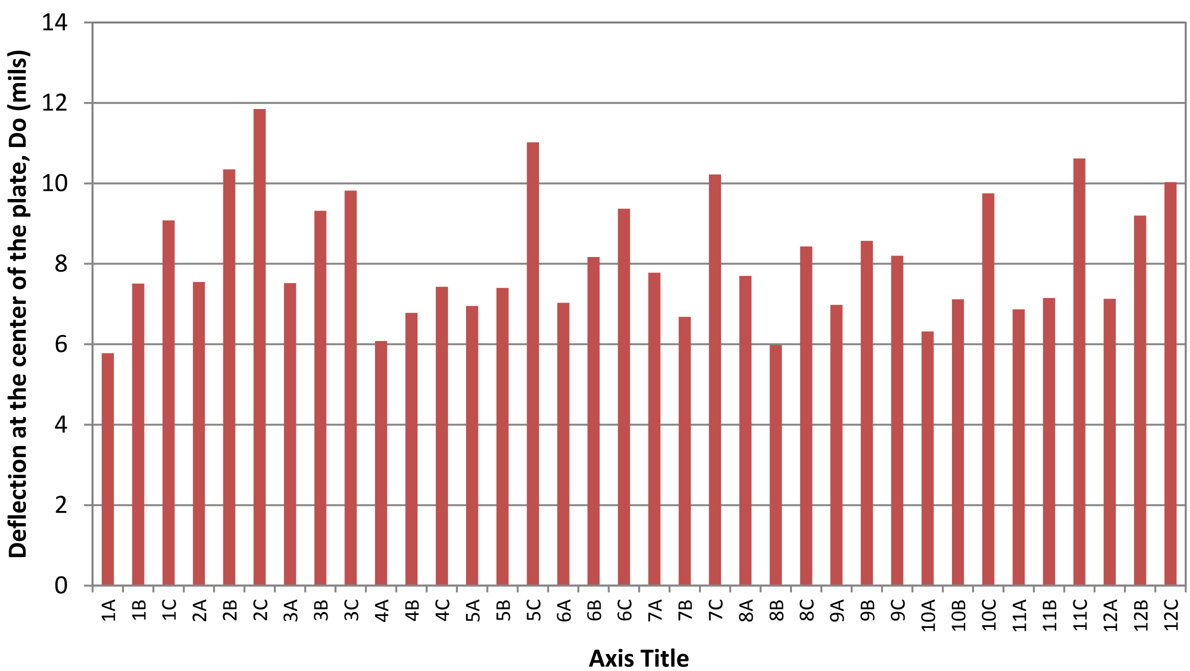

Figure B65: Distribution of average measured deflection under loading plate at LWD test points on the aggregate base layer, USH 141, Beecher.

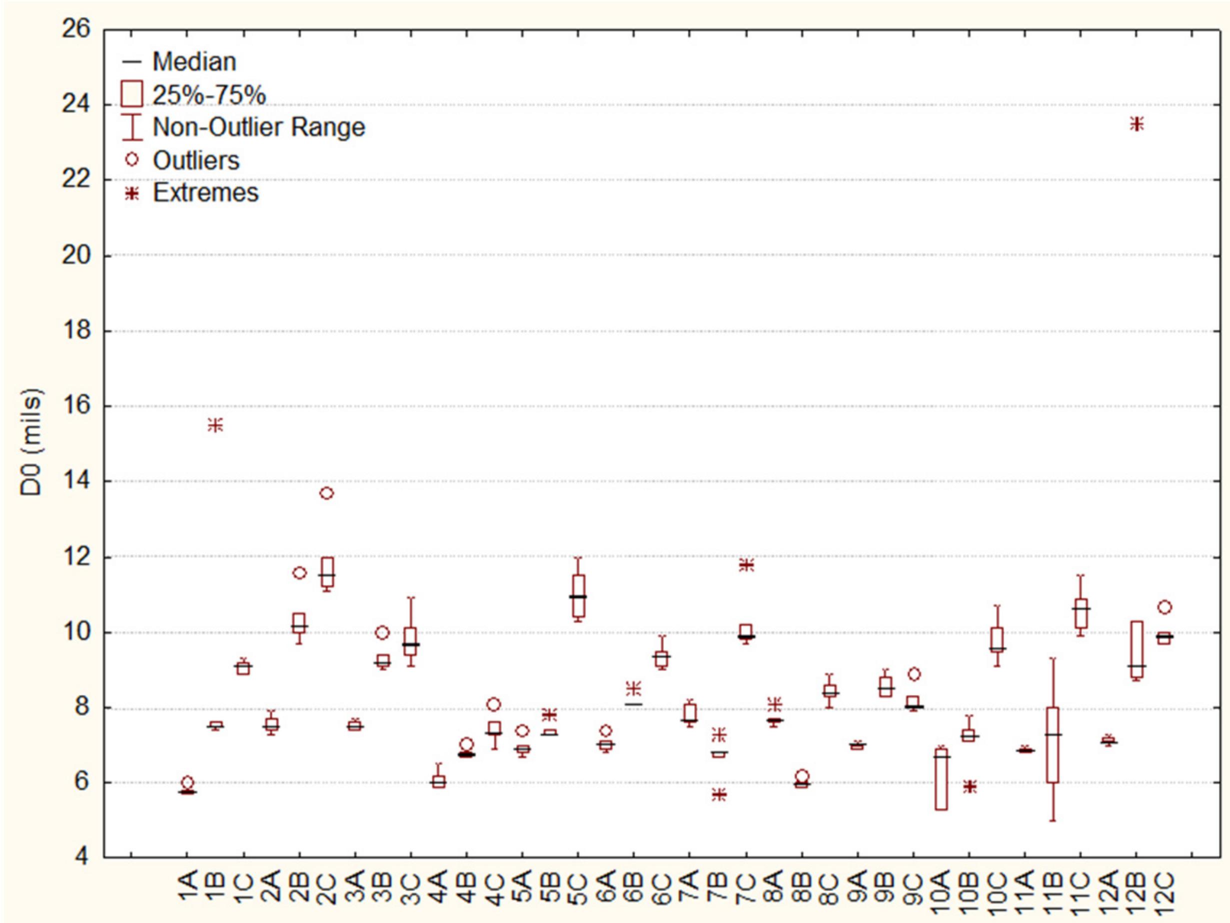

Figure B66: Whisker-box plot for the measured deflection under loading plate at LWD test points on the aggregate base layer, USH 141, Beecher.

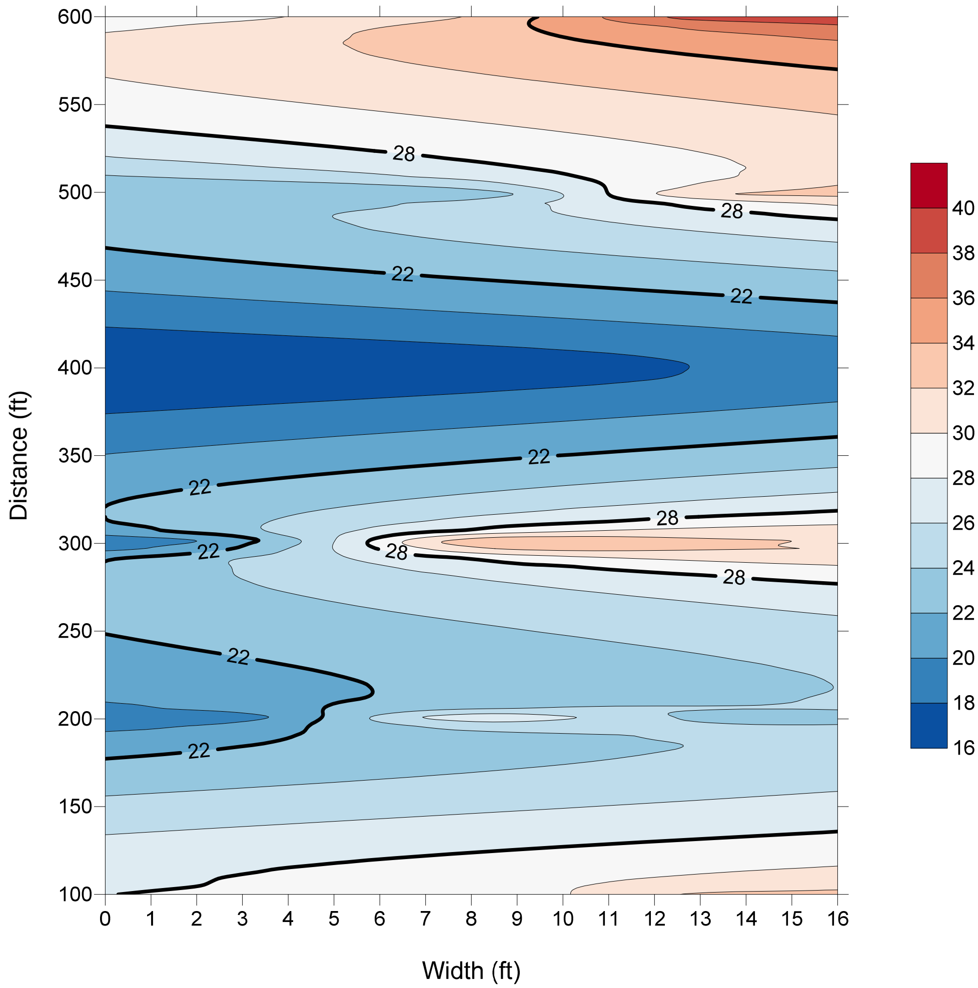

Figure B67: Contours of the calculated base layer modulus (E_{base}) based on LWD measurements, USH 141, Beecher.

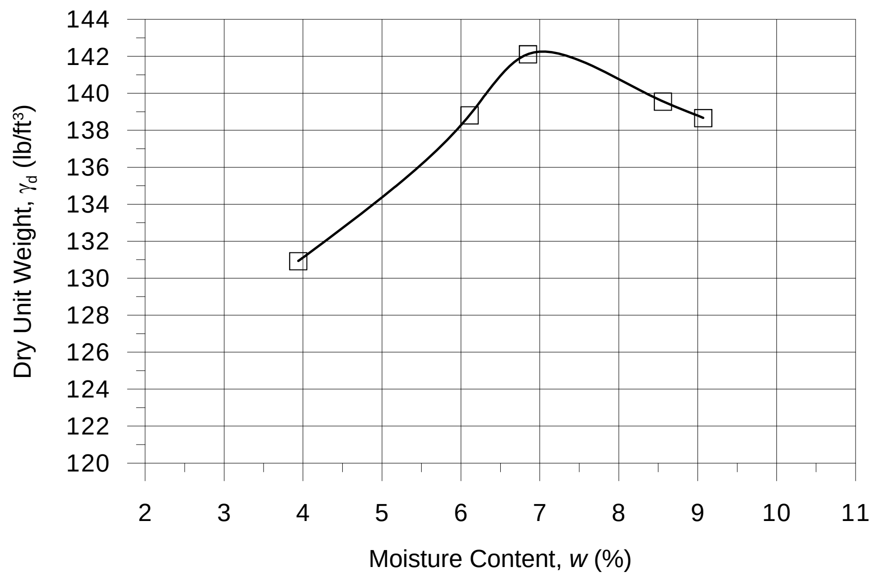

Figure B68: Compaction curve (AASHTO T 99) for base aggregate material used at STH 33, Saukville.

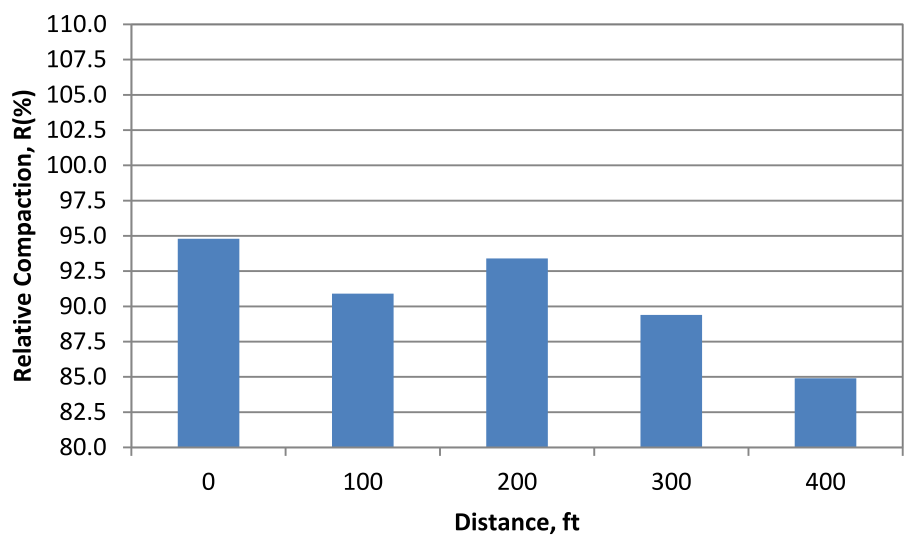

Figure B69: Variation of relative compaction with distance at test section on aggregate base layer, STH 33, Saukville.

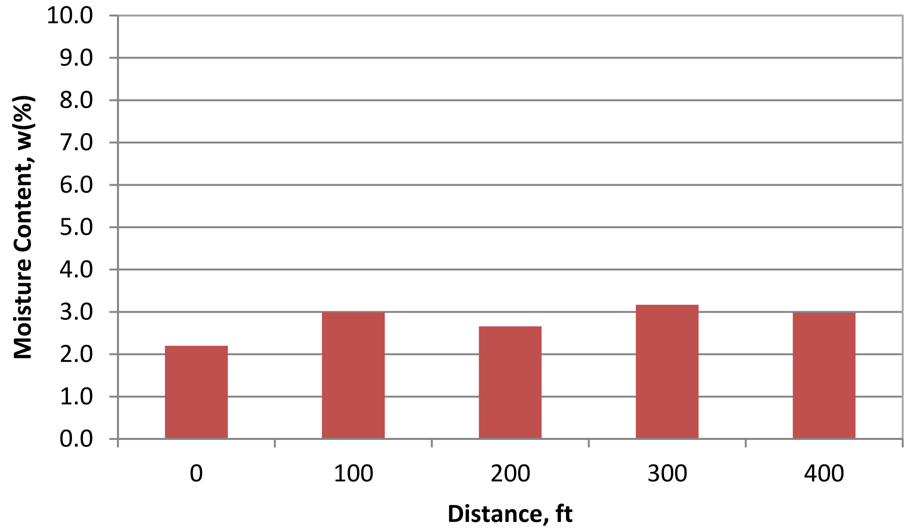

Figure B70: Variation of moisture content with distance at test section on aggregate base layer, STH 33, Saukville.

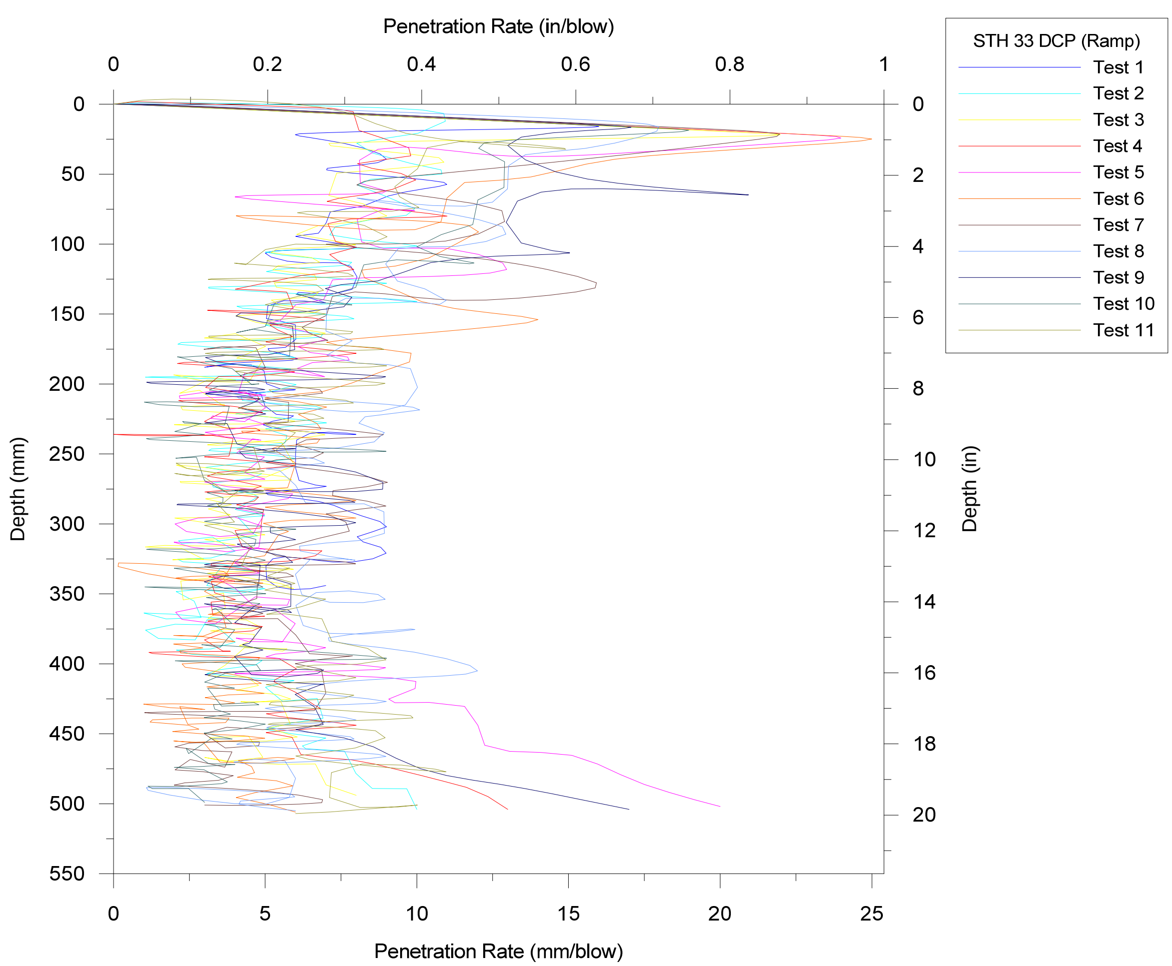

Figure B71: Penetration resistance with depth from DCP test at different points on the aggregate base layer, STH 33, Saukville.

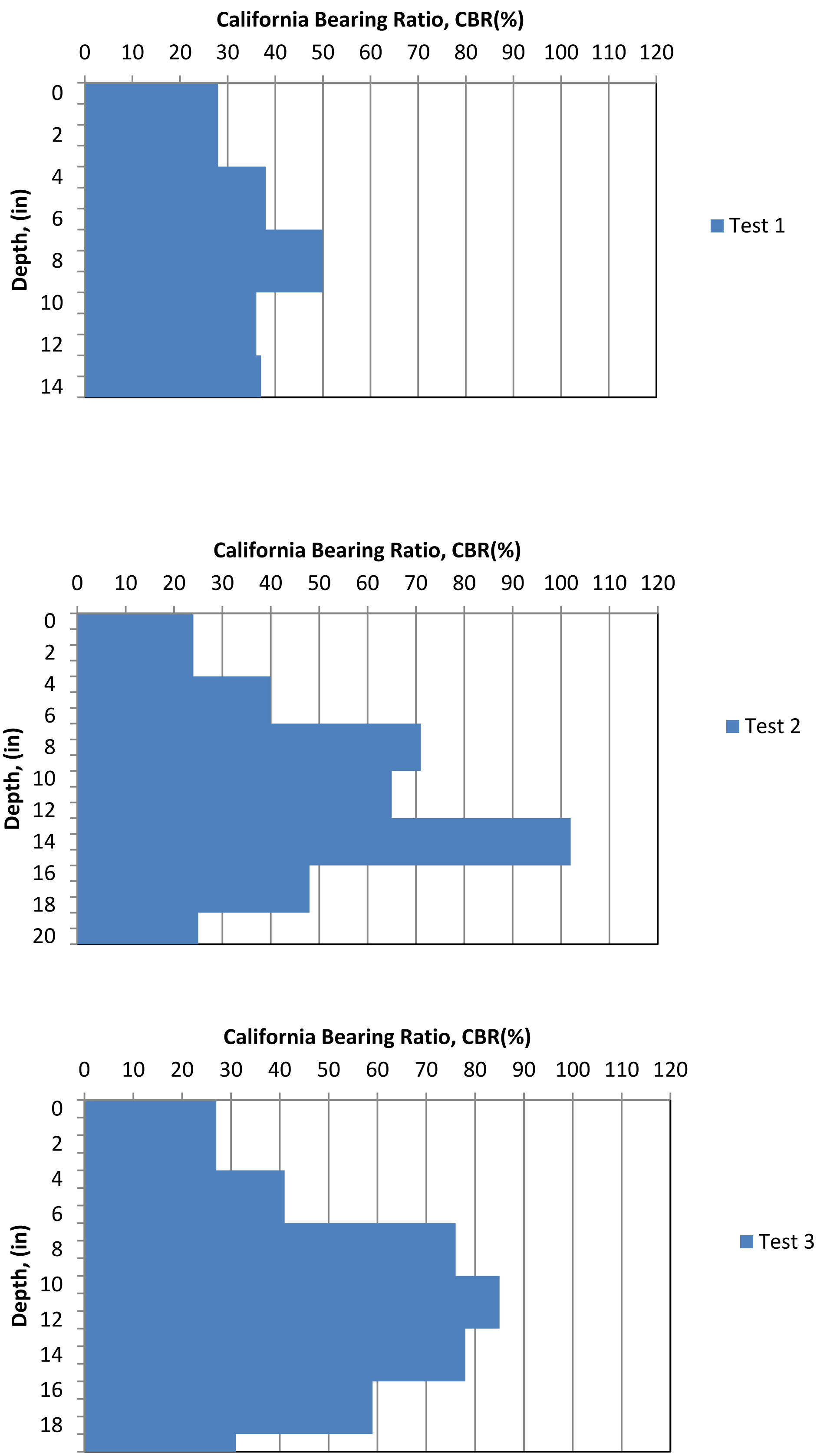

Figure B72: Variability of CBR with depth for aggregate base at STH 33, Saukville.

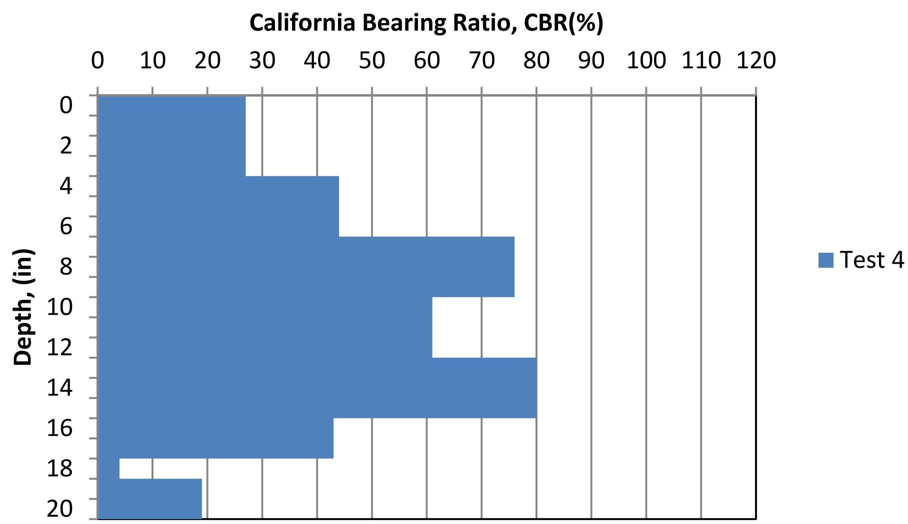

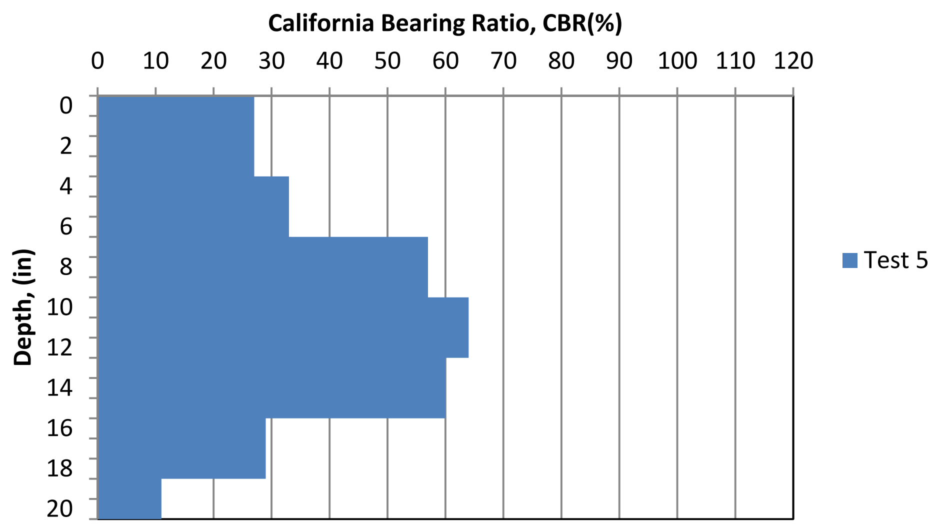

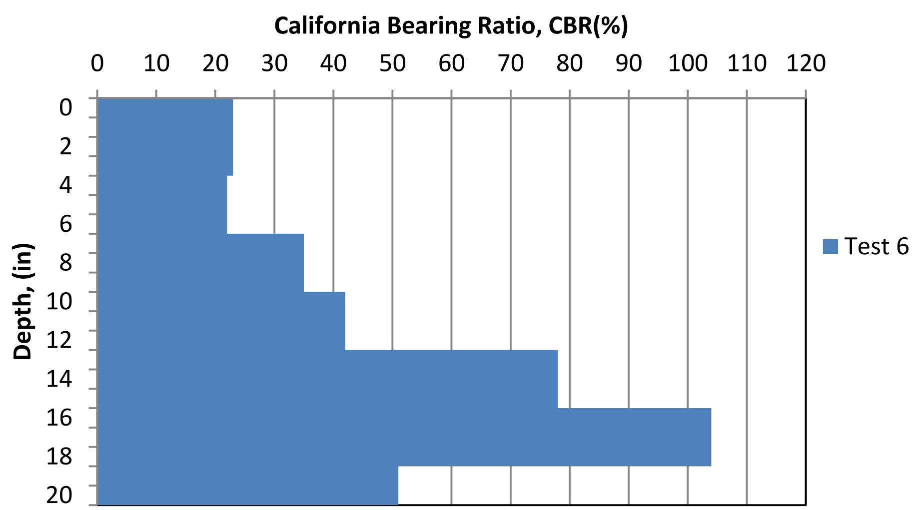

Figure B72 (Cont.): Variability of CBR with depth for aggregate base at STH 33, Saukville.

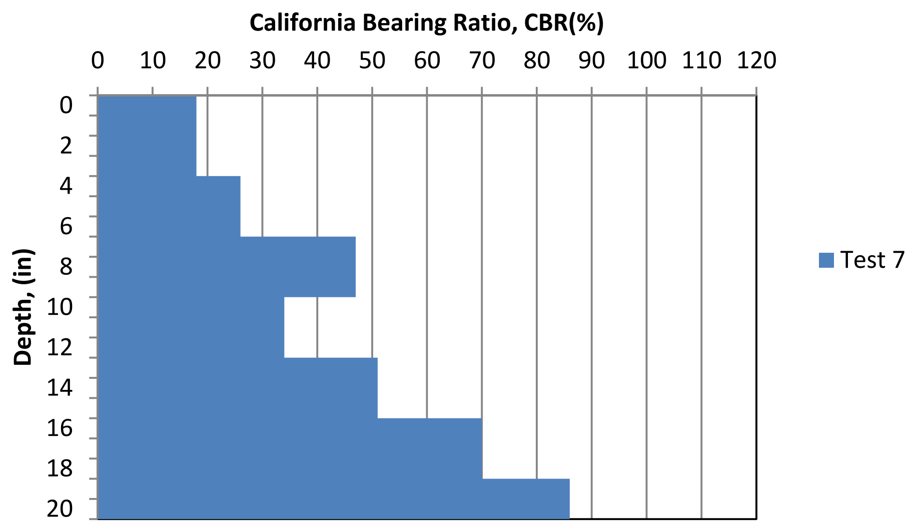

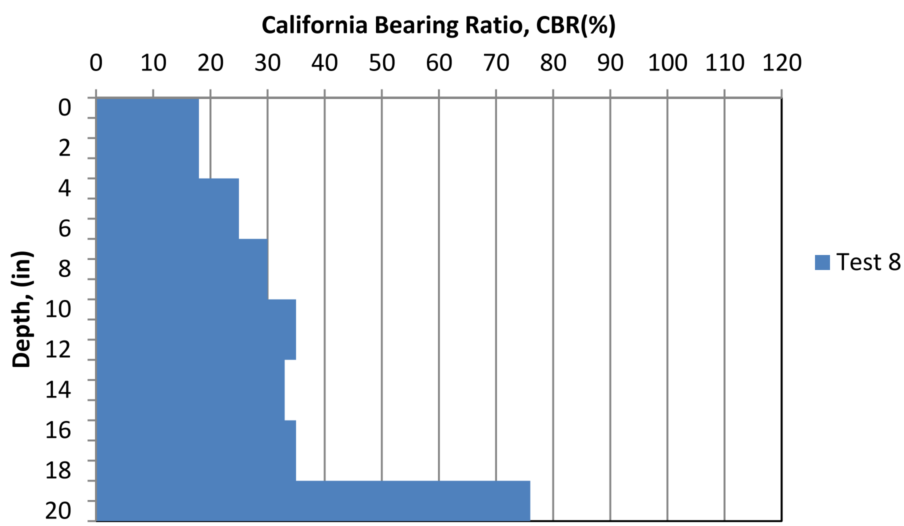

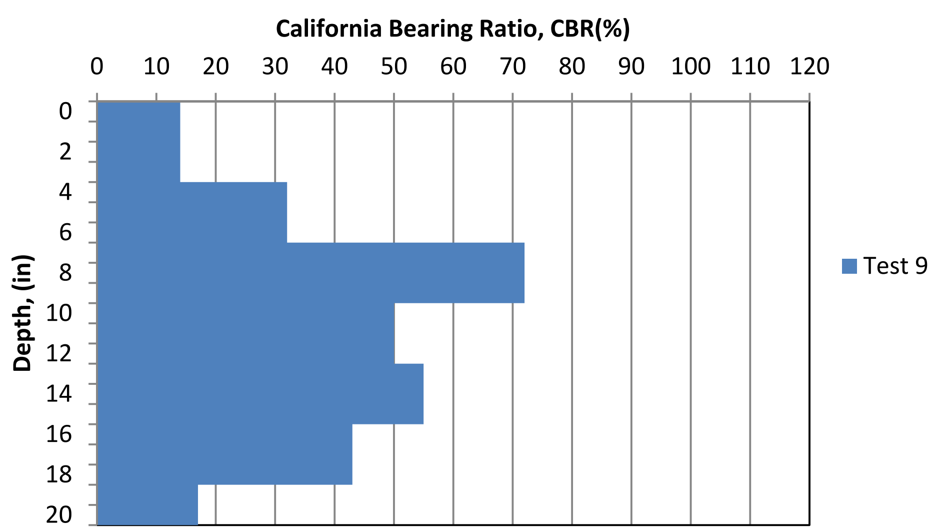

Figure B72 (Cont.): Variability of CBR with depth for aggregate base at STH 33, Saukville.

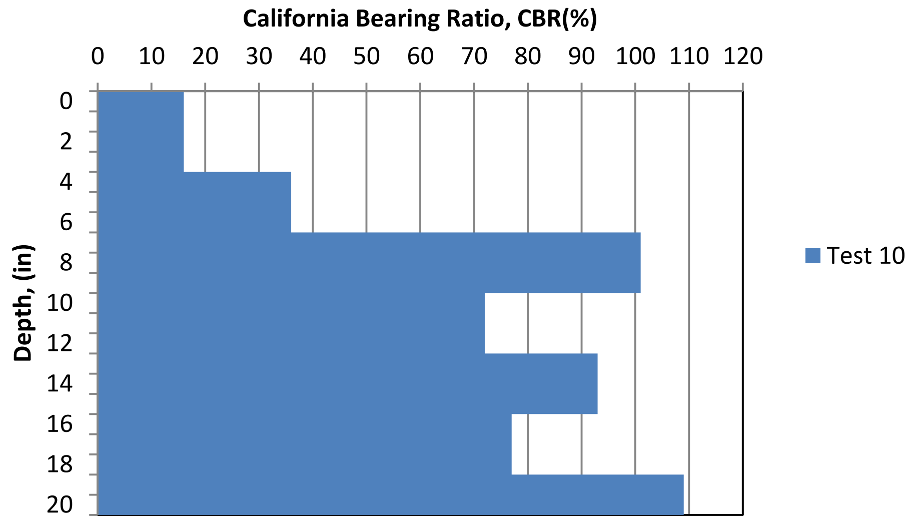

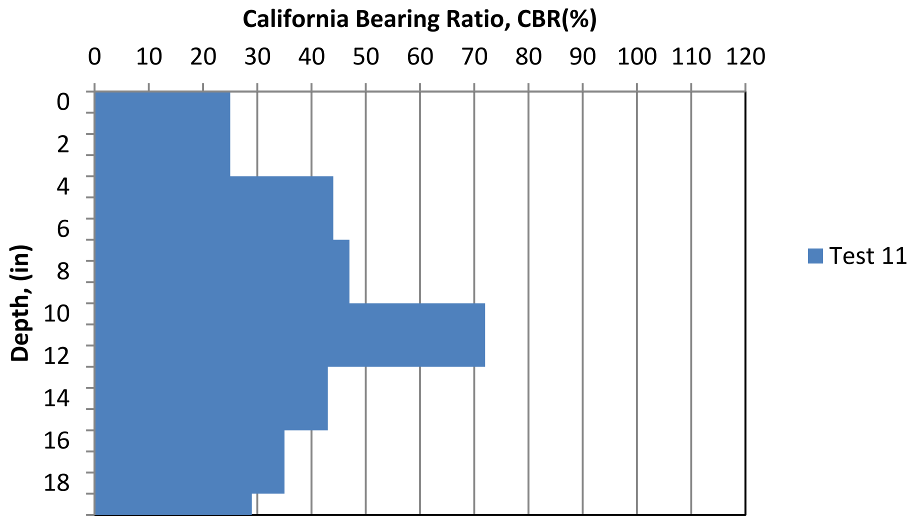

Figure B72 (Cont.): Variability of CBR with depth for aggregate base at STH 33, Saukville.

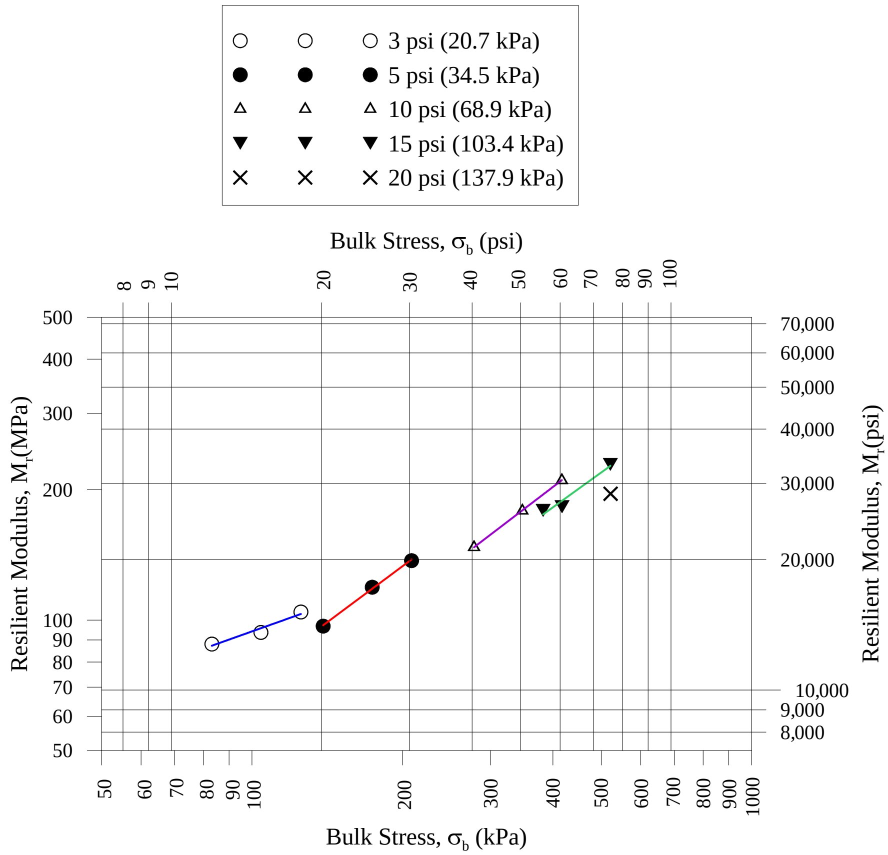

Figure B73: Results of repeated load triaxial test conducted on base aggregate specimen at maximum dry density and optimum moisture content, STH 33, Saukville.

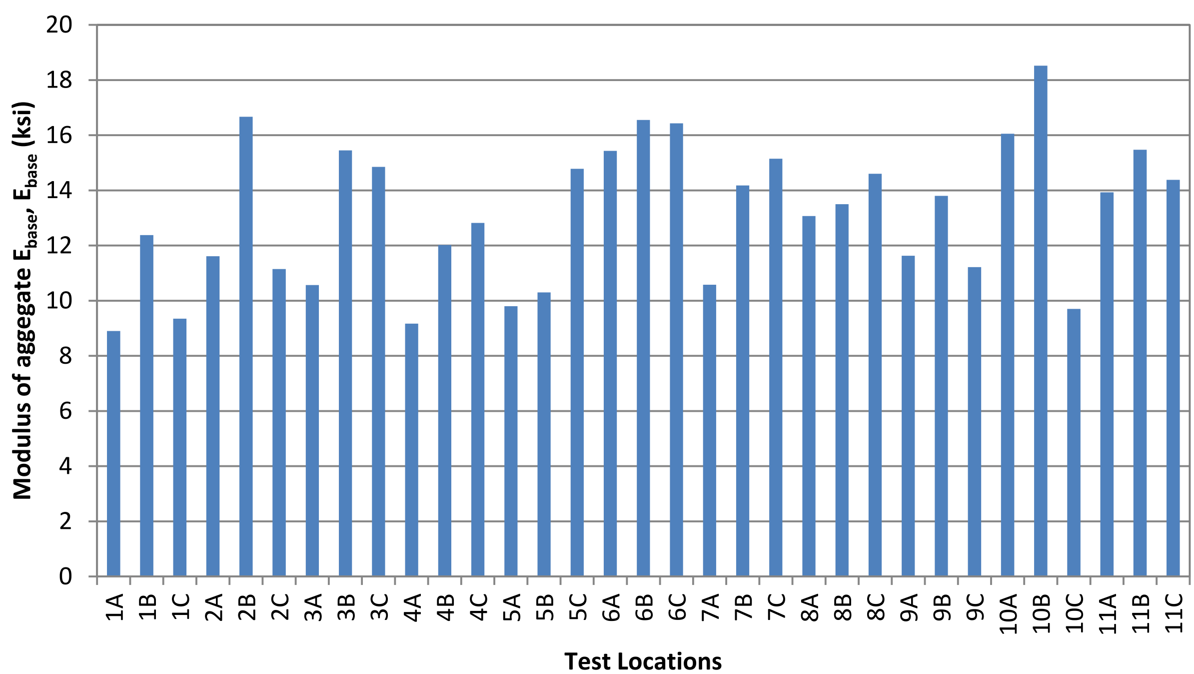

Figure B74: Distribution of average aggregate base layer modulus from LWD tests at STH 33, Saukville.

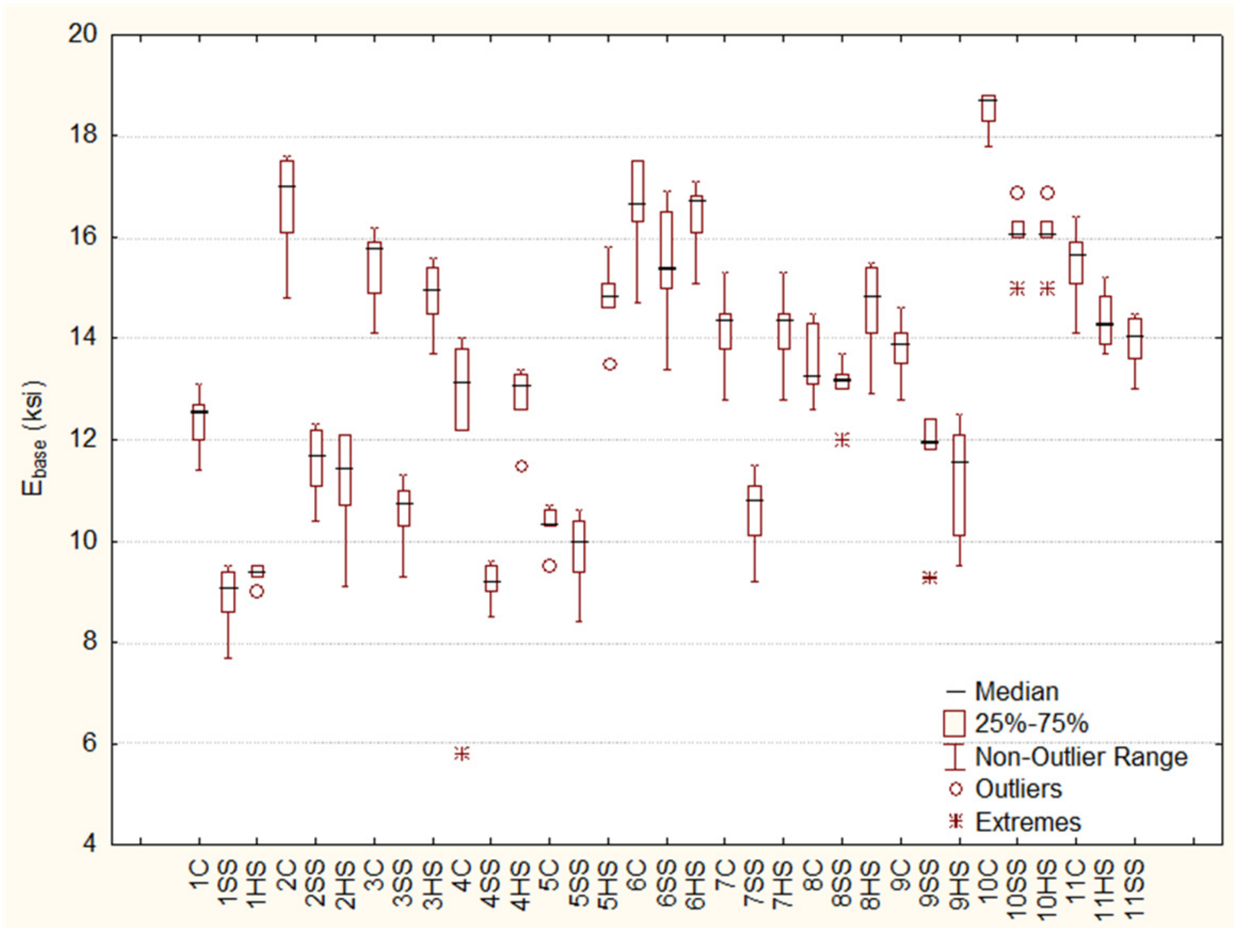

Figure B75: Whisker-box plot for the calculated aggregate base layer modulus from LWD tests, STH 33, Saukville.

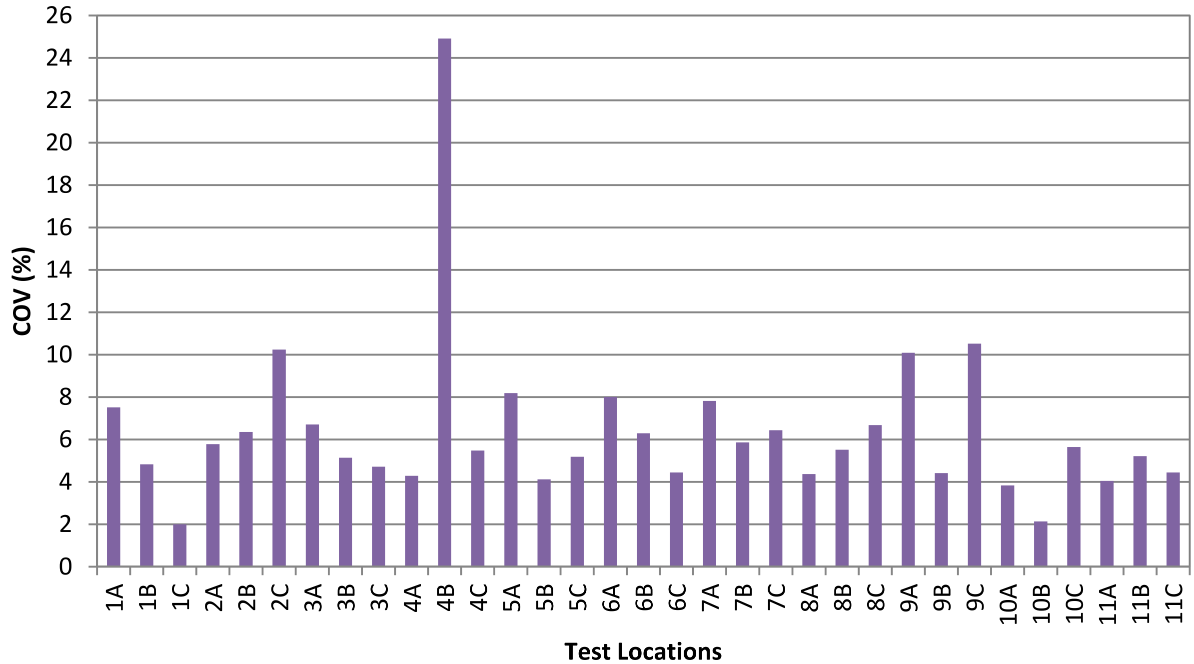

Figure B76: COV for the LWD calculated aggregate base layer modulus, STH 33, Saukville.

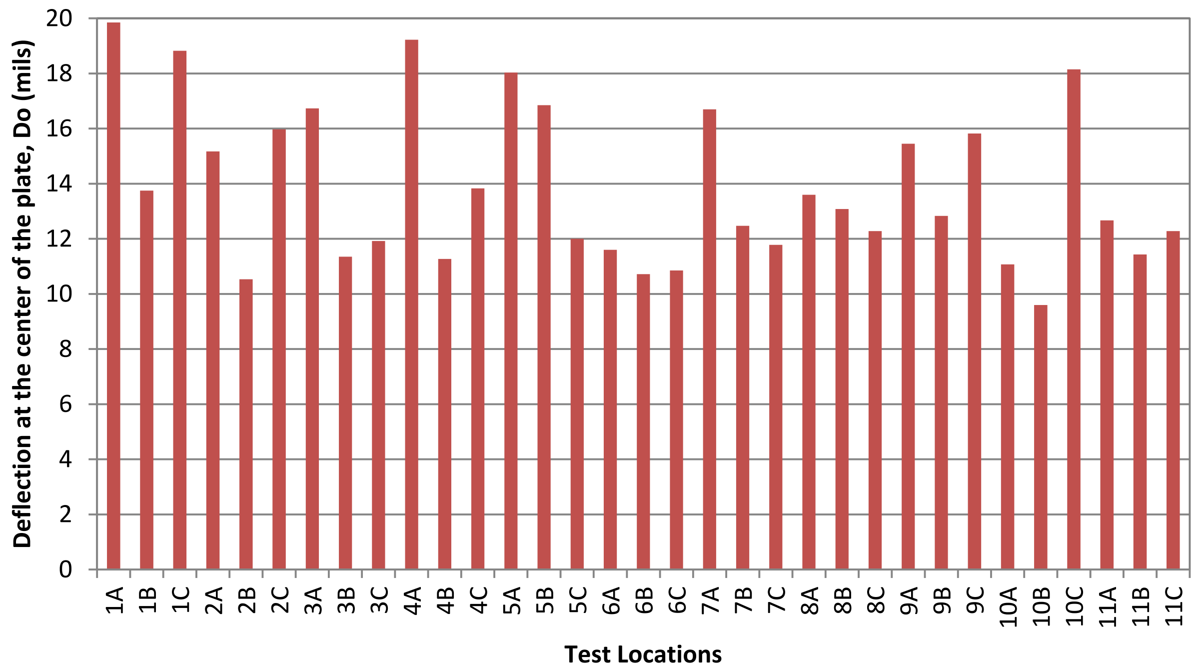

Figure B77: Distribution of average measured deflection under loading plate at LWD test points on the aggregate base layer, STH 33, Saukville.

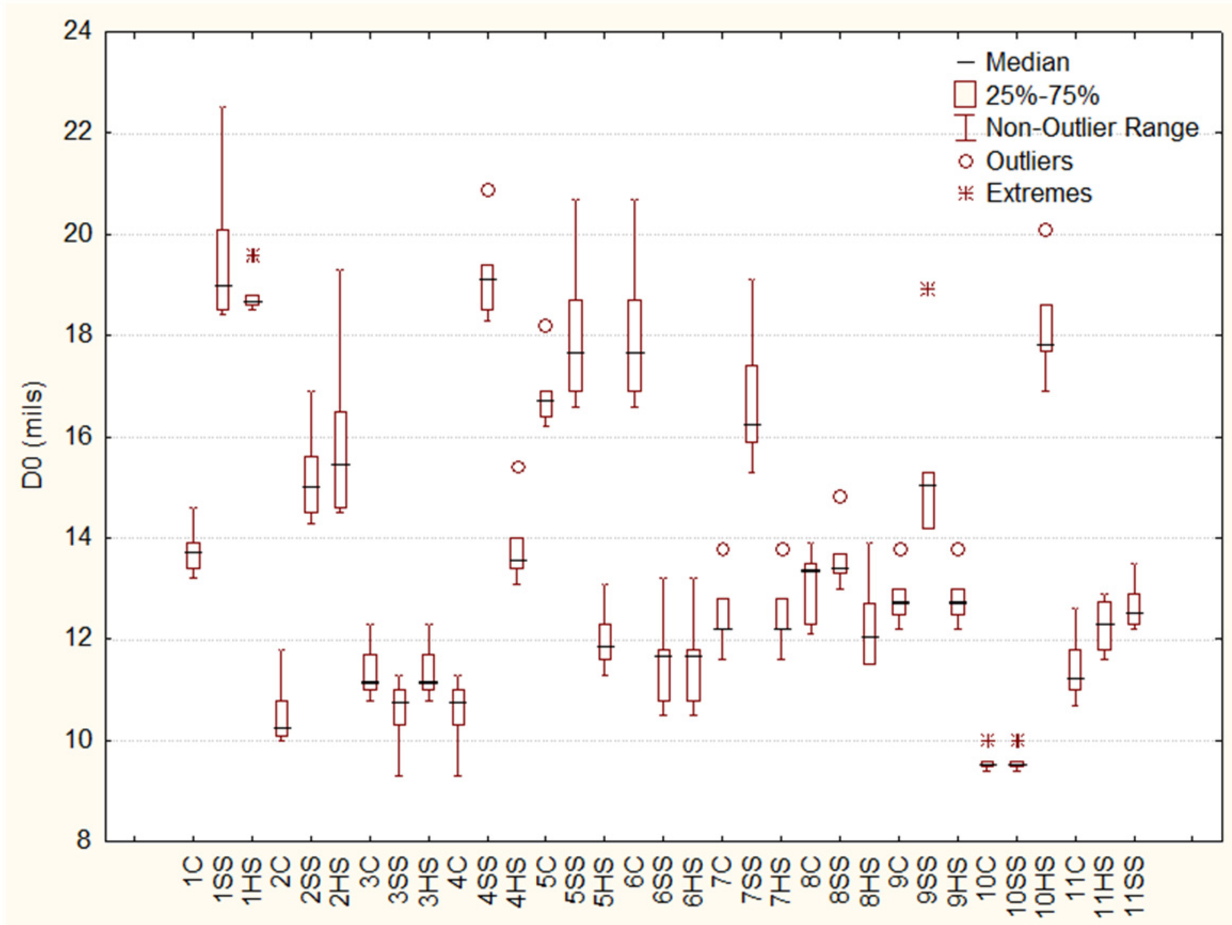

Figure B78: Whisker-box plot for the measured deflection under loading plate at LWD test points on the aggregate base layer, STH 33, Saukville.

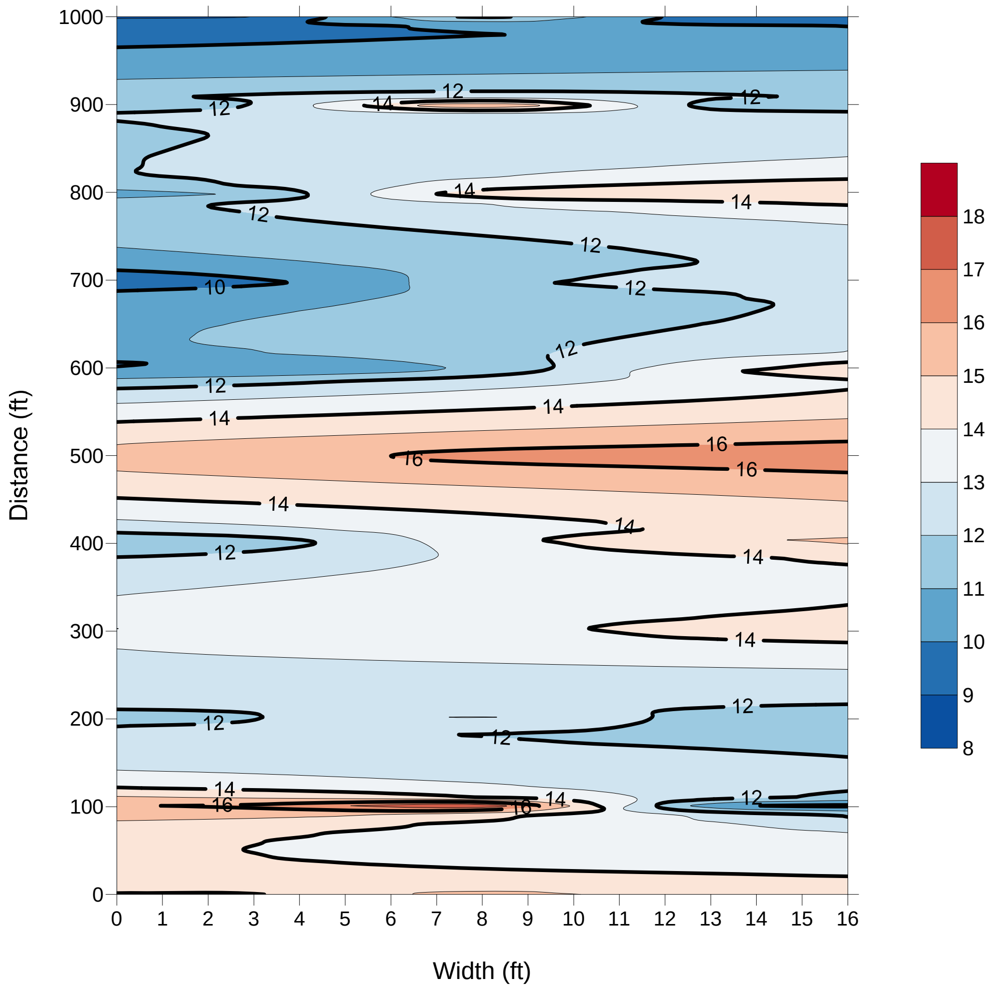

Figure B79: Contours of the calculated base layer modulus (E_{base}) based on LWD measurements, STH 33, Saukville.